Modified Zeolites and Titania Catalysts for the Conversion of Carbohydrates to 5-Hydroxymethylfurfural

A Thesis
Submitted in Partial Fulfilment of the Requirement for the Degree of

DOCTOR OF PHILOSOPHY

By

YEDLA SANTOSH KUMAR

Department of Chemical Engineering
Indian Institute of Technology Guwahati
Guwahati-781039, Assam, India
September, 2019

Dedicated To
My Supervisors and
Family Members

Indian Institute of Technology Guwahati

Department of Chemical Engineering

Statement

I, hereby declare that the content embodied in this thesis entitled "**Modified Zeolites and Titania Catalysts for the Conversion of Carbohydrates to 5-Hydroxymethylfurfural**" is the result of investigations carried out by me at the Department of Chemical Engineering, Indian Institute of Technology Guwahati, Guwahati, India, under the supervision of **Dr. Nageswara Rao Peela and Prof. Animes Kumar Golder**.

In keeping with the general practice of reporting scientific observations, due acknowledgements have been made wherever the work described is based on the findings of other investigators.

Guwahati,
September, 2019

Yedla Santosh Kumar

Indian Institute of Technology Guwahati

Department of Chemical Engineering

Certificate

It is certified that the work described in this thesis entitled "**Modified Zeolites and Titania Catalysts for the Conversion of Carbohydrates to 5-Hydroxymethylfurfural** " by Mr. Yedla Santosh Kumar for the award of degree of Doctor of Philosophy is an authentic record of the results obtained from the research work carried out under our supervision at the Department of Chemical Engineering, Indian Institute of Technology Guwahati, Guwahati, India, and this work has not been submitted elsewhere for a degree.

Dr. Nageswara Rao Peela
(Main Superviosr)
Associate Professor
Department of Chemical Engineering
IIT Guwahati, Guwahati – 781039
Assam, India

Prof. Animes Kumar Golder
(Co-Supervisor)
Professor
Department of Chemical Engineering
IIT Guwahati, Guwahati – 781039
Assam, India

ACKNOWLEDGEMENT

My doctoral dissertation would not have come to a successful completion without the help of several people. I take this opportunity to express my sincere gratitude to all of them.

First of all, I am extremely grateful to my thesis supervisors, **Dr. Nageswara Rao Peela Sir** and **Prof. Animes Kumar Golder Sir,** Department of Chemical Engineering, who motivated and made me more confident and for their valuable suggestions, incisive thinking, and cogent advice throughout whole research period. Their consistent encouragement, criticisms and painstaking planning have aided a long way for the preparation of present thesis. Their true scientific spirit, independence and self-reliance have helped me an immense to develop the quality of my research work. This feat was possible only because of the unconditional support provided by them. Whenever, I went to their office, they have always made themselves available to clarify my doubts despite their busy schedules. I always strongly believe that I am blessed by God to do my doctoral programme under their guidance. To be honest, whatever knowledge I have gained during my research period that is just because of them. It was really honoured to work under them. Thank you very much both of you sirs, for your unforgettable help and support in my life.

I would like to thank my PhD thesis oral Indian examiner **Dr. Debaprasad Shee.** I would like to also thank my doctoral committee members **Dr. Mahuya De, Prof. Vaibhav V Goud,** and **Prof. Subhendu Sekhar Bag** for their valuable suggestions and comments during all assessments of the Ph. D. program. I would like to also thank my comprehensive committee members, **Prof. G. Pugazhenthi**, **Dr. Mahuya De**, and **Prof. Vaibhav V Goud,**

I am thankful to **Prof. Ramgopal Uppaluri, Prof. Chandan Das, Prof. Nanda Kishore** Department of Chemical Engineering, IIT Guwahati and **Dr. Akshai Kumar A.S., Dr. Pavan K. Kancharla** Department of Chemistry, IIT Guwahati and **Dr. Dileep Kumar** Department of Chemical Engineering, JNTU Anantapur for given me useful suggestions and moral support during my research work. I also thank **Prof. Anugrah Singh,** Head, Department of Chemical Engineering, for his administrative support. Furthermore, I would like to thank other faculty members, research scholars, supporting staff of the Department of Chemical Engineering, IIT Guwahati for their kind cooperation in all aspects.

I take this time to express my sincere gratitude to my teacher **Krishnajee Rao Panchadi (Gurujee)** for his encouragement and motivation throughout my career.

I acknowledge Ministry of Human Resource Development **(MHRD)** and our institute for providing fellowship throughout the PhD program. The financial support provided by the Science and Engineering Research Board **(SERB, File Number: YSS/2015/000911),** New Delhi, India is gratefully acknowledged. The analytical facilities from Central Instruments Facilities **(CIF)** and analytical facilities from **Department of Chemical Engineering** of Indian Institute of Technology Guwahati are also acknowledged.

I am grateful to my senior members from our group, *Dr. Venkatanarasimha Rao Chelli*, *Dr. Raj Kumar Das*, *Dr. Vinay Kulkarni*, for their co-operative assistance and

suggestions in performing experiments. I deeply acknowledge my research group members, *Mr. Mahboob Alam, Ms. Devi Priya Mr. Rambabu, Mr. Anirban, Mr. Bharath Velaga, Mr Prasad, Mr.Ameer Suhail, Mr Hanumanth Reddy Pemmana, Mr Rammohan D, Ms pooja Saxena, Mr. Sourdip choudary Mr. paradeep soni, Mr.Madhav Solanke Mr. Nagireedi Srinu, Mr. Smruti Ranjan Dash, Ms. Paulomi Bose, and Mr P. Joy*.

I cannot forget to thank my friends *Mr Shravan Kumar, Mr. Sandup Tshering Bhutia, Mr. G. Bharath , Mr. M.M. Reddy, Mr. T. Ramesh, Mr. Prudhviraj, Mr. Satyanarayan E, Mr. Satish Raj Mani, Dr.Shyam Kumar Yadav, Mr. Dharmalingam K, Dr.Mood Mohan, Mr. Ranjeeth Kr Mishra, Mr. Amit Batghare ,Mr.Shailesh Ravi Varade Mr Sohin bir Singh. Mr. Vigneswaran, Dr Gopi Kiran, Mr. Upendar Reddy, Mr. Narendra Naik, Mr suresh (Chemistry, PhD IITG), other friends, my PhD batch mates and My juniors*, for the lovely support in making my stay at IIT Guwahati memorable.

I am deeply grateful to convey my sincere gratitude to my parents and family members for their sustained help and encouragement in all my personal and academic ventures. I feel proud and blessed to have such parents my mother **Mrs. Narayanamma** Garu and my father **Mr. Ramakrishna** Garu, my brother-in-laws **Late R.Tirupathi Rao** Garu and, **Mr. K. Jagadesawara rao** Garu and my sisters **Mrs. Lalitha** Garu, and **Mrs. Sridevi (Neelama)** Garu,. Special thanks to my one and only brother **Mahesh** and Uncle **Y. Trindha Rao** who always strengthened my morale by standing by me in all situations.

However, my compliments will be incomplete without expressing my profound gratitude to my mamayya garu **Tirupathi Rao Dannana**, his wife, Mrs **Sobha Rani**, and his daughter, **Tejaswi Chinni**). Who has always lovingly supported´ and encouraged me to pursue my career goals and try my best,

Last but not least I would like to thank my beautiful wife **Yesaswi (Bindu),** for her lovely support and patience in all these years and for encouraging me to face the difficulty. You are the source of my inspiration and happiness. Without you all this would never have been possible. My thesis acknowledgement would be incomplete without thanking my baby-son, **Nirvaan Yedla**, whose smiling face always made me happy and inspired me. Having him midway during my Ph.D. was certainly not easy for me but he has made my life wonderful.

Today, I am in this position that is just because of my Gurujee, parents and beautiful wife. I do not find words to express my gratitude to them and they are always in my heart. I feel deeply indebted to them for whatever I have achieved so far.

I wish to thank many other people whose names are not mentioned here but this does not mean that I have forgotten their help. Above all, I am thankful to GOD for giving me a wonderful and healthy life.

YEDLA SANTOSH KUMAR

ABSTRACT

The replacement of the fossil fuels with renewable sources to produce fuels and value-added chemicals is essential due to the quick depletion of fossil sources and also to meet the stringent environmental regulations. Biomass is known to be the best renewable resource because of the presence of the carbon atom in its chemical structure. Biomass consists of cellulose, hemicellulose, and lignin as its constituent biopolymers molecules. Cellulose is a polymer of glucose and these glucose molecules are bonded together with β (1→4) glycosidic bonds. So, it makes this polymer hard to break. The production of 5-Hydroxymethylfurfural (5-HMF) from the cellulose-based carbohydrates is probably one of the promising pathways for the utilization of such renewable resources for the formation of value-added chemicals because 5-HMF has many potential applications in chemical, solvent, biofuel, polymer, and pharmaceutical industries. 5-HMF could be produced with high yields from fructose, with moderate yields from glucose and with low yields from cellulose. A higher yield of 5-HMF from cellulose substrate is necessary for the industrial viability of the process.

Various homogeneous and heterogeneous catalysts have been developed for the conversion of carbohydrates to 5-HMF with high and low to moderate yields, respectively. However, homogeneous catalysts are difficult to separate out for reuse and end up with the generation of a huge quantity waste material. Alternatively, an ionic liquid (i.e. choline chloride and [BMIM]Br) encapsulated zeolites could catalyze the reactions with a high yield of 5-HMF and the catalyst separation is much easier than the homogeneous catalytic system. To the best of our knowledge, there are no reports in the open literature on the utilization of IL (either choline chloride or [BMIM]Br) encapsulated zeolites for the conversion of carbohydrates to 5-HMF. Moreover, the interactions of ILs with zeolites are not well established in the literature. In this doctoral thesis, ILs (choline chloride and [BMIM]Br) encapsulated zeolites and Ag-, Cu-, P-doped titania catalysts are prepared using an impregnation, ship-in-a-bottle, and bio-inspired methods, respectively. These catalysts are well-characterized and tested for the carbohydrates conversion to 5-HMF. In all the catalyst tests, a biphasic system with methyl isobutyl ketone (MIBK) as an extraction phase is used. NaCl is used as a salting-out agent to enhance the partition coefficient between the aqueous (reaction) and the organic (extraction) phases. The effects

of variation of operating conditions (temperature, reaction time, substrate concentration) are studied in detail.

Bare zeolites for the carbohydrates conversion to 5-HMF: At the beginning of this study, the conversion of cellulose, glucose, and fructose to 5-HMF over selected 10- and 12-membered bare zeolites, namely, HY, HBeta, HMOR, and HZSM5 is investigated. The catalysts are characterized using powder X-ray diffraction (p-XRD), N_2-sorption experiments, Field emission transmission electron microscopy (FETEM), Pyridine Fourier transformed infrared spectroscopy (Py-FTIR), and Ammonia temperature programmed desorption (NH_3-TPD). Among the catalysts tested, HBeta showed the highest 5-HMF yield of 94% with a fructose conversion of 98%. The highest yield to 5-HMF obtained with the glucose is 51.5% (at 72.9% conversion), respectively, at 180°C. HBeta showed an excellent stability with no signs of deactivation even after reuse of the same catalysts up to 5 cycles.

Choline chloride (ChCl) encapsulated zeolites for the carbohydrates conversion to 5-HMF: In the second study, a bio-based IL, ChCl is encapsulated successfully onto HMOR, HZSM5, HBeta, NaY, and HY using an impregnation method and they are then tested for the conversion of cellulose, glucose, and fructose to 5-HMF. The XRD analysis indicates the change in electron density around the zeolite pore walls. A stronger interaction of methylene carbons (N-CH_2-) in ChCl with HZSM5 is observed in ^{13}C solid-state (SS) NMR spectra. This study obtains a good 5-HMF yield of 49 (selectivity, 83%) and 55% from glucose and cellulose over ChCl/HMOR and ChCl/HY, respectively, at the optimized reaction conditions of 180°C, 1 h, substrate:catalyst ratio 3 w/w, and substrate concentration 10 wt%. The activity of the zeolites (HZSM5) with moderate silica-to-alumina ratios (SAR) is found to be enhanced by the encapsulation of ChCl due to a stronger interaction between ChCl and the zeolite as depicted from SS NMR spectra. However, this effect is negligible for the zeolites either with a low or high SAR. Similar to bare zeolites, ChCl encapsulated HZSM5 is stable and reusable up to the 5^{th} cycle tested in this study.

[BMIM]Br encapsulated zeolites for the carbohydrates conversion to 5-HMF: This study focuses on the modifications of bares zeolites using a second IL, namely, 1-Butyl-3-methylimidazolium bromide ([BMIM]Br) in a ship-in-a-bottle method. The higher temperature required for the decomposition of [BMIM]Br in zeolites as compared to that

required for the bulk [BMIM]Br indicate a stronger interaction of [BMIM]Br with the zeolite. It is found that [BMIM]Br interacts more strongly with the H-form zeolite as compared to that with Na-form zeolite. ^{27}Al SS NMR reveals that the HMOR loses its extra-framework Al with the [BMIM]Br encapsulation. The SAR increases and Na/Al ratio decreases with the incorporation of [BMIM]Br, as depicted from the EDX analysis. The decrease in Na/Al ratio indicates that some of the Na^+ cations are replaced with the $[BMIM]^+$ cations during its encapsulation into the zeolite pores. The total surface area, micropore area, and the micropore volume of the zeolites are also decreased with the encapsulation of [BMIM]Br. The modified catalysts exhibit significant improvements in the conversions of carbohydrates to 5-HMF compared to the bare zeolite counterparts. At the optimal reaction conditions (180^{o}C, substrate:catalyst ratio 3 w/w and substrate concentration 10 wt%), [BMIM]Br/NaY exhibits the highest 5-HMF yields of 80 (1 h), 62 (2 h), and 59% (3 h reaction time) with fructose, glucose, and cellulose, respectively. Moreover, these catalysts are recyclable for the production of 5-HMF with a moderate decrease in its activity till the second reuse run.

Bio-inspired Ag-, Cu- and P-doping on TiO_2 for glucose conversion to 5-HMF: Instead of zeolites as the supports, this work also explores a new bio-inspired pathway to functionalize TiO_2, a semiconductor support of amphoteric in nature. A combination of noble metal (Ag), transition metal (Cu), and inorganic (P, phosphorous) dopants are tested. The plant-based analytes present in *S. edule* extract successfully dope Ag, Cu, and P into the lattice structure of TiO_2 as evidenced from the XRD and HRTEM analyses. The surface area of the doped catalysts is found to be decreased as accordance with the lattice strain calculation. Among the catalysts, P/TiO_2 showed the highest 5-HMF yield of 50% at 81% glucose conversion at a slightly higher reaction temperature of 190°C compared to the IL encapsulated zeolite catalysts.

Upon overall comparison of the performance of the catalysts developed in this study, it could be inferred that the highest yield of 5-HMF is observed over [BMIM]Br encapsulated NaY catalyst with 62 and 59% yield from the glucose and cellulose substrates, respectively. Whereas, ChCl encapsulated HMOR catalyst showed the highest yield of 5-HMF from fructose and the highest selectivity to 5-HMF (83%) from the glucose substrate. The catalysts particularly, [BMIM]Br/NaY and ChCl/HMOR developed

in this work outperformed the catalysts reported in many earlier studies for the production of 5-HMF from carbohydrate-based substrates..

Keywords: Biomass; Carbohydrates; Value-added products; Heterogeneous catalysts; Cellulose; Glucose; Fructose; Zeolite catalysts; Titania catalysts; Brønsted acidity; Lewis acidity; Catalysts modifications; Ionic liquids; Choline chloride; 1-Butyl-3-methylimidazolium bromide; Bio-inspired doping; Metal doping; Phosphorus doping; 5-Hydroxymethylfurfural production; High conversion; High yield; Enhanced selectivity

TABLE OF CONTENTS

LIST OF FIGURE CAPTIONS

LIST OF TABLE CAPTIONS

ABBREVIATIONS

([HO_2CMMIm])Cl	1-Carboxymethyl-3-methylimidazolium chloride
[BMIM] Cl	1-butyl-3-methylimidazolium chloride
[BMIM][BF_4]	1-butyl-3-methylimidazolium tetrafluoroborate
[BMIM]Br	1-butyl-3-methylimidazolium bromide
[CMIM]Cl	1-Carboxypropyl-3-methyl imidazolium chloride
[Emim]Br	1-Ethyl-3-methyl-imidazolium-bromide
[EMIM]Cl	1-ethyl-3-methylimidazolium chloride
[HMIM][Cl]	1-hexyl-3-methylimidazolium chloride
[OMIM]Cl	1-Methyl-3-octylimidazolium chloride
5-HMF	5-hydroxymethylfurfural
AA	Acetic Acid
$Ag_3PW_{12}O_{40}$	Heteropolyacid salt
BET	Stephen Brunauer, Paul Hugh Emmett and Edward Teller
BJH	Barrett, Joyner and Halenda
ChCl	Choline chloride
DCM	Dichloromethane
DEAC	N,N-diethylethanolammonium chloride
DES	Deep eutectic solvent
DFF	2,5-Diformylfuran
DHMF	2,5-di(hydroxymethyl)furan
DMF	N,N-dimethylformamide
DMF	2,5-Dimethylfuran
DMSO	Dimethyl sulfoxid
FA	Formic acid
FF	Furfural
FTIR	Fourier transform infrared spectroscopy
GVL	Gamma-valerolactone
H_2SO_4	Sulfuric acid
H_3PO_4	Phosphoric acid
$H_3PW_{12}O_{40}$ Lab.	phosphotungstic acid

HCl	Hydrochloric acid
HPA	Heteropolyacid
HPLC	High-performance liquid chromatography
IL	Ionic liquids
LA	Levulinic acid
MCM	Mobil composition of matter
MeTHF	2-Methyltetrahydrofuran
MIBK	Methyl isobutyl ketone
MIL-101(Cr)-SO_3H	Sulfonic acid-functionalised metal–organic
MilliQ	Deionized water
mL	Millilitre
mmol	Millimole
MW	Microwave
NMR	Nuclear magnetic resonance
ppm	Parts per million
p-TSA	p-Toluenesulfonic acid
pTsOH	p-Toluenesulfonic acid
RI	Refractive index
RID	Refractive Index Detector
$Sc(OTf)_3$	Scandium trifluoromethanesulfonate
SO_3OH	Functionalised acidic ionic liquid with hydrogen sulphate anion
SO_4^{2-} /ZrO_2-Al_2O^3	Commercial solid catalyst
THF	Tetrahydrofuran
TPD	Temperature programmed desorption
TsOH	p-Toluene sulfonic acid
XRD	X-Ray diffraction
δ	Chemical shift

Mr. YEDLA SANTOSH KUMAR

Date of Birth: **05th june 1989**
Email: **k.yedla@iitg.ac.in; ysk821@gmail.com**

Educations:

Ph.D. pursuing
Department of Chemical Engineering
Indian Institute of Technology, Guwahati
Guwahati, Assam, India
2014- 2019

M. Tech in Chemical Engineering
Department of Chemical Engineering
Indian Institute of Technology, Madras
Chennai, Tamilnadu, India
2011- 2013
Marks obtained: 7.33/10.00

B. Tech in Chemical Engineering
Department of Chemical Engineering
Jawaharlal Nehru Technological University Anantapur
Anantapur, Andhra Pradesh, India
2007-2011
Marks obtained: 71.07%, 1st Class with distinction

Higher Secondary in MPC
Sri Narayana Jr. College
Visakahapatnam, Andhra Pradesh, India
2005-2007
Marks obtained: 93.9%, 1st Class with distinction

Secondary Education
Z.P.H.S, Pachipenta,
Vizinagaram, Andhra Pradesh, India
2004-2005
Marks obtained: 91.33%, 1st Class with distinction

Publications

Journal papers

1. N.R. Peela, **S.K. Yedla**, B. Velaga, A. Kumar, A.K. Golder; "Choline Chloride Functionalized Zeolites for the Conversion of Biomass Derivatives to 5-Hydroxymethylfurfural" Applied Catalysis A, General 580 (2019) 59 – 70 (DOI: 10.1016/j.apcata.2019.05.005)
2. **S.K. Yedla**, A.K. Golder, N.R. Peela, "Efficient Conversion of Carbohydrates to 5Hydroxymethylfurfural over Mesoporous Zeolites" Journal of Emerging Technologies and Innovative Research, May 2019,Volume 6, Issue 5,239-250, ISSN-2349-5162
3. **S.K. Yedla**, B.Velaga, S.Chowdary, A. Namdeo, A.K. Golder, N.R.Peela. "1-Butyl-3-Methylimidazolium Bromide Functionalized Zeolites: Nature of Interactions and Catalytic Activity for Carbohydrates Conversion to Value-added Chemicals" (Under Review)

National Conference / Inter National Conference

1. **S.K Yedla,** A. K. Golder, N. R. Peela, "Studies on the Production of 5-hydroxymethylfurfural (5-HMF) from Cellulose- A Mini Review" presented (poster) at CHEMCON 2015, December 27-30th 2015, Indian Institute of Technology Guwahati, India.
2. **S.K Yedla**, A. K. Golder, N. R. Peela, "One-Pot Production of 5-Hydroxymethylfurfural (5-HMF) from Carbohydrates by using different Solid Acid Catalysts", presented (oral) at REFLUX 2017, March 24-26th 2017, Indian Institute of Technology Guwahati, India.
3. **S.K Yedla**, A. K. Golder, N. R. Peela"Production of 5-Hydroxymethylufurfural (5-HMF) from Fructose over H-MOR Zeolite Catalyst" presented (poster) at REFLUX 2017, March 24-26th 2017, Indian Institute of Technology Guwahati, India
4. **S.K Yedla**, A. K. Golder, N. R. Peela, "Glucose Dehydration to 5-Hydroxymethylfurfural over H-Type Zeolites in a Water/MIBK Biphasic System", presented (oral) at ICPOLC-19, January, 27th 2019, Hyderabad, India.
5. **S.K Yedla,** A. K. Golder, N. R. Peela"Efficient Conversion of Carbohydrates to 5-Hydroxymethylfurfural over Mesoporous Zeolites" presented (oral) at ICET-19, March, 2nd 2019, Hyderabad, India.
6. **S.K Yedla,** A. K. Golder, N. R. Peela, "Choline Chloride Grafted Zeolites for the production of 5-Hydroxymethylfurfural from Carbohydrates Conversion" presented (poster) at RESEARCH CONCLAVE 2019, March 14-17th 2019, Indian Institute of Technology Guwahati, India.

Book Chapters

1. M. Alam, **S. K. Yedla,** S. T. Bhutia, V. V. Goud, N. R. Peela, Advancement in Development of Biodiesel Production in the Last Two Decades: An Indian Overview on Raw Materials, Synthesis, By-products, and Application. A.K. Chandel, R.K. Sukumaran (eds.), Springer, (2017), Pages (167-188)

Awards

1. Best presentation award for the paper entitled "One-Pot Production of 5-Hydroxymethylfurfural (5-HMF) from Carbohydrates by using different Solid Acid Catalysts." in Reflux-2017-Annual Chemical Engineering Symposium, Department of Chemical Engineering, 24-26 March, IIT Guwahati, Assam, India

2. Best presentation award for the paper entitled, "Choline Chloride Grafted Zeolites for the production of 5-Hydroxymethylfurfural from Carbohydrates Conversion" presented (poster) at RESEARCH CONCLAVE 2019, March 14-17th 2019, Indian Institute of Technology Guwahati, India

Job Experience:

1. Worked as a Assistant Professor in VelTech High Tech Dr. R. Rangarajan Dr. R. Sakunthala Engg College, Avadi, Chennai From June ^{1st} 2013 To April ^{11th} 2014.

Chapter 1

Background of the Work and Research Objectives

1.1 Introduction

Nowadays, most of the chemical industries are under immense pressure to develop processes to produce essential fuels and value-added chemicals from renewable resources due to depletion of fossil fuels and to meet the fast-growing needs and stringent constraints on environmental pollution. Moreover, the endeavor is to move towards more eco-friendly, cost-effective fuels and chemicals production processes and technologies. The transformations of renewable resources have a vital role considering the future sustainable supply of chemicals and energy essential for society (Binder and Raines, 2009; Corma et al., 2007).

Globally, nuclear fissile, fossil and renewable energy are the three primary sources for the production of energy, fuels, and chemicals. Fossil fuel sources are natural gas, petroleum, coal, and bitumens which were formed in early geological periods (Eminov et al., 2016). The sources of fossil fuels are not renewable, and they are distributed in specific geographical locations in a limited quantity. Today, the greatest consumption is of petroleum feedstocks over natural gas, coal, renewable and nuclear energy sources. Almost 80% of the global energy consumption is derived just from natural gas, petroleum, and coal (Demirbas, 2009; Liu et al., 2017; Mika et al., 2018). They are consumed far more rapidly than nature can replenish them. Due to the industrial growth and the blooming human population, the present consumption rate of fossil fuels is increasing exponentially. It would lead to a faster and inevitable depletion within a few decades. Moreover, the use of fossil feedstocks for the production of energy and chemicals is leading to severe environmental issues. The burning of fossil fuels leads to the emissions of CO_2 in the atmosphere which has a significant bearing on global warming and climate change (Eminov et al., 2016). Moreover, the fossil fuel reserves on the earth are not distribution uniformly. Therefore, there are strong political,

economic, and security issues worldwide related to the origin and demand based supply of fossil fuels. Such important environmental and geopolitical issues have driven the whole world to derive usable energy from renewable sources which are sustainably abundant in the nature such as solar, hydro, wind, marine, geothermal, biomass, etc. Moreover, the contaminants released to the environment are significantly lower than the conventional fossil fuel based sources (Eminov et al., 2016).

If the planet is to continue to function, the main sources of energy cannot continue to come from nonrenewable resources as these resources cause problems with energy security and environmental pollution. Therefore, there is a great need to replace nonrenewable resources (such as fossil fuels) with renewable energy resources (Demirbas, 2009). In order to store, convert, and amplify energy for the use of the global community, many different methods have been developed, and the search continues to find the most efficient method to meet our energy needs. The production of usable energy from new and renewable energy sources brings new challenges to humankind. Process efficiency and technology development are the challenges to mention a few.

Among the renewable resources, biomass is the only resource which contains carbon and thus is the most suited for fuels and chemicals production (Caratzoulas et al., 2014; Huber et al., 2006). Biomass (Eq. 1.1) is produced with the following general reaction (Mika et al., 2018):

$$6CO_2 + 6H_2O \xrightarrow{hv} C_6H_{12}O_6 \qquad (1.1)$$

Lignocellulosic biomass (plant biomass) is a globally available, non-edible and carbon neutral resource which has been used for the energy and chemicals generation since ancient times (Mika et al., 2018). The major constituents of the plant biomass are cellulose, hemicellulose, and lignin with small amounts of extractives (< 10 wt %) and ash (< 10 wt %). Cellulose is the most abundantly and naturally available biopolymer with glucose as its monomeric building block, and the glucose units are linked together by β (1 → 4) glycosidic bonds.

For cellulose separation from biomass, initially, the extractives need to be removed from the biomass using soxhlet apparatus according to the Tappi test method T204 (Kazmi et al., 2019; McCluer, 1964). After extractives removal, the cellulose is separated from hemicellulose and lignin using the following methods: (i) alkaline peroxide treatment (for hemicellulose removal), and (ii) acidified sodium chlorite treatment (for delignification) (Abdel-Halim, 2014; Crampton and Maynard, 1938; Gaudinski et al., 2005; Liu et al., 2006; Rinne et al., 2005; Sun et

al., 2004). Finally, the obtained residue (cellulose) is dried at 60°C for 16 h to remove the moisture.

The hemicellulose (Polylose) is a hetero-polymer, which mainly contains xylose, arabinose, mannose, galactose, deoxy sugar, and rhamnose. The important value-added chemicals and platform chemicals such as furfural, acetic acid, levulinic acid, and furfural alcohol are obtained from hemicellulose (Fang et al., 2000). Lignin is a phenyl propanoid-based biopolymer. It is made up of three main monomers: p-coumaryl (H), coniferyl (G), and sinapyl (S). Phenolic resins, surfactants, epoxy resins, adhesives or polyester, etc. also can be derived from lignin (Boerjan et al., 2003 ; WKazmi et al., 2019 ; Welker et al., 2015).

1.1.1 5-Hydroxymethylfurfural and its industrial importance

5-Hydroxymethylfurfural (5-HMF), Lactic acid, Formic acid (FA), and Levulinic acid (LA) are among the numerous promising biomass-derived chemicals. Among these, 5-HMF is an important bio-based platform chemical (Li et al., 2016a; Zakrzewska et al., 2011).

The 5-HMF molecule consists of hydroxyl and aldehyde groups along with a furan ring as shown in Fig. 1.1. 5-HMF is a yellow color solid with a melting point of 31°C, a boiling point of 115°C and a density of 1.206 $g.cc^{-1}$ (Van et al., 2013, Kowalski et al., 2013). 5-HMF is soluble in a variety of solvents, such as formaldehyde, water, acetone, chloroform, ethanol, methanol, benzene, ethyl acetate, etc. 5-HMF can be converted to a range of derivatives (Fig. 1.2) having potential applications (Gallezot, 2012) in the chemical industries, solvent industries, production of biofuels, polymers, pharmaceutical, etc. (Table 1.1). Kuster (1990) described the acid-catalyzed reactions for the production of 5-HMF from hexose substrate. The rehydration of 5-HMF leads to the formation of lactic acid, formic acid levulinic acid (Kuster, 1990; Van et al., 2013). The polymerization of 5-HMF results in the formation of insoluble humins. The side products formation reduces the 5-HMF yields as well as the catalyst activity. Therefore, there is an urgent need for the development of highly selective catalysts for the production of 5-HMF from carbohydrates. A review of various routes for the production of chemicals and fuels is given in the next section.

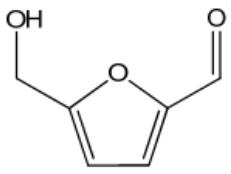

Figure 1.1: Structure of 5-Hydrtoxymethylfurfural (5-HMF).

Table 1.1: Derivatives of 5-HMF and their applications (Li et al., 2016b; Román-Leshkov et al., 2006; Van et al., 2013; Yang et al., 2012; Zakrzewska et al., 2011).

Name of the chemical	Potential applications
Formic acid	Chemicals, textiles, road salt, catalysts, fuel cells
Lactic acid	Polymers, pharmaceuticals, detergents
2,5-Diformylfuran (DFF)	Pharmaceuticals, fungicides
2,5-di(Hydroxymethyl)furan (DHMF)	Solvents, polymers
Ethoxymethylfurfural	Biofuels
2,5-Furandicarboxyaldehyde (FDC)	Polymers, resins
2-Methylfuran	Biofuel
Furfuryl alcohol	Resins, solvents
5-Hydroxymethylfuroic acid	Polymers
2,5-di(Hydroxymethyl)tetrahydrofuran (DHM-THF)	Solvents
Dimethyl furan (2,5-DMF)	Biofuels
2,5-Furandicarboxylic acid (FDCA)	Polymers, pharmaceuticals

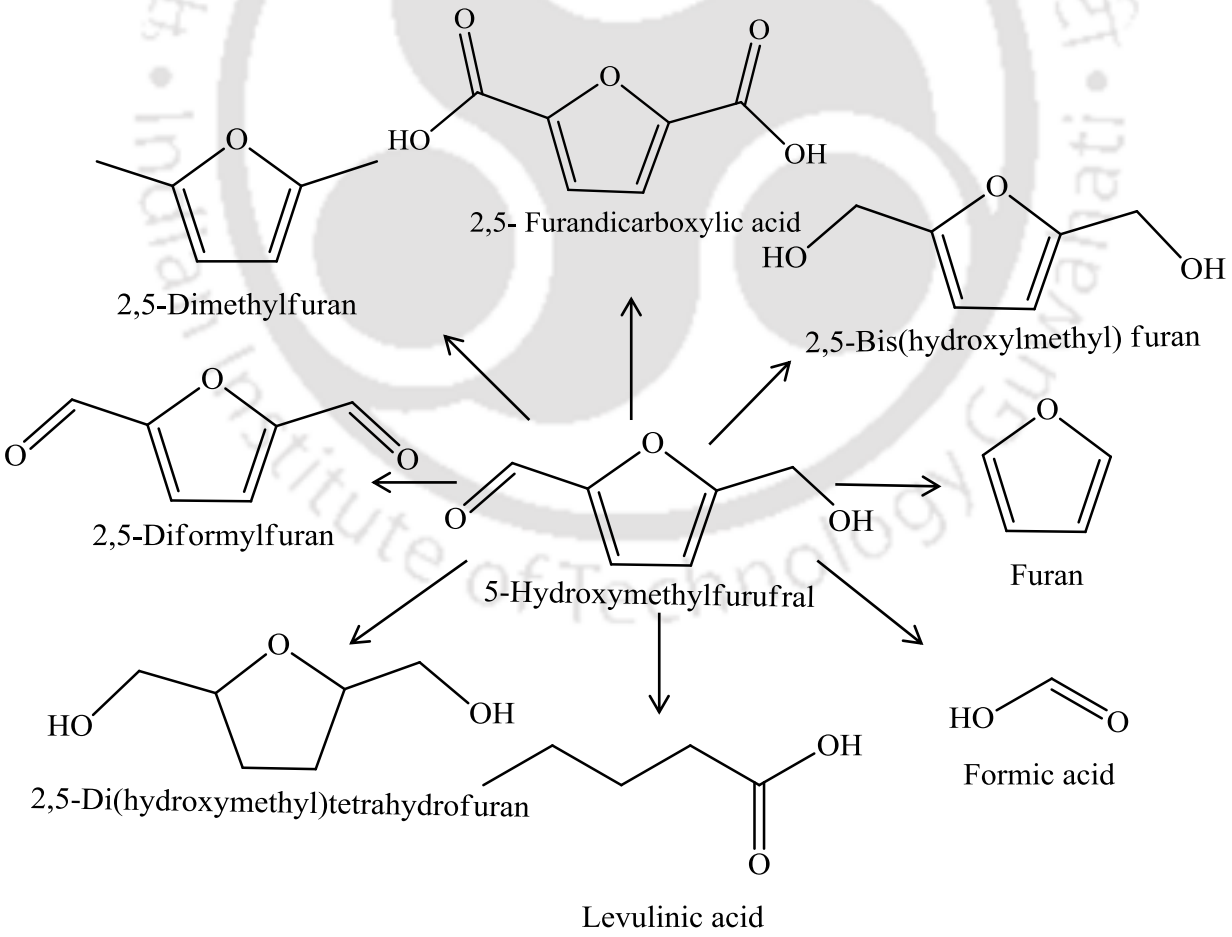

Figure 1.2: Derivatives of 5-Hydroxymethylfurfural (Gallezot, 2012).

1.1.2 Alternative routes to produce fine chemicals and fuels from biomass

Various routes have been developed for the production of chemicals and fuels (Huber et al., 2006). These routes include biochemical, gasification, pyrolysis and low-temperature chemical route. A comparison of the routes has been given in the literature (Serrano-Ruiz and Dumesic, 2011). Among these routes gasification and pyrolysis (which known to be high-temperature methods) are non-selective in the sense that the products from these routes are of wide range and types. For example, the products formed from the pyrolysis route contains up to 400 different compounds with several functional groups present in them. To produce any pure chemical from the huge number of products, separation would become a significant burden. However, this may be suitable for fuels production. In contrast, the low-temperature routes are highly selective, and the number of products formed could be significantly lower, as low as less than 10. For example, for the production of 5-HMF, the major side products would be only levulinic acid, formic acid, and humins. Therefore, this route is highly suitable for the production of value-added chemicals (Caratzoulas et al., 2014). However, one major drawback of this route is the low yields of end products produced (Serrano-Ruiz and Dumesic, 2011). Therefore, further research is required in this area to enhance the yields to make this route industrially economical.

1.2 Literature review

1.2.1 Homogeneous catalysts for carbohydrates conversion to 5-HMF

The homogeneous catalysts studied along with the reaction conditions and solvents used for the conversion of carbohydrates to 5-HMF are presented in Table 1.2.

1.2.1.1 Sulfuric acid (H_2SO_4)

H_2SO_4 has been tested for the conversion of carbohydrates (fructose, glucose, and cellulose) to 5-HMF in the temperature range of 80 to 250°C, and reaction time range of 5 s to 9 h using various solvents such as water (Várhegyi et al., 1993), Subcritical water (Bicker et al., 2003), acetone (Bicker et al., 2003), DMSO (Xiao et al., 2014), ionic liquids (ILs) (such as [BMIM]Cl (Guo et al., 2012), [EMIM]Cl (Liu and Holladay, 2013), etc.) and mixture of solvents (water + DMSO (Román-Leshkov et al., 2006), water + acetone, (Bicker et al., 2003) as shown in Table 1.2. Some studies have also been carried out with extraction phases such as methyl isobutyl ketone (MIBK) (Román-Leshkov et al., 2006), tetrahydrofuran (THF) (Moye and Goldsack, 2018), 2-butanol (Román-Leshkov et al., 2006), etc. Both monosaccharides (fructose and glucose) and polysaccharides (cellulose) are used as the feed stocks. The highest 5-HMF yield of 96% from fructose in the presence of [BMIM]Cl as reaction media at 120°C for 30 min is reported (Sievers et al., 2009). The yields of 5-HMF are reported to be varying significantly with reaction conditions (Binder and Raines, 2009).

Table 1.2: Homogeneous catalysts for the carbohydrates conversion to 5-HMF (Li et al., 2016a; Mukherjee et al., 2015; van Putten et al., 2013; Zakrzewska et al., 2011).

Sl. no.	Feed stock (Conc., Wt %)	Catalyst (concentration)	Reaction conditions					Activity		References
			Reaction phase solvent	Salting out agent	Extraction phase solvent	Temp. (°C)	Time	Conversion (%)	Yield (%)	
1	Fructose (1)	H_2SO_4 (10 mM)	Subcritical water-acetone	-	-	180	2 min	90	48	(Bicker et al., 2003)
2	Fructose (1)	H_2SO_4 (10 mM)	Acetone-water	-	-	180	2 min	98	75	(Bicker et al., 2003)
3	Fructose (1)	H_2SO_4 (10 mM)	Subcritical water	-	-	180	10 min	80	20	(Bicker et al., 2005)
4	Fructose (1)	H_2SO_4 (pH = 1.5)	Subcritical water	-	-	240	2 min	100	20	(Asghari and Yoshida, 2006a)
5	Fructose (1)	H_2SO_4 (2 mM)	Subcritical water	-	-	250	32 s	92	34	(Antal et al., 1990)
6	Fructose (7.5)	H_2SO_4 (0.25 M)	-		THF	178	5 s	N/A	56	(Moye and Goldsack, 2018)
7	Fructose (30)	H_2SO_4 (0.25 M)	Water/DMSO		MIBK/2-butanol	180	3 min	85	42	(Román-Leshkov et al., 2006)
8	Fructose (30)	H_2SO_4 (0.25 M)	Water/DMSO	-	MIBK/2-butanol	180	2.5-3 min	85	60	(Román-Leshkov et al., 2006)
9	Fructose (10)	H_2SO_4 (0.1 M)	[EMIM]Cl	-	-	84-87	5 min	100	58	(Liu and Holladay, 2013)
10	Cellulose (2)	H_2SO_4 : $AlCl_3$ (40 and 10 mol %)	DMSO	-	-	150	9 h	N/A	24	(Xiao et al., 2014)

11	Fructose (10)	H_2SO_4 (10 wt %)	[BMIM]Cl	-	-	120	1 h	100	58	(Guo et al., 2012)
12	Glucose (8)	H_2SO_4 (0.01 mmol)	[BMIM]Cl	-	-	120	3 h	93	43	(Chidambaram and Bell, 2010)
13	Fructose (10)	H_2SO_4 (6 mol %)	DMA	KCl	-	80	2 h	N/A	56	(Binder and Raines, 2009)
14	Fructose (10)	H_2SO_4 (6 mol %)	DMA	NABr	-	100	2 h	N/A	93	(Binder and Raines, 2009)
15	Fructose (10)	H_2SO_4 (6 mol %)	DMA	KI	-	100	5 h	N/A	92	(Binder and Raines, 2009)
16	Glucose (2)	H_2SO_4 (50 wt %)	Water	-	-	200[(a)]	3 min	11	2	(Qi et al., 2008a)
17	Glucose (9)	H_2SO_4 (1 mM)	Water	-	-	200	5 min	32	2	(Watanabe et al., 2005)
18	Cellulose (3)	H_2SO_4 (20 mM)	Water	-	-	215	1 h	N/A	5	(Várhegyi et al., 1993)
19	Fructose (1 g)	H_2SO_4 (40 µL)	[BMIM]Cl (20 g)	-	-	120	30 min	N/A	96	(Sievers et al., 2009)
20	Glucose (1 g)	H_2SO_4 (40 µL)	[BMIM]Cl (20g)	-	-	120	2 h	N/A	11.9	(Sievers et al., 2009)
21	Fructose (1)	HCl (pH = 4)	Subcritical water	-	-	240	2 min	63	12	(Asghari and Yoshida, 2006a)
22	Fructose (1.5)	HCl (0.08 M)	-	-	Tetrahydrofurfuryl alcohol	178	5 s	N/A	56	(Moye and Goldsack, 2018)
23	Fructose (30)	HCl (0.25 M)	Water	-	-	180	3 min	50	18	(Román-Leshkov et al., 2006)

24	Fructose (50)	HCl (0.25 M)	Water/DMSO	-	MIBK/2-butanol	180	3 min	91	47	(Román-Leshkov et al., 2006)
25	Fructose (30)	HCl (0.25 M)	Water	-	-	180	2.5-3 min	50	25	(Román-Leshkov et al., 2006)
26	Fructose (1)	HCl (pH = 1)	water	-	-	150	2 h	92	19	(de Souza et al., 2012)
27	Fructose (10)	HCl (0.25 M)	Water	-	MIBK	140	15 min	100	52	(Brasholz et al., 2011)
28	Fructose (10)	HCl (pH = 1)	Water/DMSO	-	MIBK/2-butanol	170	4 min	95	64	(Chheda et al., 2007)
29	Fructose (9)	HCl (9 mol %)	[BMIM]Cl	-	-	80	8 min	N/A	68	(Li et al., 2010)
30	Fructose (33)	HCl (9 mol %)	[BMIM]Cl	-	-	80	35 min	90	57	(Li et al., 2010)
31	Fructose (67)	HCl (9 mol %)	[BMIM]Cl	-	-	80	2 h	67	36	(Li et al., 2010)
32	Fructose (27)	HCl (1 M)	Water	-	-	130	5 min	99	28	(Hansen et al., 2009)
33	Fructose (27)	HCl (0.01 M)	Water	-	-	200[(a)]	1 min	95	53	(Hansen et al., 2009)
34	Fructose (1)	H_3PO_4 (pH = 1.5)	Subcritical water	-	-	240	2 min	100	39	(Asghari and Yoshida, 2006a)
35	Fructose (30)	H_3PO_4 (0.25 M)	Water	-	MIBK/ 2-butanol	180	3 min	65	30	(Román-Leshkov et al., 2006)
36	Fructose (3.6)	H_3PO_4 (10 mol %)	Water	-	MIBK	180[(a)]	3 min	35	25	(Kuster and Van Steen, 1977)
37	Fructose (18)	H_3PO_4 (10 mol %)	Water	-	MIBK	180[(a)]	3 min	43	25	(Kuster and Van Steen,

										1977)
38	Fructose (18)	H_3PO_4 (5 mol %)	Water	-	MIBK	180[(a)]	3 min	31	19	(Kuster and Van Steen, 1977)
39	Fructose (18)	H_3PO_4 (50 mol %)	Water	-	MIBK	180[(a)]	3 min	75	51	(Kuster and Van Steen, 1977)
40	Fructose (18)	H_3PO_4 (10 mol %)	Water	-	MIBK	190[(a)]	5 min	77	55	(Kuster and Van Steen, 1977)
41	Glucose (20)	H_3PO_4 (0.13 M)	Water	-	-	173-187	20 min	N/A	5	(Mednick, 1962)
42	Glucose (20)	Pyridine/H_3PO_4 (0.3 M/0.2 M)	Water	-	-	200-225	8.5 min	N/A	45	(Mednick, 1962)
43	Glucose (1)	H_3PO_4/Nb_2O_5 (1000 wt %)	Water	-	-	120	3 h	92	52	(Nakajima et al., 2011)
44	Fructose (30)	H_3BO_3 (85 mol %)	Water	(0.87 M NaCl)	MIBK/2-butanol	150	45 min	72	50	(Hansen et al., 2011)
45	Fructose (30)	H_3BO_3 (85 mol %)	Water	-	MIBK	150	45 min	43	22	(Hansen et al., 2011)
46	Fructose (30)	H_3BO_3 (171 mol %)	Water	(0.87 M LiCl)	MIBK	150	45 min	53	28	(Hansen et al., 2011)
47	Fructose (30)	H_3BO_3 (85 mol %)	Water	(0.87 M NaCl)	MIBK	150	45 min	69	45	(Hansen et al., 2011)
48	Fructose (30)	H_3BO_3 (85 mol %)	Water	(0.87 M KCl)	MIBK	150	45 min	70	46	(Hansen et al., 2011)
49	Fructose (30)	H_3BO_3 (85 mol %)	Water	(0.87 M $MgCl_2$)	MIBK	150	45 min	67	44	(Hansen et al., 2011)

50	Fructose (30)	H_3BO_3 (85 mol %)	Water	(0.87 M NaCl)	MIBK	150	45 min	81	52	(Hansen et al., 2011)
51	Fructose (30)	H_3BO_3 (85 mol %)	Water	-	THF	150	1.25 h	75	51	(Hansen et al., 2011)
52	Glucose (9)	H_3BO_3 (80 mol %)	DMF	-	-	120	3 h	64	7	(Ståhlberg et al., 2011)
53	Glucose (9)	H_3BO_3 (80 mol %)	DMSO	-	-	120	3 h	35	13	(Ståhlberg et al., 2011)
54	Fructose (0.05 g)	$CrCl_2$ (9 mol %)	[Bmim]Cl (0.5 g)	-	Diethyl ether (Et_2O)	100	6 h	N/A	96	(Yong et al., 2008)
55	Glucose (10)	$CrCl_2$ (0.1 M)	[EMIM]Cl	-	-	100	3 h	86	34	(Liu and Holladay, 2013)
56	Glucose (10)	$CrCl_3$ (6 mol %)	DMA	-	-	100	6 h	N/A	79	(Binder and Raines, 2009)
57	Glucose (38)	$CrCl_2$ (10 mol %)	Choline chloride	-	-	110	30 min	N/A	32	(Ilgen et al., 2009)
58	Glucose (13)	$CrCl_2$ (0.9 wt %)	TEAC	-	-	110	4 h	N/A	39	(Jadhav et al., 2012)
59	Glucose (10)	$CrCl_3.6H_2O$ (6 mol %)	[AMIM]Cl/[EMIM]Cl/[BMIM]Cl	-	-	120	30 min	93	48	(Zhang et al., 2014)
60	Glucose (9)	$CrCl_2$ (6 mol %)	[EMIM]Cl	-	-	100	3 h	94	48	(Zhao et al., 2007)
61	Glucose (3)	$CrCl_2$ (10 mol %)	[EMIM]Cl	-	-	120	3 h	100	41	(Zhang et al., 2011b)
62	Glucose (9)	$CrCl_3.6H_2O$ (6 mol %)	[EMIM]Cl	-	-	100	3 h	97	50	(Zhang et al., 2011b)
63	Glucose (3)	$CrCl_2$ (10 mol %)	P[BVIM]Cl	-	-	120	3 h	100	46	(Liu and Chen, 2013)
64	Glucose (9)	$CrCl_3.6H_2O$ (0.2 wt %)	[OMIM]Cl	-	MIBK	180	10 min	100	50	(Wei et al., 2012)

65	Glucose (9)	$CrCl_3.6H_2O$ (0.2 wt %)	[OMIM]Cl	-	Hexane	180	10 min	100	49	(Wei et al., 2012)
66	Glucose (9)	$CrCl_3.6H_2O$ (10 mol %) + $B(OH)_3$ (20 mol %)	[BMIM]Cl	-	-	120	30 min	N/A	55	(Hu et al., 2012)
67	Glucose (9)	$CrCl_3.6H_2O$ (10 mol %) + $B(OH)_3$ (20 mol %)	TEAC	-	-	120	30 min	N/A	52	(Hu et al., 2012)
68	Glucose (16)	$CrCl_2$ (0.03 M)	TEAC	-	-	120	1 h	N/A	36	(Yuan et al., 2011)
69	Glucose (9)	$CrCl_3.6H_2O$ (25 mol %)	[BMIM]Cl/ [EMIM]Cl	-	-	120	1 h	N/A	47	(Cao et al., 2011)
70	Glucose (0.036 g)	$CrCl_3.6H_2O$ (0.04 M)	[BMIM]Cl (0.3 mL)	-	Toulene	100	4 h	N/A	91	(Lima et al., 2009)
71	Glucose (0.1 g)	$CrCl_3.6H_2O$ (0.006 g)	[BMIM]Cl (0.3 mL)	-	-	100	1 h	N/A	91	(Li et al., 2009)
72	Cellulose (4)	$CrCl_2$ (25 mol %) +HCl (6 mol %)	[EMIM]Cl	-	-	140	1 h	N/A	37	(Binder and Raines, 2009)
73	Glucose (10)	$CrCl_2$ (6 mol %)	DMA	-	-	100	4 h	N/A	76	(Binder and Raines, 2009)
74	Cellulose (4)	$CrCl_2$/HCl (25 and 10 mol %)	DMA	-	-	140	2 h	N/A	22	(Binder and Raines, 2009)
75	Cellulose (4)	$CrCl_3$/HCl (25 and 10 mol %)	DMA	-	-	140	2 h	N/A	33	(Binder and Raines, 2009)
76	Cellulose (0.1 g)	$CrCl_3.6H_2O$ (0.01 g)	[BMIM]Cl (2 g)	-	-	100	2 min	N/A	61	(Li et al., 2009)
77	Cellulose (Avicel) (0.1 g)	$CrCl_3.6H_2O$ (0.01 g)	[BMIM]Cl (2 g)	-	-	100	2 min	N/A	55	(Li et al., 2009)

78	Cellulose (Sigma cell) (0.1 g)	$CrCl_3.6H_2O$ (0.01 g)	[BMIM]Cl (2 g)	-	-	100	2 min	N/A	53	(Li et al., 2009)
79	Cellulose (Spruce) (0.1 g)	$CrCl_3.6H_2O$ (0.01 g)	[BMIM]Cl (2 g)	-	-	100	2 min	N/A	62	(Li et al., 2009)
80	Cellulose (9)	$CuCl_2/CrCl_2$ (6 mol %)	[EMIM]Cl	-	-	120	4 h	N/A	33	(Su et al., 2009)
81	Cellulose (16)	$CrCl_2$ (10 mol %)	[EMIM]Cl	-	-	120	6 h	N/A	69	(Zhang et al., 2010)
82	Fructose (1)	Acetic acid (50 wt %)	Water	-	-	150	2 h	84	34	(de Souza et al., 2012)
83	Fructose (1)	Formic acid (20 wt %)	Water	-	-	150	2 h	100	38	(de Souza et al., 2012)
84	Fructose (1)	Formic acid (2.4 mM)	Subcritical water	-	-	250	32 s	56	16	(Antal et al., 1990)
85	Fructose (1)	Citric acid (pH = 1.5)	Subcritical water	-	-	240	2 min	96	35	(Asghari and Yoshida, 2006a)
86	Fructose (1)	Maleic acid (pH = 1.5)	Subcritical water	-	-	240	2 min	96	28	(Asghari and Yoshida, 2006a)
87	Fructose (1)	Oxalic acid (pH = 1.5)	Subcritical water	-	-	240	2 min	94	13	(Asghari and Yoshida, 2006a)

[a] Heating by microwave irradiation

1.2.1.2 Hydrochloric acid (HCl)

Moderate to higher yields of 5-HMF are also reported from carbohydrates using HCl as a homogeneous catalyst. For example, Kuster and Van Steen (1977) studied the conversion of fructose to 5-HMF in a biphasic system and reported a yield of 5-HMF of 68% and a conversion of 86% at a temperature of 95°C and a time of 1.5 h. A similar yield is reported in the single phase system with ionic liquid ([BMIM]Cl) as a solvent (Li et al., 2010). Yields of more than 60% is reported using the bi-phasic systems such as water-PEG/MIBK (Kuster, 1977), and water-DMSO/MIBK/2-butanol (Chheda et al., 2007), etc. When DMSO or IL is used as a solvent, the required reaction times to achieve higher yields are very short. When, water/subcritic al water is used as a solvent in a single phase process, the yields are less than 20% (Asghari and Yoshida, 2006a; de Souza et al., 2012). However, when water is combined with an extracting phase such as MIBK (Chheda et al., 2007; Román-Leshkov et al., 2006), then the yields of 5-HMF significantly greater than 50% (Brasholz et al., 2011).

1.2.1.3 Boric acid (H_3BO_3) and phosphoric acid (H_3PO_4)

H_3BO_3 has been tested for the production of 5-HMF from fructose and glucose within temperature range of 120 to 150°C, and time range of 45 min to 3 h using various solvents such as water (Hansen et al., 2009), DMSO (Ståhlberg et al., 2011) and dimethylfuran (DMF) (Ståhlberg et al., 2011) (Table 1). Some studies have also been carried out with an extraction phases such as MIBK (Hansen et al., 2009), THF (Hansen et al., 2009), and 2-butanol (Hansen et al., 2009). The highest conversion of 81% and the highest 5-HMF yield of 52% from fructose at 150°C for 45 min are reported (Hansen et al., 2009). However, a very low 5-HMF yield of 13% is reported from glucose at 120°C for 3 h (Ståhlberg et al., 2011).

H_3PO_4 has also been tested as a catalyst for the conversion of carbohydrates (fructose, glucose, and cellulose) to 5-HMF in the temperature range of 120 to 225°C, and time range of 3 min to 3 h using water and subcritical water as solvents and MIBK (Kuster and Van Steen, 1977), as an extraction phase (as shown in Table 1.2). Mednick (1962) used phosphoric acid and pyridine as co-catalysts and reported the 5-HMF yields of 44 and 46% from starch and glucose, respectively. Phosphoric acid (pH = 2) as a catalyst (Asghari and Yoshida, 2006a) reported a 5-HMF yield of 65% at 228°C and 120 s reaction time. Nakajima et al. (2011) reported a 5-HMF

yield of 52% using H_3PO_4/Nb_2O_5 as a catalyst. With H_3PO_4 as a catalyst, a 5-HMF yield of 55% from fructose in a bi-phasic system (water/MIBK) is reported (Kuster, 1977).

1.2.1.4 Chromium chlorides ($CrCl_2/CrCl_3$)

Chromium Chlorides (II & III) have been tested for the conversion of carbohydrates (fructose, glucose, and cellulose) to 5-HMF. The temperature ranges from 100 to 140°C and time ranges from 10 min to 6 h are used as reaction conditions with various solvents such as dimethylacetamide (DMA) (Binder and Raines, 2009) and ILs (such as [OMIM]Cl (Wei et al., 2012), [BMIM]Cl (Hu et al., 2012), [EMIM]Cl (Zhang et al., 2011b), etc). Some studies have also been carried out with the extraction phases such as MIBK (Wei et al., 2012), and hexane (Wei et al., 2012), (Table 1.2). Both monosaccharides (fructose and glucose), polysaccharides (cellulose) are used as the feed stocks. The highest yield of 79% is reported with glucose as the feed stock in the presence of DMA (reaction phase) at 100°C for 6h (Binder and Raines, 2009). Su et al. (2009) reported a 5-HMF yield of 55% from cellulose by using [EMIM]Cl as a reaction media and $CrCl_2/CuCl_2$ as a catalyst. Seri et al. (2002) used lanthanum (III) chloride as Lewis acid to catalyze the degradation of cellulose in water and their highest 5-HMF yield is 19% at 250°C and 150 s. Li et al. (2009) reported a $CrCl_3$-mediated production of 5-HMF (yield 60%) from cellulose in [BMIM]Cl ionic liquid, with 1 min reaction time and microwave irradiation at 400 W.

1.2.1.5 Ionic liquids

Ionic liquids can be used as solvents and/or catalysts in the synthesis of 5-HMF (Petkovic et al., 2011). Mainly, ionic liquids are liquids, and consist of salt ions at ambient temperature (Li et al., 2009) (Dongbin Zhao et al., 2002) or below 100°C (Petkovic et al., 2011). Different ionic liquids (with imidazolium as a base group), whose cations include 3-methylimidazolium ($[OMIM]^+$), 1-butyl-3- methylimidazolium ($[BMIM]^+$), 1-ethyl-3-methylimidazolium ($[EMIM]^+$), etc., have been tested in the 5-HMF production.

The main advantages of ionic liquids are recyclability, stability, low vapor pressure (Tong and Li, 2010). However, ionic liquids also have some drawbacks. Most of the ionic liquids which are tested for reactions having low biodegradability, high explosivity, high toxicity (Petkovic et al., 2011). The other drawback of the ionic liquid is high viscosity. Because of high viscosity,

mass transfer resistance increases in the liquid (Sidhpuria et al., 2011). The low vapor pressure of ionic liquid leads to difficulties in the separation of reactants or products from the solvents, and requires expensive processes such as solvent extraction. The cost of the ionic liquids is the greatest constraint; the cost is two orders of magnitude higher than that of organic solvents (Plechkova and Seddon, 2008). Cheaper ionic liquids, namely, tetraethyl ammonium chloride (Hu et al., 2012; Lima et al., 2009; Yuan et al., 2011) have been investigated for 5-HMF production from glucose and reported 88% yield of 5-HMF at 110°C with a reaction time of 30 min in the presence of [EMIM][SO_4]. Zhao et al. (2007) tested metal halides as catalysts in 1-alkyl-3-methylimidazolium chloride ([EMIM]Cl) as solvent and reasonable yields from fructose (63-83%) and glucose (68-70%) are obtained. Su et al. (2009) reported a 5-HMF yield of 55% from cellulose by using [EMIM]Cl as a reaction media and $CrCl_2$/$CuCl_2$ as a catalyst.

Some other homogeneous catalysts such as oxalic acid, citric acid, maleic acid, formic acid, acetic acid, and lactic acid are also used for the production of 5-HMF from fructose and glucose (as shown in Table 1.2).

1.2.2 Heterogeneous catalysts for carbohydrates conversion to 5-HMF

Table 1.3 gives the comprehensive list of heterogeneous catalysts (other than zeolite based catalysts) used for the conversion of carbohydrates to 5-HMF. The literature on zeolite based catalysts is presented in Table 1.4. The zeolite based catalysts are given separately because the zeolites are the major theme of this thesis. A range of solid acid catalysts has been studied for 5-HMF production. Solid acid catalysts have the advantage of easy separation and recyclability as compared to their liquid acid counter parts. Easy product recovery and adjustment of their surface acidity are some of the other advantages of solid acid catalysts (Tong and Li, 2010).

Table 1.3: Heterogeneous (other than zeolite based) catalysts for the carbohydrates conversion to 5-HMF (Li et al., 2016a; Mukherjee et al., 2015; van Putten et al., 2013; Zakrzewska et al., 2011).

Sl. no.	Feed stock (Conc., Wt %)	Catalyst (concentration)	Reaction conditions					Activity		References
			Reaction phase solvent	Salting out agent	Extraction phase solvent	Temp. (°C)	Time	Conversion (%)	Yield (%)	
Fructose Dehydration to 5-HMF in Aqueous Systems, Catalysed by Heterogeneous Catalysts										
1	Fructose (6)	AlVOP (35 wt %)	Water	-	-	80	2 h	76	58	(Carlini et al., 2004)
2	Fructose (30)	FeVOP (1.8 wt %)	Water	-	-	80	1 h	71	60	(Carlini et al., 2004)
3	Fructose (6)	Cubic ZrP_2O_7 (55 wt %)	Water	-	-	100	2 h	53	43	(Benvenuti et al., 2000)
4	Fructose (6)	γ-TiP (55 wt %)	Water	-	-	100	2 h	57	39	(Benvenuti et al., 2000)
5	Fructose (6)	γ-TiP (55 wt %)	Water	-	MIBK	100	1 h	71	67	(Benvenuti et al., 2000)
6	Fructose (2)	Dowex 50WX8-100 (100 wt %)	Water	-	-	150	30 min	54	33	(Qi et al., 2008a)
7	Fructose (2)	Dowex 50WX8-100 (100 wt %)	Water-acetone	-	-	150	15 min	90	73	(Qi et al., 2008a)
8	Fructose (6)	H_3PO_4-treated niobic Acid (63 wt %)	Water	-	-	100	0.5 h	29	28	(Armaroli et al., 2000)
9	Fructose (6)	H_3PO_4-treated niobic acid (63 wt %)	Water	-	-	100	2 h	91	22	(Armaroli et al., 2000)
10	Fructose (6)	NiP_2O_7 (71 wt %)	Water	-	-	100	0.5 h	29	29	(Armaroli et al., 2000)
11	Fructose (5.4)	Niobium phosphate (3-4 g)	Water	-	-	110	N/A	77	25	(Carniti et al., 2006)

12	Fructose (6)	NiP_2O_7 (59 wt %)	Water	-	-	100	3 h	51	30	(Carlini et al., 1999)
13	Fructose (2)	SO_4^{2-}/ZrO_2 (20 wt %)	Water	-	-	200[(a)]	5 min	59	26	(Qi et al., 2009a)
14	Fructose (2)	SO_4^{2-}/ZrO_2[b] (20 wt %)	Acetone-DMSO	-	-	180[(a)]	5 min	88	62	(Qi et al., 2009a)
15	Fructose (2)	SO_4^{2-}/ZrO_2[c] (20 wt %)	Acetone-DMSO	-	-	180[(a)]	5 min	84	63	(Qi et al., 2009a)
16	Fructose (2)	ZrO_2[b] (20 wt %)	Acetone-DMSO	-	-	180[(a)]	5 min	71	41	(Qi et al., 2009a)
17	Fructose (2)	ZrO_2[c] (20 wt %)	Acetone-DMSO	-	-	180[(a)]	5 min	37	24	(Qi et al., 2009a)
18	Fructose (9)	TiO_2 (100 wt %)	Water	-	-	200	5 min	98	22	(Watanabe et al., 2005)
19	Fructose (9)	ZrO_2 (100 wt %)	Water	-	-	200	5 min	90	15	(Watanabe et al., 2005)
20	Fructose (2)	ZrO_2 (50 wt %)	Water	-	-	200[(a)]	5 min	65	31	(Qi et al., 2008b)
21	Fructose (2)	α-TiO_2 (50 wt %)	Water	-	-	200[(a)]	5 min	84	38	(Qi et al., 2008b)
22	Fructose (1)	ZrP (50 wt %)	Water	-	-	240	2 min	81	49	(Asghari and Yoshida, 2006b)
23	Fructose (2)	$Sc(OTf)_3$ (10 wt %)	DMSO	-	-	120	2 h	100	83	(F. Wang et al., 2011)
24	Fructose (2)	$Sm(OTf)_3$ (10 wt %)	DMSO	-	-	120	2 h	100	73	(F. Wang et al., 2011)
25	Fructose (5)	Sulphated zirconia (2 wt%)	[HexylMIM]Cl	-	-	100	30 min	100	62	(Qi et al., 2011)
26	Fructose (5)	Sulphated zirconia (2 wt%)	[BMIM]Cl	-	-	120	10 min	97.3	60	(Qi et al., 2011)

27	Fructose (10)	Dowex 50WX8-200 ion exchange resin (10 wt %)	[BMIM]Cl	-	-	100	4 h	N/A	42	(Heguaburu et al., 2012)
28	Fructose (10)	1,3-Bis(2,6-diisopropyl-phenyl) imidazoly-lidene/$CrCl_2$ (9 mol %)	[BMIM]Cl	-	-	100	6 h	N/A	67	(Yong et al., 2008)
29	Fructose (8)	Amberlyst-15 (200 wt %)	BMIM+BF_4	DMSO	-	80	32 h	N/A	61	(Lansalot-Matras and Moreau, 2003)
30	Fructose (8)	Amberlyst-15 (200 wt %)	BMIM+PF_6	DMSO	-	80	24 h	N/A	55	(Lansalot-Matras and Moreau, 2003)
31	Fructose (5)	Amberlyst-15 (100 wt %)	[BMIM]Cl	-	-	80	10 min	99.6	58	(Qi et al., 2009b)
32	Fructose (20)	SBA-15-SO_3H (5 wt %)	[BMIM]Cl	-	-	120	1 h	100	57	(Guo et al., 2012)
33	Fructose (9)	P_2O_5 (50 mol %)	[BMIM]Cl	-	-	50	1 h	N/A	57	(Ray et al., 2011)
34	Fructose (6)	D001-cc ion exchange resin (6 wt %)	[BMIM]Cl	-	-	75	20 min	100	65	(Li et al., 2013)
35	Fructose (9)	Cellulose-derived catalyst (40 wt %)	[BMIM]Cl	-	-	160	15 min	N/A	57	(Hu et al., 2013)
36	Fructose (9)	Sn[$(O_3PCH_2)_2$ NCH_2 CO_2H] (25% of substrate)	[EMIM]Br	-	-	100	1.5 h	98	61	(Ning et al., 2013)
37	Fructose (9)	Zr[$(O_3PCH_2)_2$ NCH_2 CO_2H] (25% of substrate)	[EMIM]Br	-	-	100	1.5 h	N/A	55	(Ning et al., 2013)

38	Fructose (1)	-	Choline chloride citric acid monohydrate	Ethyl acetate	-	80	1 h	97.6	64	(Hu et al., 2008)
39	Fructose (38)	pTsOH (4 wt %)	Choline chloride	-	-	100	30 min	N/A	47	(Ilgen et al., 2009)
40	Fructose (7)	Glucose-TsOH (5.6 wt %)	NMP	-	-	130	1.5 h	97.9	60	(J. Wang et al., 2011)
	Fructose (7)	Glucose-TsOH (5.6 wt %)	DMSO	-	-	130	1.5 h	99.9	64	(J. Wang et al., 2011)
41	Fructose (4)	HCl (1 M); ROX 0.8 activated carbon (220 wt %)	Water	-	-	90	7 h	79	29	(Vinke and van Bekkum, 1992)
42	Fructose (4)	OC 1052 ion exchange resin (440 wt %); ROX 0.8 activated carbon (220 wt %)	Water	-	-	90	48 h	83	39	(Vinke and van Bekkum, 1992)
43	Fructose (10)	DOWEX 50WX8-100 cation exchange resin (4 wt %)	Acetone-DMSO	-	-	150	20 min	99	58	(Qi et al., 2008c)
44	Fructose (2)	Dowex 50WX8-100 (100 wt %)	Acetone-DMSO	-	-	150[(a)]	20 min	98	88	(Qi et al., 2008c)
45	Fructose (20)	Lewatitt SPC 118 ion exchange resin (0.61×10^{-3} (meq.H^+ /mol)	Water	-	MIBK	88	15 h	85	39	(Rlgal et al., 1981)
46	Fructose (20)	Spherosil S ion exchange resin (0.125×10^{-3} (meq.H^+ /mol)	Water	-	MIBK	88	15 h	100	34	(Rlgal et al., 1981)
47	Fructose (10)	Ion exchange resin (10 wt %)	Water-DMSO- PVP	-	MIBK/2-butanol	90	8-16 h	76	41	(Román-Leshkov et al., 2006)

48	Fructose (30)	Niobium phosphate (30 wt %)	Water-	-	MIBK	180	2 h	62	32	(Román-Leshkov et al., 2006)
49	Fructose (1)	Niobic acid (5 wt %)	Water	-	-	180	2 h	92	13	(de Souza et al., 2012)
50	Fructose (1)	TiO_2 (0.5 wt %)	THF	-	-	150	3 h	99	38	(Kuo et al., 2014)
51	Fructose (2)	Amberlyst-70 (3.3 wt %)	GVL-Water	-	-	130	9 min	89	50	(Gallo et al., 2013)
52	Fructose (2)	Amberlyst-70 (3.3 wt %)	GVL- Water	-	-	130	10 min	91	52	(Gallo et al., 2013)
53	Fructose (2)	Amberlyst-70 (3.3 wt %)	Water	-	THF	130	10 min	91	54	(Gallo et al., 2013)
54	Fructose (10)	Silicoalumino-phosphate (SAPO)-44 (2.9 wt %)	Water	-	MIBK	175	1 h	89	55	(Bhaumik and Dhepe, 2013)
55	Fructose (9)	$Ag_3PW_{12}O_{40}$ (0.3 wt %)	Water	-	MIBK	120	1 h	83	54	(Fan et al., 2011)
	Fructose (9)	$H_3PW_{12}O_{40}$ (0.27 wt %)	Water	-	MIBK	120	1 h	86	31	(Fan et al., 2011)
56	Fructose (0.5)	$H_3PW_{12}O_{40}$ (50 wt %)	DMSO	-	-	120	2 h	97.9	68	(Qu et al., 2012)
57	Fructose (0.5)	$[MIMPS]_3PW_{12}O_{40}$ (50 wt %)	Sec-Butanol	-	-	120	2 h	99.7	69	(Qu et al., 2012)
58	Fructose (8)	Supported-1-(tri-ethoxy silyl-propyl)-3-methyl-imidazolium hydrogen sulphate (6 wt %)	DMSO	-	-	130	30 min	99.9	44	(Sidhpuria et al., 2011)
59	Fructose (8)	Si-3-IL $-HSO_4$ (80 wt %)	DMSO	-	-	130	30 min	100	63	(Sidhpuria et al., 2011)
60	Fructose (5)	TiO_2 (50 wt %)	DMA	-	-	130[(a)]	2 min	N/A	74	(De et al., 2011)

61	Fructose (4)	TiO_2 (50 wt %)	DMA-[BMIm]Cl	-	-	130[(a)]	2 min	N/A	82	(De et al., 2011)
62	Fructose (3)	Amberlyst 15 (100 wt %)	DMF	-	-	100	1 h	100	90	(Ohara et al., 2010)
63	Fructose (3)	Amberlyst 15 (6 wt %)	DMSO	-	-	120	2 h	100	92[(d)]	(Shimizu et al., 2009)
64	Fructose (3)	Amberlyst 15 (6 wt %)	DMSO	-	-	120	2 h	100	76	(Shimizu et al., 2009)
65	Fructose (3)	Amberlyst 15 (6 wt %)	DMSO	-	-	120	2 h	100	100[(d)]	(Shimizu et al., 2009)
66	Fructose (3)	Amberlyst 15 (6 wt %)	DMSO	-	-	120	2 h	100	100	(Shimizu et al., 2009)
67	Fructose (50)	Amberlyst 15 (6 wt %)	DMSO	-	-	120	2 h	100	100[(d)]	(Shimizu et al., 2009)
68	Fructose (3)	$Cs_{2.5}H_{0.5}PW_{12}O_{40}$ (6 wt %)	DMSO	-	-	120	2 h	100	91[(d)]	(Shimizu et al., 2009)
69	Fructose (3)	$FePW_{12}O_{40}$ (6 wt %)	DMSO	-	-	120	2 h	100	97[(d)]	(Shimizu et al., 2009)
70	Fructose (3)	$FePW_{12}O_{40}$ (6 wt %)	DMSO	-	-	120	2 h	100	49[(d)]	(Shimizu et al., 2009)
71	Fructose (50)	$FePW_{12}O_{40}$ (6 wt %)	DMSO	-	-	120	2 h	N/A	48[(d)]	(Shimizu et al., 2009)
72	Fructose (3)	$H_3PW_{12}O_{40}$ (6 wt %)	DMSO	-	-	120	2 h	100	95[(d)]	(Shimizu et al., 2009)
73	Fructose (3)	Nafion (6 wt %)	DMSO	-	-	120	2 h	100	94[(d)]	(Shimizu et al., 2009)
74	Fructose (3)	Nafion (6 wt %)	DMSO	-	-	120	2 h	100	75	(Shimizu et al., 2009)
75	Fructose (3)	SO_4^{2-}/ZrO_2 (6 wt %)	DMSO	-	-	120	2 h	100	92[(d)]	(Shimizu et al., 2009)
76	Fructose (3)	WO_3/ZrO_2 (6 wt %)	DMSO	-	-	120	2 h	100	94[(d)]	(Shimizu et al., 2009)

77	Fructose (8)	Diaion PK-216 (10 mequiv)	DMSO	-	-	80	8.33 h	N/A	90	("Nakumara et al., 1980.pdf," n.d.)
78	Fructose (3)	ILIS $-SO_2Cl$ (50 mol %)	DMSO	-	-	100[(a)]	4 min	100	67	(Bao et al., 2008)
79	Fructose (3)	ILIS $-SO_3H$ (50 mol %)	DMSO	-	-	100[(a)]	4 min	100	70	(Bao et al., 2008)
80	Fructose (3)	SiO_2 $-SO_2Cl$ (50 mol %)	DMSO	-	-	100[(a)]	4 min	92	60	(Bao et al., 2008)
81	Fructose (3)	SiO_2 $-SO_3H$ (50 mol %)	DMSO	-	-	100[(a)]	4 min	95	63	(Bao et al., 2008)
82	Fructose (9)	PTA/MIL-101 (40 wt %)	DMSO	-	-	130	30 min	82	63	(Zhang et al., 2011a)
83	Fructose (7.6)	SO_4^{2-}/ZrO_2 - Al_2O_3 (20 wt %)	DMSO	-	-	130	4 h	99	57	(Yan et al., 2009)
84	Fructose (4)	TiO_2 (50 wt %)	DMSO	-	-	140[(a)]	10 min	N/A	54	(Dutta et al., 2011)
Glucose Dehydration to 5-HMF										
85	Glucose (10)	Dowex 50WX8-200 ion exchange resin (10 wt %)	[BMIM]Cl	-	-	100	4 h	N/A	49	(Heguaburu et al., 2012)
86	Glucose (10)	Amberlyst 15 ion exchange resin (10 wt %)	[BMIM]Cl	-	-	100	6 h	N/A	43	(Heguaburu et al., 2012)
87	Glucose (9)	Cellulose-derived carbonaceous catalyst (40 wt %)	[BMIM]Cl	-	-	160	15 min	77.8	33	(Hu et al., 2013)
88	Glucose (1)	NbOH (1 wt %)	Water	-	-	150	2 h	78	20	(de Souza et al., 2012)
89	Glucose (2)	Amberlyst-70 (3.3 wt %); Sn-Beta (3.3 wt %)	Water	-	GVL	130	20 min	92	41	(Gallo et al., 2013)

90	Glucose (2)	Amberlyst-70 (3.3 wt %); Sn-Beta (3.3 wt %)	Water	-	GVL	130	10 min	93	38	(Gallo et al., 2013)
91	Glucose (2)	Amberlyst-70 (3.3 wt %); Sn-Beta (3.3 wt %)	Water	-	THF	130	10 min	90	44	(Gallo et al., 2013)
92	Glucose (10)	Silicoalumino phosphate (SAPO)-44 (2.9 wt %)	Water	-	MIBK	175	4 h	83	47	(Bhaumik and Dhepe, 2013)
93	Glucose (9)	$Ag_3PW_{12}O_{40}$ (1.2 wt %)	Water	-	MIBK	130	4 h	89	53	(Fan et al., 2011)
94	Glucose (3)	Hydrotalcite/Amberlyst 15 (300 wt %)	DMA	-	-	100	3 h	97	14	(Ohara et al., 2010)
95	Glucose (3)	Hydrotalcite/Amberlyst 15 (300 wt %)	DMF	-	-	80	9 h	73	42	(Ohara et al., 2010)
96	Glucose (3)	Hydrotalcite/Amberlyst 15 (300 wt %)	DMF	-	-	100	3 h	72	41	(Ohara et al., 2010)
97	Glucose (3)	hydrotalcite/Amberlyst 15 (300 wt %)	DMF	-	-	100	4.5 h	61	45	(Ohara et al., 2010)
98	Glucose (3)	Hydrotalcite/Amberlyst 15 (300 wt %)	DMF+ Water	-	-	100	3 h	45	29	(Ohara et al., 2010)
99	Glucose (3)	Hydrotalcite/Amberlyst 15 (300 wt %)	DMSO	-	-	80	3 h	41	25	(Ohara et al., 2010)
100	Glucose (3)	Hydrotalcite/Amberlyst 15 (300 wt %)	DMSO	-	-	100	3 h	94	12	(Ohara et al., 2010)

101	Glucose (3)	Hydrotalcite/Amberlyst 15 (300 wt %)	MeCN	-	-	100	3 h	88	10	(Ohara et al., 2010)
102	Glucose (3)	Hydrotalcite/Amberlyst 15 (300 wt %)	MeCN-Water	-	-	100	3 h	91	28	(Ohara et al., 2010)
103	Glucose (7.6)	SO_4^{2-}/ZrO_2 - Al_2O_3 (20 wt %)	DMSO	-	-	130	4 h	97	48	(Yan et al., 2009)
104	Glucose (7.6)	SO_4^{2-}/ZrO_2 - Al_2O_3 (20 wt %)	DMSO	-	-	130	6 h	100	48	(Yan et al., 2009)
105	Glucose (7.6)	SO_4^{2-}/ZrO_2 - Al_2O_3 (20 wt %)	DMSO	-	-	130	15 h	100	48	(Yan et al., 2009)
106	Glucose (7.6)	CSZA-3 (1.8 wt %)	DMSO	-	-	130	6 h	100	34	(Yan et al., 2009)
107	Glucose (3.5)	SO_4^{2-}/ZrO_2 - Al_2O_3 (19 wt %)	DMSO-Water	-	-	150	4 h	N/A	56	(Yang et al., 2012)
108	Glucose (2.5)	ZrO_2 (1 wt %)	[HexylMIM][Cl]	Water	-	200	10 min	92	37	(Qi et al., 2012)
109	Glucose (16)	$AlEt_3$ (10 mol %)	[EMIM]Cl	-	-	120	6 h	100	36	(Liu and Chen, 2013)
110	Glucose (16)	$MeAl(BHT)_2$ (10 mol %)	[EMIM]Cl	-	-	120	6 h	100	35	(Liu and Chen, 2013)
111	Glucose (5)	Sn-Mont (3.3 wt %)	DMSO	-	THF	160	3 h	98.4	37	(J. Wang et al., 2012)
112	Glucose (9)	α-$Sr(PO_3)_2$ (10 Wt %)	Water	-	-	220	5 min	61	15	(Daorattanachai et al., 2012)
Dehydration of cellulose to 5-HMF										
113	Cellulose (9)	Cellulose-derived Carbonaceous catalyst (40 wt %)	[BMIM]Cl	-	-	160	15 min	N/A	32	(Hu et al., 2013)
114	Cellulose (5)	Sn-Mont (3 wt %)	Water	-	THF	160	3 h	N/A	30	(J. Wang et al., 2012)

115	Cellulose (9)	α-$Sr(PO_3)_2$ (10 wt %)	Water	-	-	230	5 min	N/A	12	(Daorattanachai et al., 2012)
116	Cellulose (5)	$Cr[(DS)H_2PW_{12}O_{40}]_3$ (15 mM)	Water	-	-	150	2 h	77	53	(Zhao et al., 2011)
117	Cellulose (5)	$Cr[H_2PW_{12}O_{40}]_3$ (15 mM)	Water	-	-	150	2 h	57	36	(Zhao et al., 2011)
118	Cellulose (5)	$H_2PW_{12}O_{40}$ (15 mM)	Water	-	-	150	2 h	33	0	(Zhao et al., 2011)
119	Cellulose (9)	ZrO_2 (100 wt %)	Water	-	-	250	5 min	34	13	(Chareonlimkun et al., 2010)
120	Cellulose (9)	TiO_2 (100 wt %)	Water	-	-	250	5 min	25	8.3	(Chareonlimkun et al., 2010)
121	Cellulose (4)	Zirconium phosphate (4 wt %)	Water	-	-	220	15 min	36	10	(Weingarten et al., 2012)
122	Cellulose (2)	$NaHSO_4$ (1.8 $mmol.g^{-1}$) + $ZnSO_4$ (2.8 $mmol.g^{-1}$)	Water	-	THF	160	1 h	96	41	(Shi et al., 2013)

[a] Heating by microwave irradiation
[b] Calcination at 500°C
[c] Calcination at 700°C
[d] Continuous flow process

Table 1.4: Zeolite based catalysts for the carbohydrates conversion to 5-HMF (Li et al., 2016a; Mukherjee et al., 2015; van Putten et al., 2013; Zakrzewska et al., 2011).

Sl. no.	Feed stock (Conc., Wt %)	Catalyst (concentration)	Reaction conditions					Activity		References
			Reaction phase solvent	Salting out agent	Extraction phase solvent	Temp. (°C)	Time	Conversion (%)	Yield (%)	
Fructose Dehydration to 5-HMF										
1	Fructose (2)	LZY zeolite (Na_{56} $(AlO_2)_{56}$ $(SiO_2)_{136}$) (100 wt%)	Water	-	-	140	2 h	70.3	1.2	(Jow et al., 1987)
2	Fructose (10)	H-mordenites (11) (29 wt %)	Water	-	-	165	-	93	73	(Moreau et al., 1996)
3	Fructose (3)	H-beta(12.5) (6.7 wt %)	DMSO	-	-	120	2 h	100	97	(Shimizu et al., 2009)
4	Fructose (3)	H-Y(2.4) (6.7 wt %)	DMSO	-	-	120	2 h	100	76	(Shimizu et al., 2009)
5	Fructose (3)	Amberlyst-15-P	DMSO	-	-	120	2 h	100	100	(Shimizu et al., 2009)
6	Fructose (3)	H-BEA zeolite (6 wt %)	DMSO	-	-	120	2 h	100	51	(Shimizu et al., 2009)
7	Fructose (50)	H-BEA zeolite (6 wt %)	DMSO	-	-	120	2 h	N/A	40[(a)]	(Shimizu et al., 2009)
8	Fructose (40)	H-mordenites (12) (20 wt %)	Water	-	-	135	-	10	6	(Ordomsky et al., 2012)
9	Fructose (6.7)	H-mordenites (12) (20 wt %)	Water	-	MIBK	165	2.5 h	30	26	(Ordomsky et al., 2012)
10	Fructose (3.5)	SiO_2/H-MOR (0.7 wt %)	Water	-	MIBK	165	5 h	75	33	(Ordomsky et al., 2012)
11	Fructose (3)	H-Beta (15) (50 wt %)	Water	-	MIBK	165	1 h	85	34	(Rivalier et al., 1995)

12	Fructose (3)	H-ZSM5 (50 wt%)	Water	-	MIBK	165	1 h	90	53	(Rivalier et al., 1995)
13	Fructose (3)	HY (10) (50 wt%)	Water	-	MIBK	165	1 h	74	41	(Rivalier et al., 1995)
14	Fructose (3)	H-mordenites (11) (50 wt%)	Water	-	MIBK	165	1 h	76	69	(Rivalier et al., 1995)
15	Fructose (2.7)	H-Beta (25) (8 wt%)	DMSO	-	-	120	2 h	72	55	(Shi et al., 2011)
16	Fructose (2.7)	H-ZSM5 (70) (8 wt%)	DMSO	-	-	120	2 h	80	65	(Shi et al., 2011)
17	Fructose (1.2)	BP2000/H-Beta (100 wt%)	Water	-	-	150	4 h	80	40	(Dornath and Fan, 2014)
18	Fructose (8.3)	KCC-1 silica (20 wt%)	DMSO	-	-	162	0.5 h	99.1	67.7	(Najafi Chermahini et al., 2016)
19	Fructose (3.6)	KIT-6 mesoporous silica (27.8 wt%)	DMSO	-	-	165	0.5 h	100	84.1	(Hafizi et al., 2016)
18	Fructose (30)	TESAS-SBA-15 (5.6 wt%)	Water	-	MIBK/2-butanol	130	141 min	84	60	(Crisci et al., 2011)
19	Fructose (2)	SBA-15-SO 3 H (packed-bed reactor)	Water	-	THF	130	-	80	50	(Tucker et al., 2012)
20	Fructose (10)	Mesoporous SBA-15-SO_3H (10 wt%)	[BMIM]Cl	-	-	120	1 h	100	81	(Guo et al., 2012)
21	Fructose (6)	SO_4 /TiO_2 -SiO_2 (21 wt%)	DMSO	-	-	110	1.5 h	77	69	(Kılıç and Yılmaz, 2015)
22	Fructose (5)	H-ZSM5 (2.5 wt %)	DMSO	-	-	110	N/A	N/A	46	(Jadhav et al., 2012)
23	Fructose (0.5)	Beta-Cal500 (0.002 wt %)	Water+DMSO	-	THF	180	3 h	96	47	(Otomo et al., 2014)
24	Fructose (8)	Zeolite H-beta (Si/Al = 25) (80 wt %)	DMSO	-	-	130	30 min	100	63	(Sidhpuria et al., 2011)

Glucose Dehydration to 5-HMF										
25	Glucose (5)	H-ZSM-5 (10 wt %)	[BMIM]Cl	--	-	110	8 h	N/A	32	(Jadhav et al., 2012)
26	Glucose (2)	Dealuminated H-Beta (15) (83 wt%)	Water+DMSO	-	THF	180	3 h	78	43	(Otomo et al., 2014)
27	Glucose (2.5)	H-Beta (Si/Al: 15)-750 (83 wt%)	Water +DMSO	-	THF	180	3 h	78	55	(Otomo et al., 2014)
28	Glucose (0.5)	Beta-Cal750 (0.4 wt %)	Water+DMSO		THF	180	3 h	78	30	(Otomo et al., 2014)
29	Glucose (10)	Sn-beta + HCl (0.5 mol%)	Water	NaCl	THF	180	70 min	79	57	(Nikolla et al., 2011)
30	Glucose (10)	Sn-Beta (0.5 mol%)	Water	NaCl	1-Butanol	160	1.5 h	75	14	(Nikolla et al., 2011)
31	Glucose (2)	Sn-Beta (3.3 wt%) +Amberlyst-70 (3.3 wt%)	Water	-	GVL	130	20 min	92	59	(Gallo et al., 2013)
32	Glucose (2)	Sn-Beta (3.3 wt%) +Amberlyst-70 (3.3 wt%)	Water	-	GHL	130	20 min	90	55	(Gallo et al., 2013)
33	Glucose (2)	Sn-Beta (3.3 wt%) +Amberlyst-70 (3.3 wt%)	Water	-	THF	130	30 min	90	63	(Gallo et al., 2013)
34	Glucose (2)	Sn-Beta (3.3 wt%) +Amberlyst-70 (3.3 wt%)	Water	-	THF+MTHF	130	40 min	90	60	(Gallo et al., 2013)
35	Glucose (10)	H-Y (5) (40 wt%)	[BMIM]Cl	-	-	140	0.5 h	24.6	11.8	(Hu et al., 2014)
36	Glucose (10)	H-mordenite (15) (40 wt%)	[BMIM]Cl	-	-	140	0.5 h	27.2	13.1	(Hu et al., 2014)
37	Glucose (10)	H-Beta (25) (40 wt%)	[BMIM]Cl	-	-	140	0.5 h	48.1	23.7	(Hu et al., 2014)
38	Glucose (10)	H-ZSM-5 (25) (40 wt%)	[BMIM]Cl	-	-	140	0.5 h	31.3	14.2	(Hu et al., 2014)
39	Glucose (10)	H-ZSM-5 (50) (40 wt%)	[BMIM]Cl	-	-	140	0.5 h	35.4	16.4	(Hu et al., 2014)

40	Glucose (10)	H-ZSM-5 (100) (40 wt%)	[BMIM]Cl	-	-	140	0.5 h	42.7	20.5	(Hu et al., 2014)
41	Glucose (10)	H-ZSM-5 (300) (40 wt%)	[BMIM]Cl	-	-	140	0.5 h	14.5	8.3	(Hu et al., 2014)
42	Glucose (10)	H-Beta (25) (40 wt%)	[BMIM]Cl	-	-	150	50 min	80.6	50.3	(Hu et al., 2014)
43	Glucose (1)	Al-MCM-41 (30 wt%)	Water	NaCl	MIBK	195	0.5 h	98	63	(Jiménez-Morales et al., 2015)
44	Glucose (1)	Al-MCM-41 (30 wt%)	Water	-	MIBK	195	2.5 h	87	36	(Jiménez-Morales et al., 2015)
45	Glucose (10)	Zr-MCM-41 (33 wt%)	Water	-	MIBK	175	2.5 h	82	23	(Jiménez-Morales et al., 2014)
46	Glucose (10)	Sn-MCM-41 (100 wt%)	[EMIM]Br	-	--	110	4 h	98	70	(Xu et al., 2014)
47	Glucose (5)	Sn-Mont	DMSO	-	THF	160	3 h	98	54	(J. Wang et al., 2012)
Cellulose conversion to 5-HMF										
48	Cellulose (5)	Sn-Mont	Water	NaCl	THF	160	3 h	N/A	39	(J. Wang et al., 2012)
49	Cellulose (6.7)	H-Y (2.5) (100 wt%)	[BMIM]Cl	$CrCl_2$ (12.5 wt%)	-	120	6 h	-	47.5	(Tan et al., 2011)
50	Cellulose (6)	Zeolite (100 wt %) + $CrCl_2$ (3 wt %)	[BMIM]Cl	-		120	6 h	N/A	37	(Tan et al., 2011)
51	Cellulose (10)	H-Y (2.5) (20 wt%)	[EMIM]Cl	LiCl (6 mol%)	-	160	0.5 h	-	70.3	(Abou-Yousef and Hassan, 2014)
52	Cellulose (2.5)	Desilicated H-ZSM-5 (30) (200 wt%)	Water	-	-	190	4 h	67	46	(Nandiwale et al., 2014)

53	Cellulose (2.4)	Dealuminated H-Beta (15) (83 wt%)	Water+DMSO	-	THF	200	5 h	100	42	(Otomo et al., 2015)

[a] Continuous flow process

Many solid catalysts are highly selective in 5-HMF production, but the substrate conversion of feedstocks is very low. The common examples are Amberlyst 15 (Shimizu et al., 2009), sulfonated resins (Daorattanachai et al., 2012), sulfonated carbon (Guo et al., 2012), sulfonic acid functionalized silica ((Amarasekara et al., 2008), 2012), WO_3/ZrO_2 (Chareonlimkun et al., 2010), ionic liquids (Hu et al., 2008), zirconium phosphate ((Asghari and Yoshida, 2006a), hierarchical H-USY zeolites (Otomo et al., 2015), niobium catalysts (Yan et al., 2009), (Carlini et al., 1999), SO_4^{2-}/Ti-MCM-41 (Guo et al., 2012; Xu et al., 2014), and dihydric phosphates with the aid of hot compressed steam (Shi et al., 2013), titanium and niobium based catalysts (Benvenuti et al., 2000), and lanthanide catalysts (Seri et al., 2002). Li et al. (2018) studied sulfonated poly (phenylene sulfide) (SPPS) catalysts for the conversion of cellulose and glucose to 5-HMF in ionic liquids and reported a 5-HMF yield of 87.2% at 140°C with glucose and the 5-HMF yield of 68.2% at 180°C with cellulose after 4 h reaction. The authors noticed that the activity of the catalyst significantly changes with the degree of sulfonation. The DFT calculation results indicated that the SO_3H group of SPPS plays a crucial role in glucose conversion into 5-HMF. The authors further emphasized that the anions and cations of ILs in combination with SO_3H-SPPS helped in stabilizing the reaction intermediates and transition states.

Beltramini's research group studied the TiO_2 based catalysts (Atanda et al., 2016, 2015b, 2015a, 2015c) and reported reasonable yields with P/TiO_2 catalysts. They reported a 5-HMF yield of 81% at a glucose conversion of 97% over P/TiO_2 catalysts at 175^{o}C and 3 h (Atanda et al., 2015a). They also identified that the biphasic system (water+THF) containing N-methyl-2-pyrrolidone is helpful in enhancing the catalytic activity of P/TiO_2 catalysts. The authors also reported a 5-HMF yield of 87% from cellulose using mechano-catalytic depolymerization (Atanda et al., 2015b).

1.2.2.1 Zeolite based catalysts

Fructose to 5-HMF: Shimizu et al. (2009) studied various solid acid catalysts ($FePW_{12}O_{40,}$ H-Beta, H-ZSM5, HY, H-Mordenite, etc.) for the conversion of fructose to 5-HMF in DMSO (solvent) as a reaction media at 120°C for 2 h in two different routes. One is by evaporation water at mild conditions to suppress the side products such as LA and FA. Another one is, by reducing the size of the catalysts particle. Among different catalysts, they reported a 5-HMF yield of 97% with H-Beta, 76% with H-Y, and 100% with Amberlyst-15-P. Authors observed that crushed and sieved Amberlyst-15-P with size 0.15 – 0.053 mm

showed the highest yield of 5-HMF. The enhanced yield is due to the improved removal of adsorbed water on the smaller particles.

Rivalier et al. (1995) studied with different zeolites catalysts (HBeta, HY, HZSM5, and HMOR) for the production of 5-HMF from fructose in a biphasic system (water/MIBK) at 165°C for 30 min and 60 min. They reported a 5-HMF yield of 34, 53, 41 and 69% over HBeta, HY, HZSM5, and HMOR, respectively, during a 60 min reaction.

Chermahini et al. (2016) synthesized KCC-1 silica nanospheres, functionalized with propylsulfonic acid groups, and tested for fructose to 5-HMF conversion with various solvents (DMSO, NMP, DMAc, DMF, and ethylene glycol). They reported the highest yield of 66.7% with DMSO at 162°C for 30 min. The same research group (Hafiz et al. (2016)) tested sulfonic acid functionalized KIT-6 mesoporous silica under similar reaction conditions and reported a 5-HMF yield of 84.1%. The catalyst activity is reported to be constant in five recycles.

Guo et al. (2012) tested propylsulfonic acid functionalized SBA-15 for the conversion of fructose to 5-HMF in [BMIM]Cl and reported a 5-HMF yield of 81% at 120°C for 1 h. Post-reaction separation of 5-HMF from reaction mixture by using THF as an extracting solvent resulted in 93% recovery of the formed 5-HMF.

Glucose to 5-HMF: Nikolla e al. (2011) studied Sn-Beta with HCl (pH = 1) for the conversion of various carbohydrates (glucose, cellobiose, starch) to 5-HMF in a biphasic system (water/THF) along with salting-out agent (NaCl). The authors reported a 5-HMF yield of 57, 36, and 52% from glucose, cellobiose, and starch, respectively, at 180°C for 70 min. They also reported a 5-HMF yield of 41% from glucose at 160°C for 90 min with a biphasic (water/1-butanol+NaCl) system.

Gallo et al. (2013) studied a combination of Sn-Beta and Amberlyst-70 for the conversion of glucose to 5-HMF with various biphasic systems. They reported the yields of 5-HMF were 59, 55, 63, and 60% using various biphasic systems namely, water/GVL, water/GHL, water/THF, water/THF + MTHF, respectively. Authors also noticed that the separation and purification of 5-HMF could be possible by distillation in the case of THF. To facilitate the separation from GHL and GVL solvent (which have boiling points similar to 5-HMF), the HMF is converted to DMF (with a yield of 46%). This low boiling product is separated by distillation.

Hu et al. (2014) studied with various zeolites catalysts (H-Beta, HY, H-ZSM5, and H-Mordenite) for the conversion of glucose to 5-HMF in the presence of [BMIM]Cl and reported a 5-HMF yield of < 24% in all cases at 140°C for 0.5 h. At temperature of 150°C for

50 min. the 5-HMF yield increases to 50.3% with H-Beta. Authors also noticed that H-Beta zeolite showed the synergistic catalytic mechanism involving both Brønsted and Lewis acid sites. They also claimed that the combination of H-Beta (Si/Al = 25) and ionic liquid ([BMIM]Cl) is an excellent reaction media for the production of 5-HMF from carbohydrates (fructose, sucrose, maltose, cellobiose, starch, and cellulose). Several speculations have been presented: i) the anionic part (Cl^-) of IL, with moderate nucleophilicity and basicity could influence glucose-fructose isomerization reactions; ii) the release of H^+ from the pores of the H-Beta zeolite is possibly promoted by the ion-exchange with $[BMIM]^+$, so as to enable the contact of fructose with the Bronsted acid sites; iii) the cationic part of IL ($[BMIM]^+$) stabilizes 5-HMF and thus reduces it's further decomposition.

Otomo et al. (2014) used steam-treated (dealuminated) H-Beta calcined at different temperatures to study the effect of these pretreatments on the direct conversion of glucose to 5-HMF. The pretreated catalysts are tested in a biphasic system (water+DMSO/THF) at 180°C for 3 h. They reported a 5-HMF yield of 55% with H-Beta and 43% with dealuminated H-beta at the same conversion of 78%. During the pretreatment, a part of Si-O-Al bonds in the framework are cleaved to form Al species in the extra-framework (Lewis acid sites) and thus resulted in the bifunctionality of the Beta zeolite. With the help of an isotopic labeling study in combination with a ^{13}C NMR analysis, the authors predicted that the glucose molecule is isomerized to fructose through an intramolecular hydride transfer.

Xu et al. (2014) tested the Sn-MCM-41 for the conversion of glucose and fructose to 5-HMF in the presence of [EMIM]Br and reported a 5-HMF yield of 70 and 80%, respectively, at 110°C for 4 h. The yield and conversion are significantly enhanced in the presence of [EMIM]Br as a solvent as compared to those in the presence of DMSO or water as solvents. Authors noticed that [EMIM]Br was not only promoting the isomerization of glucose but also for stabilizing the 5-HMF in the reaction media.

Wang et al. (2012) utilized Sn-Mont (ion-exchanged from Ca-Mont) as a catalyst for the conversion of glucose and fructose to 5-HMF in various solvents (water, DMF, THF, DMA, NMP, and DMSO) at 160°C for 3 h. They reported the highest yield of 5-HMF of 54% and 78% from glucose and fructose, respectively, with THM/DMSO (70:30, v/v ratio). The authors also reported a 5-HMF yield of 39% from cellulose with THF/H_2O-NaCl biphasic system. Good reusability of the catalyst is reported.

Jiménez-Morales et al. (2014) explored various zirconium-doped MCM-41 catalysts for the production of 5-HMF from glucose in a biphasic system (water/MIBK) and reported a 5-HMF yield of 23% at 175°C for 2.5 h over ZrO_2/MCM-41 catalyst that is activated at

550°C. Authors noticed that zirconia is highly dispersed on the surface of MCM-41 and ZrO_2/MCM-41 and the catalysts are highly stable. However, the sulfated MCM-41 catalysts are reported to be unstable in the aqueous phase, because of the sulfate leaching. The same group (Jiménez-Morales et al., (2015)) studied aluminum doped MCM-41 for the production of 5-HMF from glucose in a biphasic system (water/MIBK) with and without salting-out agent (NaCl). They reported a 5-HMF yield of 63% at 195°C for 0.5 h with NaCl and 36% at 195°C for 2.5 h without NaCl. The authors emphasized that the catalyst Al-MCM-41 is highly selective in 5-HMF production with neither LA nor furfural formation.

Cellulose to 5-HMF: Abou-Yousef and Hassan (2014) studied H-form zeolites (H-Y) for the direct conversion of cellulose to 5-HMF in [EMIM]Cl with various salting out agents (LiCl, NaCl, KCl). The authors reported the highest yield of HMF (70%) over zeolite/LiCl system at 160°C for 30 min. Tan et al. (2011) used $CrCl_2$/Zeolite/[BMIM]Cl catalyst system for the conversion of cellulose to 5-HMF and reported a maximum yield of 48% at 120°C with two-time extraction for 6 h each. Nandiwale et al. (2014) tested Bimodal (mesoporous + microporous) HZSM5 for the direct conversion of cellulose to 5-HMF in the presence of water and reported a 5-HMF yield of 46% at 190°C for 4 h. Overall, the 5-HMF yields from cellulose substrate are found to be less than 50% when heterogeneous catalysts are used. Therefore, highly effective catalysts need to be developed for this reaction which can give higher yields so as to make this process economically feasible.

Combination of the ionic liquids (as a solvent/catalyst) and zeolites showed interesting results with higher yields of 5-HMF from glucose. For example, Hu et al. (2014) reported conversion of 80% and a 5-HMF yield of about 50% with Hβ-zeolite (Si/Al = 25) as a catalyst and [BMIM]Cl as a solvent. Xu et al. (2014) obtained a 5-HMF yield of 70% from glucose in the presence of Sn-MCM-41 as a catalyst and [EMIM]Br as a solvent/catalyst. Mamo et al. (2016) studied the conversion of glucose to 5-HMF with [BMIM]Br as a solvent/catalyst and modified zeolite mordenite as a catalyst and reported an HMF yield of 64% with 98% glucose conversion. However, the presence of ILs (or DMSO) creates problems with post-separation due to their high boiling points. Moreover, the ILs (or DMSO) are not environmentally friendly solvents as compared to protic solvents as such as water (Mushrif et al., 2012). One way to circumvent this problem is to encapsulate them (ILs) in the zeolites so that they are intact inside the cavities of the zeolite (Gallezot, 2012). Moreover, ionic liquid encapsulated zeolites could act as bifunctional catalysts. Recently, Yang et al. (2015) demonstrated that IL coated on $AlCl_3/SiO_2$ gives better yields of HMF from fructose and glucose substrates. The authors observed that no IL dissolves into the organic solvent

(MIBK) used in their study. However, the catalytic activity decreases significantly with a number of experimental cycles.

1.2.2.2 Catalyst deactivation and regeneration

The catalytic activity of solid acid catalyst drops with reuse over a period of time, due to catalyst deactivation. Deposition of humins on the surface of the catalyst, leaching of the active metal or acid groups from the catalyst (Alonso et al., 2013; Hengne and Rode, 2012; Hu et al., 2013; Yang et al., 2012; Zhang et al., 2012) and dissolution of the catalysts in reaction solvents are some of the reasons for catalyst deactivation. One common method of regeneration of the used catalyst is the calcination at high temperatures (400 – 500°C) for 3 to 4 h (Zhang et al., 2012). It removes humins from the surface, which often leads to the catalytic activity recovery (Zhang et al., 2012). But, this process is inappropriate for catalysts which are thermally unstable at high temperatures (> 200^{o}C) (Alonso et al., 2013). In such cases, the catalyst can be washed with a reagents such as ethanol (Tian et al., 2013), H_2O_2 (Alonso et al., 2013), HCl (Nikolla et al., 2011), methanol (Sidhpuria et al., 2011), NaOH (Weingarten et al., 2012), acetone (Heguaburu et al., 2012), etc.

1.2.3 Role of solvents in 5-HMF production from carbohydrates

1.2.3.1 Solvents for reaction phase

Various solvents have been studied for the production of 5-HMF from carbohydrates. The suitability of solvents concerning substrate conversion, product selectivity, and yields are shown in Tables 1.2, 1.3, 1.4. Ilgen et al. (2009), explained the ecological impact of a variety of solvents and found that water is a suitable solvent. They tested the mobility, acute toxicity for aquatic organisms, chronic and acute for humans, environment persistency and bioaccumulation. The other common solvents, such as ionic liquids and DMSO, are found to be problematic on at least one front, and this is a concern that must be kept in mind when a solvent is selected for 5-HMF synthesis.

Protic solvents: Water is one of the most commonly used eco-friendly solvents. Nevertheless, it has been seen that other solvents can provide more product yields than water, particularly when 5-HMF is the desired end-product. 5-HMF can easily be rehydrated in aqueous media to levulinic acid, formic acid and it may undergo condensation reactions to form humins (Kuster, 1977). This problem should be balanced against ecological and economic factors. Other protic solvents such as butanol or in combination with water can be

used as a solvent for the production of 5-HMF. Qu et al. (2012) stated the sec-butanol (2-butanol) is the most important solvent for the fructose dehydration to 5-HMF. Román-Leshkov et al. (2006) reported that the sec-butanol is very effective as an organic co-solvent in the biphasic mixtures.

Aprotic solvents: The 5-HMF yield can be improved by using organic solvents as reaction media. Various aprotic solvents are broadly used for 5-HMF production, such as DMSO, dimethylformamide (DMF), dimethylacetamide (DMA), tetrahydrofuran (THF) and ethyl acetate (Amarasekara et al., 2008; Climent et al., 2011; Qi et al., 2008a; Shi et al., 2013). For instance, Bicker et al. (2003) reported that 5-HMF yield of 78% is obtained in an acetone-water mixture from fructose at 278°C, and the organic-water two-phase solvents also increase the yield of 5-HMF to as high as 80% (Román-Leshkov et al., 2006). When DMSO is used as a solvent for 5-HMF production, it plays a very important role. The main purpose of DMSO is the suppression of the rehydration of 5-HMF to levulinic acid and formic acid at high temperatures (> 150°C). For example, 92% of 5-HMF yield in the presence of DMSO at 150°C for 2 h is reported (Qi et al., 2008a). DMSO favorably solvates the carbonyl carbon atom of 5-HMF, controlling the further rehydration to levulinic acid and formic acid. Another work concerning the mechanism of dehydration of fructose to 5-HMF production in the presence of DMSO is accompanying with Nuclear Magnetic Resonance (NMR) by Amarasekara et al. (2008). Dimethyl sulfoxide (DMSO) as a solvent is also a known transition state (β-D-fructofuranose tautomer) stabilizer for this reaction (Mirzaei and Karimi, 2016; Mushrif et al., 2012). However, DMSO is a high boiling solvent which means it requires high energy for the separation of 5-HMF from this solvent. Moreover, DMSO is not a green solvent as compared to protic solvent as such as water (Mushrif et al., 2012; Zhang et al., 2015). The usage of innovative aprotic solvents such as N-methyl pyrrolidone (NMP) has been suggested as an eco-friendly alternative to DMSO (Chheda et al., 2007).

Ionic liquids: This category of solvents has already been discussed in the homogeneous catalysts section because the ionic liquids could also act as catalysts for the dehydration of carbohydrates to the 5-HMF reaction.

1.2.3.2 Solvents for extraction phase

Removal of 5-HMF from the reaction phase would increase the yield of 5-HMF significantly by suppressing the side reactions. An organic phase immiscible with the reaction phase and having a high partition coefficient for 5-HMF compared to the reaction media can be used as the extracting solvent (Torres et al., 2010). The partition coefficient between the

organic phase and reaction phase is very important because a lower value of the partition coefficient requires a large amount of organic solvent and a huge quantity of energy for 5-HMF separation. The extracting solvents reported in the literature include diethyl ether (Yong et al., 2008, Yadav et al., 2003), MIBK (Su et al., 2009), ethyl acetate (Qi et al., 2012), toluene (Lima et al., 2009), etc.

1.2.4 Ways to improve the 5-HMF yield

In the literature, three ways (by modifying the operating conditions) have been used to enhance the yield of 5-HMF. Continuous water removal from the reaction system by evacuation is demonstrated to be useful for the suppression of 5-HMF rehydration to LA as well as the formation of condensation products from the partially dehydrated intermediates. Shimizu et al. (2009) Addition of extraction phase which selectively extracts the formed 5-HMF is beneficial to achieve higher selectivities of 5-HMF and lower selectivities to humins (Ordomsky et al., 2012). Adsorbents such as carbon black have also been used to selectively adsorb the furanic compounds and thereby increasing their yield (Dornath and Fan, 2014).

1.2.5 Reaction mechanism

The overall mechanism is presented in Fig. 1.3. As shown in the figure, in the first stage, the cellulose undergoes hydrolysis to form its monomer glucose. The glucose then undergoes isomerization reaction to form fructose and fructose then dehydrates to form 5-HMF. There is a possibility to form side products depending on the active sites available and the reaction conditions. For example, 5-HMF may undergo rehydration to form LA and FA, or it may undergo condensation reactions to form humins, as shown in Fig. 1.3. The glucose may also undergo decomposition to form lactic acid. For the conversion of glucose to 5-HMF broadly three mechanistic pathways have been proposed. One is isomerization of glucose to fructose (over Lewis acid or Brønsted base catalysts) followed by dehydration of fructose to 5-HMF (over Brønsted acid catalysts). The second one is the direct conversion of glucose to 5-HMF via the cyclic mechanism with the assistance of Brønsted acid catalyst and with furan aldehyde as an intermediate. The third one is an open chain mechanism which also requires the only Brønsted acid catalyst to form 5-HMF with 3-deoxyglucosone as an intermediate (Li et al., 2016a).

Several studies have been carried out to understand the mechanism of glucose to fructose isomerization by homogeneous catalysis (with metal ions or acids) (Choudhary et al.,

2013; Nagorski and Richard, 2001; T. Wang et al., 2012), by enzymes (Toteva et al., 2011) and by base-catalysis (Liu et al., 2014). It has been observed that the base catalyzed reaction follows the proton transfer mechanism whereas the acid catalyzed reaction follows a hydride transfer mechanism. Significant work has been carried out by Davis' group to obtain insights on isomerization of glucose to fructose on hydrophobic, solid Lewis acid catalysts such as Sn-Beta and Ti-Beta (Bermejo-Deval et al., 2014, 2012; Moliner et al., 2010; Nikolla et al., 2011; Román-Leshkov et al., 2010). It has been identified by these researchers that the metal centers present in Sn-Beta and Ti-Beta act similar to the metal centers present in metalloenzymes towards this isomerization reaction (Moliner et al., 2010) The authors proposed "metal-assisted intramolecular hydride shift" mechanism to be responsible for glucose isomerization to fructose on these catalysts (Román-Leshkov et al., 2010).

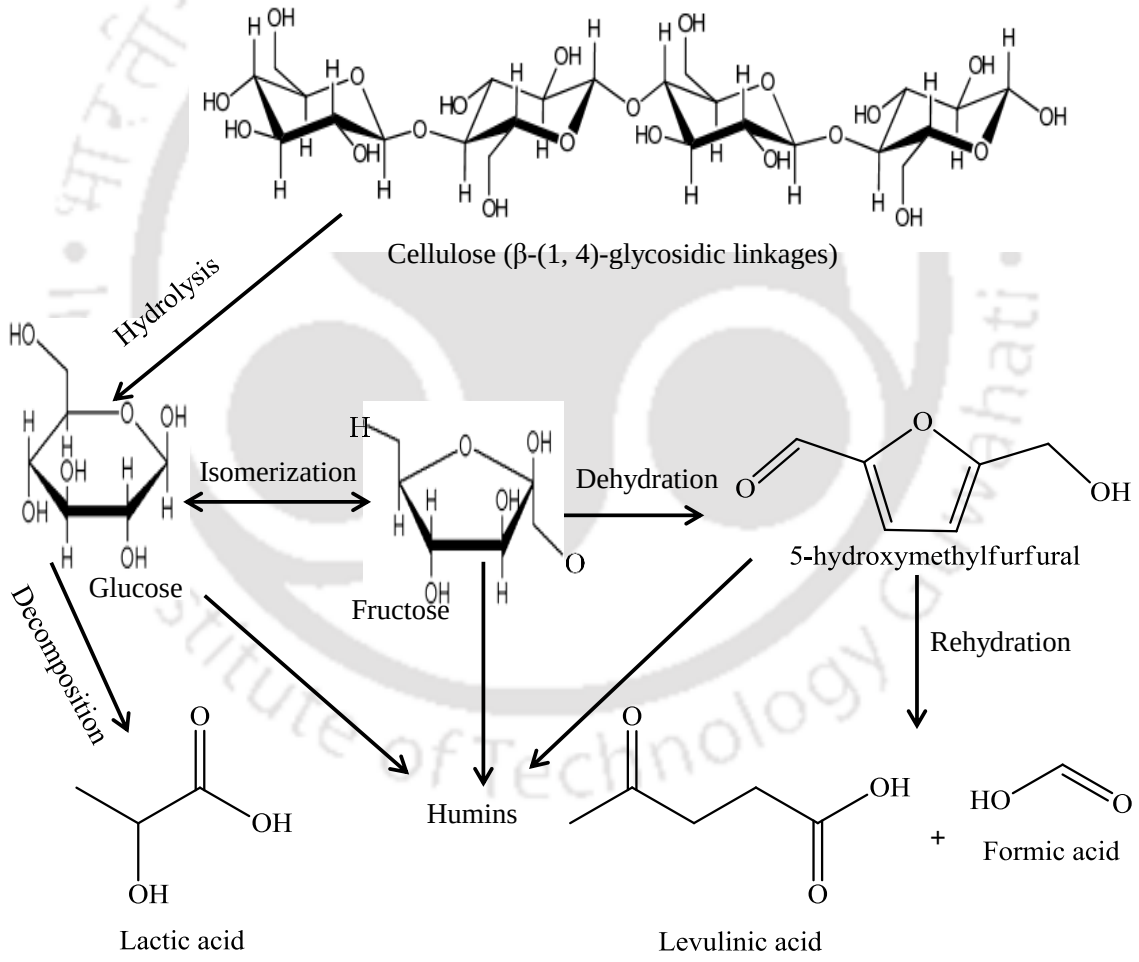

Figure 1.3: The general overall mechanism for the conversion of carbohydrates (cellulose, glucose, and fructose) to 5-HMF and other products.

1.3 Hypothesis and objectives of the work

The yields of 5-HMF from carbohydrates are reasonably high with homogeneous catalysts (Imteyaz et al., 2012; Lima et al., 2009; Zhao et al., 2007). However, the difficulty with catalysts separation and waste treatment prevents their use for the commercial 5-HMF production. As identified in the literature review, the zeolite catalysts in combination with IL solvents present an interesting reaction system for the conversion of carbohydrate-based substrates to 5-HMF with higher yields of 5-HMF. ILs, in this case, acts as both solvent and catalyst. It shows a synergistic effect in the conversion of carbohydrates to 5-HMF and therefore results in higher yields. However, the major issue with this reaction system is that ILs used are of high boiling point and requires high energy for the separation of higher boiling product (i.e. 5-HMF). In this thesis, it is hypothesized that the encapsulation of ILs in the zeolite pores could result in a similar synergistic effect as it showed in the case of zeolite + IL physical mixture. It may show even a better synergistic effect because the active sites of zeolite and IL are close to each other in the case of IL encapsulated in zeolite as compared to that of a physical mixture (zeolite + IL). Based on this hypothesis, various ionic liquids encapsulated zeolites have been synthesized and tested for the direct conversion of fructose, glucose, and cellulose to 5-HMF.

To the best of our knowledge, there are no reports in the open literature on the utilization of ILs (either choline chloride or [BMIM]Br) encapsulated zeolites for the conversion of carbohydrates to 5-HMF, except the one that is from our own group (Saxena et al., 2017). The interactions of ILs with the pure silica materials (such as SAB-15, silica gel, carbon nanotubes) are studied to some extent (Zhang et al., 2017). However, the ionic interactions of ILs with zeolites are not established in the literature, with only a few publications in this area (Mohamedali et al., 2018; Yu et al., 2014). Therefore, these are the two major knowledge gaps, which are investigated in this thesis.

Recently, we have developed a bio-inspired method for noble (Rao and Golder, 2016) and transition (Ghosh et al., 2018) metal-doping on semiconductor supports (TiO_2, ZnO, etc.). The doping test is performed at room temperature and pressure, and this technique eliminates the use of any external chemicals apart from the support materials and precursors of the dopants. The analytes present in the bio-extract is used for the incorporation of the dopants into the crystal lattice of the semiconductor supports. These catalysts are then tested for the photocatalytic decomposition of various organic pollutants with an excellent photonic efficiency (Ghosh et al., 2018; Rao and Golder, 2016). The present work also focused on this

bio-inspired technique for the doping of phosphorous along with Ag and Cu on TiO_2 for the conversion of glucose to 5-HMF which is a completely new domain of research proposed in this study. Therefore, the objectives of the thesis are designed as follows:

i. Synthesis of ChCl and [BMIM]Br encapsulated zeolites using a ship-in-a-bottle method, and metal- and phosphate-doped TiO_2 catalysts using a bio-inspired method
ii. Physicochemical characterizations of the synthesized catalysts and bare zeolites
iii. Testing of the bare zeolites for fructose, glucose, and cellulose conversion to 5-HMF
iv. Testing of the ChCl and [BMIM]Br encapsulated zeolites for the fructose, glucose, and cellulose conversion to 5-HMF
v. Testing of the metal- and phosphate-doped TiO_2 for the glucose conversion to 5-HMF

1.4 Organization of the thesis

CHAPTER 1: Background of the Work and Research Objectives

This chapter introduces the problem, includes literature survey and outlines the research objectives. A glimpse of this chapter is outlined at the beginning of this report.

CHAPTER 2: Materials and Methods

Chapter 2 describes the procedures for the modification of zeolites and TiO_2 and for the testing of these catalysts for the conversion of carbohydrates to 5-HMF in a batch autoclave reactor. The analytical procedures for catalysts characterizations and product analyses are also detailed.

CHAPTER 3: Efficient Conversion of Carbohydrates to 5-HMF over Mesoporous Zeolites

In this chapter, the performances of bare zeolites for the conversion of carbohydrates (fructose, glucose, and cellulose) to 5-HMF are reported. This study provided the platform for the necessary modifications of bare zeolites.

CHAPTER 4: Choline Chloride Encapsulated Zeolites for the Carbohydrates to 5-HMF Conversion

In this chapter, the production of 5-HMF from cellulose, glucose, and fructose using ChCl encapsulated H-MOR, H-Beta, H-ZSM-5, H-Y, and Na-Y zeolites is reported. To the best of our knowledge, no reports have been published on the ChCl impregnated zeolites for the direct cellulose conversion to 5-HMF.

CHAPTER 5: [BMIM]Br Encapsulated Zeolites for Carbohydrates Conversion to 5-HMF

In this chapter, we report the encapsulation of [BMIM]Br in zeolites using a ship-in-a-bottle method and the performance of these catalysts for the carbohydrate conversion to 5-HMF which is a step forward from the previous two chapters.

CHAPTER 6: Bio-inspired Ag-, Cu- and P-doped TiO_2 Catalysts for Conversion of Glucose to 5-HMF

In this study, an attempt is made to functionalize TiO_2 following a bio-inspired method to minimize the chemical- and energy-intensive processes in the conventional approaches. Unlike zeolites, TiO_2 is a strong amphoteric metal oxide. Furthermore, the bio-analytes are effective for the incorporation of the doped elements (Ag, Cu, and P) in the lattice structure of TiO_2.

CHAPTER 7: Major Findings and Future Directions

The salient findings of the present investigation are summarized in this Chapter. After that, the recommendations for the future work directions are appended with a brief outline of the limitations of the present work.

References

Abdel-Halim, E.S., 2014. Chemical modification of cellulose extracted from sugarcane bagasse: Preparation of hydroxyethyl cellulose. Arab. J. Chem. 7, 362–371. https://doi.org/https://doi.org/10.1016/j.arabjc.2013.05.006

Abou-Yousef, H., Hassan, E.B., 2014. A novel approach to enhance the activity of H-form

zeolite catalyst for production of hydroxymethylfurfural from cellulose. J. Ind. Eng. Chem. 20, 1952–1957. https://doi.org/10.1016/j.jiec.2013.09.016

Alonso, D.M., Gallo, J.M.R., Mellmer, M.A., Wettstein, S.G., Dumesic, J.A., 2013. Direct conversion of cellulose to levulinic acid and gamma-valerolactone using solid acid catalysts. Catal. Sci. Technol. 3, 927–931. https://doi.org/10.1039/C2CY20689G

Amarasekara, A.S., Williams, L.T.D., Ebede, C.C., 2008. Mechanism of the dehydration of d-fructose to 5-hydroxymethylfurfural in dimethyl sulfoxide at 150 °C: an NMR study. Carbohydr. Res. 343, 3021–3024. https://doi.org/10.1016/j.carres.2008.09.008

Antal, M.J., Mok, W.S.L., Richards, G.N., 1990. Mechanism of formation of 5-(hydroxymethyl)-2-furaldehyde from d-fructose and sucrose. Carbohydr. Res. 199, 91–109. https://doi.org/https://doi.org/10.1016/0008-6215(90)84096-D

Armaroli, T., Busca, G., Carlini, C., Giuttari, M., Raspolli Galletti, A.M., Sbrana, G., 2000. Acid sites characterization of niobium phosphate catalysts and their activity in fructose dehydration to 5-hydroxymethyl-2-furaldehyde. J. Mol. Catal. A Chem. 151, 233–243. https://doi.org/10.1016/S1381-1169(99)00248-4

Asghari, F.S., Yoshida, H., 2006a. Acid-catalyzed production of 5-hydroxymethyl furfural from D-fructose in subcritical water. Ind. Eng. Chem. Res. 45, 2163–2173. https://doi.org/10.1021/ie051088y

Asghari, F.S., Yoshida, H., 2006b. Dehydration of fructose to 5-hydroxymethylfurfural in sub-critical water over heterogeneous zirconium phosphate catalysts. Carbohydr. Res. 341, 2379–2387. https://doi.org/10.1016/j.carres.2006.06.025

Atanda, L., Konarova, M., Ma, Q., Mukundan, S., Shrotri, A., Beltramini, J., 2016. High yield conversion of cellulosic biomass into 5-hydroxymethylfurfural and a study of the reaction kinetics of cellulose to HMF conversion in a biphasic system. Catal. Sci. Technol. 6, 6257–6266. https://doi.org/10.1039/C6CY00820H

Atanda, L., Mukundan, S., Shrotri, A., Ma, Q., Beltramini, J., 2015a. Catalytic conversion of glucose to 5-hydroxymethyl-furfural with a phosphated TiO2catalyst. ChemCatChem 7, 781–790. https://doi.org/10.1002/cctc.201402794

Atanda, L., Shrotri, A., Mukundan, S., Ma, Q., Konarova, M., Beltramini, J., 2015b. Direct Production of 5-Hydroxymethylfurfural via Catalytic Conversion of Simple and Complex Sugars over Phosphated TiO<inf>2</inf>. ChemSusChem 8, 2907–2916. https://doi.org/10.1002/cssc.201500395

Atanda, L., Silahua, A., Mukundan, S., Shrotri, A., Torres-Torres, G., Beltramini, J., 2015c. Catalytic behaviour of TiO2-ZrO2 binary oxide synthesized by sol-gel process for

glucose conversion to 5-hydroxymethylfurfural. RSC Adv. 5, 80346–80352. https://doi.org/10.1039/c5ra15739k

Bao, Q., Qiao, K., Tomida, D., Yokoyama, C., 2008. Preparation of 5-hydroymethylfurfural by dehydration of fructose in the presence of acidic ionic liquid. Catal. Commun. 9, 1383–1388. https://doi.org/10.1016/j.catcom.2007.12.002

Benvenuti, F., Carlini, C., Patrono, P., Galletti, A.M.R., Sbrana, G., Massucci, M.A., Galli, P., 2000. Heterogeneous zirconium and titanium catalysts for the selective synthesis of 5-hydroxymethyl-2-furaldehyde from carbohydrates. Appl. Catal. A Gen. 193, 147–153. https://doi.org/10.1016/S0926-860X(99)00424-X

Bermejo-Deval, R., Assary, R.S., Nikolla, E., Moliner, M., Roman-Leshkov, Y., Hwang, S.-J., Palsdottir, A., Silverman, D., Lobo, R.F., Curtiss, L.A., Davis, M.E., 2012. Metalloenzyme-like catalyzed isomerizations of sugars by Lewis acid zeolites. Proc. Natl. Acad. Sci. 109, 9727–9732. https://doi.org/10.1073/pnas.1206708109

Bermejo-Deval, R., Orazov, M., Gounder, R., Hwang, S.J., Davis, M.E., 2014. Active sites in Sn-beta for glucose isomerization to fructose and epimerization to mannose. ACS Catal. 4, 2288–2297. https://doi.org/10.1021/cs500466j

Bhaumik, P., Dhepe, P.L., 2013. Influence of properties of SAPO's on the one-pot conversion of mono-, di- and poly-saccharides into 5-hydroxymethylfurfural. RSC Adv. 3, 17156–17165. https://doi.org/10.1039/C3RA43197E

Bicker, M., Hirth, J., Vogel, H., 2003. Dehydration of fructose to 5-hydroxymethylfurfural in sub- and supercritical acetone. Green Chem. 5, 280–284. https://doi.org/10.1039/B211468B

Bicker, M., Kaiser, D., Ott, L., Vogel, H., 2005. Dehydration of D-fructose to hydroxymethylfurfural in sub- and supercritical fluids. J. Supercrit. Fluids 36, 118–126. https://doi.org/10.1016/j.supflu.2005.04.004

Binder, J.B., Raines, R.T., 2009. Simple Chemical Transformation of Lignocellulosic Biomass into Furans for Fuels and Chemicals. J. Am. Chem. Soc. 131, 1979–1985. https://doi.org/Doi 10.1021/Ja808537j

Boerjan, W., Ralph, J., Baucher, M., 2003. Lignin Biosynthesis. Annu. Rev. Plant Biol. 54, 519–546. https://doi.org/10.1146/annurev.arplant.54.031902.134938

Brasholz, M., Von Känel, K., Hornung, C.H., Saubern, S., Tsanaktsidis, J., 2011. Highly efficient dehydration of carbohydrates to 5-(chloromethyl)furfural (CMF), 5-(hydroxymethyl)furfural (HMF) and levulinic acid by biphasic continuous flow processing. Green Chem. 13, 1114–1117. https://doi.org/10.1039/c1gc15107j

Cao, Q., Guo, X., Yao, S., Guan, J., Wang, X., Mu, X., Zhang, D., 2011. Conversion of hexose into 5-hydroxymethylfurfural in imidazolium ionic liquids with and without a catalyst. Carbohydr. Res. 346, 956–959. https://doi.org/10.1016/j.carres.2011.03.015

Caratzoulas, S., Davis, M.E., Gorte, R.J., Gounder, R., Lobo, R.F., Nikolakis, V., Sandler, S.I., Snyder, M.A., Tsapatsis, M., Vlachos, D.G., 2014. Challenges of and Insights into Acid-Catalyzed Transformations of Sugars. J. Phys. Chem. C 118, 22815–22833. https://doi.org/10.1021/jp504358d

Carlini, C., Giuttari, M., Galletti, A.M.R., Sbrana, G., Armaroli, T., Busca, G., 1999. Selective saccharides dehydration to 5-hydroxymethyl-2-furaldehyde by heterogeneous niobium catalysts. Appl. Catal. A Gen. 183, 295–302. https://doi.org/10.1016/S0926-860X(99)00064-2

Carlini, C., Patrono, P., Galletti, A.M.R., Sbrana Glauco, G., 2004. Heterogeneous catalysts based on vanadyl phosphate for fructose dehydration to 5-hydroxymethyl-2-furaldehyde. Appl. Catal. A Gen. 275, 111–118. https://doi.org/10.1016/j.apcata.2004.07.026

Carniti, P., Gervasini, A., Biella, S., Auroux, A., 2006. Niobic acid and niobium phosphate as highly acidic viable catalysts in aqueous medium: Fructose dehydration reaction. Catal. Today 118, 373–378. https://doi.org/10.1016/j.cattod.2006.07.024

Chareonlimkun, A., Champreda, V., Shotipruk, A., Laosiripojana, N., 2010. Reactions of C5 and C6-sugars, cellulose, and lignocellulose under hot compressed water (HCW) in the presence of heterogeneous acid catalysts, Fuel. https://doi.org/10.1016/j.fuel.2010.03.015

Chheda, J.N., Roman-Leshkov, Y., Dumesic, J.A., 2007. Production of 5-hydroxymethylfurfural and furfural by dehydration of biomass-derived mono- and poly-saccharides. Green Chem. 9, 342–350. https://doi.org/10.1039/B611568C

Chidambaram, M., Bell, A.T., 2010. A two-step approach for the catalytic conversion of glucose to 2,5-dimethylfuran in ionic liquids. Green Chem. 12, 1253–1262. https://doi.org/10.1039/c004343e

Choudhary, V., Mushrif, S.H., Ho, C., Anderko, A., Nikolakis, V., Marinkovic, N.S., Frenkel, A.I., Sandler, S.I., Vlachos, D.G., 2013. Insights into the interplay of lewis and Brønsted acid catalysts in glucose and fructose conversion to 5-(hydroxymethyl)furfural and levulinic acid in aqueous media. J. Am. Chem. Soc. 135, 3997–4006. https://doi.org/10.1021/ja3122763

Climent, M.J., Corma, A., Iborra, S., 2011. Converting carbohydrates to bulk chemicals and fine chemicals over heterogeneous catalysts. Green Chem. 13, 520–540.

https://doi.org/10.1039/c0gc00639d

Corma Canos, A., Iborra, S., Velty, A., 2007. Chemical routes for the transformation of biomass into chemicals. Chem. Rev. 107, 2411–2502. https://doi.org/10.1021/cr050989d

Crisci, A.J., Tucker, M.H., Lee, M.Y., Jang, S.G., Dumesic, J.A., Scott, S.L., 2011. Acid-functionalized SBA-15-type silica catalysts for carbohydrate dehydration. ACS Catal. 1, 719–728. https://doi.org/10.1021/cs2001237

Daorattanachai, P., Khemthong, P., Viriya-Empikul, N., Laosiripojana, N., Faungnawakij, K., 2012. Conversion of fructose, glucose, and cellulose to 5-hydroxymethylfurfural by alkaline earth phosphate catalysts in hot compressed water. Carbohydr. Res. 363, 58–61. https://doi.org/10.1016/j.carres.2012.09.022

De, S., Dutta, S., Patra, A.K., Bhaumik, A., Saha, B., 2011. Self-assembly of mesoporous TiO2nanospheres via aspartic acid templating pathway and its catalytic application for 5-hydroxymethyl-furfural synthesis. J. Mater. Chem. 21, 17505–17510. https://doi.org/10.1039/c1jm13229f

de Souza, R.L., Yu, H., Rataboul, F., Essayem, N., 2012. 5-Hydroxymethylfurfural (5-HMF) Production from Hexoses: Limits of Heterogeneous Catalysis in Hydrothermal Conditions and Potential of Concentrated Aqueous Organic Acids as Reactive Solvent System. Challenges 3, 212–232. https://doi.org/10.3390/challe3020212

Demirbas, A., 2009. Progress and recent trends in biodiesel fuels. Energy Convers. Manag. 50, 14–34. https://doi.org/10.1016/j.enconman.2008.09.001

Dongbin Zhao, Wu, M., Kou, Y., Min, E., 2002. Ionic liquids: applications in catalysis. Catal. Today 74, 157–189. https://doi.org/10.1016/j.ccr.2004.04.015

Dornath, P., Fan, W., 2014. Dehydration of fructose into furans over zeolite catalyst using carbon black as adsorbent. Microporous Mesoporous Mater. 191, 10–17. https://doi.org/10.1016/j.micromeso.2014.02.031

Dutta, S., De, S., Patra, A.K., Sasidharan, M., Bhaumik, A., Saha, B., 2011. Microwave assisted rapid conversion of carbohydrates into 5-hydroxymethylfurfural catalyzed by mesoporous TiO2nanoparticles. Appl. Catal. A Gen. 409–410, 133–139. https://doi.org/10.1016/j.apcata.2011.09.037

Eminov, S., Filippousi, P., Brandt, A., Wilton-Ely, J., Hallett, J., 2016. Direct Catalytic Conversion of Cellulose to 5-Hydroxymethylfurfural Using Ionic Liquids. Inorganics 4, 32. https://doi.org/10.3390/inorganics4040032

Fan, C., Guan, H., Zhang, H., Wang, J., Wang, S., Wang, X., 2011. Conversion of fructose and glucose into 5-hydroxymethylfurfural catalyzed by a solid heteropolyacid salt.

Biomass and Bioenergy 35, 2659–2665. https://doi.org/10.1016/j.biombioe.2011.03.004

Fang, J.M., Sun, R.C., Tomkinson, J., 2000. Isolation and characterization of hemicelluloses and cellulose from rye straw by alkaline peroxide extraction 87–107.

Gallezot, P., 2012. Conversion of biomass to selected chemical products. Chem. Soc. Rev. 41, 1538–1558. https://doi.org/10.1039/c1cs15147a

Gallo, J.M.R., Alonso, D.M., Mellmer, M.A., Dumesic, J.A., 2013. Production and upgrading of 5-hydroxymethylfurfural using heterogeneous catalysts and biomass-derived solvents. Green Chem. 15, 85–90. https://doi.org/10.1039/c2gc36536g

Ghosh, P., Chelli, V.R., Giri, A.S., Golder, A.K., 2018. Steroid glycosides as potential analytes for Cu-doping on TiO2for photocatalytic water treatment. Environ. Prog. Sustain. Energy 00, 1–9. https://doi.org/10.1002/ep.12879

Guo, X., Cao, Q., Jiang, Y., Guan, J., Wang, X., Mu, X., 2012. Selective dehydration of fructose to 5-hydroxymethylfurfural catalyzed by mesoporous SBA-15-SO3H in ionic liquid BmimCl. Carbohydr. Res. 351, 35–41. https://doi.org/10.1016/j.carres.2012.01.003

Hafizi, H., Najafi Chermahini, A., Saraji, M., Mohammadnezhad, G., 2016. The catalytic conversion of fructose into 5-hydroxymethylfurfural over acid-functionalized KIT-6, an ordered mesoporous silica. Chem. Eng. J. 294, 380–388. https://doi.org/10.1016/j.cej.2016.02.082

Hansen, T.S., Mielby, J., Riisager, A., 2011. Synergy of boric acid and added salts in the catalytic dehydration of hexoses to 5-hydroxymethylfurfural in water. Green Chem. 13, 109–114. https://doi.org/10.1039/c0gc00355g

Hansen, T.S., Woodley, J.M., Riisager, A., 2009. Efficient microwave-assisted synthesis of 5-hydroxymethylfurfural from concentrated aqueous fructose. Carbohydr. Res. 344, 2568–2572. https://doi.org/10.1016/j.carres.2009.09.036

Heguaburu, V., Franco, J., Reina, L., Tabarez, C., Moyna, G., Moyna, P., 2012. Dehydration of carbohydrates to 2-furaldehydes in ionic liquids by catalysis with ion exchange resins. Catal. Commun. 27, 88–91. https://doi.org/10.1016/j.catcom.2012.07.002

Hengne, A.M., Rode, C. V., 2012. Cu–ZrO2 nanocomposite catalyst for selective hydrogenation of levulinic acid and its ester to γ-valerolactone. Green Chem. 14, 1064. https://doi.org/10.1039/c2gc16558a

Hu, L., Sun, Y., Lin, L., 2012. Efficient conversion of glucose into 5-hydroxymethylfurfural by chromium(III) chloride in inexpensive ionic liquid. Ind. Eng. Chem. Res. 51, 1099–1104. https://doi.org/10.1021/ie202174f

Hu, L., Wu, Z., Xu, J., Sun, Y., Lin, L., Liu, S., 2014. Zeolite-promoted transformation of glucose into 5-hydroxymethylfurfural in ionic liquid. Chem. Eng. J. 244, 137–144. https://doi.org/10.1016/j.cej.2014.01.057

Hu, L., Zhao, G., Tang, X., Wu, Z., Xu, J., Lin, L., Liu, S., 2013. Catalytic conversion of carbohydrates into 5-hydroxymethylfurfural over cellulose-derived carbonaceous catalyst in ionic liquid. Bioresour. Technol. 148, 501–507. https://doi.org/10.1016/j.biortech.2013.09.016

Hu, S., Zhang, Z., Zhou, Y., Han, B., Fan, H., Li, W., Song, J., Xie, Y., 2008. Conversion of fructose to 5-hydroxymethylfurfural using ionic liquids prepared from renewable materials. Green Chem. 10, 1280–1283. https://doi.org/10.1039/b810392e

Huber, G.W., Iborra, S., Corma, A., 2006. Synthesis of transportation fuels from biomass: Chemistry, catalysts, and engineering. Chem. Rev. 106, 4044–4098. https://doi.org/10.1021/cr068360d

Ilgen, F., Ott, D., Kralisch, D., Reil, C., Palmberger, A., König, B., 2009. Conversion of carbohydrates into 5-hydroxymethylfurfural in highly concentrated low melting mixtures. Green Chem. 11, 1948–1954. https://doi.org/10.1039/b917548m

Imteyaz Alam, M., De, S., Dutta, S., Saha, B., 2012. Solid-acid and ionic-liquid catalyzed one-pot transformation of biorenewable substrates into a platform chemical and a promising biofuel. RSC Adv. 2, 6890–6896. https://doi.org/10.1039/c2ra20574b

Jadhav, H., Taarning, E., Pedersen, C.M., Bols, M., 2012. Conversion of d-glucose into 5-hydroxymethylfurfural (HMF) using zeolite in [Bmim]Cl or tetrabutylammonium chloride (TBAC)/CrCl2. Tetrahedron Lett. 53, 983–985. https://doi.org/10.1016/j.tetlet.2011.12.059

Jiménez-Morales, I., Moreno-Recio, M., Santamaría-González, J., Maireles-Torres, P., Jiménez-López, A., 2015. Production of 5-hydroxymethylfurfural from glucose using aluminium doped MCM-41 silica as acid catalyst. Appl. Catal. B Environ. 164, 70–76. https://doi.org/10.1016/j.apcatb.2014.09.002

Jiménez-Morales, I., Santamaría-González, J., Jiménez-López, A., Maireles-Torres, P., 2014. Glucose dehydration to 5-hydroxymethylfurfural on zirconium containing mesoporous MCM-41 silica catalysts. Fuel 118, 265–271. https://doi.org/10.1016/j.fuel.2013.10.079

Jow, J., Rorrer, G.L., Hawley, M.C., 1987. Dehydration of D-fructose to Levulinic Acid over LYZ Zeolite Catalyst. Biomass 14, 185–194.

Kazmi, M.Z.H., Karmakar, A., Michaelis, V.K., Williams, F.J., 2019. Separation of cellulose/hemicellulose from lignin in white pine sawdust using boron trihalide reagents.

Tetrahedron 75, 1465–1470. https://doi.org/https://doi.org/10.1016/j.tet.2019.02.009

Kılıç, E., Yılmaz, S., 2015. Fructose Dehydration to 5-Hydroxymethylfurfural over Sulfated TiO_2–SiO_2, Ti-SBA-15, ZrO_2, SiO_2, and Activated Carbon Catalysts. Ind. Eng. Chem. Res. 54, 5220–5225. https://doi.org/10.1021/acs.iecr.5b00628

Kowalski, S., Lukasiewicz, M., Duda-Chodak, A., Zięc, G., 2013. 5-hydroxymethyl-2-furfural (HMF) -heat-induced formation, occurrence in food and biotransformation - A review. Polish J. Food Nutr. Sci. 63, 207–225. https://doi.org/10.2478/v10222-012-0082-4

Kuo, C.-H., Poyraz, A.S., Jin, L., Meng, Y., Pahalagedara, L., Chen, S.-Y., Kriz, D.A., Guild, C., Gudz, A., Suib, S.L., 2014. Heterogeneous acidic TiO2 nanoparticles for efficient conversion of biomass derived carbohydrates. Green Chem. 16, 785. https://doi.org/10.1039/c3gc40909k

Kuster, B.F.M., 1990. 5-Hydroxymethylfurfural (HMF). A Review Focussing on its Manufacture. Starch - Stärke 42, 314–321. https://doi.org/10.1002/star.19900420808

Kuster, B.F.M., 1977. The influence of water concentration on the dehydration of d-fructose. Carbohydr. Res. 54, 177–183. https://doi.org/https://doi.org/10.1016/S0008-6215(00)84807-7

Kuster, B.F.M., Van Steen, H.J.C. Der, 1977. Preparation of 5-Hydroxymethylfurfural Part I. Dehydration of Fructose in a Continuous Stirred Tank Reactor. Starch - Stärke 29, 99–103. https://doi.org/10.1002/star.19770290306

Lansalot-Matras, C., Moreau, C., 2003. Dehydration of fructose into 5-hydroxymethylfurfural in the presence of ionic liquids. Catal. Commun. 4, 517–520. https://doi.org/10.1016/S1566-7367(03)00133-X

Li, C., Zhang, Z., Zhao, Z.K., 2009. Direct conversion of glucose and cellulose to 5-hydroxymethylfurfural in ionic liquid under microwave irradiation. Tetrahedron Lett. 50, 5403–5405. https://doi.org/10.1016/j.tetlet.2009.07.053

Li, C., Zhao, Z.K., Wang, A., Zheng, M., Zhang, T., 2010. Production of 5-hydroxymethylfurfural in ionic liquids under high fructose concentration conditions. Carbohydr. Res. 345, 1846–1850. https://doi.org/10.1016/j.carres.2010.07.003

Li, H., Fang, Z., Smith, R.L., Yang, S., 2016a. Efficient valorization of biomass to biofuels with bifunctional solid catalytic materials. Prog. Energy Combust. Sci. 55, 98–194. https://doi.org/10.1016/j.pecs.2016.04.004

Li, H., Yang, S., Riisager, A., Pandey, A., Sangwan, R.S., Saravanamurugan, S., Luque, R., 2016b. Zeolite and zeotype-catalysed transformations of biofuranic compounds. Green

Chem. 18, 5701–5735. https://doi.org/10.1039/c6gc02415g

Li, Y., Liu, H., Song, C., Gu, X., Li, H., Zhu, W., Yin, S., Han, C., 2013. The dehydration of fructose to 5-hydroxymethylfurfural efficiently catalyzed by acidic ion-exchange resin in ionic liquid. Bioresour. Technol. 133, 347–353. https://doi.org/10.1016/j.biortech.2013.01.038

Li, Z., Su, K., Ren, J., Yang, D., Cheng, B., Kim, C.K., Yao, X., 2018. Direct catalytic conversion of glucose and cellulose. Green Chem. 20, 863–872. https://doi.org/10.1039/c7gc03318d

Lima, S., Neves, P., Antunes, M.M., Pillinger, M., Ignatyev, N., Valente, A.A., 2009. Conversion of mono/di/polysaccharides into furan compounds using 1-alkyl-3-methylimidazolium ionic liquids. Appl. Catal. A Gen. 363, 93–99. https://doi.org/10.1016/j.apcata.2009.04.049

Liu, C.-F., Ren, J.-L., Xu, F., Liu, J.-J., Sun, J.-X., Sun, R.-C., 2006. Isolation and Characterization of Cellulose Obtained from Ultrasonic Irradiated Sugarcane Bagasse. J. Agric. Food Chem. 54, 5742–5748. https://doi.org/10.1021/jf060929o

Liu, C., Carraher, J.M., Swedberg, J.L., Herndon, C.R., Fleitman, C.N., Tessonnier, J.P., 2014. Selective base-catalyzed isomerization of glucose to fructose. ACS Catal. 4, 4295–4298. https://doi.org/10.1021/cs501197w

Liu, D.D.J., Chen, E.Y.X., 2013. Polymeric ionic liquid (PIL)-supported recyclable catalysts for biomass conversion into HMF. Biomass and Bioenergy 48, 181–190. https://doi.org/10.1016/j.biombioe.2012.11.020

Liu, L., Chang, H.M., Jameel, H., Park, J.Y., Park, S., 2017. Catalytic Conversion of Biomass Hydrolysate into 5-Hydroxymethylfurfural. Ind. Eng. Chem. Res. 56, 14447–14453. https://doi.org/10.1021/acs.iecr.7b03635

Liu, W., Holladay, J., 2013. Catalytic conversion of sugar into hydroxymethylfurfural in ionic liquids. Catal. Today 200, 106–116. https://doi.org/10.1016/j.cattod.2012.07.008

Mamo, W., Chebude, Y., Márquez-Álvarez, C., Díaz, I., Sastre, E., 2016. Comparison of glucose conversion to 5-HMF using different modified mordenites in ionic liquid and biphasic media. Catal. Sci. Technol. 6, 2766–2774. https://doi.org/10.1039/c5cy02070k

McCluer, R.H., 1964. Methods in carbohydrate chemistry. Volume 3, Cellulose (Whistler, Roy L.; Wolfrom, M. L.; ed.s). J. Chem. Educ. 41, 352. https://doi.org/10.1021/ed041p352.3

Mednick, M.L., 1962. The Acid-Base-Catalyzed Conversion of Aldohexose into 5-(Hydroxymethyl)-2-furfural. J. Org. Chem. 27, 398–403.

https://doi.org/10.1021/jo01049a013

Mika, L.T., Cséfalvay, E., Németh, Á., 2018. Catalytic Conversion of Carbohydrates to Initial Platform Chemicals: Chemistry and Sustainability. Chem. Rev. 118, 505–613. https://doi.org/10.1021/acs.chemrev.7b00395

Mirzaei, H.M., Karimi, B., 2016. Sulphanilic acid as a recyclable bifunctional organocatalyst in the selective conversion of lignocellulosic biomass to 5-HMF. Green Chem. 18, 2282–2286. https://doi.org/10.1039/c5gc02440d

Mohamedali, M., Ibrahim, H., Henni, A., 2018. Incorporation of acetate-based ionic liquids into a zeolitic imidazolate framework (ZIF-8) as efficient sorbents for carbon dioxide capture. Chem. Eng. J. 334, 817–828. https://doi.org/10.1016/j.cej.2017.10.104

Moliner, M., Roman-Leshkov, Y., Davis, M.E., 2010. Tin-containing zeolites are highly active catalysts for the isomerization of glucose in water. Proc. Natl. Acad. Sci. 107, 6164–6168. https://doi.org/10.1073/pnas.1002358107

Moreau, C., Durand, R., Razigade, S., Duhamet, J., Faugeras, P., Rivalier, P., Pierre, R., Avignon, G., 1996. Dehydration of fructose to 5-hydroxymethylfurfural over H-mordenites. Appl. Catal. A Gen. 145, 211–224. https://doi.org/10.1016/0926-860X(96)00136-6

Moye, C.J., Goldsack, R.J., 2018. Reaction of ketohexoses with acid in certain non-aqueous sugar solvents. J. Appl. Chem. 16, 206–208. https://doi.org/10.1002/jctb.5010160703

Mukherjee, A., Dumont, M.J., Raghavan, V., 2015. Review: Sustainable production of hydroxymethylfurfural and levulinic acid: Challenges and opportunities. Biomass and Bioenergy 72, 143–183. https://doi.org/10.1016/j.biombioe.2014.11.007

Mushrif, S.H., Caratzoulas, S., Vlachos, D.G., 2012. Understanding solvent effects in the selective conversion of fructose to 5-hydroxymethyl-furfural: A molecular dynamics investigation. Phys. Chem. Chem. Phys. 14, 2637–2644. https://doi.org/10.1039/c2cp22694d

Nagorski, R.W., Richard, J.P., 2001. Mechanistic Imperatives for Aldose - Ketose Isomerization in Water : Specific , General Base- and Metal Ion-Catalyzed Isomerization of Glyceraldehyde with Proton and Hydride Transfer 794–802. https://doi.org/10.1021/ja003433a

Najafi Chermahini, A., Shahangi, F., Dabbagh, H.A., Saraji, M., 2016. Production of 5-hydroxymethylfurfural from fructose using a spherically fibrous KCC-1 silica catalyst. RSC Adv. 6, 33804–33810. https://doi.org/10.1039/c6ra03382b

Nakajima, K., Baba, Y., Noma, R., Kitano, M., N. Kondo, J., Hayashi, S., Hara, M., 2011.

Nb2O5•nH2O as a heterogeneous catalyst with water-tolerant lewis acid sites. J. Am. Chem. Soc. 133, 4224–4227. https://doi.org/10.1021/ja110482r

Nakumara et al., 1980.pdf, n.d.

Nandiwale, K.Y., Galande, N.D., Thakur, P., Sawant, S.D., Zambre, V.P., Bokade, V. V., 2014. One-pot synthesis of 5-hydroxymethylfurfural by cellulose hydrolysis over highly active bimodal micro/mesoporous H-ZSM-5 catalyst. ACS Sustain. Chem. Eng. 2, 1928–1932. https://doi.org/10.1021/sc500270z

Nikolla, E., Román-Leshkov, Y., Moliner, M., Davis, M.E., 2011. "One-pot" synthesis of 5-(hydroxymethyl)furfural from carbohydrates using tin-beta zeolite. ACS Catal. 1, 408–410. https://doi.org/10.1021/cs2000544

Ning, H., Song, J., Hou, M., Yang, D., Fan, H., Han, B., 2013. Efficient dehydration of carbohydrates to 5-hydroxymethylfurfural in ionic liquids catalyzed by tin(IV) phosphonate and zirconium phosphonate. Sci. China Chem. 56, 1578–1585. https://doi.org/10.1007/s11426-013-4944-3

Ohara, M., Takagaki, A., Nishimura, S., Ebitani, K., 2010. Syntheses of 5-hydroxymethylfurfural and levoglucosan by selective dehydration of glucose using solid acid and base catalysts. Appl. Catal. A Gen. 383, 149–155. https://doi.org/10.1016/j.apcata.2010.05.040

Ordomsky, V. V., Van Der Schaaf, J., Schouten, J.C., Nijhuis, T.A., 2012. Fructose dehydration to 5-hydroxymethylfurfural over solid acid catalysts in a biphasic system. ChemSusChem 5, 1812–1819. https://doi.org/10.1002/cssc.201200072

Otomo, R., Tatsumi, T., Yokoi, T., 2015. Beta zeolite: a universally applicable catalyst for the conversion of various types of saccharides into furfurals. Catal. Sci. Technol. 5, 4001–4007. https://doi.org/10.1039/C5CY00719D

Otomo, R., Yokoi, T., Kondo, J.N., Tatsumi, T., 2014. Dealuminated Beta zeolite as effective bifunctional catalyst for direct transformation of glucose to 5-hydroxymethylfurfural. Appl. Catal. A Gen. 470, 318–326. https://doi.org/10.1016/j.apcata.2013.11.012

Petkovic, M., Seddon, K.R., Rebelo, L.P.N., Pereira, C.S., 2011. Ionic liquids: A pathway to environmental acceptability. Chem. Soc. Rev. 40, 1383–1403. https://doi.org/10.1039/c004968a

Plechkova, N. V., Seddon, K.R., 2008. Applications of ionic liquids in the chemical industry. Chem. Soc. Rev. 37, 123–150. https://doi.org/10.1039/b006677j

Qi, X., Guo, H., Li, L., 2011. Efficient conversion of fructose to 5-hydroxymethylfurfural catalyzed by sulfated zirconia in ionic liquids. Ind. Eng. Chem. Res. 50, 7985–7989.

https://doi.org/10.1021/ie200488k

Qi, X., Watanabe, M., Aida, T.M., Smith, R.L., 2012. Synergistic conversion of glucose into 5-hydroxymethylfurfural in ionic liquid-water mixtures. Bioresour. Technol. 109, 224–228. https://doi.org/10.1016/j.biortech.2012.01.034

Qi, X., Watanabe, M., Aida, T.M., Smith, R.L., 2009a. Sulfated zirconia as a solid acid catalyst for the dehydration of fructose to 5-hydroxymethylfurfural. Catal. Commun. 10, 1771–1775. https://doi.org/10.1016/j.catcom.2009.05.029

Qi, X., Watanabe, M., Aida, T.M., Smith, R.L., 2009b. Efficient process for conversion of fructose to 5-hydroxymethylfurfural with ionic liquids. Green Chem. 11, 1327–1331. https://doi.org/10.1039/b905975j

Qi, X., Watanabe, M., Aida, T.M., Smith, R.L., 2008a. Catalytic dehydration of fructose into 5-hydroxymethylfurfural by ion-exchange resin in mixed-aqueous system by microwave heating. Green Chem. 10, 799–805. https://doi.org/10.1039/b801641k

Qi, X., Watanabe, M., Aida, T.M., Smith, R.L., 2008b. Catalytical conversion of fructose and glucose into 5-hydroxymethylfurfural in hot compressed water by microwave heating. Catal. Commun. 9, 2244–2249. https://doi.org/10.1016/j.catcom.2008.04.025

Qi, X., Watanabe, M., Aida, T.M., Smith, R.L., 2008c. Selective Conversion of D -Fructose to 5-Hydroxymethylfurfural by Ion-Exchange Resin in Acetone/Dimethyl sulfoxide Solvent Mixtures. Ind. Eng. Chem. Res. 47, 9234–9239. https://doi.org/10.1021/ie801016s

Qu, Y., Huang, C., Zhang, J., Chen, B., 2012. Efficient dehydration of fructose to 5-hydroxymethylfurfural catalyzed by a recyclable sulfonated organic heteropolyacid salt. Bioresour. Technol. 106, 170–172. https://doi.org/10.1016/j.biortech.2011.11.069

Rao, C.V., Golder, A.K., 2016. Development of a bio-mediated technique of silver-doping on titania. Colloids Surfaces A Physicochem. Eng. Asp. 506, 557–565. https://doi.org/10.1016/j.colsurfa.2016.07.031

Ray, D., Mittal, N., Chung, W.J., 2011. Phosphorous pentoxide mediated synthesis of 5-HMF in ionic liquid at low temperature. Carbohydr. Res. 346, 2145–2148. https://doi.org/10.1016/j.carres.2011.08.006

Rinne, K.T., Boettger, T., Loader, N.J., Robertson, I., Switsur, V.R., Waterhouse, J.S., 2005. On the purification of α-cellulose from resinous wood for stable isotope (H, C and O) analysis. Chem. Geol. 222, 75–82. https://doi.org/https://doi.org/10.1016/j.chemgeo.2005.06.010

Rivalier, P., Moreau, C., Durand, R., 1995. Reactor With Simultaneous Extraction of an

Intermediate Product. Catal. Letters 24, 165–171.

Rlgal, L., Gaset, A., Gorrlchon, J.P., 1981. Selective Conversion of D-Fructose to 5-Hydroxymethyl-2-furancarboxaldehyde Using a Water-Solvent-Ion-Exchange Resin Triphasic System. Ind. Eng. Chem. Prod. Res. Dev. 20, 719–721. https://doi.org/10.1021/i300004a025

Román-Leshkov, Y., Chheda, J.N., Dumesic, J.A., 2006. Phase Modifiers Promote Efficient Production of Hydroxymethylfurfural from Fructose. Science (80-.). 312, 1933 LP – 1937.

Román-Leshkov, Y., Moliner, M., Labinger, J.A., Davis, M.E., 2010. Mechanism of glucose isomerization using a solid lewis acid catalyst in water. Angew. Chemie - Int. Ed. 49, 8954–8957. https://doi.org/10.1002/anie.201004689

Saxena, P., Velaga, B., Peela, N.R., 2017. Ionic Liquid-Encapsulated Zeolite Catalysts for the Conversion of Glucose to 5-Hydroxymethylfurfural. ChemistrySelect 2, 10379–10386. https://doi.org/10.1002/slct.201701955

Seri, K., Sakaki, T., Shibata, M., Inoue, Y., Ishida, H., 2002. Lanthanum(III)-catalyzed degradation of cellulose at 250 degrees C. Bioresour. Technol. 81, 257–260. https://doi.org/10.1016/S0960-8524(01)00145-6

Serrano-Ruiz, J.C., Dumesic, J.A., 2011. Catalytic routes for the conversion of biomass into liquid hydrocarbon transportation fuels. Energy Environ. Sci. 4, 83–99. https://doi.org/10.1039/c0ee00436g

Shi, N., Liu, Q., Zhang, Q., Wang, T., Ma, L., 2013. High yield production of 5-hydroxymethylfurfural from cellulose by high concentration of sulfates in biphasic system. Green Chem. 15, 1967–1974. https://doi.org/10.1039/c3gc40667a

Shi, Y., Li, X., Hu, J., Lu, J., Ma, Y., Zhang, Y., Tang, Y., 2011. Zeolite microspheres with hierarchical structures: Formation, mechanism and catalytic performance. J. Mater. Chem. 21, 16223–16230. https://doi.org/10.1039/c1jm11669j

Shimizu, K. ichi, Uozumi, R., Satsuma, A., 2009. Enhanced production of hydroxymethylfurfural from fructose with solid acid catalysts by simple water removal methods. Catal. Commun. 10, 1849–1853. https://doi.org/10.1016/j.catcom.2009.06.012

Sidhpuria, K.B., Daniel-Da-Silva, A.L., Trindade, T., Coutinho, J.A.P., 2011. Supported ionic liquid silica nanoparticles (SILnPs) as an efficient and recyclable heterogeneous catalyst for the dehydration of fructose to 5-hydroxymethylfurfural. Green Chem. 13, 340–349. https://doi.org/10.1039/c0gc00690d

Sievers, C., Musin, I., Marzialetti, T., Olarte, M.B.V., Agrawal, P.K., Jones, C.W., 2009.

Acid-catalyzed conversion of sugars and furfurals in an ionic-liquid phase. ChemSusChem 2, 665–671. https://doi.org/10.1002/cssc.200900092

Ståhlberg, T., Rodriguez-Rodriguez, S., Fristrup, P., Riisager, A., 2011. Metal-free dehydration of glucose to 5-(Hydroxymethyl)furfural in ionic liquids with boric acid as a promoter. Chem. - A Eur. J. 17, 1456–1464. https://doi.org/10.1002/chem.201002171

Su, Y., Brown, H.M., Huang, X., Zhou, X. dong, Amonette, J.E., Zhang, Z.C., 2009. Single-step conversion of cellulose to 5-hydroxymethylfurfural (HMF), a versatile platform chemical. Appl. Catal. A Gen. 361, 117–122. https://doi.org/10.1016/j.apcata.2009.04.002

Sun, J.X., Sun, X.F., Zhao, H., Sun, R.C., 2004. Isolation and characterization of cellulose from sugarcane bagasse. Polym. Degrad. Stab. 84, 331–339. https://doi.org/https://doi.org/10.1016/j.polymdegradstab.2004.02.008

Tan, M.X., Zhao, L., Zhang, Y., 2011. Production of 5-hydroxymethyl furfural from cellulose in CrCl2/Zeolite/BMIMCl system. Biomass and Bioenergy 35, 1367–1370. https://doi.org/10.1016/j.biombioe.2010.12.006

Tian, G., Tong, X., Cheng, Y., Xue, S., 2013. Tin-catalyzed efficient conversion of carbohydrates for the production of 5-hydroxymethylfurfural in the presence of quaternary ammonium salts. Carbohydr. Res. 370, 33–37. https://doi.org/10.1016/j.carres.2013.01.012

Tong, X., Li, Y., 2010. Efficient and selective dehydration of fructose to 5-hydroxymethylfurfural catalyzed by brønsted-acidic ionic liquids. ChemSusChem 3, 350–355. https://doi.org/10.1002/cssc.200900224

Torres, A.I., Daoutidis, P., Tsapatsis, M., 2010. Continuous production of 5-hydroxymethylfurfural from fructose: A design case study. Energy Environ. Sci. 3, 1560–1572. https://doi.org/10.1039/c0ee00082e

Toteva, M.M., Silvaggi, N.R., Allen, K.N., Richard, J.P., 2011. Binding energy and catalysis by d -xylose isomerase: Kinetic, product, and X-ray Crystallographic analysis of enzyme-catalyzed isomerization of (R)-glyceraldehyde. Biochemistry 50, 10170–10181. https://doi.org/10.1021/bi201378c

Tucker, M.H., Crisci, A.J., Wigington, B.N., Phadke, N., Alamillo, R., Zhang, J., Scott, S.L., Dumesic, J.A., 2012. Acid-functionalized SBA-15-type periodic mesoporous organosilicas and their use in the continuous production of 5-hydroxymethylfurfural. ACS Catal. 2, 1865–1876. https://doi.org/10.1021/cs300303v

van Putten, R.-J., van der Waal, J., de Jong, E., Rasrendra, B., Heeres, H.J., de Vries, J.G.,

2013. Hydroxymethylfurfural, A Versatile Platform Chemical Made from Renewable Resources. Chem.Rev. 113, 1499–1597. https://doi.org/10.1021/cr300182k

Várhegyi, G., Szabó, P., Mok, W.S.-L., Antal, M.J., 1993. Kinetics of the thermal decomposition of cellulose in sealed vessels at elevated pressures. Effects of the presence of water on the reaction mechanism. J. Anal. Appl. Pyrolysis 26, 159–174. https://doi.org/https://doi.org/10.1016/0165-2370(93)80064-7

Vinke, P., van Bekkum, H., 1992. The Dehydration of Fructose Towards 5-Hydroxymethylfurfural Using Activated Carbon as Adsorbent. Starch - Stärke 44, 90–96. https://doi.org/10.1002/star.19920440303

Wang, F., Shi, A.W., Qin, X.X., Liu, C.L., Dong, W.S., 2011. Dehydration of fructose to 5-hydroxymethylfurfural by rare earth metal trifluoromethanesulfonates in organic solvents. Carbohydr. Res. 346, 982–985. https://doi.org/10.1016/j.carres.2011.03.009

Wang, J., Ren, J., Liu, X., Xi, J., Xia, Q., Zu, Y., Lu, G., Wang, Y., 2012. Direct conversion of carbohydrates to 5-hydroxymethylfurfural using Sn-Mont catalyst. Green Chem. 14, 2506–2512. https://doi.org/10.1039/c2gc35699f

Wang, J., Xu, W., Ren, J., Liu, X., Lu, G., Wang, Y., 2011. Efficient catalytic conversion of fructose into hydroxymethylfurfural by a novel carbon-based solid acid. Green Chem. 13, 2678–2681. https://doi.org/10.1039/c1gc15306d

Wang, T., Gallo, J.M.R., Shanks, B.H., Dumesic, J.A., 2012. Production of 5-Hydroxymethylfurfural from Glucose Using a Combination of Lewis and Brønsted Acid Catalysts in Water in a Biphasic Reactor with an Alkylphenol Solvent. https://doi.org/10.1021/cs300192z

Watanabe, M., Aizawa, Y., Iida, T., Aida, T.M., Levy, C., Sue, K., Inomata, H., 2005. Glucose reactions with acid and base catalysts in hot compressed water at 473 K. Carbohydr. Res. 340, 1925–1930. https://doi.org/10.1016/j.carres.2005.06.017

Wei, Z., Liu, Y., Thushara, D., Ren, Q., 2012. Entrainer-intensified vacuum reactive distillation process for the separation of 5-hydroxylmethylfurfural from the dehydration of carbohydrates catalyzed by a metal salt-ionic liquid. Green Chem. 14, 1220–1226. https://doi.org/10.1039/c2gc16671b

Weingarten, R., Conner, W.C., Huber, G.W., 2012. Production of levulinic acid from cellulose by hydrothermal decomposition combined with aqueous phase dehydration with a solid acid catalyst. Energy Environ. Sci. 5, 7559–7574. https://doi.org/10.1039/c2ee21593d

Welker, M.C., Balasubramanian, K.V., Petti, C., Rai, M.K., DeBolt, S., Mendu, V., 2015.

Engineering Plant Biomass Lignin Content and Composition for Biofuels and Bioproducts. Energies . https://doi.org/10.3390/en8087654

Xiao, S., Liu, B., Wang, Y., Fang, Z., Zhang, Z., 2014. Efficient conversion of cellulose into biofuel precursor 5-hydroxymethylfurfural in dimethyl sulfoxide-ionic liquid mixtures. Bioresour. Technol. 151, 361–366. https://doi.org/10.1016/j.biortech.2013.10.095

Xu, Q., Zhu, Z., Tian, Y., Deng, J., Shi, J., Fu, Y., 2014. Sn-MCM-41 as efficient catalyst for the conversion of glucose into 5-hydroxymethylfurfural in ionic liquids. BioResources 9, 303–315.

Yadav, J.S., Reddy, B.V.S., Premalatha, K., 2003. 1-Butyl-3-methylimidazolium Tetrafluoroborate ([Bmim]BF4) Ionic Liquid: A Novel and Recyclable Reaction Medium for the Synthesis of vic-Diamines. Adv. Synth. Catal. 345, 948–952. https://doi.org/10.1002/adsc.200303029

Yan, H., Yang, Y., Tong, D., Xiang, X., Hu, C., 2009. Catalytic conversion of glucose to 5-hydroxymethylfurfural over SO42-/ZrO2and SO42-/ZrO2-Al2O3solid acid catalysts. Catal. Commun. 10, 1558–1563. https://doi.org/10.1016/j.catcom.2009.04.020

Yang, J., De Vigier, K.O., Gu, Y., Jérôme, F., 2015. Catalytic dehydration of carbohydrates suspended in organic solvents promoted by ALCL3/SiO2coated with choline chloride. ChemSusChem 8, 269–274. https://doi.org/10.1002/cssc.201402761

Yang, Y., Xiang, X., Tong, D., Hu, C., Abu-Omar, M.M., 2012. One-pot synthesis of 5-hydroxymethylfurfural directly from starch over SO(4)(2-)/ZrO2-Al2O3 solid catalyst. Bioresour. Technol. 116, 302–306. https://doi.org/10.1016/j.biortech.2012.03.081

Yong, G., Zhang, Y., Ying, J.Y., 2008. Efficient catalytic system for the selective production of 5-hydroxymethylfurfural from glucose and fructose. Angew. Chemie - Int. Ed. 47, 9345–9348. https://doi.org/10.1002/anie.200803207

Yu, Y., Mai, J., Wang, L., Li, X., Jiang, Z., Wang, F., 2014. Ship-in-a-bottle synthesis of amine-functionalized ionic liquids in NaY zeolite for CO2capture. Sci. Rep. 4, 1–8. https://doi.org/10.1038/srep05997

Yuan, Z., Xu, C., Cheng, S., Leitch, M., 2011. Catalytic conversion of glucose to 5-hydroxymethyl furfural using inexpensive co-catalysts and solvents. Carbohydr. Res. 346, 2019–2023. https://doi.org/10.1016/j.carres.2011.06.007

Zakrzewska, M.E., Bogel-łukasik, E., Bogel-łukasik, R., 2011. Ionic Liquid-Mediated Formation of 5-Hydroxymethylfurfural s A Promising Biomass-Derived Building Block 397–417.

Zhang, J., Cao, Y., Li, H., Ma, X., 2014. Kinetic studies on chromium-catalyzed conversion

of glucose into 5-hydroxymethylfurfural in alkylimidazolium chloride ionic liquid. Chem. Eng. J. 237, 55–61. https://doi.org/10.1016/j.cej.2013.10.007

Zhang, J., Yu, X., Zou, F., Zhong, Y., Du, N., Huang, X., 2015. Room-Temperature Ionic Liquid System Converting Fructose into 5-Hydroxymethylfurfural in High Efficiency. ACS Sustain. Chem. Eng. 3, 3338–3345. https://doi.org/10.1021/acssuschemeng.5b01015

Zhang, S., Zhang, J., Zhang, Y., Deng, Y., 2017. Nanoconfined Ionic Liquids. Chem. Rev. 117, 6755–6833. https://doi.org/10.1021/acs.chemrev.6b00509

Zhang, Y., Degirmenci, V., Li, C., Hensen, E.J.M., 2011a. Phosphotungstic acid encapsulated in metal-organic framework as catalysts for carbohydrate dehydration to 5-hydroxymethylfurfural. ChemSusChem 4, 59–64. https://doi.org/10.1002/cssc.201000284

Zhang, Y., Du, H., Qian, X., Chen, E.Y.X., 2010. Ionic liquid-water mixtures: Enhanced Kwfor efficient cellulosic biomass conversion. Energy and Fuels 24, 2410–2417. https://doi.org/10.1021/ef1000198

Zhang, Y., Pidko, E.A., Hensen, E.J.M., 2011b. Molecular Aspects of Glucose Dehydration by Chromium Chlorides in Ionic Liquids. Chem. – A Eur. J. 17, 5281–5288. https://doi.org/10.1002/chem.201003645

Zhang, Z., Liu, B., Zhao, Z., 2012. Conversion of fructose into 5-HMF catalyzed by GeCl4in DMSO and [Bmim]Cl system at room temperature. Carbohydr. Polym. 88, 891–895. https://doi.org/10.1016/j.carbpol.2012.01.032

Zhao, H., Holladay, J.E., Brown, H., Zhang, Z.C., 2007. Metal Chlorides in Ionic Liquid Solvents Convert Sugars to 5-Hydroxymethylfurfural. Science (80-.). 316, 1597 LP – 1600.

Zhao, S., Cheng, M., Li, J., Tian, J., Wang, X., 2011. One pot production of 5-hydroxymethylfurfural with high yield from cellulose by a Brønsted-Lewis-surfactant-combined heteropolyacid catalyst. Chem. Commun. 47, 2176–2178. https://doi.org/10.1039/c0cc04444j

Chapter 2

Materials and Methods

This chapter details the experimental investigations, procedures, and the methods of analyses followed throughout the study. It includes the determination of physicochemical properties, such as structural morphology, size, and crystallinity along with catalyst activities, of zeolites, choline chloride impregnated zeolites, [BMIM]Br encapsulated zeolites and metal-doped semiconductor materials. Specifications of all reagents and chemicals are documented in this chapter. Any specific change or deviation from what is stated here is detailed in the respective section(s) / chapter(s).

2.1 Materials and reagents

Cellulose microcrystalline (purity > 99.5%, w/w), Dextrose (purity > 99.5%, w/w), D-Fructose (purity > 99.5%, w/w) were obtained from Himedia (India) and used as reactants. 5-HMF (purity > 98%, w/w), Levulinic acid (purity > 97%), Lactic acid (purity), and Formic acid (purity 98%, w/w) were procured from SRL (India) and Merck, Mumbai (India). The chemical structure of 5-HMF, Levulinic acid, Lactic acid, Formic acid, and Acetic acid are shown in Fig. 2.1. Other chemicals and reagents were procured mostly from Merck, Mumbai (India). The chemical and reagent details are listed in Table 2.1.

All the zeolite catalysts, i.e., HBeta, HY, NH_3ZSM5, NaY, and NH_3MOR were obtained from Alfa Aesar, the USA. The NH_3 forms of ZSM5 and MOR were converted to H-form by calcining at 400°C for 2 h. The mole ratio (SiO_2/Al_2O_3) of the catalyst is listed in Table 2.2.

Deionized (DI) water (conductivity 0.055 $\mu S.cm^{-1}$) of Millipore Filtration Unit (Elix-3, USA) was used to prepare all the reagents and solutions. All the plastic wares used were made of polypropylene procured from Tarson Products Pvt. Ltd., Kolkata (India). Glassware with a low coefficient of thermal expansion was mostly obtained from Borosil, Mumbai (India).

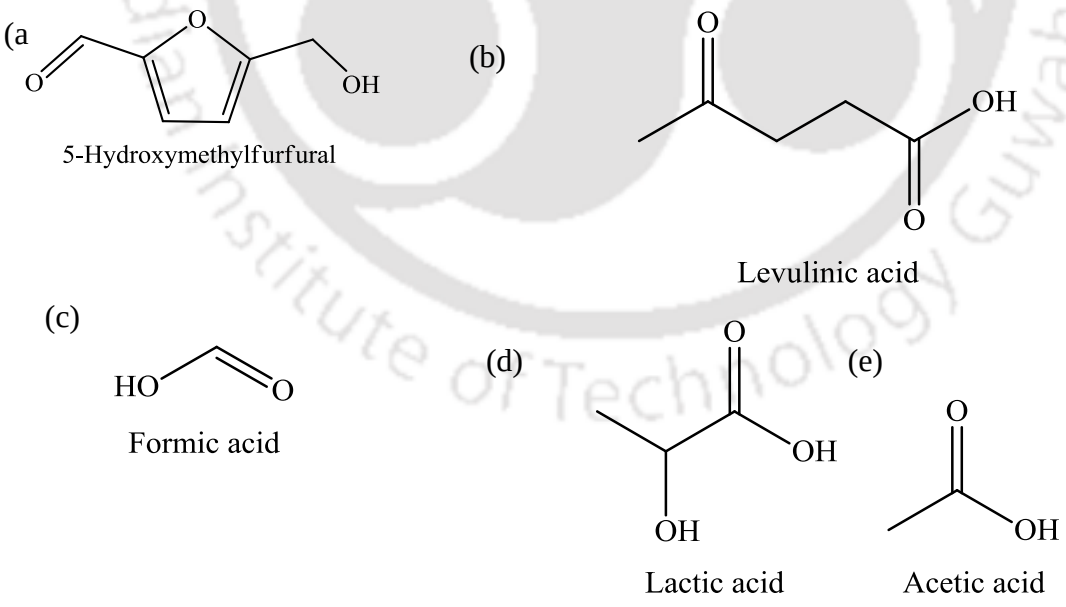

Figure 2.1: Chemical structure of (a) 5-HMF, (b) Levulinic acid, (c) Formic acid, (d) Lactic acid, and (e) Acetic acid.

Table 2.1: List of chemicals/reagents used to prepare model effluent and reagents/ solutions to carry out this work.

Reagents/chemicals	Purity (%)	Grade	Make
5-HMF ($C_6H_6O_3$)	98	GR	SRL (India)
D-Fructose ($C_6H_{12}O_6$)	99.5	AR	Hi-media (India)
Cellulose microcrystalline	99.5	AR	
Dextrose ($C_6H_{12}O_6$)	99.5	AR	
Acetic acid (CH_3COOH)	99.6	AR	
Methyl isobutyl ketone ($C_6H_{12}O$)	98	AR	
Formic acid (CH_2O_2)	98	GR	Loba-Chemie, Mumbai (India)
Furfural ($C_5H_4O_2$)	98.5	GR	
Lactic acid ($C_3H_6O_3$)	97	GR	
Choline chloride ($C_5H_{14}ClNO$)	98	AR	Merck (India)
1,4 Dioxane ($C_4H_8O_2$)	99.5	AR	
Levulinic acid ($C_3H_8O_3$)	97	GR	
Copper(II) nitrate trihydrate ($Cu(NO_3)_2.3H_2O$)	98	AR	
Acetone (C_3H_6O)	≥ 99.8	AR	
Silicone oil	-	-	
Methanol (CH_3OH)	99	AR	
Potassium bromide (KBr)	99.5	GR	
Sodium chloride (NaCl)	99.5	GR	
Silver nitrate ($AgNO_3$)	99	AR	
Sulphuric acid (H_2SO_4)	98	AR	
Di-Sodium hydrogen phosphate anhydrous (Na_2HPO_4)	> 99	AR	
1-Butyl-3-methylimidazolium bromide [BMIM]Br ($C_8H_{15}BrN_2$)	> 97	AR	Sigma Aldrich (India)
Titanium dioxide (TiO_2)	99.5	AR	
Ethanol (C_2H_5OH)	99.9	AR	Changshu Yangyuan Chemicals (China)
Pyridine (C_5H_5N)	99	AR	Alfa aser (USA)
Nickel nitrate hexahydrate ($Ni(NO_3)_2.6H_2O$)	99	AR	
Palladium nitrate ($Pd(NO_3)_2$)	98.5	AR	

Table 2.2: The SiO_2/Al_2O_3 mole ratio of various zeolites used in this study.

Zeolite	SiO_2/Al_2O_3 mole ratio
HBeta	360:1
HY	80:1
HZSM5	80:1
HMOR	20:1
HY	5.1:1
NaY	5.1:1

2.1.1 Selection of *Sechium Edule* and fruit-extract preparation

In this study, metal doped onto TiO_2 were synthesized using the bio-extract prepared from the fruit of *Sechium edule* (or simply *S. edule*) (Fig. 2.2a). It grows abundantly in the North Eastern part of India, and fruits are available in almost all seasons. *S. edule* is fleshy-fibrous and come in different sizes (3-11 cm wide and 4.3-26.5 cm long), colors (from dark or light green to white to pale yellow), and shapes (elongated pyriform, pyriform, subovoid, ovoid, globose) (Cadena-Iñiguez et al., 2007). The surface of these fruits contains woody ridges and, the pulp is whitish pale or green and tastes sweet or insipid. The seed is ovoid, smooth, compressed, and germinates within the fruit. The composition of the *S. edule* is shown in Table 2.3.

This species was originally discovered by Browne (1756) in Jamaica (Browne, 1756) and in 1763 it was classified simultaneously as *Sicyos edulis* by Jacquin (Cadena-Iñiguez et al., 2007) and as *Chocho edulis* by Adanson (Cadena-Iñiguez et al., 2007). Later, Jacquin (1788) changed it to *C. edulis* and placed it in genus Chayota. A few years later, Swartz (1800) became the first to include this species in *Sechium*, when he proposed the combination by which it is still known, *Sechium edule* or *S. edule*.

The major producer countries are Mexico, Costa Rica, Brazil, and the Dominican Republic with 360, 170, 50, and 2.3 thousand tons per year. In Mexico, *S. edule* is in fourth place after avocado, tomato, and coffee as an export product (Cadena-Iñiguez et al., 2007).

In India, Mizoram has the largest production of *S. edule* mainly in Sihphir area being a cooler climate (8 – 32ºC) and good annual rainfall (2500 – 3000 mm) (Singh et al., 2015). In Mizoram, the area of *S. edule* production is increased to 714 hectare (hec) in 2008 from 535 hectare in 2002 and, a typical production is in between 20 and 25 $ton.hec^{-1}$ in organic-rich soil. The production of *S. edule* in Assam (India) is about 20 – 22 $ton.hec^{-1}$ with a total production area of 110 hec in Assam, and the average production in India is about 10 – 15 $ton.hec^{-1}$ based on the total area for vegetable cultivation (Morton, 1981).

The fruit extracts exhibit strong reducing power and, it could convert potassium ferricyanide to potassium ferrocyanide of about 2000 ASE/mg which was used for the antioxidant activity test (Ordonez et al., 2006). ASE means that reducing the power of 1 mg sample is equivalent (E) to reducing the power of 1 nmol ascorbic acid (AS). The analytes present in the extract act as strong electron and hydrogen donors. It could break the radical chain reaction and convert the free radicals into stable products. In fact, this particular study

provides the foundation for the selection of *S. edule* for the bio-mediated synthesis of bio-mediated TiO_2 doping using metal dopants such as Ag, Cu.

Table 2.3: *S. edule* plant details and chemical composition. Data are reported per 100 g of dry matter (Cadena-Iñiguez et al., 2007; Shiga et al., 2015).

Botanical name	*Sechium edule*
Family	Cucurbits
Genus	Sechium
Kingdom	Plant
Tribe	Sicyeae
Order	Cucurbitales
Species	*S. edule*

Composition	**Leaf**	**Fruit**	**Root**
Ascorbic acid, mg	16	29.8	19
Flavonoid content, g	35	19.3	30.5
Energy, cal	60	26 - 30	79
Protein, g	4	0.9 - 1.1	2
Carbohydrates, g	4.7	3.5 - 8.4	17.8
Phosphorus, µg	108	20 - 27	34
Calcium, mg	21.7 - 69.5	6.1 - 19	6.1 - 17.5
Nitrogen, g	0.49 - 0.778	0.95 - 0.156	0.332
Thiamine, mg	0.043 - 0.0119	0.03 - 0.33	0.041 - 0.08
Roboflavin, mg	0.124 - 0.208	0.03 - 0.37	0.05 - 0.028
Niacin, mg	0.919 - 1.19	0.35 - 1.1	0.7 - 1.04

2.1.2 Preparation of bio-extract

S. edule (Fig. 2.2a) was purchased from the market located at Indian Institute of Technology Guwahati, India. The cleaned fruits were cut into small pieces (10 mm × 10 mm × 10 mm) and, the bio-extract was prepared by heating 1 g fruit pieces (Fig. 2.2b) per 8 mL deionized water (DI water) for 12 h at 90±2°C. The clear bio-extract was collected after the filtration using the nylon mesh followed by the membrane filter (0.45 µm, Pall membrane filter, India). The color of the bio-extract was slightly yellowish (Fig. 2.2c) without a distinct spectral absorption peak, but it exhibited a broad absorption band between 200 and 250 nm (Fig. 2.3). The fresh bio-extract was employed immediately for the AgNPs synthesis.

Ascorbic acid (AS) present in *Sechium edule* was first extracted in water and, after that AS concentration in the bio-extract was determined using high-performance liquid chromatography (Model: 26462, Make: Shimadzu, Japan).

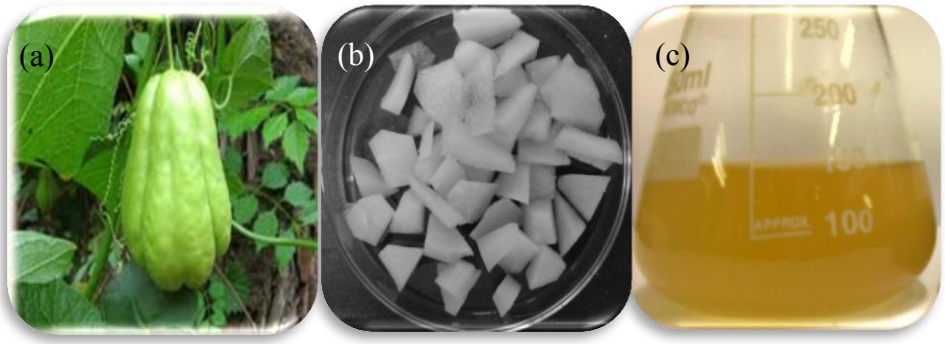

Figure 2.2: Pictorial view of fruits (a), fruit pieces (b) and aqueous bio-extract (c) of *S. edule*.

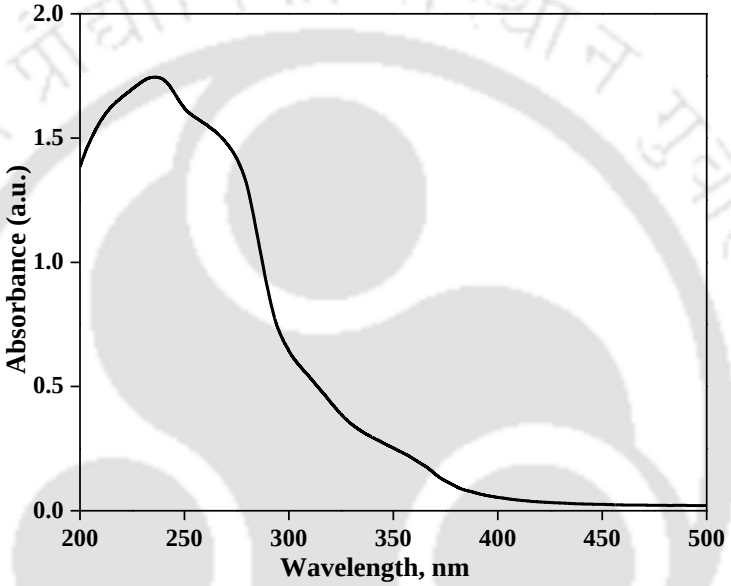

Figure 2.3: Spectral absorbance of *S. edule* fruit aqueous extract at natural pH of 5.8.

2.2 Analytical techniques

2.2.1 Concentration determination of 5-HMF, LA, FA, lactic acid, AA, fructose, and glucose

The samples obtained from the catalyst testing experiments (Chapter 2, Section 2.4) were analyzed by using a High-performance liquid chromatography (HPLC, Model: series 200, Make: Perkin Elmer, Switzerland), equipped with a quaternary pump, a refractive index (RI) detector, and a Hi-Plex H column (300 mm × 7.7 mm). The column temperature was set at 60°C. The mobile phase (0.01M aq. H_2SO_4) was pumped at a flow rate of 0.6 mL.min^{-1}. Glucose, fructose, 5-HMF, lactic acid, acetic acid (AA), formic acid (FA), and levulinic acid (LA) were quantified using 1,4-dioxane as an external calibration standard. The suspended particles appeared, if any, were removed by filtration using 0.2 µm cellulose acetate filter

(Make: Pall India Pvt. Ltd., India; serial no. 08091ID0683). The concentration of (a) glucose, (b) fructose, (c) lactic acid, (d) formic acid, (e) acetic acid, (f) levulinic acid, and (g) 5-HMF were determined from the areas obtained in the HPLC and using the respective calibration curves (Fig. 2.4) and the corresponding retention times are (a) 11.08 min, (b) 11.892 min, (c) 15.383, (d) 16.451 min, (e) 18.01 min, (f) 19.232 min, and (g) 36.147 min, respectively, (Fig. 2.5). The calibration factor was calculated using the following equation (Eq. 2.1).

$$C_i = \frac{\text{Area of i}/\text{Area of 1,4-dioxane}}{\text{Wt.\% of i}/\text{Wt.\% of 1,4-dioxane}} \qquad (2.1)$$

Where, i = Glucose, fructose, 5-HMF, LA, FA, AA or lactic acid. The experiments were usually conducted for two times, and the corresponding errors in the analytical results are shown in the graphs.

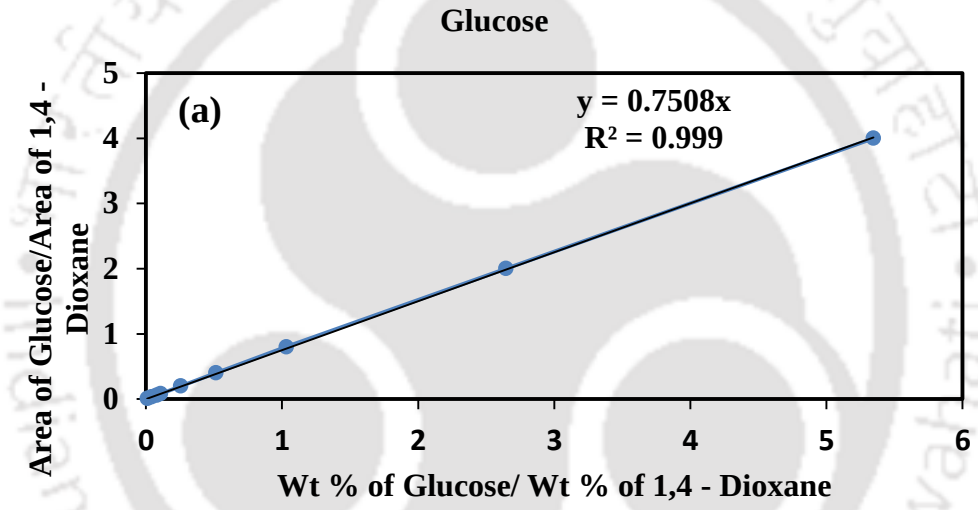

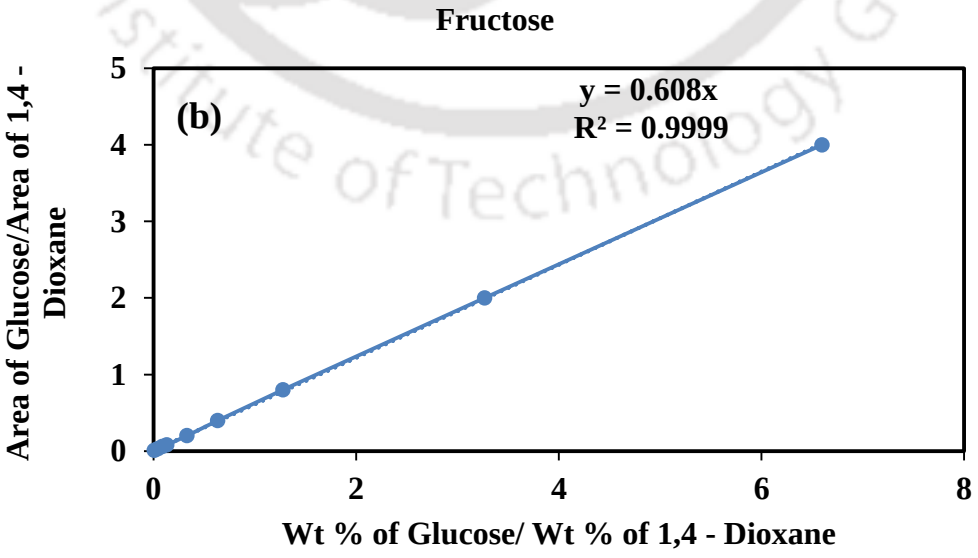

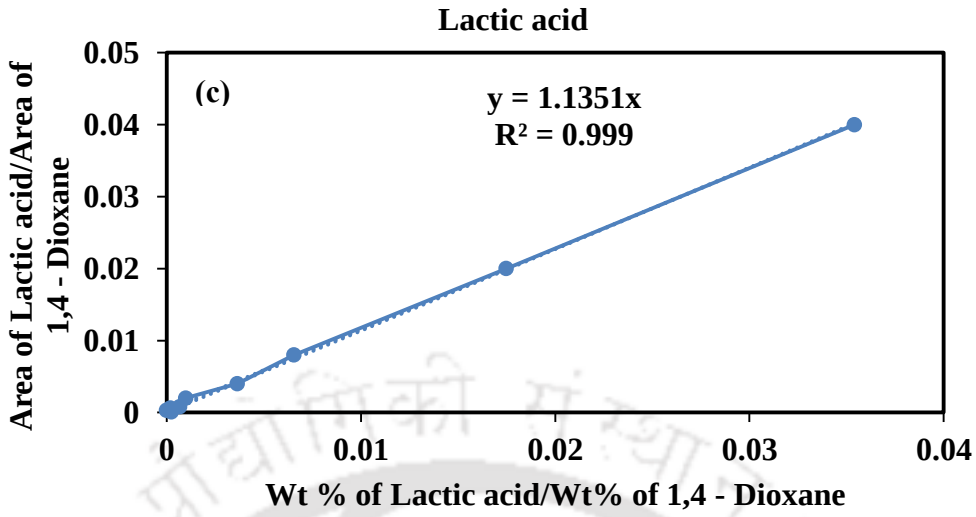

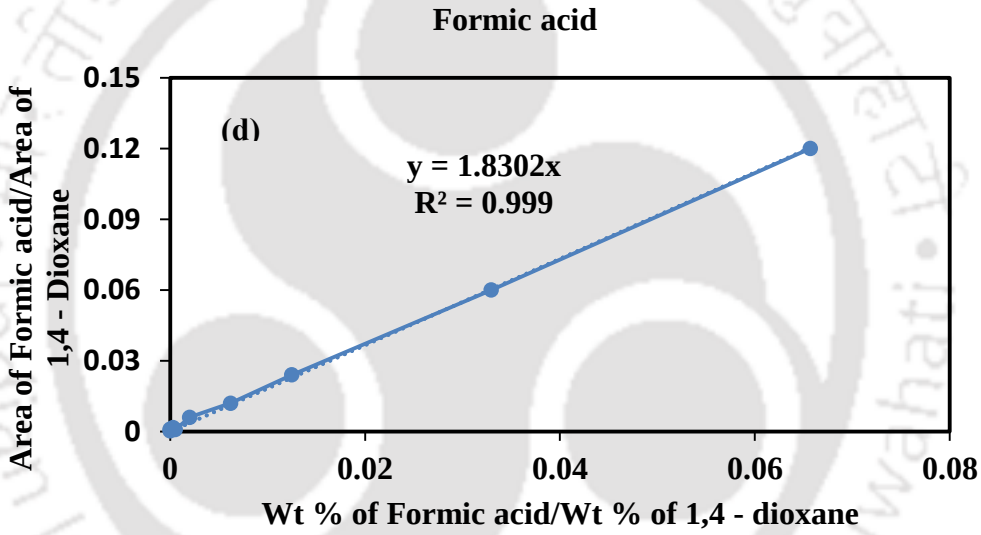

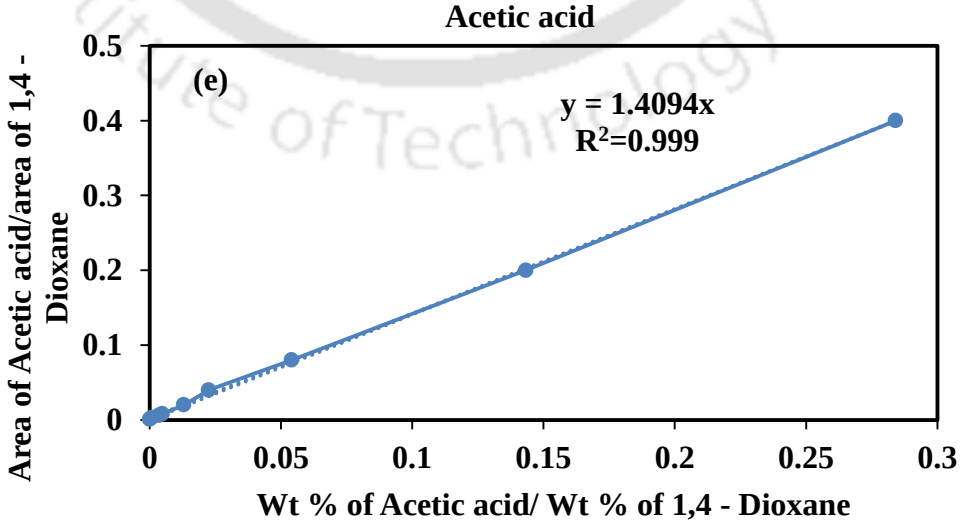

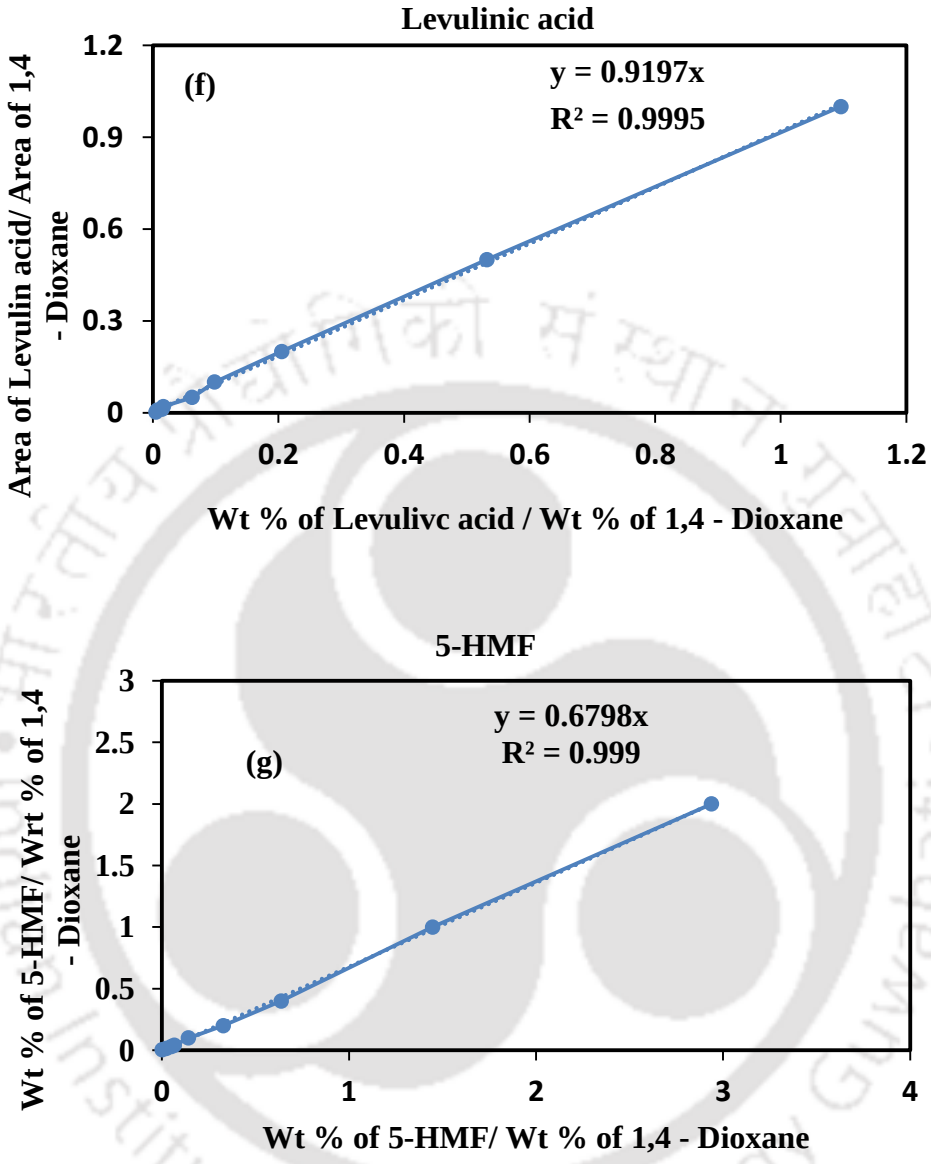

Figure 2.4. Calibration curves of (a) Glucose, (b) Fructose, (c) Lactic acid, (d) Formic acid, (e) Acetic acid, (f) Levulinic acid, and (g) 5-HMF obtained from HPLC.

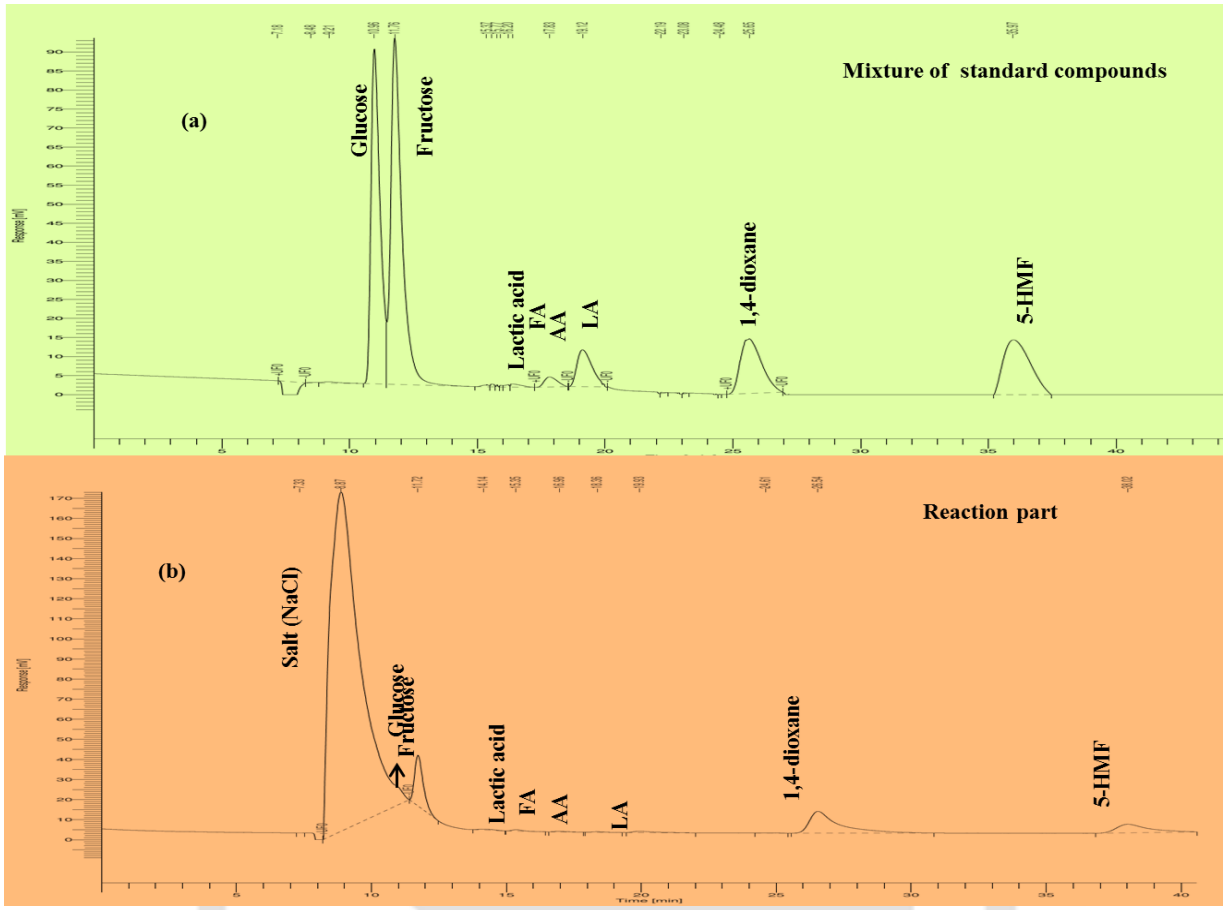

Figure 2.5: Representative HPLC chromatograms of (a) mixture of standard compounds, and (b) reaction products (5-HMF, LA, FA, AA, lactic acid, fructose, and glucose) obtained from HPLC.

2.2.2 FTIR and Py-FTIR spectroscopic analysis

The presence of different functional groups in the bare zeolites as well as on the doped catalysts was confirmed by acquiring the FTIR spectra using the KBr pellet method. KBr salt was dried in a hot air oven (model: N-101, Navyug, India) at 105°C. KBr to the sample in the ratio of 99:1 (w/w) was ground in a clean mortar and pestle for homogenization. It was then transferred to the pellet casting die. The pressure of 5 to 7 tons was imposed to create a thin pellet. The background correction was done with pure KBr pellet by scanning from 450 – 4500 cm^{-1} with a resolution of 4 cm^{-1}. The number of scans was 40 for each specimen for noise reduction. For the liquid sample, a small drop of the bio-extract was added on KBr pellet film. An FTIR spectrophotometer (Model: IR affinity 1, Make: Shimadzu, Japan) was employed for this work.

The concentration of Brønsted (C_{BAS}) and Lewis acid (C_{LAS}) sites was determined by FTIR spectrophotometry (Model: IR Affinity 1, Make: Shimadzu, Japan) in a wavelength

range of 1400 - 1600 cm^{-1} with 30 scans and a resolution of 4 cm^{-1}, using pyridine as a probe molecule. The samples were first heated to 400°C for 1 h, cooled to ambient temperature under vacuum and then purged with N_2. The pyridine was injected under the N_2 atmosphere at room temperature. After soaking the sample in pyridine for about 30 min, the excess pyridine was removed by evacuation at 100°C for 2 h. The C_{LAS} and C_{BAS} were calculated using the extinction coefficients reported by (Emeis, 1993).

2.2.3 Ammonia temperature programmed desorption (NH_3-TPD)

The total acidity of the samples was also determined using ammonia temperature programmed desorption (NH_3-TPD, Model: BELCAT-II, Make: MicrotracBEL, Japan) equipped with a thermal conductivity detector (TCD). In a typical analysis, the sample was pretreated at 400°C for 1 h under helium (He) gas flow (50 $mL.min^{-1}$) and then cooled to 50°C. The sample was saturated with 10% of NH_3/He mixture for 60 min at 50°C. The physisorbed NH_3 was removed under helium flow at 100°C for 10 min. Finally, desorption of ammonia was carried out in the temperature range from 100 to 800°C with a heating rate of 10°C.min^{-1} under helium flow.

2.2.4 Atomic absorption spectroscopy (AAS)

The concentration of metal ions like Ag^{+} and Cu^{2+} in solution during bio-mediated catalyst-doping were determined using AAS (model: AA240FS, Varian, USA). The calibration curve was obtained in the range of 1 to 10 $mg.L^{-1}$ for all metal ions separately, and calibration samples were prepared each time before the analysis. Air-acetylene gas at a flow rate of 400 $L.h^{-1}$ for drying and 150 $L.h^{-1}$ for sheathing were purged. The specific metal hollow cathode lamps were used during analysis.

2.2.5 BET surface area analyzer

The catalyst surface area was obtained using BET analyzer (Model: Autosorb-IQ MP, Make: Quantachrome, USA). Before N_2 adsorption, an amount of 50 mg either bare or doped catalyst powders were degassed at 200°C for 4 h. The parameters such as pore size, pore volume, and Barrett, Joyner, Halenda (BJH) surface area, adsorption or desorption curve were obtained from BET analysis.

2.2.6 Electron microscopic analyses

The size and surface morphology of zeolites and modified zeolites catalyst were obtained using transmission electron microscopy (TEM) (Model: JEM 2100; Make: JEOL, Japan). A quantity of 10 mg specimen particles was dispersed in 25 mL acetone and, the suspension was then placed in the ultrasonic bath for about 30 min to segregate individual particles. One drop suspension was deposited onto the carbon-coated copper grid, and the film on the TEM grid was left for 2 min. The grid was allowed to dry in the hot air oven for about 1 h at 60°C. High-resolution TEM (HRTEM), and selected area diffraction pattern (SAED) were also measured to find out the interplanar spacing and crystal planes with the same instrument.

The same sample preparation procedure was also adopted for field emission scanning electron microscopy (FESEM) using a glass slide instead of a copper grid (model: Sigma, Zeiss, Germany). Energy-dispersive X-ray (EDX) spectroscopy equipped with FESEM was employed for the surface elemental analyses.

2.2.7 Solid-state NMR

Solid-state NMR spectra of ^{27}Al and ^{13}C nuclei were collected using the SS NMR facility (Model: ECX400; Make: JEOL) available at Sophisticated Instruments Facility (SIF), IISc Bangalore, India

2.2.8 Elemental analysis (CHNS)

The CHNS analysis was carried out to determine the ChCl concentrations in the zeolites by using the CHNS analysis facility (Model: EuroEA3000 Elemental Analyser; Make: Euro Vector, Italy) available at Guwahati biotech park, IIT Guwahati, India.

2.2.9 Thermalgravimetric analyses (TGA)

The mass losses of zeolites, modified zeolites and metal-doped and P-doped TiO_2 particles with the temperature were studied by a Thermalgravimetric analyzer (model: TG 209 F1 Libra, NETZSCH, Germany) in the temperature range of 30 to 950°C under nitrogen gas at a heating rate of 10°C min^{-1}. An amount of 10 mg sample was used for the analyses.

2.2.10 X-ray diffraction

The crystallinity of the synthesized modified zeolites and metal-doped semiconductor were studied by employing an X-ray diffractometer (model: D8 Advance, Bruker, Germany) with λ = 0.15406 nm of CuKα radiation at 5° per min scan rate. An amount of 20 mg dried sample was placed into the holder and the XRD patterns were recorded between 5 and 50° 2θ angle for zeolites and modified zeolites. In the case of TiO_2 based catalysts, the XRD patterns were recorded between 20 and 80° 2θ angle.

2.2.11 Zeta potential and particle size measurements

The hydrodynamic particle diameter and zeta-potential were obtained by the dynamic light scattering (DLS) and electrophoretic light scattering (ELS) methods (model: Delsa Nano-C, Beckman Coulter, Switzerland). An amount of 0.2 g catalyst powder was dispersed in 100 mL DI water and then placed in the ultrasonic bath for 20 min at different pH (3-10). The suspended particles were filtrated using 0.2 µm membrane syringe filter (Part no.: C-129M, Axiva Sichem Biotech, India), and the final sample pH was measured (pH/ion 510, Eutech Instruments, Malaysia) before zeta potential measurement. After that, the particle size distribution with average size, polydispersity index, and zeta potential values was recorded.

The details of various instruments used in different parts of this work are summarized in Table 2.4.

Table 2.4: Instrumental details for analysis of modified zeolites and titania catalysts characterizations, and experimental work.

Instrument	Model and make	Purpose	Detection/ working/performance range
Atomic absorption spectrometer	Model: AA240FS Make: Varian, USA	Metal ion concentration determination	Concentration: 1 – 100 $mg.L^{-1}$
Analytical balance	Model: BSA 224S-CW Make: Sartorius, India	Weight measurement	0 to 220 g Resolution: 0.1 mg
BET surface area analyzer	Model: Autosorb-IQ MP, Make: Quantachrome, USA	Surface area determination	Surface area: 0 to 5000 $m^2.g^{-1}$
Field emission scanning electron	Model: Sigma Make: Zeiss,	Size and surface morphology	

microscopy	Germany		
FTIR spectrometer	Model: IR affinity 1 Make: Shimadzu, Japan	Functional group characterization	Frequency: 350 to 4500 cm^{-1}
Hot air oven	Model: ISO 9001-2008 Make: Navyug, India	Moisture removal	Temperature: 30 to 250°C
HPLC instrument	Model: series 200, Make: Perkin Elmer, Switzerland	Concentration determination	0.01 to 1 $\mu g.mL^{-1}$
Magnetic stirrer	Model: Spinot 6020 Make: Tarson, India	Mixing/agitation	Stirrer speed: 100 to 1000 rpm
Micropipette	Model: T100 & T1000 Make: Tarsons products Pvt Ltd., India	µL range liquid dispensing for analytical work	Capacity T100:10 to 100 µL T1000:100 to 1000 µL
CHNS analyzer	Model: EuroEA3000 Elemental Analyser; Make: Euro Vector, Italy	Elemental Concentration determination	Lowest detection limit: 0.2 mg
Microwave oven	Model: MH-2046HB Make: LG Electronics, India	Microwave assisted drying of glassware	Frequency: 2450 MHz (fixed) Microwave: 800 W (fixed)
Millipore water purification unit	Model: Elix 3 Make: Millipore, USA	Preparation of all reagent and test solutions	TOC: < 30 $\mu g\ L^{-1}$ Pyrogens (endotoxins): < 0.001 EU mL^{-1} Water resistivity (@ 25°C): > 5 MΩ.cm
Orbital shaker	Model: LSI-3016R Make: Lab Tech, Korea	Agitation	Maximum speed: 350 rpm Temperature: ± 0.5°C
Delsa Nano	Model No.: Delsa Nano C; Make: M/s Beckman Coulter, Switzerland	Particle size and zeta potential determination	Zeta potential: –100 to + 100 mV Size: 0.6 nm to 30 µm
pH meter	Model: pH 510 Make: Eutech Instruments, Singapore	pH measurement	pH: 0 to 14 Resolution: 0.01 pH
Temperature program reduction	Model: I2720 Make: Micrometrics, Germany	Reducibility of catalyst	Temperature: 0 to 1500°C
Thermal gravimetric analyses	Model: TG 209 F1 Libra Make: NETZSCH, Germany	Mass loss determination	Temperature: 30 to 1100°C
Filed Transmission	Model: JEM 2100	Size and surface	Size: 0.6 nm to 250 µm

electron microscopy	Make: JEOL, Japan	morphology	
Ultrasonic bath	Model: Lab Companion UC-02 Make: Jeiotech, Korea	Mixing	Frequency (sound wave): 40 kHz (fixed) Ultrasonic power: 70 W (fixed)
Ammonia temperature programmed desorption (NH_3-TPD)	Model: BELCAT-II, Make: MicrotracBEL, Japan	Total acidity measurement	
X-ray diffraction	Model: D8 Advance Make: Bruker, Germany	Crystal structure of bare and modified catalysts	2θ = 2 to 100°

2.3 Synthesis of catalysts

2.3.1 Choline chloride impregnation onto zeolites

For the preparation of ChCl/zeolite catalysts, the ChCl was impregnated onto the zeolites using a similar method reported in previous work (Saxena et al., 2017). In brief, 1.00 g of zeolite powder was suspended in 3 mL of methanol and stirred for 1 h and the required amount of ChCl was added slowly to the suspension, under stirring. The mixture was stirred for another 1 h at room temperature. The obtained catalyst was first filtered and then vacuum dried at room temperature. The list of catalysts prepared by this method is presented in Table 2.5.

Table 2.5: List of bare and modified catalysts to carry out this work.

S.No	Catalyst	Method used	Nominal (SAR)	Code used in the further study
1	NaY	Commercial	5.1:1	NaY_5.1.
2	HY	Commercial	5.1:1	HY_5.1
3	HY	Commercial	80:1	HY_80
4*	HMOR	Commercial	20:1	HMOR_20
5*	HZSM5	Commercial	80:1	HZSM5_80
6	HBeta	Commercial	360:1	HBeta_80
7	ChCl/NaY	Impregnation	5.1:1	ChCl/NaY_5.1
8	ChCl/HY	Impregnation	5.1:1	ChCl/HY_5.1
9	ChCl/HY	Impregnation	80:1	ChCl/HY_80
10	ChCl/HMOR	Impregnation	20:1	ChCl/HMOR_20
11	ChClHZSM5	Impregnation	80:1	ChClHZSM5_80
12	ChCl/HBeta	Impregnation	360:1	ChCl/HBeta_360
13	BMIMBr/NaY	Encapsulation	5.1:1	[BMIM]Br/NaY_5.1
14	BMIMBr/HMOR	Encapsulation	20:1	[BMIM]Br/HMOR_20
15	BMIMBr/HY	Encapsulation	80:1	[BMIM]Br/HY_80
16	TiO_2	Commercial	N/A	TiO_2

17	Ag/TiO_2	Bio-mediated doping	N/A	Ag/TiO_2
18	Cu/TiO_2	Bio-mediated doping	N/A	Cu/TiO_2
19	P/TiO_2	Bio-mediated doping	N/A	P/TiO_2
* NH_3-ZSM5 (80) and NH_3-MOR (20) were obtained from Alfa Aesar, the USA. The NH_3 forms of ZSM-5 and MOR were converted to H-form by calcining at 400°C for 2 h. N/A- Not Applicable				

2.3.2 [BMIM]Br encapsulation onto zeolites by a ship-in-a-bottle method

Ionic liquid Butyl-methyl imidazolium bromide ([BMIM]Br) was incorporated within the supercages of zeolites. [BMIM]Br could not be incorporated directly into the zeolite cages/pores as the size of this ionic liquid is much larger than the pore aperture of the zeolites. Hence, the precursors (in this case, N-methylimidazole and 1-bromobutane) of the ionic liquid, much smaller in size, were directed to and allowed them to react within the pores of zeolites. The resultant product of the reaction, [BMIM]Br, was trapped within the zeolite cavities as shown in Fig. 2.6.

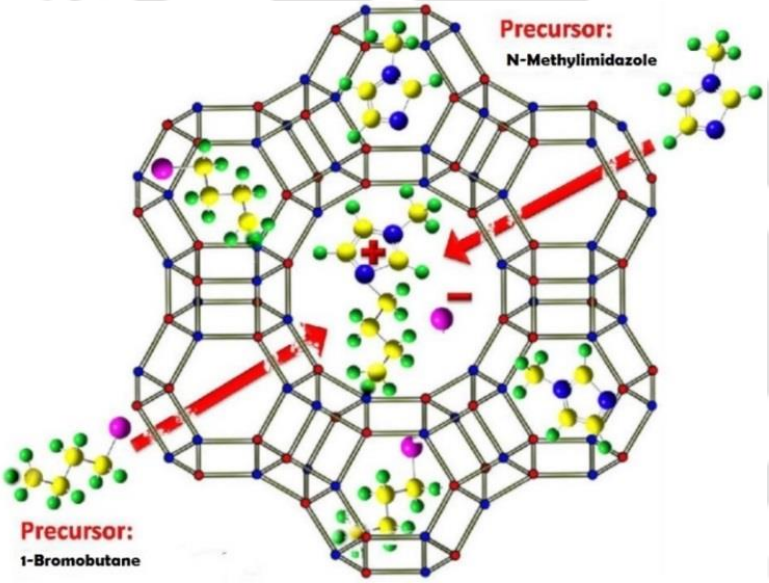

Figure 2.6: Ship- in-bottle strategy for the synthesis of ionic liquid encapsulated zeolites (Yu et al., 2014)**.**

The ionic liquid encapsulated zeolite was prepared according to the following steps as followed from the work of (Yu et al., 2014). An amount of 0.82 g N-methylimidazole and 3 g of zeolite were added to 10 g of ethanol in a conical flask and was continuously stirred for 24 h at room temperature. After 24 h, a solution of 1.36 g 1-bromobutane in 10 g ethanol was added to the flask and the contents of the flask were shifted to a round bottom flask and refluxed for another 24 h. This step enables the reaction to occur. The mixture obtained after

refluxing was washed and filtered with ethanol (3 × 20 ml) prior to Soxhlet extraction for 24 h with ethanol as solvent. Soxhlet extraction was used to remove any loosely bonded ILs and the unreacted reactants. The product obtained after extraction was then dried in a vacuum oven for 24 h at 80ºC. The final product obtained was white solid powder. The list of catalysts prepared by this method is presented in Table 2.5.

2.3.3 Bio-mediated doping method

An amount of 2 g of semiconductor supports, i.e., TiO_2 powder was dispersed in 200 mL of $AgNO_3$ solution (ethanol: water = 1: 99 v/v) corresponding to Ag-concentration from 0.25 to 2 g per 100 g catalyst, and adjusted the solution pH (3 to 11) using 0.1 N H_2SO_4 or NaOH (Fig. 2.7). Ethanol acts as e^- donor to react irreversibly with h^+ leading to the suppression of e^- and h^+ recombination (Chowdhury et al., 2012; Rao and Golder, 2016). The obtained dispersion was stirred for 60 min to equilibrate Ag^+ adsorption onto TiO_2. It was then centrifuged at 4500 rpm for 20 min, and the clear solution obtained was separated for the residual Ag^+ concentration determination. Ag^+/TiO_2 residue was collected and rinsed with DI water to remove loosely or un-adsorbed Ag^+ ions. The true Ag-loading onto the surface of TiO_2 was determined from the concentration of un-adsorbed Ag^+ in the discards. Thus formed residue was again dispersed in 180 mL DI water, and a 20 mL *Sechium edule* extract was added under a continuous stirring at 320 rpm on a magnetic stirrer of Tarsons (Spinnot, India). The stirring was continued for 24 h to achieve the complete reduction of Ag^+. The reaction time was determined by the highest concentration of Ag^+ used in bio-mediated doping, however, without TiO_2. In fact, the color of the reaction mixture was turned from milky white to light brown even within 3 h of reaction, which was indicative to the conversion of Ag^+ ions to AgNPs on the semiconductor surface. The resulting brown colored Ag-doped semiconductor was collected by filtration using 0.45 µm filter paper (Pall membrane filter, India) and rinsed 4 times with ethanol followed by DI water to eliminate the bio-residuals. Ag/TiO_2 was then dried at 100 ºC in a hot-air oven (N-101, Navyug, India) for 12 h and ground in a mortar and pestle. The functionalization of metal-doped titania (TiO_2) at different stages is shown in Figure 2.9. The synthesized particles were stored in an airtight container in the dark before the characterizations and catalyst activity test. A similar procedure was employed for the preparation of Cu- and P-doped TiO_2 catalysts. The precursors used for the doping of Cu and P were Copper (II) nitrate trihydrate and di-sodium hydrogen phosphate anhydrous, respectively. The list of catalysts prepared by this method is presented in Table 2.5.

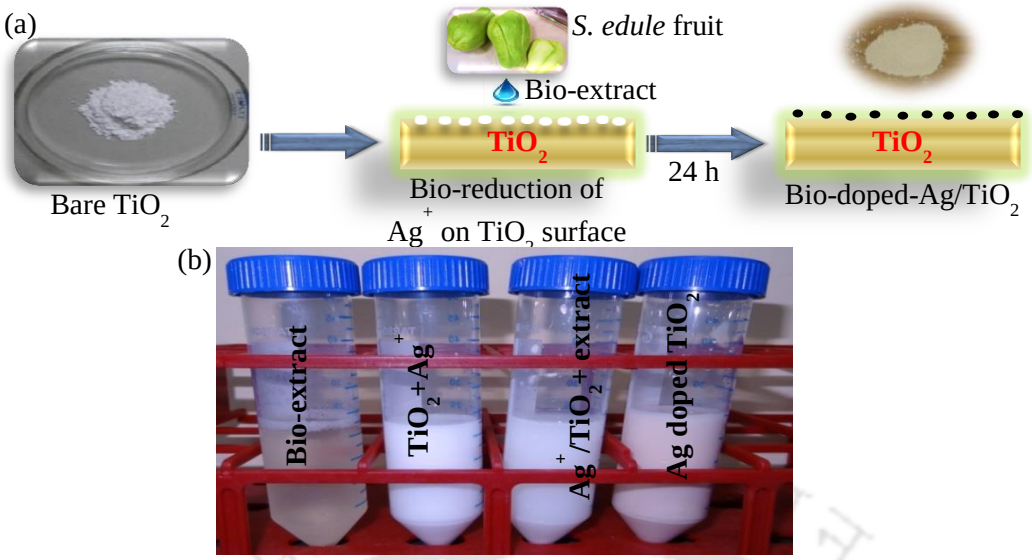

Figure 2.7: (a) Schematic steps showing functionalization of metal-doped TiO_2 catalyst using Ag-dopant. (b) The pictorial view of bio-extract and reaction mixture.

2.4 Catalyst testing experimental procedure

The required amounts of the reaction mixture (water + carbohydrate substrate (cellulose, glucose or fructose) + NaCl + catalyst) and extraction phase (MIBK) were added to a Teflon lined stainless steel autoclave reactor (the schematic diagram is shown in Fig. 2.8) and sealed properly to avoid any leaks. The reactor was placed in an oil bath which was pre-stabilized at desired reaction temperature. After the run, the reaction was quenched by placing the reactor in an ice bath. The catalyst and the solid products formed were separated from the liquid using a 0.2 µm nylon membrane filter. Then, the reaction and extraction phases were separated by using a separating funnel.

The compounds present in both the phases were quantified separately using an HPLC (as described in the Section 2.2.1). The conversion of carbohydrate and yield of products were calculated using the following formulae (Eq. 2.2 – 2.4):

$$\text{Conversion of carbohydrate (\%)} = \frac{(\text{Mass of carbohydrate fed} - \text{Mass of carbohydrate remained})}{\text{Mass of carbohydrate fed}} \times 100 \qquad 2.2$$

$$\text{Yield of i (\%)} = \frac{\text{Moles of i formed}}{\text{Moles of carbohydrate fed}} \times 100 \qquad 2.3$$

$$\text{where i is } 5-\text{HMF, LA, FA, AA or Fructose}$$

$$\text{Selectivity to } 5-\text{HMF (\%)} = \frac{\text{Moles of } 5-\text{HMF formed}}{\text{Moles of carbohydrate converted}} \times 100 \qquad 2.4$$

Note: In the case of cellulose, the yield was calculated based on the equivalent glucose units (molecular weight 164.12 $g.mol^{-1}$).

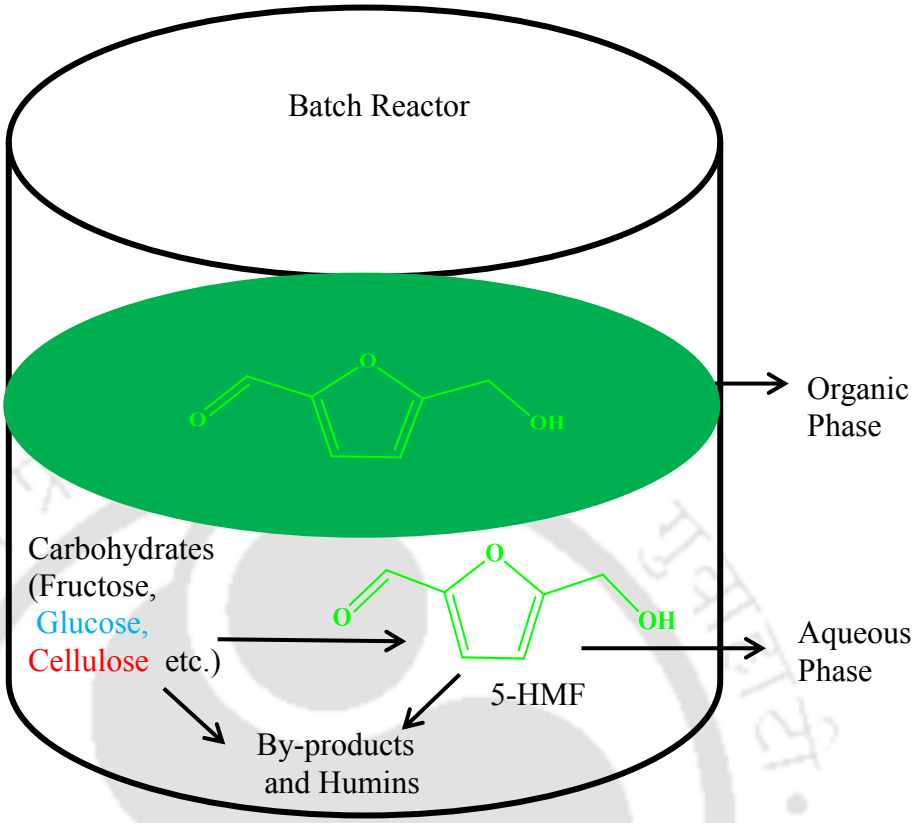

Figure 2.8: The batch process for the production of 5-HMF from carbohydrates. The green part indicates the organic phase (MIBK) and white part contains the aqueous phase which contains carbohydrates, catalyst, sodium chloride, DI water (dH_2O) (Nikolla et al., 2011).

2.4.1 Catalyst stability test

The reusability of catalysts was investigated at the optimal conditions. The catalyst sample obtained after each reaction was washed two times with dH_2O (5 mL) and used in the next experiment without any further treatment.

References

Browne, P., 1756. Civil and natural history of Jamaica. London, England.

Cadena-Iñiguez, J., Arévalo-Galarza, L., Avendaño-Arrazate, C.H., Soto-Hernández, M., Ruiz-Posadas, L. del M., Santiago-Osorio, E., Acosta-Ramos, M., Cisneros-Solano, V.M., Aguirre-Medina, J.F., Ochoa-Martínez, D., 2007. Production, genetics, postharvest management and pharmacological characteristics of Sechium edule (Jacq.) Sw. Fresh Prod. 1, 41–53.

Chowdhury, P., Moreira, J., Gomaa, H., Ray, A.K., 2012. Visible-solar-light-driven

photocatalytic degradation of phenol with dye-sensitized TiO2: Parametric and kinetic study. Ind. Eng. Chem. Res. 51, 4523–4532.

De Graaf, J., Van Dillen, A.J., De Jong, K.P., Koningsberger, D.C., 2001. Preparation of highly dispersed Pt particles in zeolite Y with a narrow particle size distribution: Characterization by hydrogen chemisorption, TEM, EXAFS spectroscopy, and particle modeling. J. Catal. 203, 307–321. https://doi.org/10.1006/jcat.2001.3337

Emeis, C.A., 1993. Determination of integrated molar extinction coefficients for infrared absorption bands of pyridine adsorbed on solid acid catalysts. J. Catal. https://doi.org/10.1006/jcat.1993.1145

Morton, J.F., 1981. The chayote, A perennial, climbing, subtropical vegetable. Proc. Florida State Hortic. Soc. 94, 240–245.

Nikolla, E., Román-Leshkov, Y., Moliner, M., Davis, M.E., 2011. "One-pot" synthesis of 5-(hydroxymethyl)furfural from carbohydrates using tin-beta zeolite. ACS Catal. 1, 408–410. https://doi.org/10.1021/cs2000544

Ordonez, A.A.L., Gomez, J.D., Vattuone, M.A., Isla, M.I., 2006. Antioxidant activities of Sechium edule (Jacq.) Swartz extracts. Food Chem. 97, 452–458. https://doi.org/10.1016/j.foodchem.2005.05.024

Rao, C.V., Golder, A.K., 2016. Development of a bio-mediated technique of silver-doping on titania. Colloids Surfaces A Physicochem. Eng. Asp. 506, 557–565. https://doi.org/10.1016/j.colsurfa.2016.07.031

Saxena, P., Velaga, B., Peela, N.R., 2017. Ionic Liquid-Encapsulated Zeolite Catalysts for the Conversion of Glucose to 5-Hydroxymethylfurfural. ChemistrySelect 2, 10379–10386. https://doi.org/10.1002/slct.201701955

Shiga, T.M., Peroni-Okita, F.H.G., Carpita, N.C., Lajolo, F.M., Cordenunsi, B.R., 2015. Polysaccharide composition of raw and cooked chayote (Sechium edule Sw.) fruits and tuberous roots. Carbohydr. Polym. 130, 155–165. https://doi.org/10.1016/j.carbpol.2015.04.055

Singh, B.K., Ramakrishna, Y., Verma, V.K., 2015. Chow-chow (Sechium edule): Best alternative to shifting cultivation in Mizoram. Indian J. Hill Farming 28, 158–161.

Yu, Y., Mai, J., Wang, L., Li, X., Jiang, Z., Wang, F., 2014. Ship-in-a-bottle synthesis of amine-functionalized ionic liquids in NaY zeolite for CO2capture. Sci. Rep. 4, 1–8. https://doi.org/10.1038/srep05997

Chapter 3

Efficient Conversion of Carbohydrates to 5-HMF over Mesoporous Zeolites

3.1 Specific overview

The research on biomass conversion to value-added chemicals is gaining significant attention in recent years. The second generation (lignocellulosic) biomass such as agricultural and forest residues, contains cellulose, hemicellulose, and lignin as major building blocks (Besson et al., 2014; Chatterjee et al., 2015; Corma Canos et al., 2007; Luterbacher et al., 2014; Taarning et al., 2011). 5-HMF is an important platform chemical that can be derived from biomass, particularly from cellulose which is a polymer of glucose (Zhang et al., 2015). 5-HMF has numerous applications in polymers, solvent industries, and bio-fuels (Fonseca and Rafael, 2013; Li et al., 2016b; Zakrzewska et al., 2011).

5-HMF could be produced from fructose, an isomer of glucose, with high yields (Zakrzewska et al., 2011) However, it is costlier and less abundant. Therefore, the direct conversion of glucose and cellulose to 5-HMF has been explored. This process requires the presence of both Brønsted and Lewis acid sites. However, some researchers reported a mechanism which suggests the direct conversion of glucose to 5-HMF without the formation of fructose, which indicates that only Brønsted acid sites are sufficient for the reaction (Li et al., 2016a).

In the early years, homogeneous catalysts have been explored for the direct conversion of glucose and cellulose to 5-HMF. Mineral acids such as H_2SO_4 and HCl are tested for this reaction, but obtained low yields (13% with H_2SO_4 (Qi et al., 2014) and 10% with HCl (Nikolla et al., 2011). Metal chlorides such as $CrCl_3$ alone also resulted in low yields (~10%) (Jia et al., 2014). Higher yields are reported when $CrCl_3$ is used in combination with ionic liquids (IL) or mineral acids (> 70% with IL (Zhao et al., 2007) and 59% with HCl (Zhang et al., 2013). The major issues in using the above mentioned homogeneous catalysts are the

reactor and equipment corrosion, and the difficulty in product separation and catalyst recycle. In contrast, solid acid catalysts have numerous advantages over homogeneous catalysts in terms of product separation, catalyst–life, –recovery, and –recycle (Agirrezabal-Telleria et al., 2014; Hu et al., 2014; Taarning et al., 2011)

Zeolites have also been studied for this reaction (Li et al., 2016b). Hu et al. (2014) studied various zeolites with IL ([BMIM]Cl) as a solvent, and reported 50% yield of 5-HMF from glucose over Beta zeolite. Otomo et al. (2014) tested the Beta zeolites calcined at different temperatures for glucose dehydration. The authors claimed that the high calcination temperatures (750°C) resulted in higher yields of 5-HMF (55%) due to the generation of Lewis acid sites. Most of the studies on zeolites as well as other solid acid catalysts involve the use of either dimethylsulfoxide (DMSO) or IL as solvents (Li et al., 2016b; Shahangi et al., 2018; Zhang et al., 2017). However, these high boiling solvents require high energy for the product (5-HMF) separation from them.

In the present study, zeolite catalysts i.e., HBeta, HMOR, HY, and HZSM5 have been tested for the conversion of carbohydrates (fructose, glucose, and cellulose) to 5-HMF in a biphasic system containing eco-friendly solvents (water as reaction phase and MIBK as extraction phase). The effect of reaction conditions such as reaction time, temperature, and the substrate on conversion and yield is studied. Further, the stability (recyclability) of the best catalyst is investigated in this work.

3.2 Results and discussion

3.2.1 Catalyst characterizations

The XRD patterns of HBeta, HMOR, HZSM5, and HY (Fig. 3.1) are matched with the patterns typically found for these catalysts (Mamo et al., 2016; Moreno-Recio et al., 2017). N_2 sorption isotherms of all the zeolites are shown in Fig. 3.2. As expected, all the zeolites are exhibited type IV isotherms, and both micropore and mesopore textures. This is in accordance with the literature (Moreno-Recio et al., 2017). The ratio of mesopore to micropore surface area varied significantly among the catalysts (Table 3.1). For example, for HMOR, the ratio of micropore to mesopore area is 14.5, whereas that for HBeta is 1.49. The BET surface area of HMOR is nearly equal to that of HZSM5. However, the micropore area and micro to mesopore volume ratio of HMOR are higher than those of HZSM5. The average pore size of all the zeolite catalysts is in the similar range of 2.8 – 3.2 nm. Even though

HZSM5 has 10-membered ring structure, the average pore size is similar to that of other 12-membered ring zeolites. This can be attributed to its higher fraction of mesopores.

The NH_3-TPD patterns are shown in Fig. 3.3a. All the zeolites except HMOR exhibit three distinct peaks corresponding to ammonia desorbed from weak, moderate and strong acid sites of the zeolites. Based on the peak temperatures and the corresponding quantity of ammonia desorbed, the acid strength is found to be in the following order: HMOR > HBeta > HY > HZSM5. The NH_3-TPD patterns of the zeolites and their acid strengths are similar to those reported in the literature (Dumitriu and Hulea, 2003; Kulawang, 2015; Srivastava et al., 2015). The total acidity from NH_3-TPD varied as follows: HMOR > HBETA ≈ HZSM5 > HY (Table 3.2). From Py-FTIR spectra, it can be observed that the concentration of Lewis acid sites (C_{LAS}) is increased and the concentration of Brønsted acid sites (C_{BAS}) is decreased with the SiO_2/Al_2O_3 ratio (SAR) (Table 3.2 and Fig. 3.3b). The highest C_{BAS} observed with HMOR zeolite may be due to the higher Al concentration (lower SAR). The highest C_{BAS} observed with HMOR zeolite may be due to the higher Al concentration (lower SAR). The higher Al concentration accommodates more protons, which in turn result in higher Brønsted acidity (Lobo, 2008).

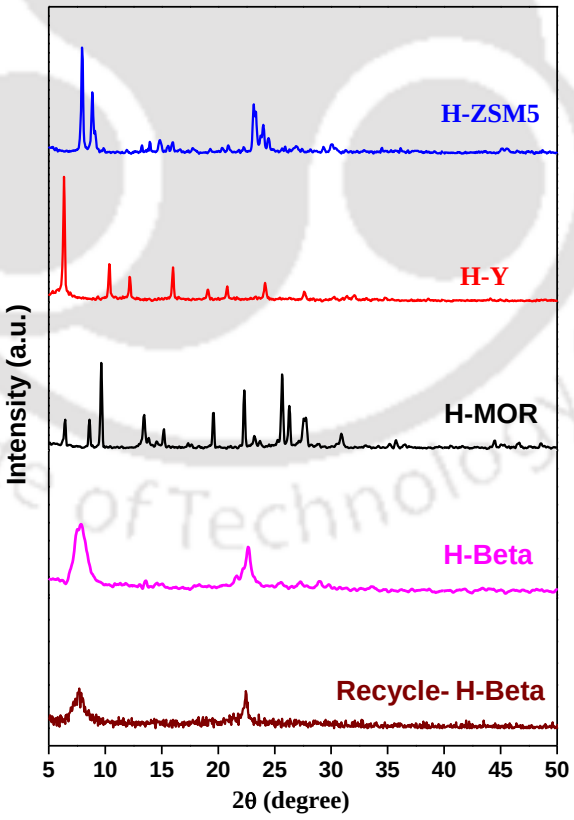

Figure 3.1: The powder XRD patterns of various zeolite catalysts used in this study.

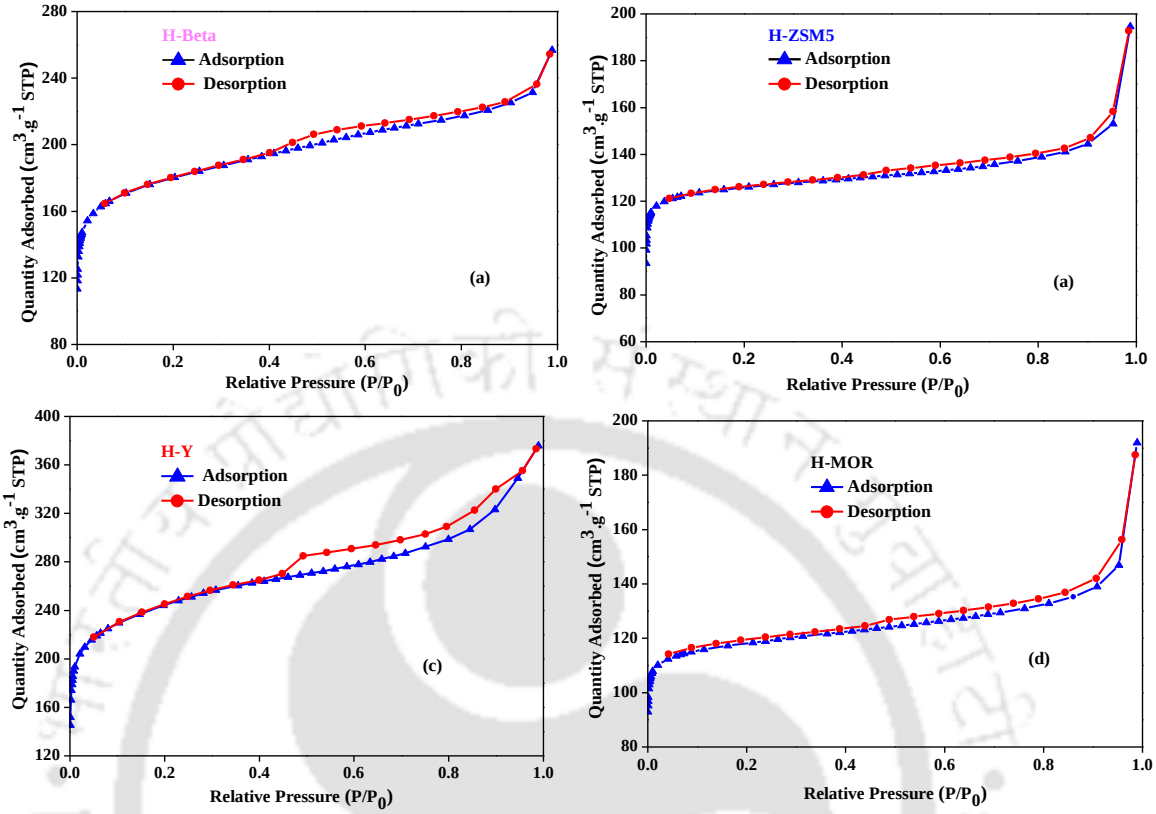

Figure 3.2: N_2 adsorption-desorption isotherms: (a) HBeta, (b) HZSM5, (c) HY, (d) HMOR.

Table 3.1: Textural properties of the catalysts used in this study.

Zeolite (SAR[a])	S_{BET}[b], $m^2.g^{-1}$	S_{BJH}[c], $m^2.g^{-1}$	V_{BJH}[d], $cm^3.g^{-1}$	$S_{t\text{-}plot}$[e], $m^2.g^{-1}$	$V_{t\text{-}plot}$[f], $cm^3.g^{-1}$	V_{TP}[g], $cm^3.g^{-1}$	P_D[h], nm
HBeta (360:1)	563	223	0.206	333	0.179	0.398	2.82
HY (80:1)	773	113	0.229	439	0.231	0.581	2.88
HZSM5 (80:1)	381	70	0.133	315	0.167	0.301	3.16
HMOR (20:1)	386	23	0.093	334	0.164	0.273	2.83

[a]SAR - SiO_2/AlO_3 ratio
[b]S_{BET} - BET surface area
[c]S_{BJH} - BJH mesopore surface area from desorption
[d]V_{BJH} - BJH mesopore volume from desorption
[e]$S_{t\text{-}plot}$ - t-plot micropore surface area
[f]$V_{t\text{-}plot}$ - t-plot micropore volume
[g]V_{TP} - total pore volume calculated at P/Po = 0.99
[h]P_D - Average pore diameter

Table 3.2: Acid site concentration from Py-FTIR and NH_3-TPD analysis.

Sl. no.	Catalyst (SAR[a])	C_{BAS} ($\mu mol.g^{-1}$)[b]	C_{LAS} ($\mu mol.g^{-1}$)[b]	B/L ratio[b]	Total acid site concentration[c] ($\mu mol\ NH_3$).g^{-1}
1	HBeta (360)	119.2	484.8	0.23	47
2	HY (80)	126.5	331.4	0.39	36
3	HZSM5 (80)	179.0	173.1	1.03	44
4	HMOR (20)	926.0	89.2	10.38	143

[a]SAR - SiO_2/AlO_3 ratio
[b]C_{BAS} (concentration of Brønsted acid sites), C_{LAS} (concentration of Lewis acid sites) and B/L (Brønsted acid sites/Lewis acid sites) ratio are measured using FTIR with pyridine as a probe molecule
[c]Total acid site concentration measured from the NH_3-TPD analysis

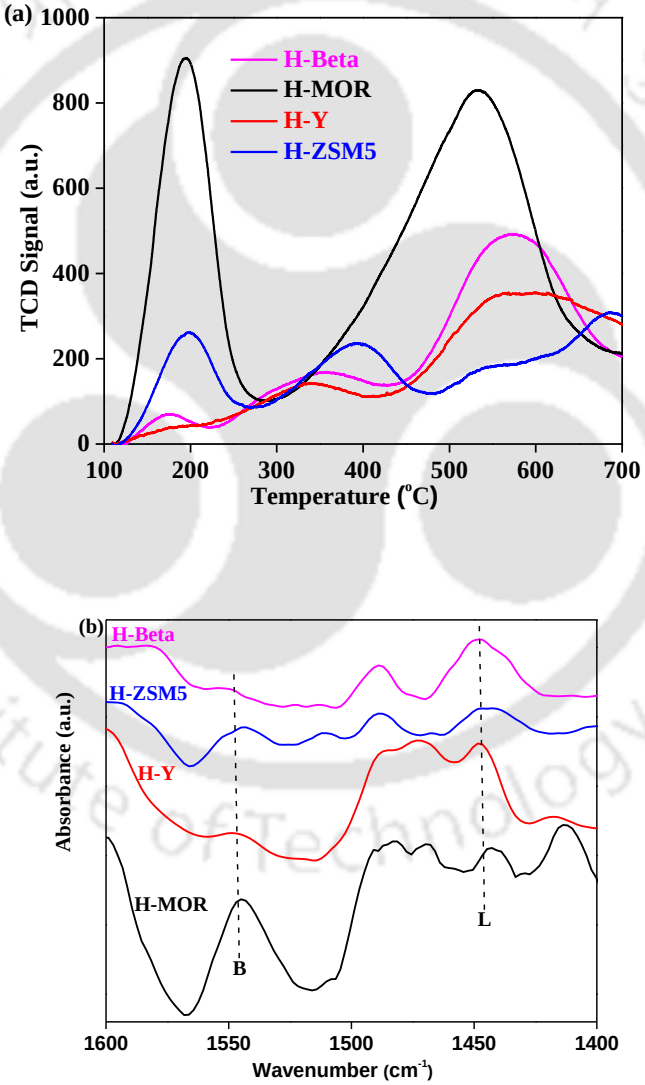

Figure 3.3: Acidity measurements by (a) NH_3–TPD and (b) Pyridine-FTIR, of zeolites HBeta, HMOR, HY, and HZSM5.

3.2.2 Optimization of reaction conditions

Catalyst loading: With the increase in the amount of catalyst from 0.033 to 0.1 g (glucose: catalyst weight ratio = 6:1 – 2:1), at constant glucose weight of 0.2 g, the conversion increases from 31 to 87% (Figure 3.4). However, the maximum 5-HMF yield is found at glucose: catalyst weight ratio of 3:1. A decrease in 5-HMF yield is observed at higher catalyst weights. This can be attributed to side products (LA and FA) formation, as evident from Figure 3.4, due to the availability of higher acid sites than just required for the glucose dehydration reaction (Nandiwale et al., 2014).

NaCl concentration: The addition of NaCl (in the range of 10 – 30%) has a significant influence on the 5-HMF production from glucose (Figure 3.5). In the case of no NaCl but in the presence of the catalyst, the conversion and yields are 26 and 5.8%, respectively. However, even with small amounts of NaCl (10%) addition with H-MOR, the conversion increases to 60% and the yield increases to 25%. Further, the increase in NaCl to its saturation value of 30% resulted in a marginal increase in the conversion (80%) and yield (34%) (Dumesic, 2009).

Water to MIBK ratio: The effect of the ratio of reaction phase (dH_2O) to extraction phase (MIBK) on conversion and yield is shown in Figure 3.6. When no MIBK is used in the experiment, the conversion is 46%, but the yield of 5-HMF is only 5%. As MIBK added as an extraction phase to the reaction system at 1:1 weight ratio, the 5-HMF yield increases significantly to 19% and it further increases to 34% as the ratio increases to 1:2. However, the further increase in the amount of MIBK, the 5-HMF yield decreases marginally. This may be attributed to higher miscibility of MIBK in water with the increase of its portion, which may lead to side product formation. Change in the acidity of the reaction phase, due to a higher concentration of MIBK in it, could be another reason (Dumesic, 2009; Wang et al., 2012).

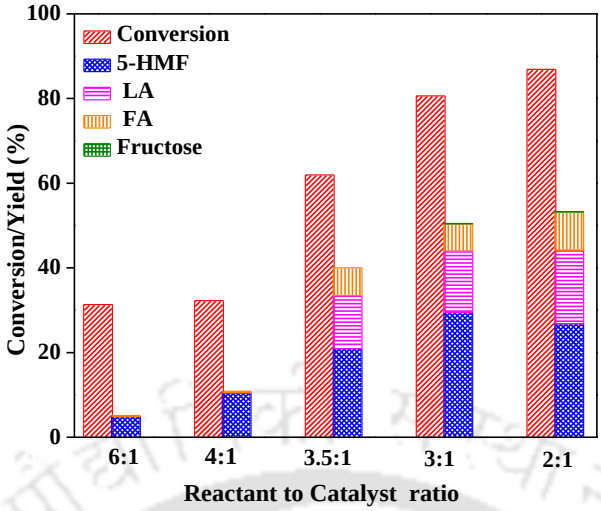

Figure 3.4: Effect of catalyst weight on the conversion of glucose to 5-HMF using HMOR catalyst.

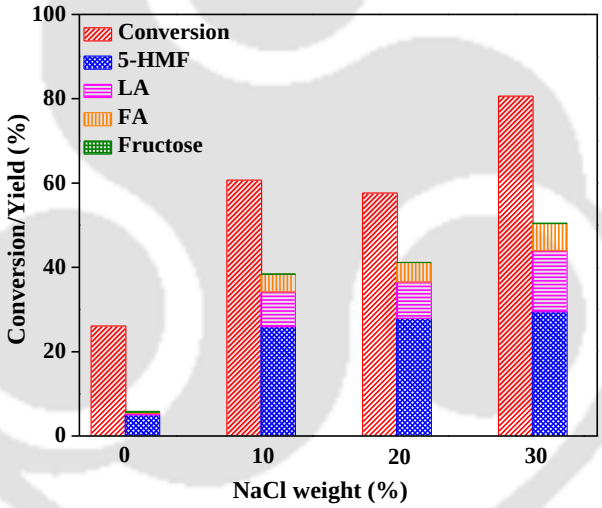

Figure 3.5: Conversion of glucose and yield reaction products (5-HMF, LA, FA, and fructose at different NaCl concentration using HMOR catalyst.

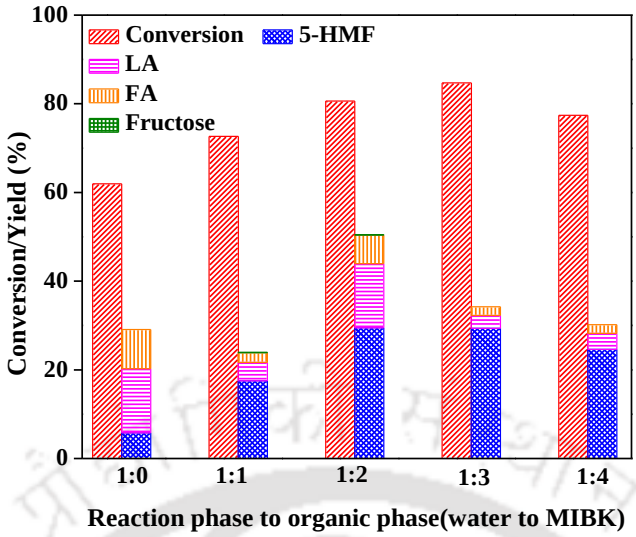

Figure 3.6: Conversion of glucose and yield reaction products (5-HMF, LA, FA, and fructose) at different water to MIBK ratio using H-MOR catalyst.

3.2.3 Performance of various zeolites in glucose to 5-HMF conversion

The effect of reaction temperature (in the range of 160 – 180°C) and reaction time (1.5 – 3 h) on glucose conversion and product yields over HZSM5 is shown in Fig. 3.7 (for experimental conditions please see entries 1 – 6, Table 3.3). The reaction temperature has a significant influence on glucose conversion as well as on the yield of 5-HMF. The glucose conversion and 5-HMF yield are increased from 16 to 71% and from 12 to 46%, respectively, with the temperature. The yields of other reaction products such as LA and FA are increased and that of acetic acid (AA) is nearly constant (~3%) with the temperature. The selectivity to 5-HMF is first increased and then decreased, and selectivities to LA and FA are increased, with the temperature. This implies that HZSM5 favors the rehydration of 5-HMF to LA and FA at high temperatures.

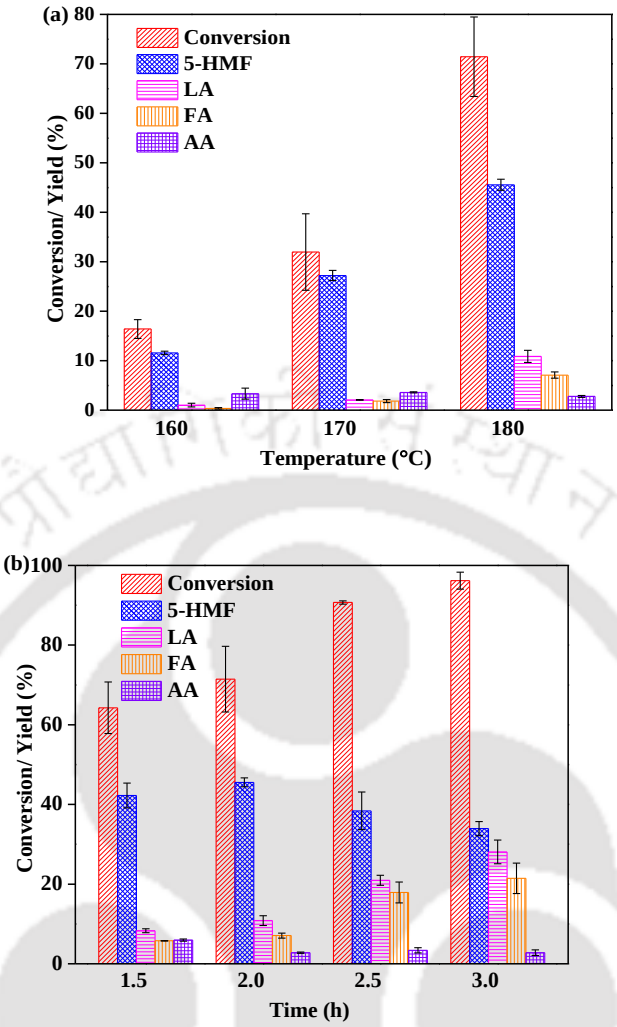

Figure 3.7: Variation of conversion of glucose and yield of reaction products (5-HMF, LA, FA, and fructose) as a function of (a) reaction temperature and (b) reaction time using HZSM5 catalyst.

Table 3.3: Detailed experimental conditions used in this study.

Sl. no.	Temp. (^{o}C), Time (h)	Substrate	Catalyst	Reaction phase composition in 2 g of water			Extraction phase
				NaCl (g)	Catalyst (g)	Substrate (g)	MIBK (g)
1	180, 1.5	Glucose	HZSM5	0.6	0.0667	0.2	4
2	180, 2	Glucose	HZSM5	0.6	0.0667	0.2	4
3	180, 2.5	Glucose	HZSM5	0.6	0.0667	0.2	4
4	180, 3	Glucose	HZSM5	0.6	0.0667	0.2	4
5	160, 2	Glucose	HZSM5	0.6	0.0667	0.2	4
6	170, 2	Glucose	HZSM5	0.6	0.0667	0.2	4

7	180, 2.83	Glucose	HBeta	0.6	0.0667	0.2	4
8	180, 1.58	Glucose	HMOR	0.6	0.0667	0.2	4
9	180, 2	Glucose	HY	0.6	0.0667	0.2	4
10	180, 2	Glucose	HBeta	0	0.0667	0.2	4
11	180, 2	Glucose	HBeta	0	0.0667	0.2	0
12	180, 2	Glucose	HBeta	0.6	0.0667	0.2	0
13	180, 1	Fructose	HBeta	0.6	0.0667	0.2	4
14	180, 2	Cellulose	HBeta	0.6	0.0667	0.2	4
15	180, 3	Cellulose	HBeta	0.6	0.0667	0.2	4
16	180, 4	Cellulose	HBeta	0.6	0.0667	0.2	4
17	180, 3	Cellulose	HBeta-R2	0.6	0.0667	0.2	4
18	180, 3	Cellulose	HBeta-R3	0.6	0.0667	0.2	4
19	180, 3	Cellulose	HBeta-R4	0.6	0.0667	0.2	4
20	180, 3	Cellulose	HBeta-R5	0.6	0.0667	0.2	4

With the reaction time, the glucose conversion is increased from 64 to 96% and the yield of 5-HMF is exhibited a maximum of 46% at 2 h (Fig. 3.7b). The yields of LA and FA are increased with the prolonged reaction time, indicating that the higher residence time is not favorable for the selective conversion of glucose to 5-HMF (Wang et al., 2017). Therefore, a reaction temperature of 180°C and a reaction time of 2 h are found to be the optimum for this catalyst.

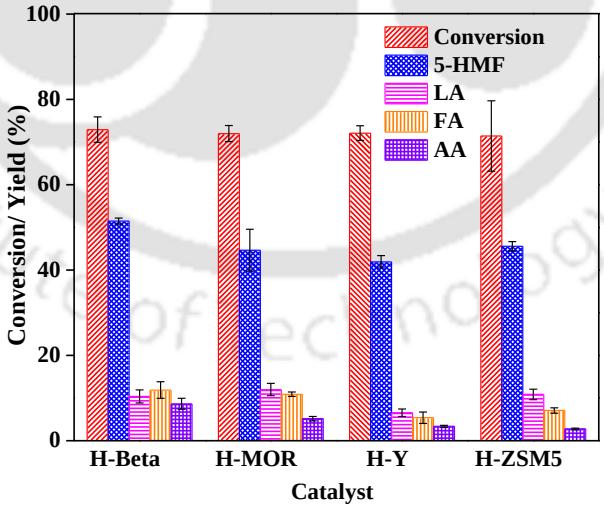

Figure 3.8: Conversion of glucose and yield of reaction products (5-HMF, LA, FA, and AA). (Reaction conditions: 2 g of DI water, 0.2 g of the substrate, glucose: catalyst = 3:1 w/w, 4 g of MIBK, 0.6 g of NaCl, 120 min of reaction time for H-Y and H-ZSM5,170 min for H-Beta, 95 min for H-MOR and 180°C of reaction temperature).

The yields of 5-HMF, LA, FA, and AA over various catalysts (H-Beta, H-MOR, H-Y, and H-ZSM5) are shown in Fig. 3.8. No traces of fructose (not shown in the figure) were found in the reaction products. This indicates that either the fructose was converted to 5-HMF soon after its formation or the reaction proceeds through either open-chain or cyclic mechanism. In the second case, no formation of fructose could be observed. Among the various zeolites, H-Beta exhibited the highest yield of 5-HMF (51.5%) at similar glucose conversion level (72.9%). It might be due to lower C_{BAS} and higher mesoporosity which was revealed by the N_2–sorption data (Table 3.1). The micropore surface area may not be accessible to the reaction due to the larger molecular sizes of reactant and products of the present study. Even if it accessible by the acyclic hexose molecule, the 5-HMF formed may rearrange to higher molecular weight compounds or it will rehydrate to form LA and FA (Agirrezabal-Telleria et al., 2014; Otomo et al., 2015). The catalyst having higher mesoporosity is expected to show a higher yield of 5-HMF (Moreno-Recio et al., 2016; Nandiwale et al., 2014) and that is what we observed in this study. For example, the HBeta (S_{BJH} = 223 $m^2.g^{-1}$) shows a higher yield of 5-HMF (46%) as compared to that (36%) over HMOR (S_{BJH} = 23 $m^2.g^{-1}$). However, the mesoporosity is not playing any role in enhancing the glucose conversion. The lower conversion over HBeta could be attributed to the lower C_{BAS}, as evident from the Py-FTIR. The yields of LA and FA are significantly higher with HMOR as compared to that on other zeolites. The higher C_{BAS} of HMOR may be responsible for the side products formation by rehydration of 5-HMF (Nandiwale et al., 2014). Though the yields of 5-HMF are similar over the zeolites HBeta (45.9%) and HZSM5 (45.6%), the selectivity is significantly higher with the HBeta (73.6 vs. 63.8%). Therefore, the HBeta is used in further study.

The effects of NaCl and the presence of extraction phase on the conversion and yields are also studied over HBeta (entries 10 – 13, Table 3.3; Fig. 3.9). The conversions of glucose (the yield of 5-HMF) without NaCl and in the presence and absence of extraction phase (MIBK) are 24% (16%) and 7% (5%), respectively. Whereas, the conversions of glucose (yields of 5-HMF) with NaCl and in the presence and absence of extraction phase (MIBK) are 62% (46%) and 63% (28%), respectively. Both extraction phase, as well as NaCl, have a significant synergistic effect on the conversion of glucose and yield of 5-HMF. The synergy can be attributed to two primary reasons: (i) salting-out effect, which means upon the addition of NaCl to the biphasic system, the partition coefficient increases (Moreno-Recio et al., 2016; Nandiwale et al., 2014; Román-Leshkov et al., 2007; Wang et al., 2017) and (ii)

reaction mechanism itself may change in the presence of NaCl (Tyrlik et al., 1996; T. Wang et al., 2012) (Combs et al., 2013).

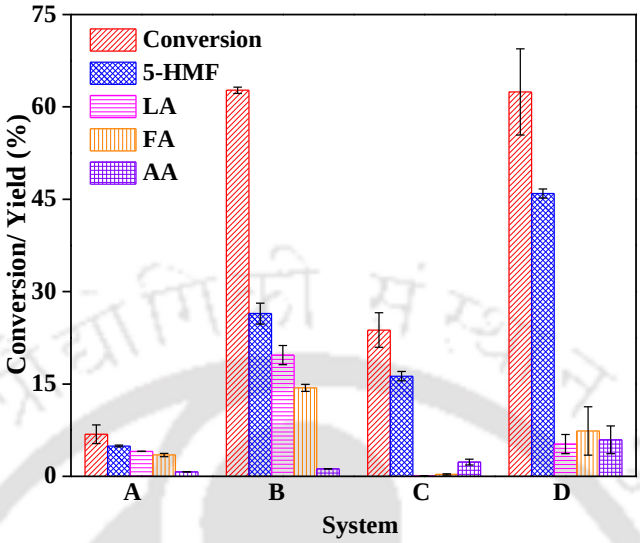

Figure 3.9: Conversion of glucose and yield reaction products (5-HMF, LA, FA, and glucose) over H-Beta catalyst, without (A) and with (B) NaCl in a single phase system and without (C) and with (D) NaCl in a biphasic system; at 180^{o}C and 2 h reaction time.

Mamo et al. (Mamo et al., 2016) compared glucose dehydration with differently modified mordenite zeolites in IL at 100°C for 6 h and reported a 5-HMF yield of 25% with similar pretreatment conditions of the catalyst used in this study. Otomo et al. (Otomo et al., 2014) reported a 5-HMF yield of 9.4% with water as a solvent and of 32% with DMSO, at 180°C and 3 h reaction time. Hu et al. (Hu et al., 2014) used HMOR for glucose dehydration in the presence of IL at 140°C for 30 min and reported a very low 5-HMF yield of 13.1%. Therefore, based on the above comparison of previous studies with the present one, the toxic and uneconomical solvents (such as ILs and DMSO) can be avoided and still obtain better yields by using the mesoporous zeolite.

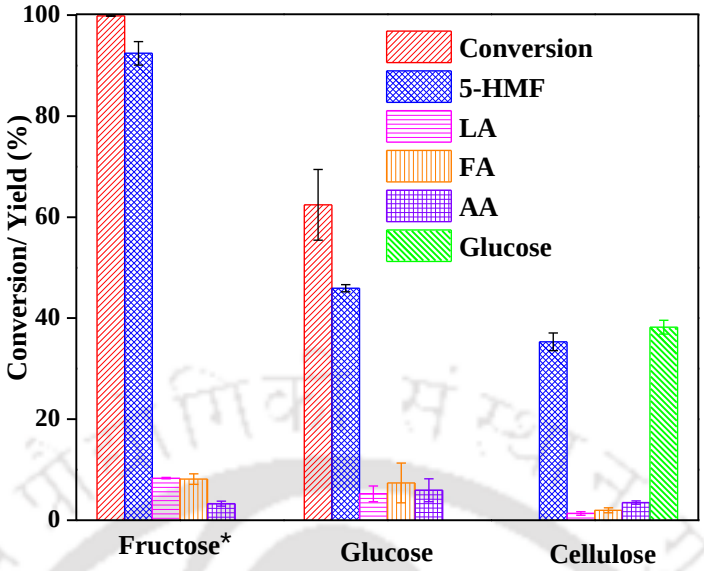

Figure 3.10: Conversion and yield of reaction products with various substrates (Fructose, Glucose and cellulose) over HBeta zeolite catalyst (Reaction conditions: 2 g DI water, 0.2 g substrate, substrate: catalyst = 3:1 w/w, 4 g MIBK, 0.6 g NaCl, 2 h reaction time, and 180°C reaction temperature). *With Fructose the reaction time is 1 h and other conditions are same as above. Note: The yield of glucose from cellulose is also included.

3.2.4 Performance of HBeta with cellulose, glucose, and fructose

The conversion of carbohydrate and yields of various products with the substrates (fructose, glucose, and cellulose) over HBeta are shown in Fig. 3.10 (for experimental conditions please see entries 12 – 14, Table 3.3). With fructose, the reaction time used is 1 h and the other reaction conditions are identical (2 g DI water, 0.2 g substrate, substrate:catalyst = 3:1 w/w, 4 g MIBK, 0.6 g NaCl, and 180°C reaction temperature). With fructose as a substrate, the conversion is 100% and the yield of 5-HMF is 92%. The cellulose conversion is 99% and yields of glucose and 5-HMF are 38 and 35%, respectively. With glucose as substrate, the conversion is lower (62%) but the yield of 5-HMF is higher (45%) than that with the cellulose. The comparison of data from all the three substrates indicates that either the conversion of glucose to fructose or the direct conversion of glucose to 5-HMF is a rate-limiting step in the direct conversion of cellulose (or glucose) to 5-HMF. This hypothesis is also supported by the fact that in all the experiments (with glucose or cellulose as a substrate) the fructose yield is zero. The yields of LA and FA are < 10% in the case of fructose and < 3% in the case of cellulose. The lower Brønsted acidity and the higher mesoporosity of HBeta are favoring maintain lower yields of LA and FA by suppressing 5-HMF rehydration.

The suppression of 5-HMF rehydration could, in turn, be attributed to the good mass transport of the 5-HMF from the mesopores.

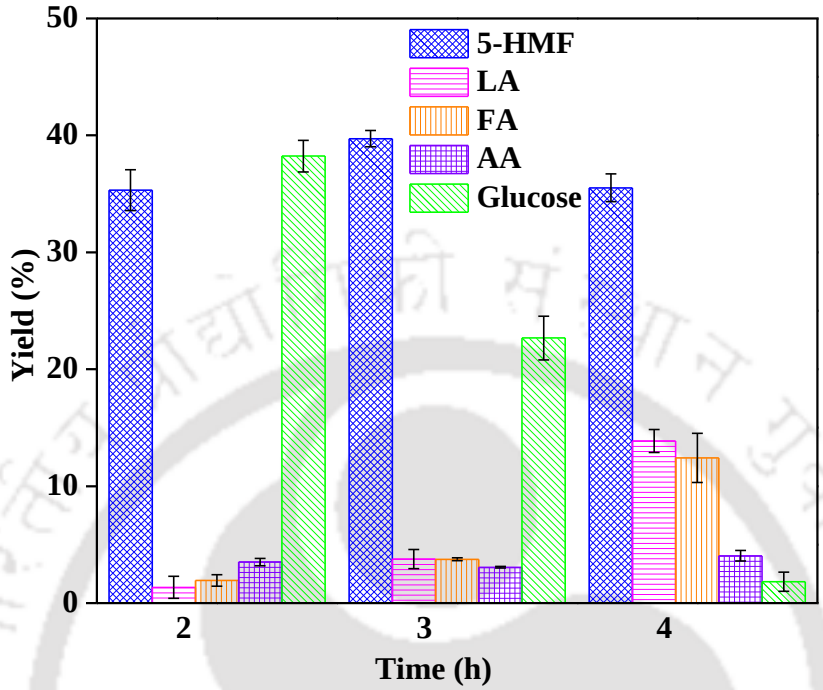

Figure 3.11: Conversion of cellulose and yields of reaction products as a function of reaction time over HBeta.

The conversion of cellulose is nearly constant with reaction time (Fig. 3.11). The yield of glucose is decreased with the reaction time and became negligible at 4 h. The yield of 5-HMF passed through a maximum at 3 h reaction time with a maximum yield of 40%. Therefore, the optimum reaction time for the cellulose to 5-HMF conversion is found to be 3 h at 180^{o}C. Otomo et al., (2015) reported a 5-HMF yield of 42% with HBeta zeolite as a catalyst and in a solvent mixture of water, DMSO and tetrahydrofuran (THF) at 200^{o}C for 5 h. Similar yield (46%) of 5-HMF from cellulose have been reported by Nandiwale et al., (2014) with a bimodal Micro/Mesoporous HZSM5 zeolite at 190^{o}C for 4 h. Lanzafame et al., (2012) reported a very low selectivity to 5-HMF from the cellulose of 10% at 190^{o}C for 5 h. The conversion of the substrate and yield of 5-HMF are better or similar to those reported in the literature with similar catalysts. The better activity obtained in this study could be attributed to the mesoporosity or the framework topology of the HBeta.

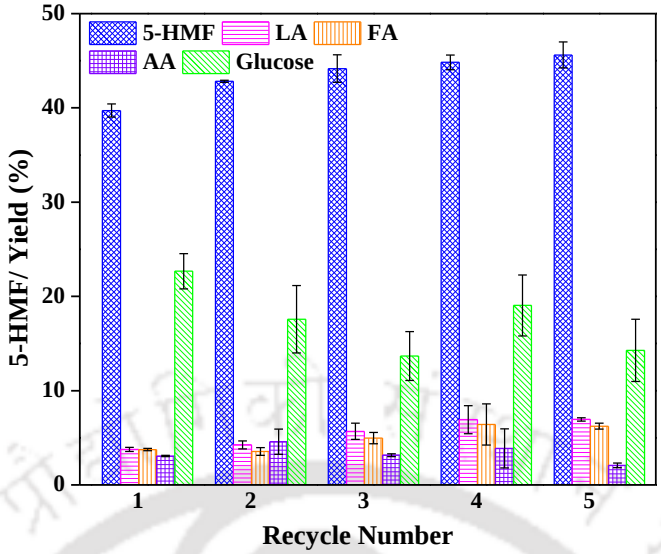

Figure 3.12: Conversion of cellulose and yields of reaction products as a function of catalyst recycle number over HBeta.

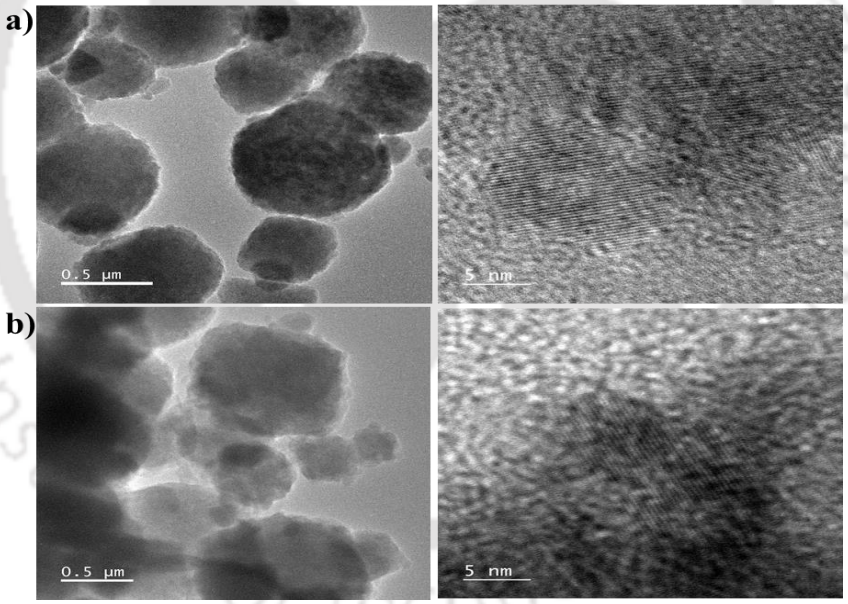

Figure 3.13: FETEM images of (a) fresh and (b) recycled HBeta catalyst.

3.2.5 Recycle of catalyst

The conversion of cellulose, as well as the yield of 5-HMF, are nearly constant for all the 5 cycles (entries 15, 17 – 20, Table 3.3) tested in this study (Fig. 3.12). On comparison of XRD patterns of fresh and used HBeta catalyst, it can be observed that the exposure of the catalyst to reaction conditions does not result in significant change in the crystal structure (Fig. 1). The comparison of FETEM micrographs of fresh and spent HBeta catalysts is

indicated that there is no carbonaceous material formed during the reaction (Fig. 3.13). The excellent stability of the zeolite could be attributed to higher SAR (360:1) of HBeta used in this study. The higher SAR gives rise to the hydrophobic nature of the zeolite and makes the zeolite framework more stable in water at high temperatures. Similar results in terms of stability are obtained by other researchers (Nandiwale et al., 2014).

3.3 Conclusions

In summary, high yields of 5-HMF from carbohydrates (fructose, glucose, and cellulose) are obtained over zeolites with high mesoporosity. Among the zeolites tested, HBeta showed the highest 5-HMF yield of 94% with a fructose conversion of 98% at 180°C for 1 h. The highest selectivities to 5-HMF obtained with the glucose and cellulose substrates are 74% (conversion 62%) and 41% (conversion 98%), respectively, at 180°C. The HBeta is highly selective to 5-HMF production with a negligible concentration of side products (< 3%). The HBeta showed excellent stability with no signs of deactivation even after 5 cycles of reuse. Finally, this study shows that a zeolite with high mesoporosity and high SAR results in higher yield and excellent stability in 5-HMF direct production from cellulose.

References

Agirrezabal-Telleria, I., Gandarias, I., Arias, P.L., 2014. Heterogeneous acid-catalysts for the production of furan-derived compounds (furfural and hydroxymethylfurfural) from renewable carbohydrates: A review. Catal. Today 234, 42–58. https://doi.org/10.1016/j.cattod.2013.11.027

Besson, M., Gallezot, P., Pinel, C., 2014. Conversion of biomass into chemicals over metal catalysts. Chem. Rev. 114, 1827–1870. https://doi.org/10.1021/cr4002269

Chatterjee, C., Pong, F., Sen, A., 2015. Chemical conversion pathways for carbohydrates. Green Chem. 17, 40–71. https://doi.org/10.1039/c4gc01062k

Combs, E., Cinlar, B., Pagan-torres, Y., Dumesic, J.A., Shanks, B.H., 2013. In fl uence of alkali and alkaline earth metal salts on glucose conversion to 5-hydroxymethylfurfural in an aqueous system. CATCOM 30, 1–4. https://doi.org/10.1016/j.catcom.2012.10.011

Corma Canos, A., Iborra, S., Velty, A., 2007. Chemical routes for the transformation of biomass into chemicals. Chem. Rev. 107, 2411–2502. https://doi.org/10.1021/cr050989d

Dumesic, Æ.J.A., 2009. Solvent Effects on Fructose Dehydration to 5-Hydroxymethylfurfural in Biphasic Systems Saturated with Inorganic Salts 297–303.

https://doi.org/10.1007/s11244-008-9166-0

Dumitriu, E., Hulea, V., 2003. Effects of channel structures and acid properties of large-pore zeolites in the liquid-phase tert-butylation of phenol. J. Catal. 218, 249–257. https://doi.org/10.1016/S0021-9517(03)00159-3

Fonseca, R. Da, Rafael, R.D.S., 2013. Different cell disruption methods for astaxanthin recovery by Phaffia rhodozyma. African J. Biotechnol. 10, 1165–1171. https://doi.org/10.5897/AJB10.1034

Hu, L., Wu, Z., Xu, J., Sun, Y., Lin, L., Liu, S., 2014. Zeolite-promoted transformation of glucose into 5-hydroxymethylfurfural in ionic liquid. Chem. Eng. J. 244, 137–144. https://doi.org/10.1016/j.cej.2014.01.057

Jia, S., Liu, K., Xu, Z., Yan, P., Xu, W., Liu, X., Zhang, Z.C., 2014. Reaction media dominated product selectivity in the isomerization of glucose by chromium trichloride: From aqueous to non-aqueous systems. Catal. Today 234, 83–90. https://doi.org/10.1016/j.cattod.2014.02.038

Kulawang, sittichai, 2015. Acidity of modified Mordenites synthesized from rice husk silica and catalytic transformation of methyl butanol. Quim Nov. 38, 191–195.

Lanzafame, P., Temi, D.M., Perathoner, S., Spadaro, A.N., Centi, G., 2012. Direct conversion of cellulose to glucose and valuable intermediates in mild reaction conditions over solid acid catalysts. Catal. Today 179, 178–184. https://doi.org/10.1016/j.cattod.2011.07.018

Li, H., Fang, Z., Smith, R.L., Yang, S., 2016a. Efficient valorization of biomass to biofuels with bifunctional solid catalytic materials. Prog. Energy Combust. Sci. 55, 98–194. https://doi.org/10.1016/j.pecs.2016.04.004

Li, H., Yang, S., Riisager, A., Pandey, A., Sangwan, R.S., Saravanamurugan, S., Luque, R., 2016b. Zeolite and zeotype-catalysed transformations of biofuranic compounds. Green Chem. 18, 5701–5735. https://doi.org/10.1039/c6gc02415g

Lobo, R., 2008. Chemical diversity of Zeolite Catalytic Sites. AIChE J. 54. https://doi.org/10.1002/aic

Luterbacher, J.S., Martin Alonso, D., Dumesic, J.A., 2014. Targeted chemical upgrading of lignocellulosic biomass to platform molecules. Green Chem. 16, 4816–4838. https://doi.org/10.1039/c4gc01160k

Mamo, W., Chebude, Y., Márquez-Álvarez, C., Díaz, I., Sastre, E., 2016. Comparison of glucose conversion to 5-HMF using different modified mordenites in ionic liquid and biphasic media. Catal. Sci. Technol. 6, 2766–2774. https://doi.org/10.1039/c5cy02070k

Moreno-Recio, M., Jiménez-Morales, I., Arias, P.L., Santamaría-González, J., Maireles-

Torres, P., 2017. The Key Role of Textural Properties of Aluminosilicates in the Acid-Catalysed Dehydration of Glucose into 5-Hydroxymethylfurfural. ChemistrySelect 2, 2444–2451. https://doi.org/10.1002/slct.201700097

Moreno-Recio, M., Santamaría-González, J., Maireles-Torres, P., 2016. Brönsted and Lewis acid ZSM-5 zeolites for the catalytic dehydration of glucose into 5-hydroxymethylfurfural. Chem. Eng. J. 303, 22–30. https://doi.org/10.1016/j.cej.2016.05.120

Nandiwale, K.Y., Galande, N.D., Thakur, P., Sawant, S.D., Zambre, V.P., Bokade, V. V., 2014. One-pot synthesis of 5-hydroxymethylfurfural by cellulose hydrolysis over highly active bimodal micro/mesoporous H-ZSM-5 catalyst. ACS Sustain. Chem. Eng. 2, 1928–1932. https://doi.org/10.1021/sc500270z

Nikolla, E., Román-Leshkov, Y., Moliner, M., Davis, M.E., 2011. "One-pot" synthesis of 5-(hydroxymethyl)furfural from carbohydrates using tin-beta zeolite. ACS Catal. 1, 408–410. https://doi.org/10.1021/cs2000544

Otomo, R., Tatsumi, T., Yokoi, T., 2015. Beta zeolite: a universally applicable catalyst for the conversion of various types of saccharides into furfurals. Catal. Sci. Technol. 5, 4001–4007. https://doi.org/10.1039/C5CY00719D

Otomo, R., Yokoi, T., Kondo, J.N., Tatsumi, T., 2014. Dealuminated Beta zeolite as effective bifunctional catalyst for direct transformation of glucose to 5-hydroxymethylfurfural. Appl. Catal. A Gen. 470, 318–326. https://doi.org/10.1016/j.apcata.2013.11.012

Qi, L., Mui, Y.F., Lo, S.W., Lui, M.Y., Akien, G.R., Horváth, I.T., 2014. Catalytic Conversion of Fructose, Glucose, and Sucrose to 5-(Hydroxymethyl)furfural and Levulinic and Formic Acids in γ-Valerolactone As a Green Solvent. ACS Catal. 4, 1470–1477. https://doi.org/10.1021/cs401160y

Román-Leshkov, Y., Barrett, C.J., Liu, Z.Y., Dumesic, J.A., 2007. Production of dimethylfuran for liquid fuels from biomass-derived carbohydrates. Nature 447, 982–985. https://doi.org/10.1038/nature05923

Shahangi, F., Najafi Chermahini, A., Saraji, M., 2018. Dehydration of fructose and glucose to 5-hydroxymethylfurfural over Al-KCC-1 silica. J. Energy Chem. 27, 769–780. https://doi.org/10.1016/j.jechem.2017.06.004

Srivastava, R., Sarmah, B., Satpati, B., 2015. Nanocrystalline ZSM-5 based bi-functional catalyst for two step and three step tandem reactions. RSC Adv. 5, 25998–26006. https://doi.org/10.1039/c4ra16697c

Taarning, E., Osmundsen, C.M., Yang, X., Voss, B., Andersen, S.I., Christensen, C.H., 2011.

Zeolite-catalyzed biomass conversion to fuels and chemicals. Energy Environ. Sci. 4, 793–804. https://doi.org/10.1039/c004518g

Tyrlik, S.K., Szerszen, D., Olejnik, M., Danikiewicz, W., 1996. Concentrated water solutions of salts as solvents for reaction of carbohydrates. Part 2. Influence of some magnesium salts and some ruthenium species on catalysis of dehydration of glucose. J. Mol. Catal. A Chem. 106, 223–233. https://doi.org/10.1016/1381-1169(95)00275-8

Wang, C., Zhang, L., Zhou, T., Chen, J., Xu, F., 2017. Synergy of Lewis and Brønsted acids on catalytic hydrothermal decomposition of carbohydrates and corncob acid hydrolysis residues to 5-hydroxymethylfurfural. Sci. Rep. 7, 40908.

Wang, J., Ren, J., Liu, X., Xi, J., Xia, Q., Zu, Y., Lu, G., Wang, Y., 2012. Direct conversion of carbohydrates to 5-hydroxymethylfurfural using Sn-Mont catalyst. Green Chem. 14, 2506–2512. https://doi.org/10.1039/C2GC35699F

Wang, T., Gallo, J.M.R., Shanks, B.H., Dumesic, J.A., 2012. Production of 5-Hydroxymethylfurfural from Glucose Using a Combination of Lewis and Brønsted Acid Catalysts in Water in a Biphasic Reactor with an Alkylphenol Solvent. https://doi.org/10.1021/cs300192z

Zakrzewska, M.E., Bogel-Łukasik, E., Bogel-Łukasik, R., 2011. Ionic liquid-mediated formation of 5-hydroxymethylfurfural-A promising biomass-derived building block. Chem. Rev. 111, 397–417. https://doi.org/10.1021/cr100171a

Zhang, Hongbin, Hu, Z., Huang, L., Zhang, Hongxia, Song, K., Wang, L., Shi, Z., Ma, J., Zhuang, Y., Shen, W., Zhang, Y., Xu, H., Tang, Y., 2015. Dehydration of Glycerol to Acrolein over Hierarchical ZSM-5 Zeolites: Effects of Mesoporosity and Acidity. ACS Catal. 5, 2548–2558. https://doi.org/10.1021/cs5019953

Zhang, L., Yu, H., Wang, P., 2013. Solid acids as catalysts for the conversion of d-xylose, xylan and lignocellulosics into furfural in ionic liquid. Bioresour. Technol. 136, 515–521. https://doi.org/10.1016/j.biortech.2013.03.054

Zhang, Z., Song, J., Han, B., 2017. Catalytic Transformation of Lignocellulose into Chemicals and Fuel Products in Ionic Liquids. Chem. Rev. 117, 6834–6880. https://doi.org/10.1021/acs.chemrev.6b00457

Zhao, H., Holladay, J.E., Brown, H., Zhang, Z.C., 2007. Metal Chlorides in Ionic Liquid Solvents Convert Sugars to 5-Hydroxymethylfurfural. Science (80-.). 316, 1597 LP – 1600.

Chapter 4

Choline Chloride Encapsulated Zeolites for the Carbohydrates to 5-HMF Conversion

4.1 Specific overview

The cellulose conversion to 5-HMF using homogeneous catalysts (such as $CrCl_3$) and ionic liquids (ILs) as catalyst/solvent resulted in yields of 5-HMF up to 89% (Zakrzewska et al., 2011; Zhang et al., 2017). For example, Sweygers et al. (2018) studied the microwave-assisted conversion of bamboo biomass to 5-HMF in a biphasic system (water + methyl isobutyl ketone (MIBK)) with HCl as a catalyst and reported a 5-HMF yield of 42%. However, homogeneous catalysts pose environmental problems in terms of difficulty in separation and recyclability of the catalysts in addition to waste streams production. To circumvent these issues, researchers have tested heterogeneous catalysts such as zeolites (Li et al., 2016) for biomass conversions and obtained the 5-HMF yields in the range of 25 – 45%. Nandiwale et al. (2014) reported a 5-HMF yield of 46% from cellulose over the micro/mesoporous HZSM5 catalyst with water as a solvent. The authors attributed the high yields to the mesoporosity of the HZSM5.Otomo et al. (2015) studied the direct conversion of cellulose to 5-HMF over HBeta zeolite with water + DMSO as a solvent, and tetrahydrofuran (THF) as an extraction phase and reported a yield of 42% at 200°C for 5 h.

The yields are in the range of 20 – 60% with Cr-based solid catalysts when used in IL solvents (Zhang et al., 2017). Zhang et al. (2013) tested a combination of mixed solvents (water + dimethyl sulfoxide, DMSO), lithium chloride (LiCl) and a polymer-supported sulfonic acid catalyst for carbohydrates to 5-HMF conversion and reported up to 54% 5-HMF yield from cellulose. The combination of the ionic liquids (as solvent/catalyst) and zeolites also showed reasonable yields of 5-HMF from cellulose. For example, Abou-Yousef and Hassan(Abou-

Yousef and Hassan, 2014) used HY for the production of 5-HMF from cellulose in the presence of 1-ethyl-3-methylimidazolium chloride ([EMIM]Cl) and reported a yield of 70%. Recently Li et al. (2018) tested carbon quantum dots for the cellulose to 5-HMF conversion in the presence of DMSO + water as a solvent and obtained a 5-HMF yield of 22%. However, ILs and DMSO are high boiling solvents, which require high energy for 5-HMF separation. One way to circumvent this problem is to immobilize the IL in the zeolites so that they are intact inside the cavities of the zeolite (Gallezot, 2012). Recently, Yang et al. (2015) have demonstrated that IL coated on $AlCl_3/SiO_2$ gives better yields of 5-HMF from fructose and glucose substrates. In our previous study, we obtained higher yields of 5-HMF from glucose using IL encapsulated zeolites (Saxena et al., 2017). Most of the ILs used for these studies is imidazolium-based which are non-biodegradable and toxic. An alternative to these ILs is the choline based ILs, (in particularly, choline chloride (ChCl)) which are biodegradable, non-toxic and find various applications (Gadilohar and Shankarling, 2017).

In the previous chapter, we presented the performance of bare zeolite catalysts for the carbohydrates conversion to 5-HMF. In this chapter, the production of 5-HMF from cellulose, glucose, and fructose using ChCl impregnated zeolites (HMOR, HBeta, HZSM5, HY, NaY) as catalysts is reported. ChCl is impregnated onto the zeolites using the wet-impregnation method. Various characterization techniques are employed to understand the interaction of ChCl with the zeolite particles. To the best of our knowledge, no reports have been published on the ChCl impregnated zeolites for the direct cellulose conversion to 5-HMF.

4.2. Results and discussions

4.2.1. Characteristics and physiochemical attributes

The amount of ChCl impregnated in each zeolite is calculated based on the CHNS analysis and presented in Table 4.1. As can be seen from the table, except for ChCl/HY_80, ChCl in all the zeolites is varied within a narrow range, i.e., from 50 to 60 mg/g. For ChCl/HY_80, it is approximately 40 mg/g.

Table 4.1: ChCl concentration in the zeolites.

Sl. no.	Sample name	ChCl ($mg.g^{-1}$)
1	ChCl/HBeta_360	59.6
2	ChCl/HZSM5_80	49.3
3	ChCl/HY_80	39.1

4	ChCl/HMOR_20	60.7
5	ChCl/NaY_5.1	49.3
6	ChCl/HY_5.1	54.9

4.2.1.1 Crystallinity of modified and unmodified catalysts

The XRD patterns and crystallite size of bare and modified zeolites are shown in Fig. 4.1. All the zeolite catalysts exhibited distinct peaks for the diffraction from their typical lattice planes as shown in Figs. 1a and 1b. The presented XRD data is normalized w.r.t. the highest intensity peak of each pattern. For comparison, the XRD pattern of ChCl is also presented. The major diffraction peaks of ChCl at 2θ = 16.75°, 26.7°, 34.23°, 39.68° are assigned to [0 2 0], [4 0 1], [4 1 1], and [4 2 1] lattice planes. The XRD patterns of the bare zeolites are well matched with their standard diffraction patterns (COD #7051100 (HBeta_360), COD #9003355 (HMOR_20), COD #2004384 (HY_80), COD #9011266 (HZSM5_80), COD #9013434, (HY_5.1), and COD #9000124 (NaY_5.1)) as well as with their patterns from standard IZA structure commission. There is no change in the crystal structure of the zeolites after ChCl impregnation. When the actual intensities are compared, zeolites with higher SARs hardly show any change in intensity upon ChCl encapsulation. However, the XRD patterns of zeolites with lower SARs show a decrease in intensity when ChCl is encapsulated. The reason for the decrease of intensity is the decrease in the difference between the electron densities of the walls and the pores, which in turn is due to the pore filling with the ChCl. The relative intensity of the peaks is increased with most of the high 2θ values of all modified zeolites except in modified HBeta_360. For example, on a comparison of HY_80 and ChCl/HY_80, the intensity is the same at a 2θ of 6.16°. However, the peaks at higher 2θ angles show higher relative intensity from ChCl/HY_80 as compared to that from HY_80. The introduction of ChCl in HBeta_360 resulted in the increase and decrease of intensities from the [3 0 2] and [1 0 1] planes, respectively. It can be concluded that only intensities from major planes of the most of the zeolites are affected by the ChCl encapsulation.

The same phenomenon has been represented in literature for ionic liquid impregnated on NaY zeolite (Eguizábal et al., 2011; Yu et al., 2014). No diffraction peak is observed for ChCl in the modification of zeolites, which could be attributed to a uniform and high dispersion of ChCl in the zeolite. The same phenomenon has been reported in the literature for ChCl-HMOR (Saxena et al., 2017). The XRD patterns for ChCl/HZSM5_80 with various ChCl loadings are shown in Fig. 4.2 and indicated no changes in the intensity with the increase of ChCl loading.

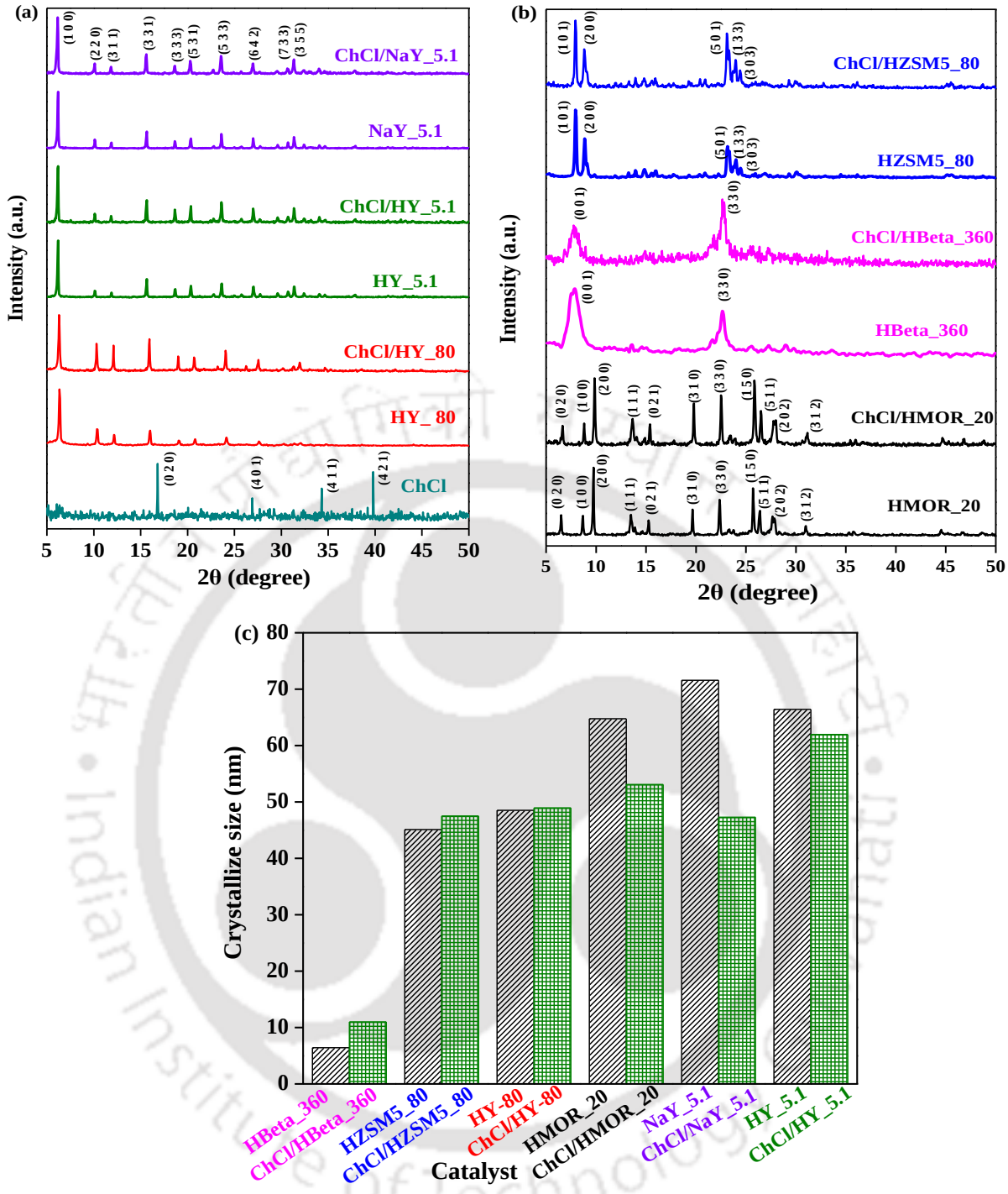

Figure 4.1: The powder XRD patterns (a, b) and average crystallize size (c) of various zeolite catalysts used in this study.

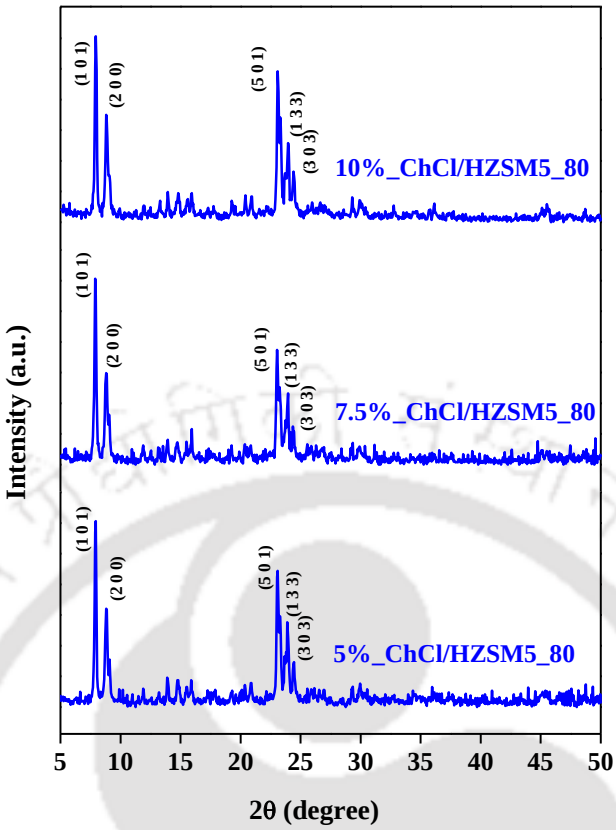

Figure 4.2: The XRD patterns for ChCl/HZSM5_80 with various ChCl loadings.

The average crystallite sizes of bare and modified zeolites are calculated using Scherer's equation (Fig. 1c). Irrespective of the topology of the zeolite, the crystallite sizes of both bare and modified zeolites are increased with decrease of SAR, within the experimental error. With the addition of ChCl, the crystallite size is decreased at lower SAR, however, it is nearly constant at higher SAR. The highest decrease in crystallite size is observed with NaY_5.1 with a difference of 25 nm. With ChCl/HY_5.1, the decrease in crystallite size is observed to be less (< 5 nm) upon addition of ChCl. Another reason for the changes in relative intensity (and the changes in crystallite size) is an ion-exchange reaction between the cation (H^+ or Na^+ in this case) on the zeolite and the cation of the ChCl. Similar changes have been reported in the literature for mesoporous titania upon addition of ionic liquids (Preethi et al., 2017).

4.2.1.2 N_2 sorption behavior of bare and ChCl impregnated zeolites

The N_2-sorption data is presented in Table 4.2 and the isotherms are shown in Fig. 4.3. All the zeolites, including the ChCl encapsulated ones, exhibited the Type II isotherm, which is typical for micro- and mesoporous materials. In bare zeolites studied in this work, the mesopore

area is increased with SAR, irrespective of the topology. It is the lowest with the HY_5.1 and is the highest with the HBeta_360. For almost all zeolites when encapsulated with the ChCl, the total surface area, micropore surface area and total pore volume are decreased and the average pore size increased. The mesopore area is either unchanged or slightly increased with the encapsulation, except for HBeta. In the case of HBeta, the mesoporosity decreased significantly from 223 to 55 $m^2.g^{-1}$ and the micropore area is nearly constant at approximately of 330 $m^2.g^{-1}$. The micropore area of the HMOR became zero upon encapsulation. When HY_5.1 and NaY_5.1 are compared, the effect of encapsulation is more significant on NaY_5.1 zeolite, with the total surface area decreased from 712 to 484 $m^2.g^{-1}$ and the micropore area decreased from 672 to 396 $m^2.g^{-1}$ (compare entries 11 and 12, Table 4.2). The differences in the sorption characteristics of ChCl encapsulated HY_5.1 and NaY_5.1 indicates the differences in the interactions of ChCl with H^+ and Na^+ ions of the zeolites (Yu et al., 2014). The decrease of the total surface area and micropore area and the increase of average pore size in all cases, except HBeta, reiterates the fact that the ChCl fills the micropores. The pore filling mechanism is different in the case of HBeta as compared to others. In this case, the ChCl is adsorbed on the surface of the mesopores but not filled (or partially filled) the micropores which is why there is a significant decrease in the mesopore area but hardly any change in the micropore area. A similar result has been reported by Arellano et al. (2016) who studied the IL impregnated mesoporous silica beads for CO_2 adsorption. The mesopore area of ChCl/HZSM5_80 and ChCl/HBeta_360 are nearly the same.

Table 4.2: The textural properties of zeolite catalysts used in this study.

Zeolite (Si/Al)	S_{BET} ($m^2.g^{-1}$)	S_{μ} ($m^2.g^{-1}$)	V_{μ} ($cm^3.g^{-1}$)	V_p ($cm^3.g^{-1}$)	Avg. pore size (nm)	BJH method		S_{micro} / S_{des}	V_{mico} / V_{des}
						S_{des} ($m^2.g^{-1}$)	V_{des} ($cm^3.g^{-1}$)		
HZSM5_80	381	315	0.167	0.301	3.16	70	0.133	4.5	1.25
ChCl/HZSM5_80	272	191	0.096	0.233	3.43	60	0.109	3.16	0.83
HBeta_360	563	333	0.179	0.398	2.82	223	0.206	1.49	0.86
ChCl/HBeta_360	477	322	0.160	0.341	2.86	55	0.112	5.85	1.43
HMOR_20	386	334	0.164	0.273	2.83	23	0.093	14.5	1.76
ChCl/HMOR_20	44	0	0	0.123	11.09	21	0.107	0	0
HY_80	773	440	0.231	0.581	3.00	113	0.229	3.89	1.008
ChCl/HY_80	708	353	0.184	0.599	3.38	138	0.292	2.56	0.63
HY_5.1	570	535	0.279	0.333	2.34	14	0.040	38.21	6.975
ChCl/HY_5.1	543	470	0.244	0.351	2.59	31	0.078	15.16	3.13
NaY_5.1	712	672	0.351	0.409	2.30	15	0.042	44.8	8.357
ChCl/NaY_5.1	484	396	0.209	0.298	2.46	21	0.053	18	3.94

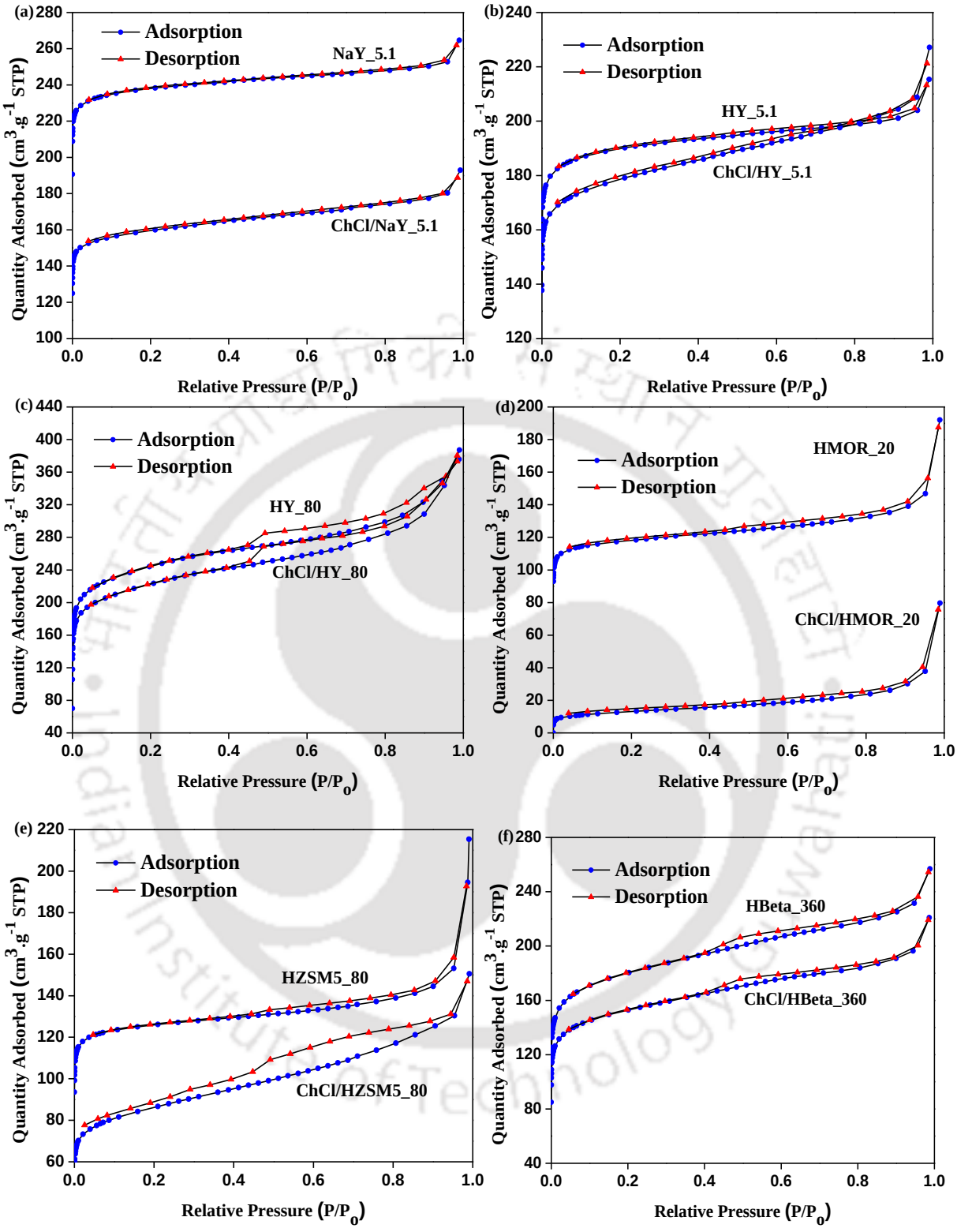

Figure 4.3: N_2 adsorption – desorption isotherms: (a) NaY_5.1 and ChCl/NaY_5.1, (b) HY_5.1 and ChCl/HY_5.1, (c) HY_80 and ChCl/HY_80, (d) HMOR_20 and ChCl/HMOR_20, (e) HZSM5_80, and ChCl/HZSM5_80 (f) HBeta_360, and ChCl/HBeta_360.

4.2.1.3 ^{27}Al and ^{13}C SS NMR analysis

The solid-state NMR spectra for the bare and ChCl encapsulated zeolites are shown in Fig. 4.4. The changes in the environment of framework Al upon incorporation of ChCl into the zeolites are reflected by the corresponding changes in the ^{27}Al SS NMR peak positions. In general, there is an up-field shift of framework Al atoms upon ChCl encapsulation into the zeolites. The framework Al of zeolite NaY_5.1 showed an upfield shift of 1.5 ppm upon ChCl encapsulation. The framework Al showed a more pronounced upfield shift of 8.7 ppm when ChCl was impregnated into HY_5.1. In addition, the interaction of ChCl with HY_5.1 resulted in the loss of extra-framework Al atom which was indicated by disappearance of the peak at 3.38 ppm in the ^{27}Al SS NMR. However, HY_80 exhibited neither a significant upfield shift of framework Al nor a disappearance of extra-framework Al atom upon ChCl encapsulation. Similar to HY_5.1, ^{27}Al SS NMR analysis of the ChCl incorporated zeolite HBeta_360 showed the disappearance of extra-framework Al but with a lower up-field shift (1.2 ppm) of framework Al atoms. In contrast, characterization of ChCl impregnated zeolite HMOR_20 indicated the formation of new extra-framework Al (appearance of peak at 4.06 ppm) in addition to an up-field shift of framework Al by about 1.9 ppm. Upon incorporation of ChCl, the zeolite HZSM5_80 showed a up-field shift of framework Al atoms (1.8 ppm) which is very similar to that observed by NaY_5.1.

Similarly, comparison of the ^{13}C SS NMR shifts of the carbon atoms present in impregnated choline chloride with the corresponding ^{13}C shifts (liquid phase) of carbon atoms in free ChCl provides valuable information. In this case, there is a general down-field (by 0.5 – 1.0 ppm) shift of all the carbons of ChCl upon interaction with HY_5.1, NaY_5.1, HY_80, HBeta_360, and HMOR_20. In all these cases, for a given ChCl-zeolite system, the methyl and methylene carbons are down-field shifted to similar extents. However, for the ChCl interacting with zeolite HZSM5_80, an exceptionally high down-field shift (2.0 ppm) for the methylene (N-CH_2-) carbons is observed. In addition, contrary to other zeolites, the methyl and the methylene (O-CH_2-) carbons of ChCl- HZSM5_80 are down-field shifted to a lesser extent (1.0 ppm) compared to methylene (N-CH_2-) carbon.

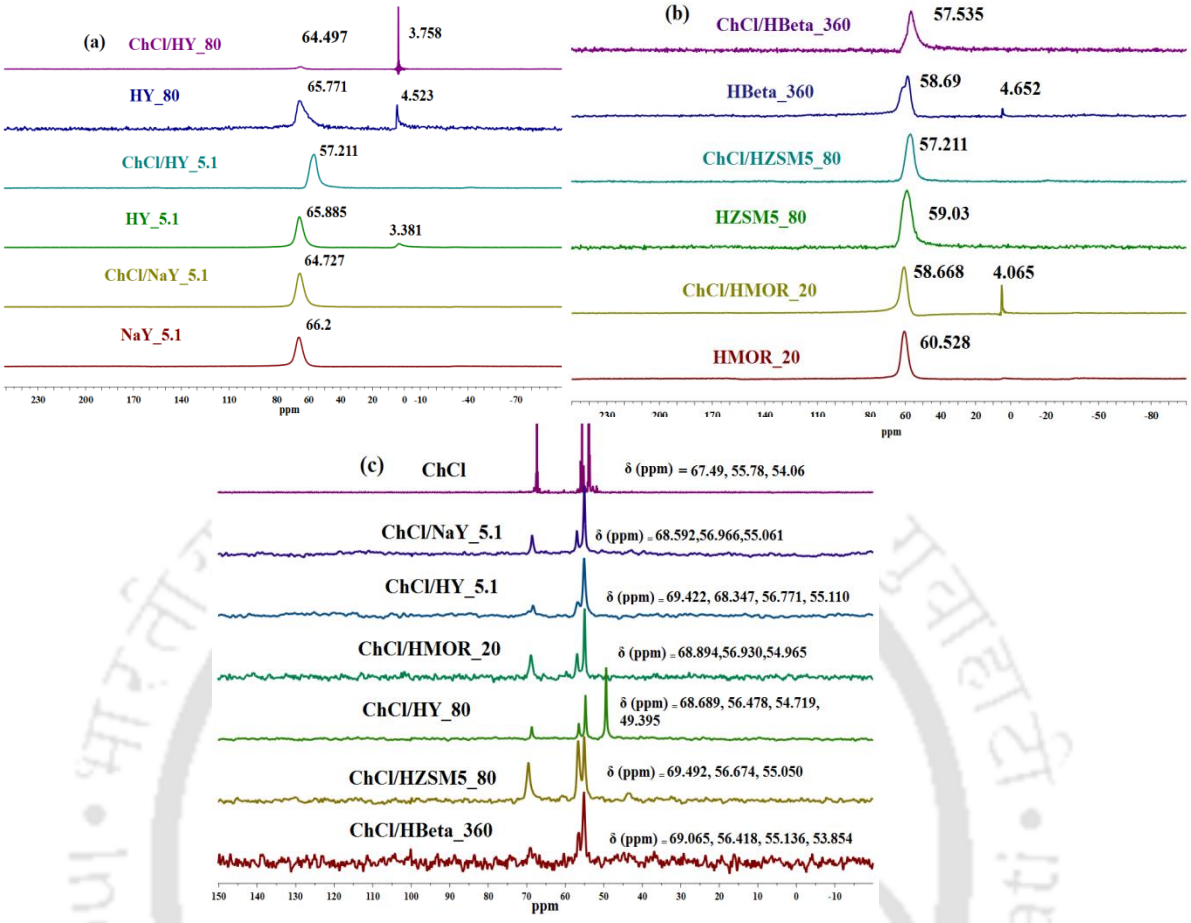

Figure 4.4: The solid state NMR spectra of ^{27}Al (a and b) and ^{13}C (c) nuclei of various zeolites used in this study.

4.2.2 Catalyst test results

The detailed experimental conditions used in this study are summarized in the Table 4.3.

Table 4.3: Detailed experimental conditions used in this study (MIBK and NaCl amounts are constant in all the experiments at 4 g and 0.6 g, respectively. The x in xChCl/HZSM5_80 indicate the wt % of ChCl. When the ChCl wt % is 5% then the number is not given. The experiments are numbered in the order of their appearance in this chapter).

Sl. no.	Temp. (°C), Time (h)	Substrate	Catalyst	Reaction phase	
				Catalyst (g)	Substrate (g)
1	180, 1	Glucose (10%)	HMOR_20	0.0667	0.2
2	180, 1	Glucose (10%)	ChCl/HMOR_20	0.0667	0.2
3	180, 1.5	Glucose (10%)	ChCl/HMOR_20	0.0667	0.2
4	180, 2	Glucose (10%)	ChCl/HMOR_20	0.0667	0.2

5	180, 1	Fructose (10%)	ChCl/HMOR_20	0.0667	0.2
6	180, 1	Cellulose (10%)	ChCl/HMOR_20	0.0667	0.2
7	180, 2	Cellulose (10%)	ChCl/HMOR_20	0.0667	0.2
8	180, 3	Cellulose (10%)	ChCl/HMO_20	0.0667	0.2
9	180, 1	Cellulose (10%)	HMOR_20	0.0667	0.2
10	180, 2	Cellulose (10%)	HMOR_20	0.0667	0.2
11	180, 3	Cellulose (10%)	HMOR_20	0.0667	0.2
12	180, 3	Cellulose (10%)	HY_80	0.0667	0.2
13	180, 3	Cellulose (10%)	ChCl/HY_80	0.0667	0.2
14	180, 1	Cellulose (10%)	HY_5.1	0.0667	0.2
15	180, 3	Cellulose (10%)	ChCl/HY_5.1	0.0667	0.2
16	180, 3	Cellulose (10%)	NaY_5.1	0.0667	0.2
17	180, 3	Cellulose (10%)	ChCl/NaY_5.1	0.0667	0.2
18	180, 3	Cellulose (10%)	HBeta_360	0.0667	0.2
19	180, 3	Cellulose (10%)	ChCl/HBeta_360	0.0667	0.2
20	180, 3	Cellulose (10%)	HZSM5_80	0.0667	0.2
21	180, 3	Cellulose (10%)	ChCl/HZSM5_80	0.0667	0.2
22	180, 0.75	Cellulose (10%)	ChCl/HY_5.1	0.0667	0.2
23	180, 1	Cellulose (10%)	ChCl/HY_5.1	0.0667	0.2
24	180, 2	Cellulose (10%)	ChCl/HY_5.1	0.0667	0.2
25	180, 3	Cellulose (10%)	7.5ChCl/HZSM5_80	0.0667	0.2
26	180, 3	Cellulose (10%)	10ChCl/HZSM5_80	0.0667	0.2
27	180, 3	Cellulose (15%)	ChCl/HZSM5_80	0.1	0.3
28	180, 3	Cellulose (5%)	ChCl/HZSM5_80	0.0333	0.1
29	180, 3.5	Cellulose (5%)	ChCl/HZSM5_80	0.0333	0.1
30	180, 4	Cellulose (5%)	ChCl/HZSM5_80	0.0333	0.1
31	180, 2	Cellulose (5%)	ChCl/HZSM5_80	0.0333	0.1
32	180, 3	Cellulose (5%)	ChCl/HZSM5_80	0.0333	0.1
33	180, 3	Cellulose (5%)	ChCl/HZSM5_80	0.0333	0.1
34	180, 3	Cellulose (5%)	ChCl/HZSM5_80	0.0333	0.1
35	180, 3	Cellulose (5%)	ChCl/HZSM5_80	0.0333	0.1

4.2.2.1 Glucose to 5-HMF conversion

Effect of ChCl addition on zeolites functionality: The catalytic activity of HMOR_20 and ChCl/HMOR_20 are compared in Fig. 4.5a. With the ChCl encapsulation, both glucose conversion, as well as the yield of 5-HMF are increased, significantly, from 30 to 60% and 27 to 49%, respectively. The yields of other compounds (LA, FA and AA) are less than 5% but increased with ChCl/HMOR_20. The enhancement in activity is seen despite the fact that the micropore area and total surface area are decreased significantly after the addition of ChCl to HMOR (Table 1). SS NMR spectra shows that the ChCl impregnated zeolite possess a peak at 5.02 ppm and is absent in the bare zeolite. This peak corresponds to the octahedral Al sites of the zeolite. This indicates that the incorporation of ChCl in the HMOR zeolite forms the extra-framework octahedral Al sites and this may be responsible for the higher activity of ChCl/HMOR_20. Therefore, the enhanced conversion could be attributed to the synergistic

effect of the ChCl and HMOR. In our previous work (Saxena et al., 2017), the effect of ChCl encapsulation into the zeolite HMOR is showed to be negative in terms of 5-HMF yield at the reaction conditions 170^{o}C for 3 h. At these reaction conditions, the 5-HMF yield is decreased from 35% (over bare HMOR) to 20% (over ChCl/HMOR). In this study, the 5-HMF yield increased significantly from 27% (over bare HMOR) to 49% (over ChCl/HMOR) at 180^{o}C for 1 h. This indicates the significant effect of reaction conditions on selective conversion of glucose to 5-HMF. Significant effects of operating conditions on glucose conversion to 5-HMF over various catalysts have also been reported by other research groups (Guo et al., 2017; Jiménez-Morales et al., 2015; Mamo et al., 2016; Shahangi et al., 2018). The detailed experimental conditions are presented in Table 4.3.

Effect of reaction time on 5-HMF formation from glucose: The conversion of glucose is increased (from 60 to 100%) and the yield of 5-HMF is decreased (from 49 to 8%), as the reaction time increases from 1 to 2 h, over ChCl/HMOR_20 (Fig. 4.5b). Whereas, the yield of LA and FA increased (LA: from 5 to 50% and FA: from 5 to 38%) and that of AA is nearly constant (at ~5%) with reaction time. This clearly indicates that the LA is formed at the expense of 5-HMF at higher reaction times. Therefore, it can be said that the catalyst favours the higher glucose conversion at higher reaction times. However, the rehydration of 5-HMF to LA and FA is also favored under the same conditions, which is undesirable. Therefore, a reaction time of 1 h is optimum for the glucose conversion to 5-HMF over this catalyst.

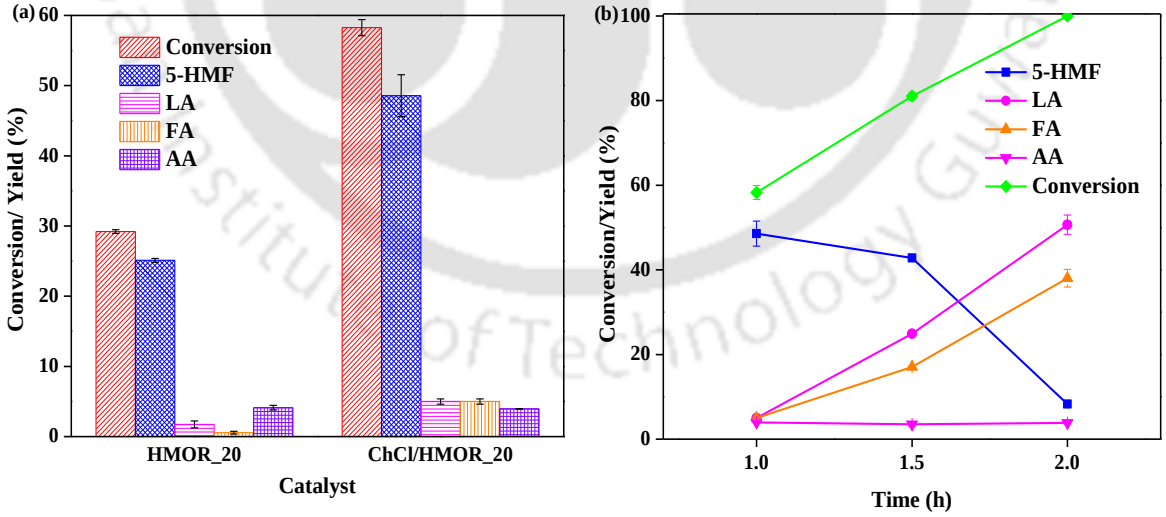

Figure 4.5: Variation of conversion of glucose and yields of reaction products (5-HMF, LA, FA, and AA) over HMOR_20 and ChCl/HMOR_20 catalysts (a) and as a function of reaction time over ChCl/HMOR_20 catalyst (b) (Reaction conditions: 2 g DI water, 0.2 g substrate, substrate: catalyst = 3:1 w/w, 4 g MIBK, 0.6 g NaCl, 1 h reaction time, and 180°C temperature).

4.2.2.2 Substrate variation

As a next step, various substrates (fructose, glucose, and cellulose) are tested for 5-HMF production over ChCl/HMOR_20 (Fig. 4.6). With fructose as substrate, the conversion is 99% and the 5-HMF yield is 98% and the yields of other products are very small. As compared to fructose, glucose as substrate resulted in a lower conversion as well as 5-HMF yield. In the case of cellulose, the yield of glucose is significant. It is anticipated that the increase in reaction time may result in higher 5-HMF yield (Fig. 4.7a). However, the increase in reaction time rather resulted in the increase of side products (LA and FA) and no enhancement in the 5-HMF yield is observed. The 5-HMF yield is higher at 2 h reaction time and it is decreased significantly with the increase of reaction time to 3 h with the formation of rehydration products (LA and FA).

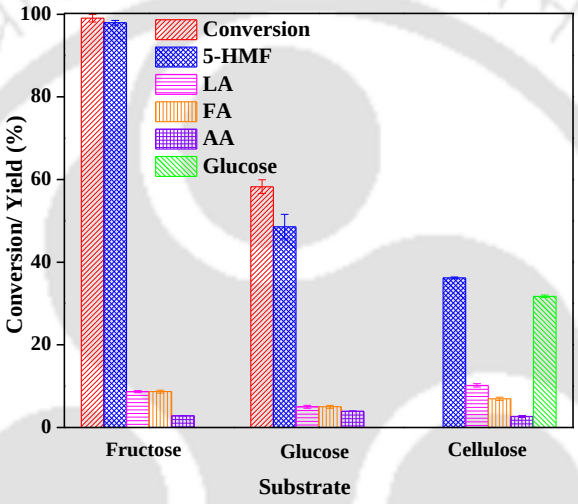

Figure 4.6: Yields of reaction products and conversion variation with different substrates (Fructose, Glucose and cellulose) over ChCl/HMOR_20 zeolite catalyst (Reaction conditions: 2 g DI water, 0.2 g substrate, substrate: catalyst = 3:1 w/w, 4 g MIBK, 0.6 g NaCl, 1 h reaction time, and 180°C reaction temperature).

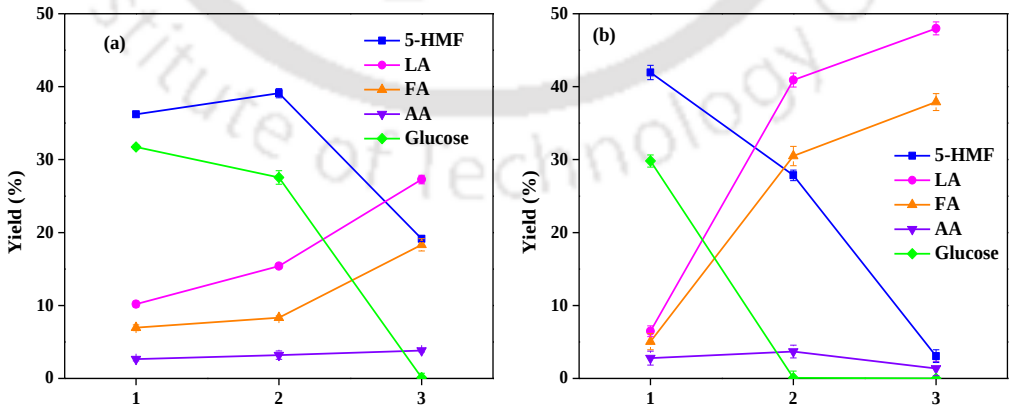

Figure 4.7: Variation of yield of reaction products (5-HMF, LA, FA, AA and Glucose) as a function of reaction time using (a) ChCl/HMOR_20 and (b) HMOR_20. (Reaction conditions: 2 g DI water, 0.2 g cellulose, substrate: catalyst = 3:1 w/w, 4 g MIBK, 0.6 g NaCl, and 180°C reaction temperature).

4.2.2.3 Role of catalysts for cellulose to 5-HMF conversion

The yields of various products obtained over different catalysts are shown in Fig. 4.8. Overall, the effect of ChCl addition to zeolite on the yield of 5-HMF is either positive or negligible. For example, the yield of 5-HMF over HY_80 is increased from 30 to 36% and that over HZSM5_80 is increased from 36 to 44% upon the encapsulation of ChCl. When the changes in yields of side-products (particularly LA) up on ChCl encapsulation are compared, it can be observed that the LA yield is lower in the case of ChCl/HY_80 as compared to that over HY_80 (5 vs. 14%). Whereas, the LA yield is higher over ChCl/HZSM5_80 as compared to that over HZSM5_80 (15 vs. 11%). Moreover, the glucose yield is higher over ChCl/HY_80 (14%) as compared to that over ChCl/HZSM5_80 (9%) This data indicates that the higher yield of 5-HMF over ChCl/HY_80 is due to suppression of the rehydration reaction of 5-HMF to LA over this catalyst. While, the higher yield of 5-HMF over ChCl/HZSM5_80 is due to the overall higher activity of this catalyst. There is slight decrease in the yield of 5-HMF in the case of ChCl/HMOR_20 as compared to that over HMOR_20. This is in contrast to the result that is obtained when glucose is used as reactant (Fig. 3a) where a significant increase in 5-HMF yield (from 27 to 49%) is observed.

To compare the effect of reaction time on the yield of 5-HMF over HMOR_20 and ChCl/HMOR_20 catalysts, a time study is carried out with these catalysts. On comparison of the Fig. 4.7a and b, it can be seen that the glucose yield reached 0% in 2 h reaction time over HMOR_20 and it took 3 h time for the glucose yield to reach 0% over ChCl/HMOR_20. The maximum yield of 5-HMF that is obtained over HMOR_20 is 42% at 1 h reaction time and that over ChCl/HMOR_20 is 39% at 2 h reaction time. The LA yield increased with reaction time over both the catalysts and reached 48% over HMOR_20 and 27% over ChCl/HMOR_20, at the reaction time of 3 h. The overall data indicates that the catalyst HMOR_20 is more active as compared to ChCl/HMOR_20 for the selective conversion of cellulose to 5-HMF. All other catalysts (NaY_5.1, HY_5.1 and HBeta_360) resulted in negligible change in the yield of 5-HMF upon impregnation with ChCl.

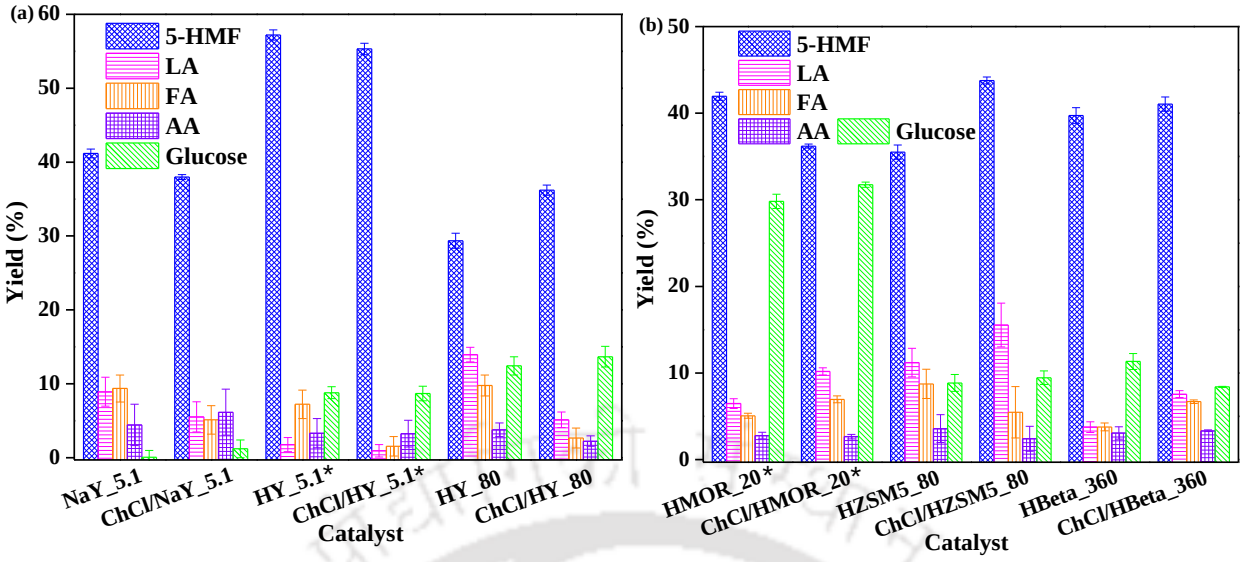

Figure 4.8: Yields of reaction products (5-HMF, LA, FA, AA and Glucose). (Reaction conditions: 2 g of DI water, 0.2 g of substrate, cellulose: catalyst = 3:1 w/w, 4 g of MIBK, 0.6 g of NaCl, 3 h of reaction time, and 180°C of reaction temperature). *With HY_5.1, ChCl/HY_5.1, HOMR_20 and ChCl/HMOR_20 catalysts, the reaction time is 1 h and all other conditions are same as above.

The HY_5.1 is initially tested for 3 h reaction time but resulted in significant amounts of side products (LA and FA). Therefore, time study is carriedout to find out the suitable reaction time. The yield of 5-HMF is first increased and then decreased with the reaction time (Fig. 4.9). The yields of side products (LA and FA) are lower at low reaction times and increased monotonically with reaction time. Whereas, glucose yield is the highest at the lowest reaction time, decreased with reaction time and finally became negligible above 2 h of reaction time. The yield of acetic acid (AA) is nearly constant with reaction time. Therefore, the yields obtained at 1 h reaction time are presented in the catalyst activity comparison (Fig. 4.9). The H-form Y zeolites showed a higher yield of 5-HMF as compared to that of Na-form Y with same SAR. This may be due to lower Brønsted acid sites present in the case of NaY. The HY_5.1 zeolites (both with and without ChCl), as compared to their NaY_5.1 counter-parts, showed a good ability to suppress the side-product (LA) formation, while maintaining the higher yields of 5-HMF. When the yields of 5-HMF over HY zeolites with different SAR are compared, it can be noticed that the HY with lower SAR gives a higher yield of 5-HMF which can again be attributed to higher Brønsted acid sites in the case of HY with lower SAR. The zeolites with moderate SAR values resulted in enhanced 5-HMF yield upon impregnation with the ChCl, irrespective of the type of zeolite (compare HY_80 and HZSM5_80 zeolites with others in Fig. 4.9. In case of zeolites with SAR = 80 (HY_80 and HZSM5_80), ChCl may be binding to Si

sites and work in tandem with the Al sites towards bifunctional catalysis which enhances the catalytic activity. In case of HY_5.1, ChCl finds a large number of Al sites resulting in ready inhibition of these active sites, which may not be the case when one uses the zeolites with high SAR. For SAR = 360, though the ChCl binds to Si and participates in catalysis, the corresponding number of Al sites is too few to demonstrate any significant effect of dual functionality.

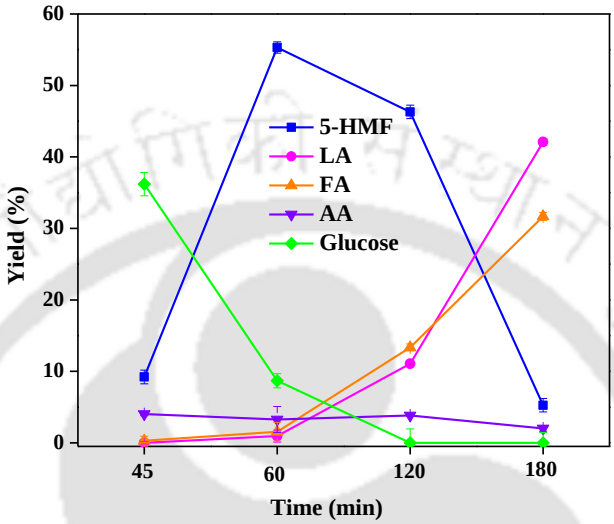

Figure 4.9: Variation of the yields of reaction products (5-HMF, LA, FA, AA and Glucose) as a function of reaction time using ChCl/HY_5.1 catalyst. (Reaction conditions: 2 g DI water, 0.2 g cellulose, substrate: catalyst = 3:1 w/w, 4 g MIBK, 0.6 g NaCl, and 180°C reaction temperature)

The encapsulation of ChCl onto the zeolites would result in the donation of electron density from either the N atom or the O atom in ChCl to the Lewis acidic sites of the zeolite. Al^{3+} being more Lewis acidic than Si^{4+}, the effect of ChCl interaction should be reflected in the ^{27}Al NMR shifts. As expected, an up-field NMR shift in the ^{27}Al signals is observed in the case of all zeolites (Fig. 4.4a and b). However, as the ^{27}Al SS NMR studies show that the signals shift to similar extents upon ChCl impregnation into the zeolites, it is difficult to correlate the ^{27}Al shifts to the observed activity. A different observation is made when the corresponding shifts of the ChCl carbons were analyzed in the ^{13}C NMR. In this case, a downfield shift of the methyl and methylene (O-CH_2-, N-CH_2-) carbons is expected upon encapsulation of ChCl and such a shift is observed with all zeolites (Fig. 4.4c). Further, the catalyst ChCl/HZSM5_80 which showed the best activity exhibited a pronounced ^{13}C shift only for the N-CH_2- methylene carbon compared to methyl and the O-CH_2- methylene carbon. Such an observation was not made in case of other zeolites. This indicates the better interaction of ChCl with HZSM5_80 with the N atom interacting better than O atom.

4.2.2.4 Effect of ChCl loading, the cellulose dosage and the reaction time on cellulose conversion to 5-HMF

The effect of ChCl loading in the catalyst is tested by varying the ChCl loading from 0 to 10% in the zeolite (Fig. 4.10). With the increase of ChCl concentration in the zeolite, the 5-HMF yield is first increased till 6% then decreased and finally leveled-off. The decrease of 5-HMF yield at higher loadings of ChCl may be attributed to the capping effect of ChCl which means that the impregnated ChCl, at higher loadings, may completely cover the active surface of the zeolites, resulting in lower yields.

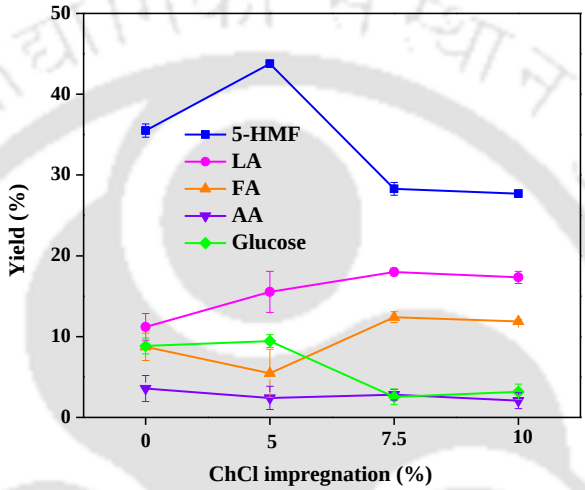

Figure 4.10: Yields of various reaction products as a function of ChCl concentration in the ChCl/HZSM5_80 zeolite.

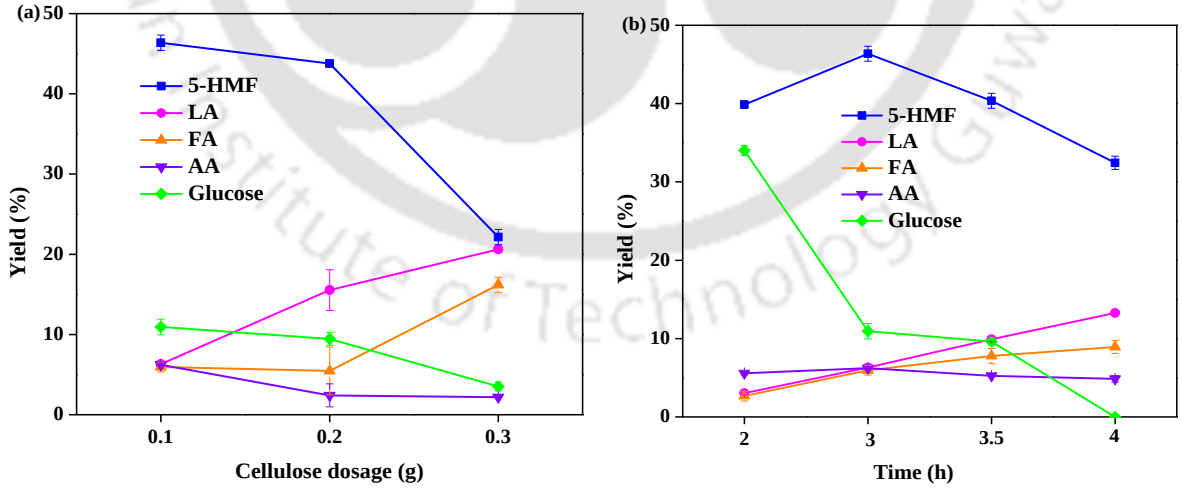

Figure 4.11: (a) Effect of variation of cellulose dosage on the product yields over ChCl/HZSM5_80. (Reaction conditions: 2 g of DI water, cellulose: catalyst = 3:1 w/w, 4 g of MIBK, 0.6 g of NaCl, 3 h of reaction time, and 180°C of reaction temperature). **(b)** Variation of product yields as a function of reaction time over ChCl/HZSM5_80. (Reaction conditions: 2 g DI water, 0.1 g cellulose, substrate: catalyst = 3:1 w/w, 4 g MIBK, 0.6 g NaCl, and 180°C reaction temperature)

As a next step cellulose dossage is varied to see its effect on the conversion and yield of 5-HMF. As the cellulose dossage increases, the yields of 5-HMF, glucose and AA are decreased and those of LA and FA are increased (Fig. 4.11a). Therefore, 0.1 g dossage of cellulose is chosen for the further study

The variation of yields of various products as a function of reaction time is shown in Fig. 4.11b. As can be seen from the figure, the 5-HMF yield is first increased and then decrease with the reaction time. The yield of glucose decreased, and those of LA and FA increased with the reaction time. The yield of AA is nearly constant with the reaction time. From these results it can be seen that the glucose formation is higher at lower reaction times but as the time increases from 2 to 3 h, the glucose is converted to 5-HMF. With the further increase of time beyond 3 h, the formed 5-HMF is rehydrated to LA and FA. Similar trend has been reported by Li et al. (2018) who studied the direct conversion of cellulose to 5-HMF over sulfonated poly(phenylene sulfide). Therefore, 3 h is the optimum reaction time for the conversion of cellulose to 5-HMF with higher yields over ChCl/HZSM5_80.

4.2.3 Recycle test of used catalyst

From the above study, with cellulose as a substrate, the ChCl/HZSM5_80 catalyst at 180^{o}C for 3 h is found to show the highest effect of ChCl on the yield of 5-HMF. Therefore, the recycle test is carriedout using the same conditions. The yields of 5-HMF is nearly constant with the recycle, indicating that the catalyst is highly stable up to five cycles, under the reaction conditions used in this study (Fig. 4.12). The yield of glucose is increased marginally from 12 (over fresh catalyst) to 20% (over the re-used catalyst). Whereas, there is a decrease of yield of LA from 6 (over fresh catalyst) to 3% (over the re-used catalyst). These data indicate that the catalyst is stable up to five cycles, under the reaction conditions used in this study. However, the catalytic sites required for rehydration of 5-HMF to LA and FA were decreased. In addition, it appears that undesired reactions such as formation of humins (Fig 4.16), occurs more readily with fresh catalysts than with recycled ones, thus explaining the higher yields of glucose in subsequent cycles. The TGA of fresh and recycled ChCl/HZSM5_80 (Fig. 4.13 and Table 4.4) revealed that the weight loss (in the temperature range of 200 – 600^{o}C) difference is less than 8% indicating that the humins formation is minimal with this catalyst. FESEM and FETEM (Fig. 4.14) images indicate that there is no significant coke/humins formation during the reaction. As shown in the Fig. 4.15, the NMR spectra show that there is no leaching of ChCl is occurred during the reaction. This indicates that the encapsulation of ChCl resulted in mutual protection of

ChCl and Al species in the catalyst due to bonding with each other. This may be another reason for the good stability of the catalyst during the recycle test. Other researchers also reported high stability of HZSM5 catalysts in 5-HMF production. For example, Wang et al. (2016) studied microalgae conversion to 5-HMF over the commercial HZSM5 catalyst and reported a nearly stable operation up to 6 cycles.

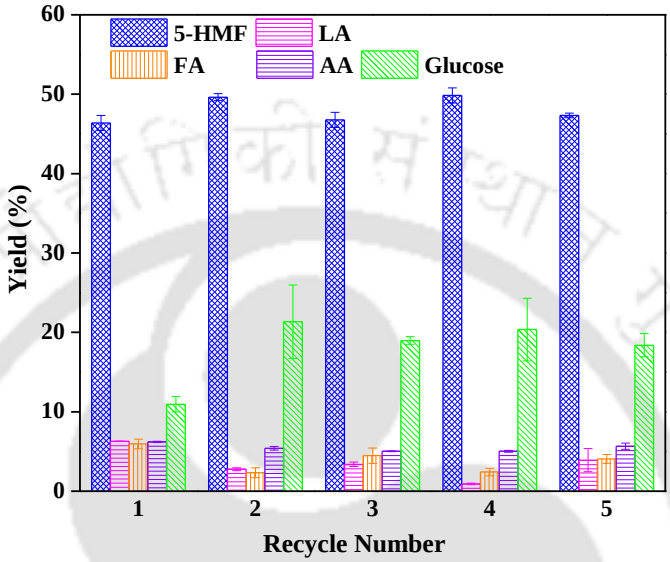

Figure 4.12: Variation of yields of reaction products as a function of catalyst recycle number over ChCl/HZSM5_80.

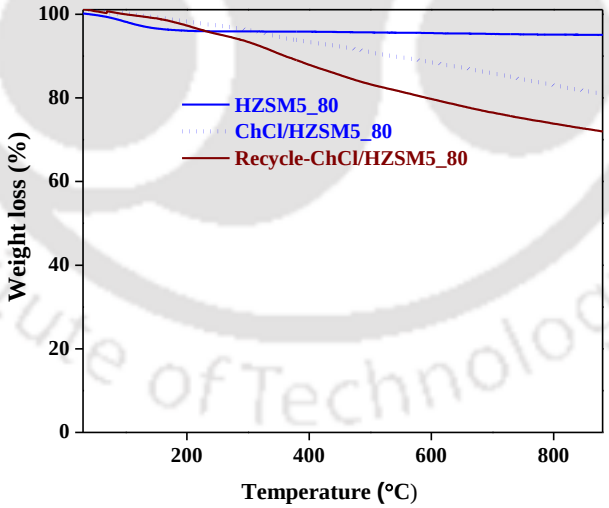

Figure 4.13: TGA profiles of HZSM5_80, ChCl/HZSM5_80 and recycled ChCl/HZSM5_80

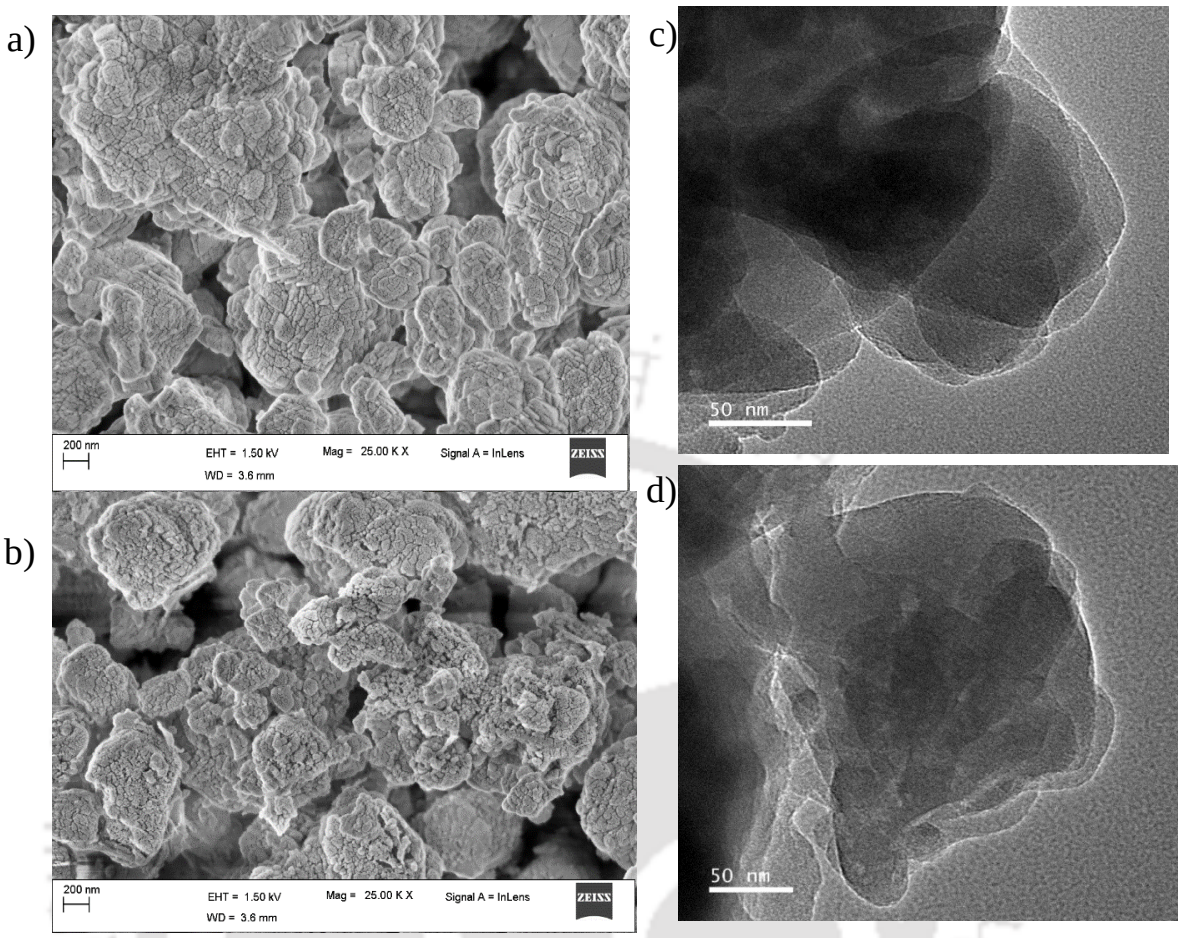

Figure 4.14: FESEM (a & b) and FETEM (c & d) images of (a & c) fresh and (b & d) recycled ChCl/HZSM5_80.

Table 4.4: Weight losses in TGA in the temperature range of 200 - 600^{o}C

Sample	Weight loss (%)
HZSM5_80	0.5
ChCl/HZSM5_80	9.7
Recycle ChCl/HZSM5_80	17.5

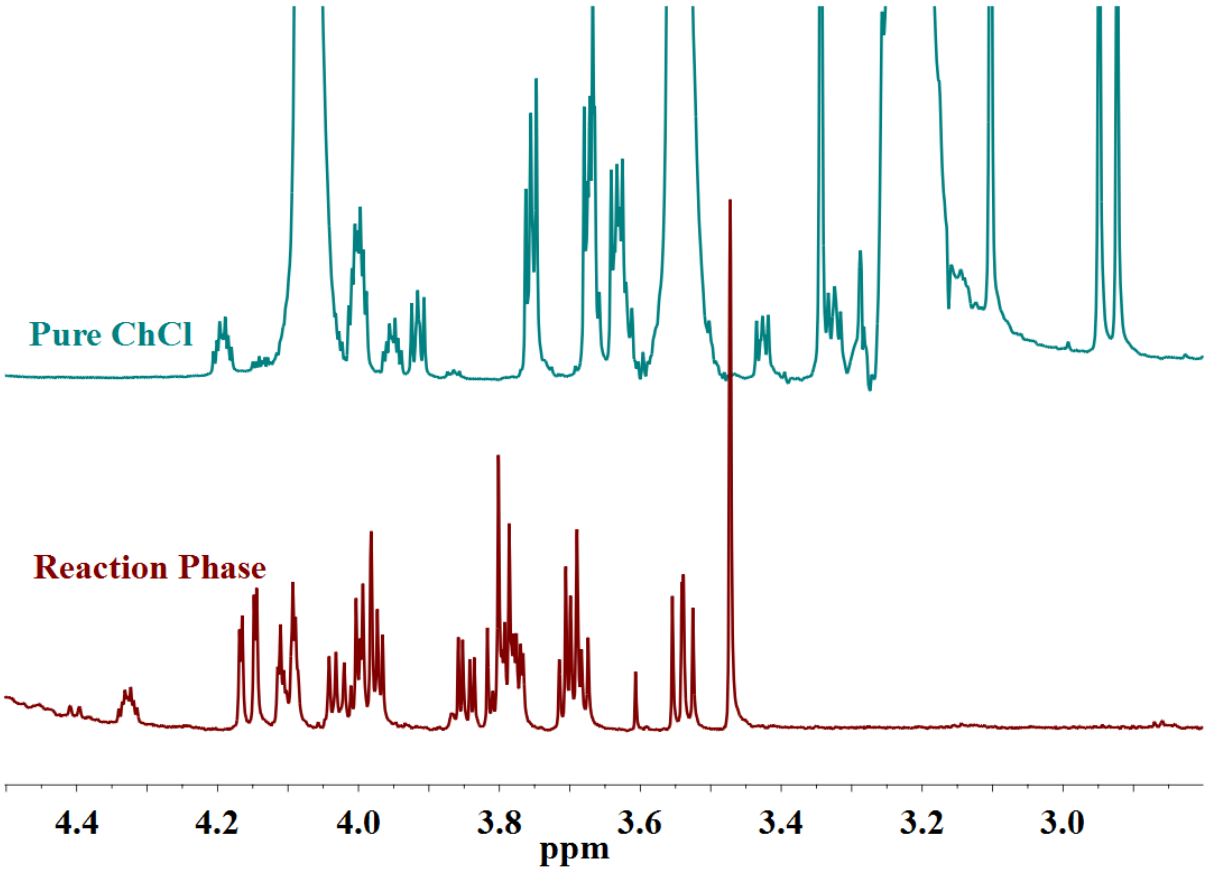

Figure 4.15: ^{1}H NMR of Pure ChCl and the reaction phase.

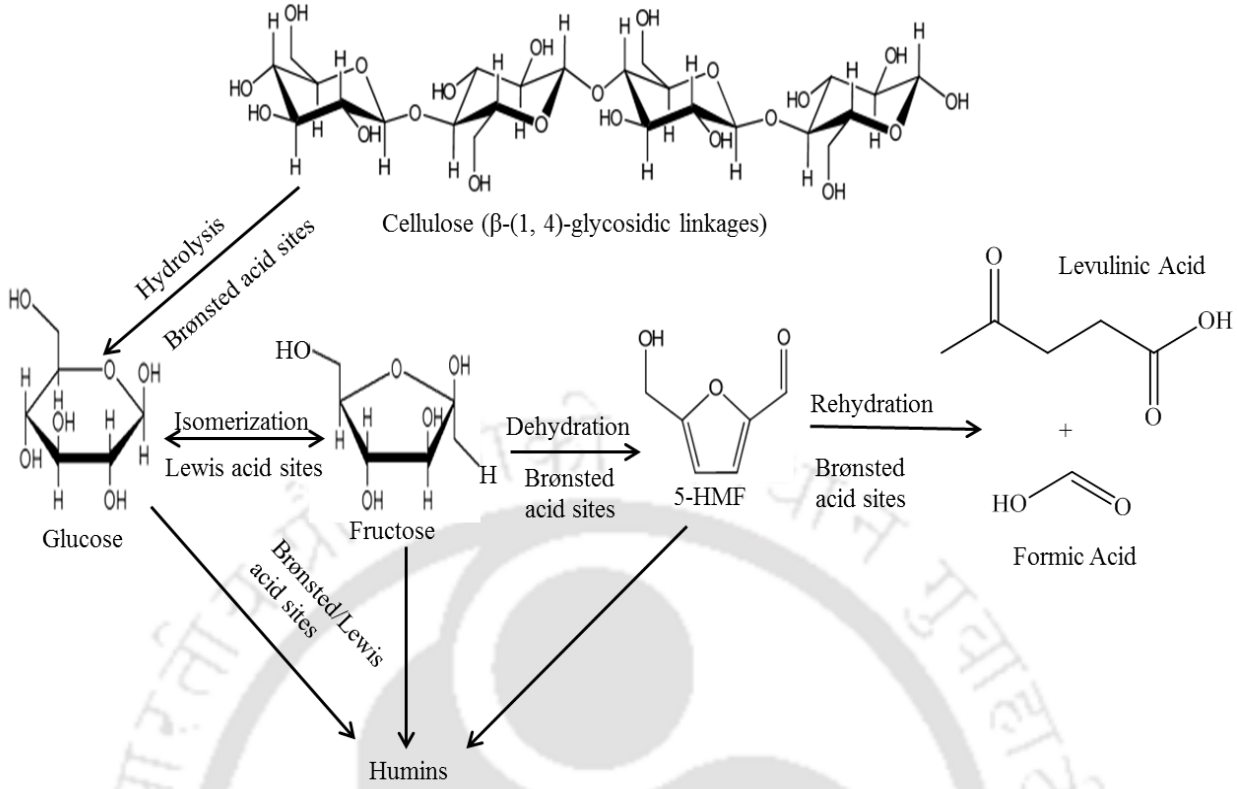

Figure 4.16: A plausible reaction mechanism for the conversion cellulose to 5-HMF and other side products.

4.3 Conclusions

The choline chloride impregnated HMOR, HZSM5, HBeta, NaY, and HY zeolites are highly active for cellulose, glucose and fructose conversion to 5-HMF. The crystal size is decreased for the zeolites with lower silica-to-alumina ratio upon impregnation with the ChCl. The 5-HMF yield from glucose and cellulose are the highest at 49 and 55% over ChCl/HMOR_20 and ChCl/HY_5.1, respectively. The activity of the zeolites with moderate silica-to-alumina ratios (SAR) is enhanced by the impregnation of ChCl on to these zeolites, particularly HZSM5. This is attrubted to the better interaction of ChCl with HZSM5 throgh N-atoms of ChCl. However, the effect is negligible for the zeolites with either low or high SAR. The ChCl impregnated HZSM5 catalyst remained stable up to five consecutive cycles.

References

Abou-Yousef, H., Hassan, E.B., 2014. A novel approach to enhance the activity of H-form zeolite catalyst for production of hydroxymethylfurfural from cellulose. J. Ind. Eng. Chem. 20, 1952–1957. https://doi.org/10.1016/j.jiec.2013.09.016

Arellano, I.H., Madani, S.H., Huang, J., Pendleton, P., 2016. Carbon dioxide adsorption by zinc-functionalized ionic liquid impregnated into bio-templated mesoporous silica beads. Chem. Eng. J. 283, 692–702. https://doi.org/10.1016/j.cej.2015.08.006

Eguizábal, A., Lemus, J., Urbiztondo, M., Moschovi, A.M., Ntais, S., Soler, J., Pina, M.P., 2011. Ammonium based ionic liquids immobilized in large pore zeolites: Encapsulation procedures and proton conduction performance. J. Power Sources 196, 4314–4323. https://doi.org/10.1016/j.jpowsour.2010.12.019

François, J., Vigier, K.D.O., 2017. Catalytic Conversion of Carbohydrates to Furanic Derivatives in the Presence of Choline Chloride 1–11. https://doi.org/10.3390/catal7070218

Gadilohar, B.L., Shankarling, G.S., 2017. Choline based ionic liquids and their applications in organic transformation. J. Mol. Liq. 227, 234–261. https://doi.org/10.1016/j.molliq.2016.11.136

Gallezot, P., 2012. Conversion of biomass to selected chemical products. Chem. Soc. Rev. 41, 1538–1558. https://doi.org/10.1039/c1cs15147a

Guo, J., Zhu, S., Cen, Y., Qin, Z., Wang, J., Fan, W., 2017. Ordered mesoporous Nb–W oxides for the conversion of glucose to fructose, mannose and 5-hydroxymethylfurfural. Appl. Catal. B Environ. 200, 611–619. https://doi.org/10.1016/j.apcatb.2016.07.051

Jiménez-Morales, I., Moreno-Recio, M., Santamaría-González, J., Maireles-Torres, P., Jiménez-López, A., 2015. Production of 5-hydroxymethylfurfural from glucose using aluminium doped MCM-41 silica as acid catalyst. Appl. Catal. B Environ. 164, 70–76. https://doi.org/10.1016/j.apcatb.2014.09.002

Li, H., Yang, S., Riisager, A., Pandey, A., Sangwan, R.S., Saravanamurugan, S., Luque, R., 2016. Zeolite and zeotype-catalysed transformations of biofuranic compounds. Green Chem. 18, 5701–5735. https://doi.org/10.1039/c6gc02415g

Li, K., Chen, J., Yan, Y., Min, Y., Li, H., Xi, F., Liu, J., Chen, P., 2018. Quasi-homogeneous carbocatalysis for one-pot selective conversion of carbohydrates to 5-hydroxymethylfurfural using sulfonated graphene quantum dots. Carbon N. Y. 136, 224–233. https://doi.org/10.1016/j.carbon.2018.04.087

Li, Z., Su, K., Ren, J., Yang, D., Cheng, B., Kim, C.K., Yao, X., 2018. Direct catalytic

conversion of glucose and cellulose. Green Chem. 20, 863–872. https://doi.org/10.1039/c7gc03318d

Mamo, W., Chebude, Y., Márquez-Álvarez, C., Díaz, I., Sastre, E., 2016. Comparison of glucose conversion to 5-HMF using different modified mordenites in ionic liquid and biphasic media. Catal. Sci. Technol. 6, 2766–2774. https://doi.org/10.1039/c5cy02070k

Nandiwale, K.Y., Galande, N.D., Thakur, P., Sawant, S.D., Zambre, V.P., Bokade, V. V., 2014. One-pot synthesis of 5-hydroxymethylfurfural by cellulose hydrolysis over highly active bimodal micro/mesoporous H-ZSM-5 catalyst. ACS Sustain. Chem. Eng. 2, 1928–1932. https://doi.org/10.1021/sc500270z

Otomo, R., Tatsumi, T., Yokoi, T., 2015. Beta zeolite: a universally applicable catalyst for the conversion of various types of saccharides into furfurals. Catal. Sci. Technol. 5, 4001–4007. https://doi.org/10.1039/C5CY00719D

Pidko, E.A., Hensen, E.J.M., van Santen, R.A., 2012. Self-organization of extraframework cations in zeolites. Proc. R. Soc. A Math. Phys. Eng. Sci. 468, 2070–2086. https://doi.org/10.1098/rspa.2012.0057

Preethi, T., Padmapriya, M.P., Abarna, B., Rajarajeswari, G.R., 2017. Choline chloride-zinc chloride ionic liquid as a green template for the sol-gel synthesis of mesoporous titania. RSC Adv. 7, 10081–10091. https://doi.org/10.1039/c6ra28478g

Saxena, P., Velaga, B., Peela, N.R., 2017. Ionic Liquid-Encapsulated Zeolite Catalysts for the Conversion of Glucose to 5-Hydroxymethylfurfural. ChemistrySelect 2, 10379–10386. https://doi.org/10.1002/slct.201701955

Shahangi, F., Najafi Chermahini, A., Saraji, M., 2018. Dehydration of fructose and glucose to 5-hydroxymethylfurfural over Al-KCC-1 silica. J. Energy Chem. 27, 769–780. https://doi.org/10.1016/j.jechem.2017.06.004

Sweygers, N., Harrer, J., Dewil, R., Appels, L., 2018. A microwave-assisted process for the in-situ production of 5-hydroxymethylfurfural and furfural from lignocellulosic polysaccharides in a biphasic reaction system. J. Clean. Prod. 187, 1014–1024. https://doi.org/10.1016/j.jclepro.2018.03.204

Wang, J.J., Tan, Z.C., Zhu, C.C., Miao, G., Kong, L.Z., Sun, Y.H., 2016. One-pot catalytic conversion of microalgae (Chlorococcum sp.) into 5-hydroxymethylfurfural over the commercial H-ZSM-5 zeolite. Green Chem. 18, 452–460. https://doi.org/10.1039/c5gc01850a

Yang, J., De Vigier, K.O., Gu, Y., Jérôme, F., 2015. Catalytic dehydration of carbohydrates

suspended in organic solvents promoted by ALCL3/SiO2coated with choline chloride. ChemSusChem 8, 269–274. https://doi.org/10.1002/cssc.201402761

Yu, Y., Mai, J., Wang, L., Li, X., Jiang, Z., Wang, F., 2014. Ship-in-a-bottle synthesis of amine-functionalized ionic liquids in NaY zeolite for CO2capture. Sci. Rep. 4, 1–8. https://doi.org/10.1038/srep05997

Zakrzewska, M.E., Bogel-Łukasik, E., Bogel-Łukasik, R., 2011. Ionic liquid-mediated formation of 5-hydroxymethylfurfural-A promising biomass-derived building block. Chem. Rev. 111, 397–417. https://doi.org/10.1021/cr100171a

Zhang, Z., Du, B., Zhang, L.J., Da, Y.X., Quan, Z.J., Yang, L.J., Wang, X.C., 2013. Conversion of carbohydrates into 5-hydroxymethylfurfural using polymer bound sulfonic acids as efficient and recyclable catalysts. RSC Adv. 3, 9201–9205. https://doi.org/10.1039/c3ra41912f

Zhang, Z., Song, J., Han, B., 2017. Catalytic Transformation of Lignocellulose into Chemicals and Fuel Products in Ionic Liquids. Chem. Rev. 117, 6834–6880. https://doi.org/10.1021/acs.chemrev.6b00457

Chapter 5

[BMIM]Br Encapsulated Zeolites for the Carbohydrates Conversion to 5-HMF

5.1 Specific overview

Ionic liquids (ILs) are emerging both as green solvents and catalysts for biomass processing (Zhang et al., 2017). The major advantage of ILs is that the cation and anion part of the ILs, which could be varied to tune their catalytic properties. However, higher cost, difficulty in separation, and high viscosity pose challenges in using ILs as catalysts at an industrial scale. Therefore, IL functionalized heterogeneous catalysts such as zeolites are being developed (Sudarsanam et al., 2018). Three methods/strategies are commonly used for the zeolite functionalization; namely, i) ship-in-a-bottle, ii) bottle around a ship and iii) wet impregnation. In the first strategy, the precursors of IL are initially adsorbed onto the pores/cages of the support and allow them to react and form the IL inside the pores/cages (Saxena et al., 2017). Imidazolium-based ILs are mostly encapsulated using this method (Yu et al., 2014b). In a bottle-around-a-ship strategy, the IL and precursors for the support are used to synthesize the support over the IL. Here, IL may act as solvent and template. This method is similar to template-assisted zeolite synthesis, but the calcination step is avoided so as to preserve the IL inside the pores of the support (Yuan et al., 2015). In the impregnation method, the ILs such as choline chloride are adsorbed directly onto the support (Peela et al., 2019). The ILs, when used as solvents facilitate the reaction and stabilize the intermediate compounds (e.g. 5-hydroxymethylfurfural (5-HMF) in carbohydrates conversion) thereby suppress the side reactions (Hu et al., 2013). However, due to their high boiling points, separation and recyclability are challenging. To enable easy separation and recyclability, the ILs can be immobilized and be tested whether they can still provide the same benefits or not. Therefore,

this study targets the utilization of 1-butyl-3-methylimidazolium bromide ([BMIM]Br) functionalized zeolites for the conversion of carbohydrates to 5-HMF.

Lignocellulosic biomass comprises cellulose (45-50%), hemicellulose (25-35%) and lignin (25-35%), and their composition varies with the sources (Hsu et al., 2011). A catalyst possessing mesoporosity, and both Lewis and Brønsted acid sites can be used to convert carbohydrates selectively to 5-HMF (Kang et al., 2018). Tan et al. (2011) tested various zeolites such as HY, HBETA, HMOR, HZSM-5 in 1-butyl-3-methylimidazolium chloride ([BMIM]Cl) along with the $CrCl_3$ system and reported a maximum 5-HMF yield of 36% with HY at 120°C and 6 h. Though the yields are reasonable with the zeolite catalysts in the IL solvent system, the separation of product from high boiling IL is still an issue.

An interesting way to avoid the separation issue associated with ILs is to immobilize them on solid support (Sudarsanam et al., 2018). Yang et al. (2015) studied the $AlCl_3/SiO_2$ coated with choline chloride (ChCl) for the dehydration of carbohydrates and reported a 5-HMF yield of 38% from glucose. The higher yield is attributed to the *in-situ* formation of a deep eutectic liquid phase between ChCl and carbohydrate. One way to circumvent this issue is to synthesize the IL in-situ zeolite pores/cages to trap it in the cages of zeolite (Yu et al., 2014a; Zhang et al., 2017). The IL functionalized zeolites combine the individual properties of the ILs and the zeolites (Sudarsanam et al., 2018). The functionalization may also induce new properties due to synergistic IL-zeolite interaction. Moreover, one can reduce the requirement of costlier ILs to a great extent in the reaction mixture (Olivier-Bourbigou et al., 2010).

5.2 Results and discussion

5.2.1 Characteristics and physiochemical attributes

5.2.1.1 XRD characterization

All the bare zeolites used in this study are highly crystalline and exhibit the diffraction patterns corresponding to their standard patterns from IZA (Baerlocher and McCusker L.B.). In all the cases of ionic liquid encapsulated catalysts, the XRD pattern (Fig. 5.1) is similar to that of the corresponding bare zeolites. It confirms that ionic liquid (IL) encapsulation is not destroying the parent zeolite structure. The ionic liquid encapsulated zeolites showed slightly higher crystal size than that of the bare zeolites (Table 5.1). For example, the crystal size is 71 and 58 nm for [BMIM]Br/NaY_5.1 and NaY_5.1, 56 and 49 nm for [BMIM]Br/HY_80 and HY_80, and 65 and 62 nm for [BMIM]Br/HMOR_20 and HMOR_20, respectively. The

detailed analysis of the XRD pattern, in the case of Y zeolite, reveals that the relative intensities from planes [2 2 0] and [3 3 1] increased with the ionic liquid encapsulation. Similar relative intensities are also noticed for HMOR_20 zeolite, the intensities from planes [3 3 0], [1 5 0], and [2 0 2] are higher with ionic liquid encapsulation. The increase of relative intensities is higher in the case of H-form zeolite than that of the Na-form zeolite. It could be due to the change in interaction strength between the cation of the zeolite and the ionic liquid. Earlier reports on ionic liquid encapsulation in the zeolite also reports a similar trend (Saxena et al., 2017; Yu et al., 2014b). Yu et al. (2014b) explained that this phenomenon could be due to the fact that the large organic cations facilitate the redistribution of randomly distributed cations (Na^+ and H^+) into the specific sites of the zeolite framework. This results in the variation of electron density with IL encapsulation (Mohamedali et al., 2018).

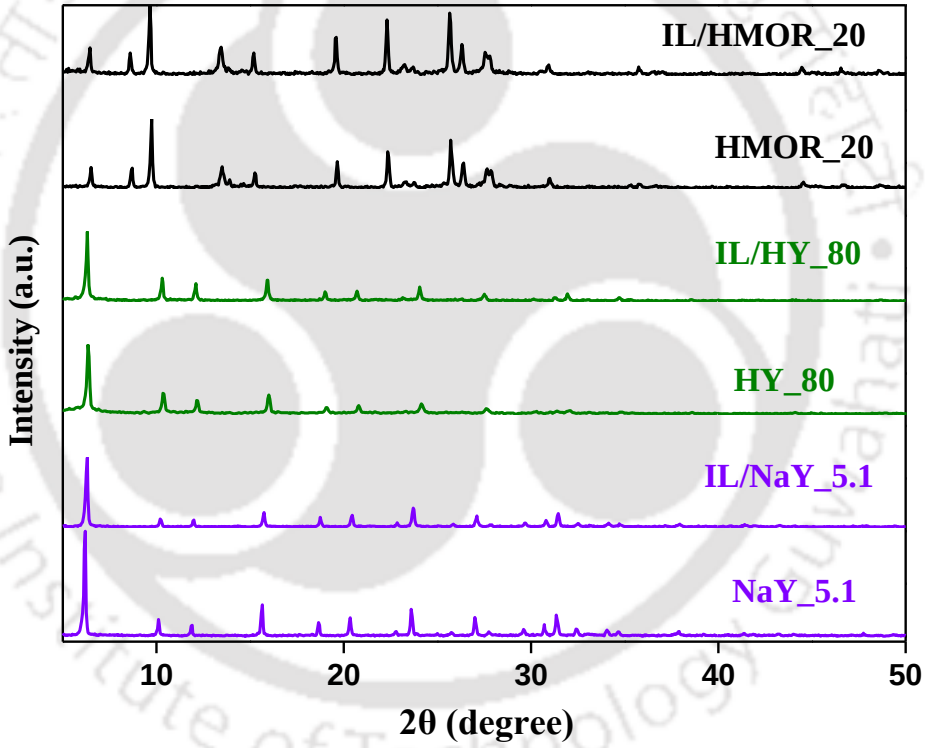

Figure 5.1: XRD patterns of bare and [BMIM]Br encapsulated zeolites.

Table 5.1: Confirmation of presence of [BMIM]Br in zeolite by various characterization techniques and its effect on crystal size, position of Al, SiO_2/Al_2O_3, and Na_2O/Al_2O_3 ratios of the zeolites.

Catalyst	Crystal size (nm) [a]	[BMIM]Br in zeolite (Wt.%)		^{27}Al NMR chemical shift (ppm)	SiO_2/Al_2O_3 [b]	Na_2O/Al_2O_3 [b]
		From TGA	From CHNS			
NaY_5.1	58	NA	NA	66.2	5.12	1.07
[BMIM]Br/NaY_5.1	71	3.6	8.7	65.423	7.46	0.15
HY_80	49	NA	NA	65.789,	88.02	0.32

				4.817		
[BMIM]Br/HY_80	56	1.4	6.5	65.771, 4.523	95	0.22
HMOR_20	62	NA	NA	60.528, 4.817	19.44	0.02
[BMIM]Br/HMOR_20	65	6.8	7.9	59.93	22.38	0.01
[a]from XRD using Scherrer's equation [b]from EDX analysis NA – Not applicable						

5.2.1.2 TGA and CHNS Analysis

Quantification of [BMIM]Br encapsulated in the zeolite is carried out by TGA weight loss measurements and from CHNS analysis. Thermal stability profiles of all the bare and [BMIM]Br encapsulated zeolites are shown in Fig. 5.2a. The bare zeolites exhibit one major weight loss in the initial temperature range i.e., 50 – 200°C. The weight loss in this region could be due to the removal of the framework-bound moisture present inside the pores of the zeolite. After 200°C, the weight loss is very minimal, indicating that all parent bare zeolites are thermally stable. In the case of [BMIM]Br encapsulated zeolites, the weight loss in the range of 200 – 800°C is attributed to the decomposition of [BMIM]Br. This weight loss for [BMIM]Br encapsulated zeolites is much higher than that of the parent zeolite confirming that the encapsulation of ionic liquid inside the pores of the zeolites (Table 5.1). All [BMIM]Br encapsulated zeolites exhibited two major DTG peaks (Fig. 5.2b). The 1-butyl-3-methylimidazolium [BMIM] made up of imidazolium and butyl chain (alkyl). It shows two stages of decomposition in TGA analysis as shown in Fig. 5.2b. It is speculated that the decomposition step from 430 to 475°C corresponds to the decomposition of alkyl chain of [BMIM] (Maton et al., 2013; Mohamedali et al., 2018). However, for confirmation we need to perform the TGA-MS, which gives the complete information on the fragments formed at different temperatures. The second DTG peak corresponds to the total decomposition of [BMIM]Br (Mohamedali et al., 2018). The thermal stability of zeolite confined [BMIM]Br is significantly higher as compared to their bulk counterparts. Yu et al. (2014b) also reported similar thermal profile for [BMIM]Br encapsulated in NaY zeolite. The thermal stability of confined ILs in silica is lower as compared to their bulk counterparts as reported in the literature (Chen et al., 2012), which is in contrast to what we observed with zeolites.

Further investigation of TGA profiles reveals that the decomposition temperatures of IL varied with the variation of cation (Na^+ and H^+) in the zeolite as well as with the type of zeolite. The two DTG peaks are at 433 and 550°C for [BMIM]Br/NaY_5.1, 450 and 586°C

for [BMIM]Br/HY_80, and 475 and 588°C for [BMIM]Br/HMOR_20, respectively. The difference in the second decomposition temperature, i.e., 550°C (for [BMIM]Br/NaY_5.1) vs. 588°C (for [BMIM]Br/HY_80) is due to variation of the ionic interaction of [BMIM]Br with the cation (Na^+ or H^+) of the zeolite framework. A similar two-stage decomposition is observed by Mohamedali et al. (2018) in their work on [BMIM][Ac]@ZIF. The authors reported that the shift in decomposition temperature is due to different decomposition mechanism and variation of ionic interactions of IL with ZIF-8 pores. To summarize the TGA data, it can be said that the weight loss from TGA corresponds to the [BMIM]Br loading and the shift in decomposition peaks signifies the interaction of IL with the zeolite. The [BMIM]Br weight present in the zeolite is also analyzed using CHNS elemental analyzer (Table 5.1). Amount of [BMIM]Br presence is calculated from the percentage of C present (as determined by CHNS analyzer). The [BMIM]Br amounts encapsulated in NaY_5.1, HY_80 and HMOR_20 are 8.7, 6.5, and 7.9 wt %, respectively. The difference in wt % of [BMIM]Br obtained from TGA and CHNS analysis could be attributed to the incomplete decomposition of [BMIM]Br.

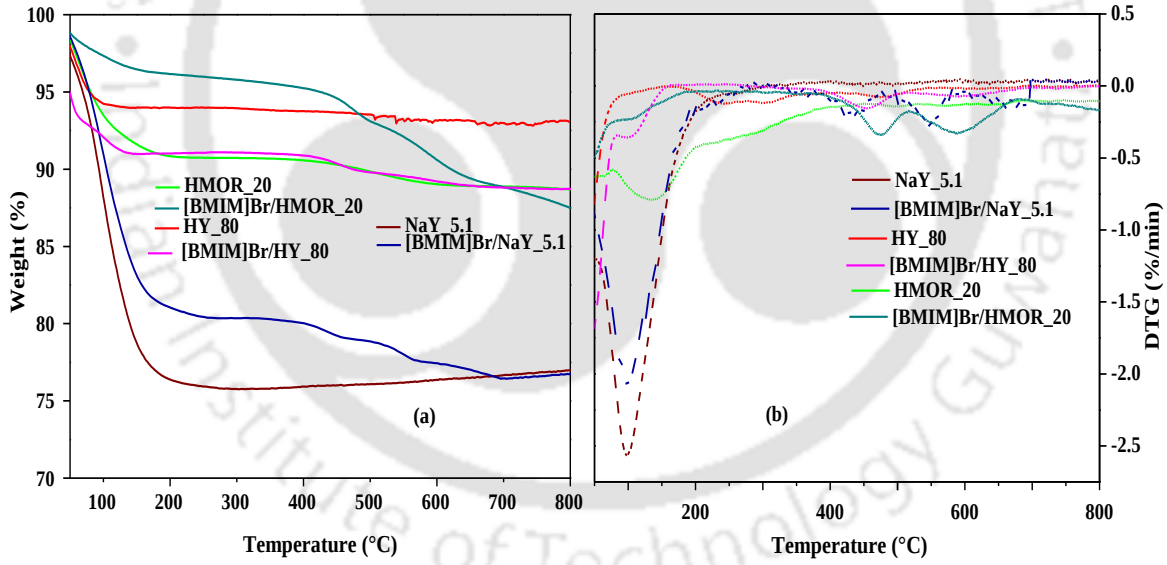

Figure 5.2: TGA profiles of bare and [BMIM]Br encapsulated zeolite catalysts.

5.2.1.3 N_2 sorption studies

Fig. 5.3 shows the N_2 isotherm of bare and [BMIM]Br encapsulated zeolites. All the [BMIM]Br zeolites exhibited similar type isotherm as that of the parent zeolites. NaY_5.1 and [BMIM]Br/NaY_5.1 zeolites display type I isotherm indicating the typical microporous nature. HY_80 and HMOR_20 exhibited a combination of both type I and IV isotherms indicating the presence of both mesoporosity and microporosity. The BET surface area (S_{BET})

decreases significantly (712 to 473 m^2g^{-1} for NaY_5.1, 773 to 673 $m^2.g^{-1}$ for HY_80, and 365 to 36 $m^2.g^{-1}$ for HMOR_20) in all the cases of [BMIM]Br encapsulated zeolite which signifies the presence of [BMIM]Br in the pores of the zeolite structure. The percentage variation of S_{BET} with and without [BMIM]Br leaves an insight of the variation of [BMIM]Br loading in the zeolite pores. The percentage decrease of $(S_{BET})_{IL}$ to $(S_{BET})_{without\text{-}IL}$ is as follows: HMOR_20 (~10 times) > NaY_5.1 (~1.5) > HY_80 (~1.1) and it is similar to that of the TGA weight loss (Table 5.1). The micropore areas (S_μ) of all the three zeolites are also decreased significantly (672 to 439 $m^2.g^{-1}$ for NaY_5.1, 440 to 343 $m^2.g^{-1}$ for HY_80, and 306 to 0 $m^2.g^{-1}$ for HMOR_20). However, the incorporation of [BMIM]Br in NaY_5.1 and HY_80 zeolite showed only a marginal effect on the ratio of S_μ to S_{BET}, which is essentially remained constant at 0.94 and 0.54, respectively, for these two zeolites (Table 5.2). Whereas, in HMOR_20 zeolite, the [BMIM]Br encapsulation showed a significant effect on the microporosity, making the S_μ/S_{BET} ratio zero.

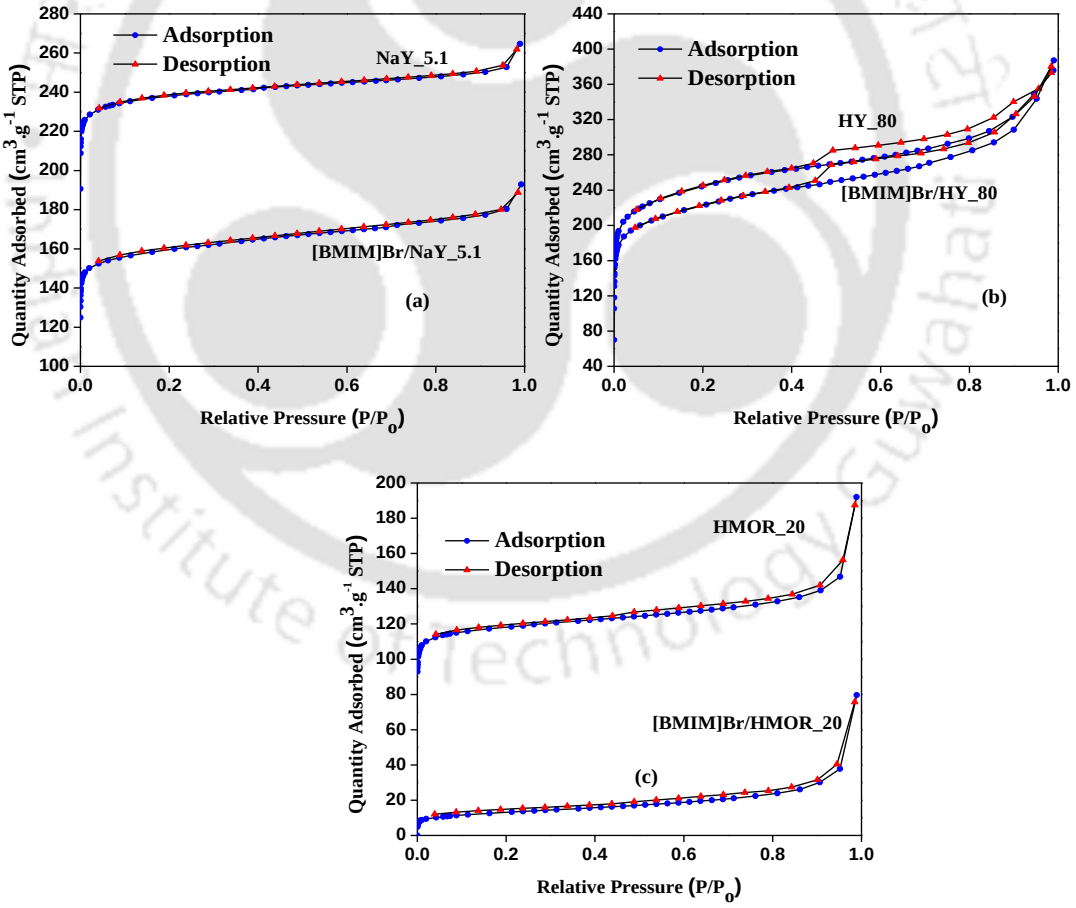

Figure 5.3: N_2 sorption data of bare and [BMIM]Br encapsulated zeolites.

Table 5.2: N_2 sorption data of bare and [BMIM]Br encapsulated zeolites.

Zeolite Name (Si/Al)	S_{BET} ($m^2.g^{-1}$)	S_{μ} $m^2.g^{-1}$)	V_{μ} ($cm^3.g^{-1}$)	V_p ($cm^3.g^{-1}$)	Avg. pore size (nm)	BJH Method		S_{μ}/ S_{BET}	REF
						S_{des} ($m^2.g^{-1}$)	V_{des} ($cm^3.g^{-1}$)		
NaY_5.1	712	672	0.351	0.409	2.30	15	0.04	0.94	PW
[BMIM]Br/NaY_5.1	473	439	0.227	0.262	2.41	18	0.05	0.93	PW
HY_80	773	440	0.231	0.581	1.50	333	0.35	0.57	A
[BMIM]Br/HY_80	671	343	0.180	0.530	3.16	328	0.35	0.52	A
HMOR_20	365	306	0.160	0.273	3.00	59	0.11	0.83	A
[BMIM]Br/HMOR_20	36	-	-	0.15	16.24	36	0.15	-	A

S_{BET} - BET surface area
S_{des} - BJH desorption surface area
S_{μ}- t-plot micropore surface area
P_D - Average pore diameter
V_P - total pore volume calculated at P/Po = 0.99
V_{μ}- t-plot micropore volume
V_{des} - BJH pore volume from desorption
A - (Saxena et al., 2017)
PW- Present Wotk

5.2.1.4 Spectroscopy analysis

Further, spectroscopy analysis (FTIR, Raman, EDX, and ^{27}Al NMR) confirms the existence/interaction of [BMIM]Br inside/with the zeolite pores. In the case of NaY_5.1 and [BMIM]Br/NaY_5.1, the Raman spectra exhibited a peak at 500 cm^{-1} (Fig. 5.4). It is the characteristic peak of NaY_5.1 zeolite attributed to framework T-O stretching. Some additional peaks are observed in [BMIM]Br/NaY_5.1 at 1023, 1332, and 1416 cm^{-1}. These peaks are the characteristic peaks of BMIM[Br] corresponding to CH_3 bending and ring bending (Yu et al., 2014a; Yuan et al., 2010), ring stretching and CH_3 symmetrical bending (Yu et al., 2014a; Yuan et al., 2010). Similarly, FTIR also exhibited the characteristic peaks of BMIM[Br]. IR band at 2800 – 3000 cm^{-1} attributed to C-H stretching vibrations of [BMIM]Br cation. Similar Raman and IR bands are observed in the earlier studies (Moumene et al., 2015; Yu et al., 2014a, 2014b; Yuan et al., 2010).

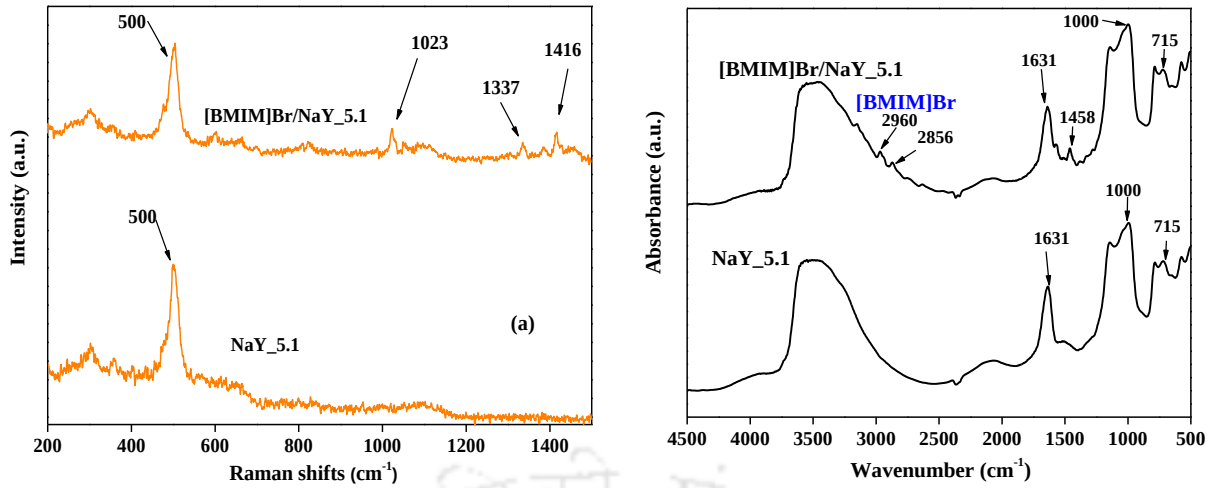

Figure 5.4: Raman and FTIR spectra of bare and [BMIM]Br encapsulated NaY_5.1 zeolite.

From EDX, the effect of ionic liquid encapsulation on silica to alumina ratio (SAR) is analyzed (Table 5.1). Encapsulation of [BMIM]Br in the zeolite had a significant effect on the molar ratios (i.e., SiO_2/Al_2O_3 and Na_2O/Al_2O_3). An increase in SAR and decrease in Na_2O/Al_2O_3 are observed with [BMIM]Br encapsulation in zeolites. For example, the SAR increased from 2.56 to 3.73 upon encapsulation of [BMIM]Br in NaY_5.1. The variation of SAR in this study is in line with the literature (Moliner et al., 2013; Yuan et al., 2015; Zhu et al., 2013). Zhu et al. (2013) encapsulated the N-methylpyridinium (NMP) iodide as SDA in the synthesis of high silica Y zeolite. The author explains the decrease in Na_2O/Al_2O_3 ratio is due to the partial replacement of sodium cation by the NMP cation to balance the charges of the zeolite framework (Zhu et al., 2013). All these results suggest that [BMIM]Br is incorporated into the zeolite pores, which tends to balance the charge on the zeolite, therefore $[BMIM]^+$ cation partially replaces the sodium cation or proton of the zeolite and results in the change in electron density around the Al. This change in electron density is confirmed by the ^{27}Al Solid-state NMR analysis.

From ^{27}Al Solid-state NMR spectroscopy analysis, the effects of ionic liquid encapsulation on the position of alumina (in the framework or in the extra-framework, etc.), as well as the change in electron density, are analyzed (Fig. 5.5). In H-form (HY_80 and HMOR_20) zeolites, an extra framework is observed at 4.817 ppm, resulted from the calcination of ammonia exchanged zeolite. However, in all the cases of [BMIM]Br encapsulation, a slight upfield shift is observed for the framework alumina (Table 5.1). The slight peak shift with [BMIM]Br encapsulation could be attributed to the change in the chemical environment of the framework Al. For example, the framework Al in NaY_5.1

zeolite has an upfield shift by 0.777 ppm. For HMOR_20, the peak (4.817 ppm) corresponding to the extra framework Al is disappeared, and a slight upfield shift of 0.593 ppm is observed for the peak corresponding to framework Al, upon IL encapsulation. Similarly, for HY_80, an upfield shift of 0.294 ppm is observed in the extra framework Al, upon encapsulation with [BMIM]Br. The change in electron density (due to the incorporation of IL in zeolite pores) results in charge imbalance on the zeolite and loses some Al atoms (Zhu et al., 2013).

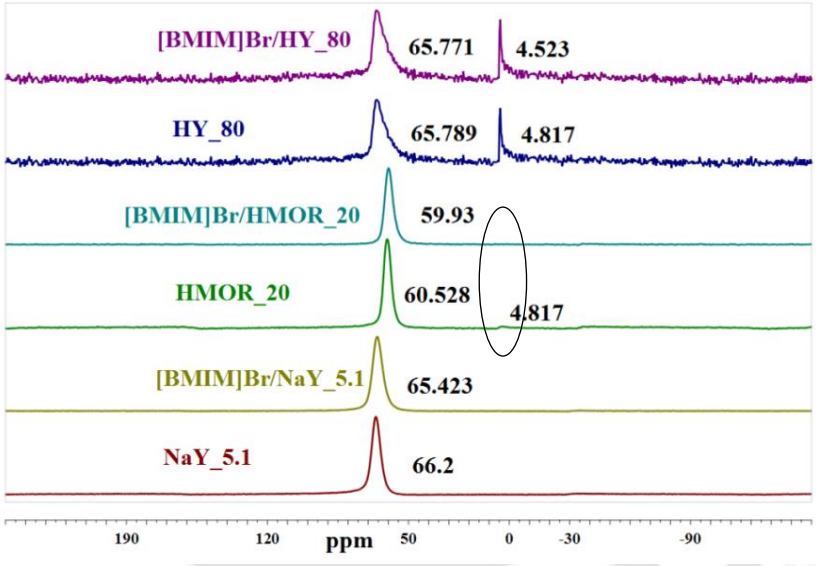

Figure 5.5: ^{27}Al NMR spectra of bare and [BMIM]Br encapsulated zeolites.

5.2.1.5 Morphology analysis

Morphology and d-spacing of the NaY_5.1 and IL/NaY_5.1 are analyzed using FETEM (Fig. 5.6). No effect of IL encapsulation is noticed on the morphology of the zeolite. The d-spacing with and with-out IL has a marginal effect and is consistent with XRD analysis. The d-spacing for NaY_5.1 and [BMIM]Br/NaY_5.1 are 1.42 nm and 1.64 nm, respectively. The IL encapsulated zeolite ([BMIM]Br/NaY_5.1) showed a poly-crystallinity structure which could be a combination of IL and the parent zeolite crystallinity (NaY_5.1).

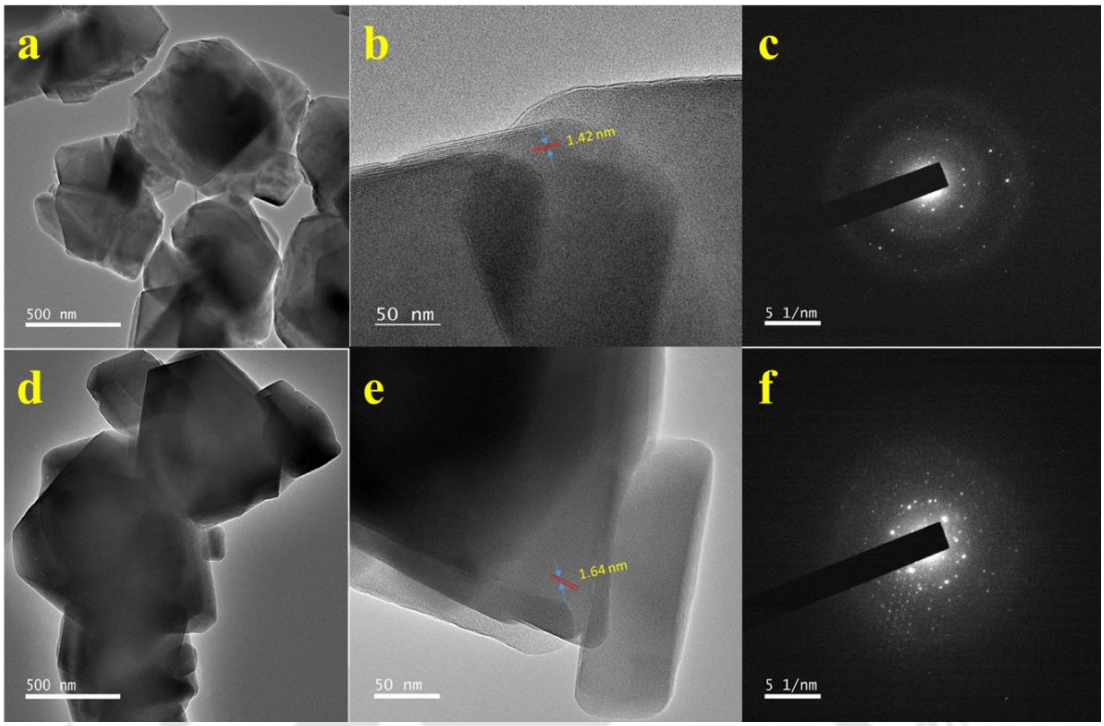

Figure 5.6: FETEM of various catalysts: NaY_5.1 (a, b and c) and [BMIM]Br/NaY_5.1 (d, e and f).

5.2.2 Catalyst testing

The bare and IL encapsulated zeolites catalytic activity are tested for the conversion of various carbohydrates (cellulose, glucose, and fructose) to 5-HMF. The optimal reaction conditions (reaction temperature and time) are obtained with the monosaccharide (glucose). At the optimal conditions, the performance of various catalysts is tested with different substrates. Recycle study is conducted for the best catalyst at the optimized parameters. All the catalyst testing conditions used in this study are presented in Table 5.3.

Table 5.3: Reaction conditions used for the catalyst testing (other reaction conditions are constant at: 2 g water; 0.6 g NaCl; 0.0667 g catalyst; 0.2 g substrate and 4 g MIBK).

Sl. no.	Temperature (°C), Time (h)	Substrate	Catalyst
01	180, 1	Glucose	[BMIM]Br/HMOR_20
02	180, 3	Cellulose	[BMIM]Br/NaY_5.1
03	180, 3	Cellulose	[BMIM]Br/HY_80
04	180, 3	Cellulose	[BMIM]Br/HMOR_20
05	180, 3	Cellulose	NaY_5.1

06	180, 3	Cellulose	HY_80
07	180, 3	Cellulose	HMOR_20
08	180, 1	Fructose	[BMIM]Br/NaY_5.1
09	180, 1	Glucose	[BMIM]Br/NaY_5.1
10	180, 1.5	Glucose	[BMIM]Br/NaY_5.1
11	180, 2	Glucose	[BMIM]Br/NaY_5.1
12	180, 2.5	Glucose	[BMIM]Br/NaY_5.1
13	180, 3	Cellulose	[BMIM]Br/NaY_5.1
14	180, 3	Cellulose	[BMIM]Br/NaY_5.1
15	180, 3	Cellulose	[BMIM]Br/NaY_5.1
16	180, 3	Cellulose	[BMIM]Br/NaY_5.1

5.2.2.1 Effect of catalyst types

Effect of [BMIM]Br encapsulation over different zeolites is studied for the conversion of cellulose (Fig. 5.7). The 5-HMF yield varies over bare zeolites in the following order: NaY_5.1 > HY_80 > HMOR_20. Whereas, the side products (LA and FA) follows the opposite trend, i.e., $(LA)_{HMOR\_20} > (LA)_{HY\_80} > (LA)_{NaY\_5.1.}$ This signifies that the formed 5-HMF undergo rehydration to LA and FA. It is understood from literature (Choudhary et al., 2013; Li et al., 2016) and our previous work (Saxena et al., 2017; Velaga and Peela, 2019) that rehydration of 5-HMF occur via Brønsted acid sites. Therefore, higher rehydration rate of HMOR_20 could be due to the presence of higher Brønsted acid sites in HMOR_20 as compared to that in the remaining two zeolites. However, the yield of glucose over HY_80 (~12%) is higher than that over NaY_5.1 (~0.5%) and HMOR_20 (~0.5%). It could be due to the presence of Lewis acid sites resulted from the extra framework alumina as noticed from ^{27}Al SS NMR data (Kruger et al., 2013). In all the cases of zeolites with IL encapsulation showed the positive effect on the yield and selectivity of 5-HMF. For example, the 5-HMF yield is increased from 41 to 59% over [BMIM]Br/NaY_5.1. While the yield of the intermediate product increased, i.e., glucose (0.5 to 6%) and side products such as LA (8 to 6%), FA (8.5 to 5.5%), and AA (5 to 4%) decreased with IL encapsulation. Similarly, for HY_80 and HMOR_20, the yield of 5-HMF is increased from 29 to 39% and 18 to 40% respectively with IL encapsulation. The percentage increase in the yield of 5-HMF over the zeolites with and without IL encapsulation is in relation to the amount of IL loading. The behaviour is like $(5\text{-HMF})_{[BMIM]Br/MOR\_20}$ to $(5\text{-HMF})_{MOR\_20}$ > $(5\text{-HMF})_{[BMIM]Br/NaY\_5.1}$ to $(5\text{-HMF})_{NaY\_5.1}$ > $(5\text{-HMF})_{[BMIM]Br/HY\_80}$ to $(5\text{-HMF})_{HY\_80}$ which is similar manner as explained

in the TGA and N_2 sorption study. Whereas the yield of side products (LA, FA) decreased with ionic liquid encapsulation which could be due to stabilization of 5-HMF by IL with the formation of a hydrogen bond with IL and 5-HMF as explained by Hu et al. (2014). The increase in glucose yield is due to the rearrangement of Al in the zeolite framework with the $[BMIM]^+$ cation, which in turn tends to reduce the Brønsted acid sites. The phenomena of the rearrangement of the cation of zeolite with incoming IL are explained in XRD and EDX analyses. Our results are consistent with the literature, where the increase of SAR of zeolites increase the selectivity to 5-HMF (Jiménez-Morales et al., 2015; Kruger et al., 2013). In overall, ionic liquid encapsulated zeolites showed higher activity than bare parental zeolite, among the [BMIM]Br/zeolites, [BMIM]Br/NaY_5.1 showed the highest activity in terms of 5-HMF yield. Therefore, further studies are performed using [BMIM]Br/NaY_5.1.

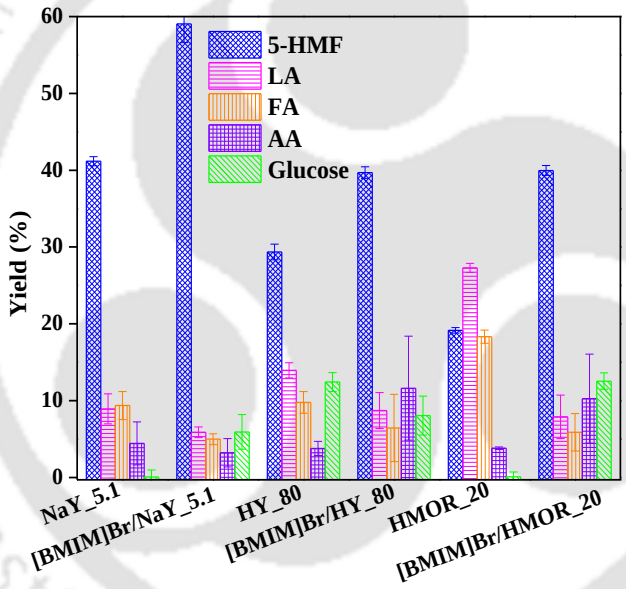

Figure 5.7: Yields of 5-HMF and side products over bare and [BMIM]Br encapsulated zeolites (Reaction conditions: 2 g DI water, 0.2 g substrate, substrate: catalyst = 3:1 w/w, 4 g MIBK, 0.6 g NaCl, 3 h reaction time and 180°C temperature).

5.2.2.2 Effect of reaction time

Effect of reaction time on the yield of 5-HMF and other products from glucose is shown in Fig 5.8. Glucose conversion increased from 76% at 60 min and reached 100% at 120 min. The yield of 5-HMF initially increased with time up to 120 min and then decreased at 150 min, reaching a maximum of 62%. The decrease at higher reaction times could be attributed to the formation of side products such as humins. The yield of levulinic acid and formic acid also increased up to 120 min reaction time and then leveled-off at higher times.

However, the maximum yield of these side products is less than 10%. The yield of AA is nearly constant with reaction time. The optimum parameters are found to be 180°C and 2 h reaction time for the conversion of glucose, with a maximum yield of desired product.

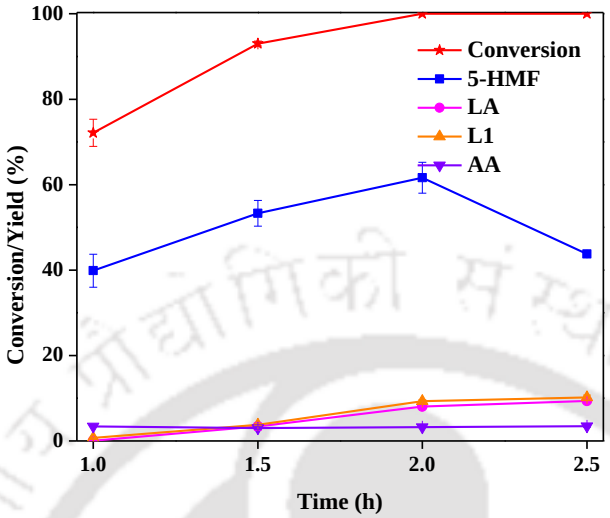

Figure 5.8: Effect of reaction time on conversion of glucose and yields of reaction products (reaction conditions: 2 g DI water, 0.2 g substrate, substrate: catalyst ([BMIM]Br/NaY_5.1) = 3:1 w/w, 4 g MIBK, 0.6 g NaCl, and 180°C reaction temperature).

5.2.2.3 Influence of reaction substrates on 5-HMF yield

Various carbohydrates such as fructose, glucose, cellulose, and xylose are studied to determine the role of the reactant on the 5-HMF and furfural yield and product distribution over [BMIM]Br/NaY_5.1 zeolite at the above optimized parameters. Fig. 5.9 shows the product distribution with the variation of reactant. The yield of 5-HMF is varied in the following order: fructose (80%) > glucose (62%) > cellulose (59%). As understood from literature (Ennaert et al., 2016; Kang et al., 2018; Kuster, 1990; Li et al., 2016), the conversion of cellulose to 5-HMF involves the formation of intermediates such as glucose, fructose. As cellulose conversion is a cascade reaction, it may require higher reaction time. Therefore, cellulose to 5-HMF experiment is performed at longer times compared to glucose or fructose. In the case of cellulose, the yield of 5-HMF is 59% with an intermediate product (glucose) yield of 8% and side product yields of LA, FA, and AA of 8, 7, and 5%, respectively. In the case of glucose and fructose, the experiments are carried out at 2 and 1 h, respectively. The conversion of both fructose and glucose of 100% is obtained with a 5-HMF yield of 80 and 60%, respectively. The side products (LA and FA) formation is slightly higher from glucose as compared to that from fructose. The 5-HMF yield from cellulose is as good as from glucose. On other hands, an increase in reaction time to 2 h for fructose or 3 h

for glucose, leaning to lower 5-HMF yield and higher side products, as observed glucose time study. Our results are consistent with the literature (Hu et al., 2014; 2013).

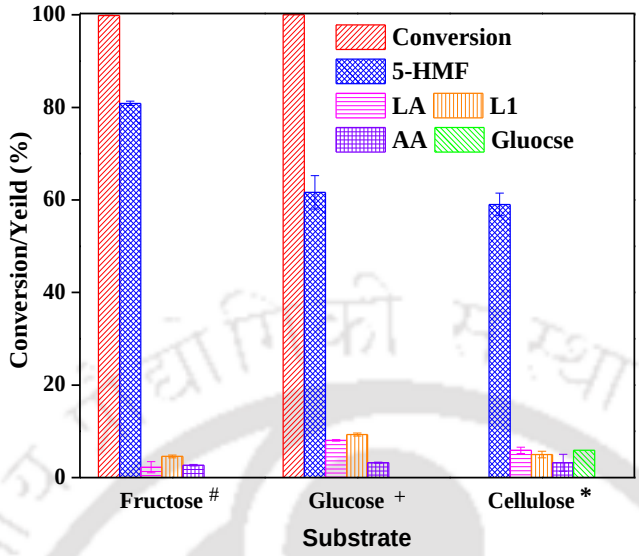

Figure 5.9: Conversion and yields of reaction products with various substrates (Fructose, Glucose, and Cellulose) over [BMIM]Br/NaY_5.1 zeolite catalyst (Reaction conditions: 2 g DI water, 0.2 g substrate, substrate: catalyst = 3:1 w/w, water/extractive phase-1:2 (w/w), 0.6 g NaCl, and 180°C reaction temperature). #With Fructose, the reaction time is 1 h, +With glucose, the reaction time is 2 h and *With cellulose, the reaction time is 3 h.

Effect of reactants on the 5-HMF yield is compared with literature and tabulated in Table 5.4. Most of the previous works report the use of ionic liquid as a co-catalyst/solvent for the production of 5-HMF from various carbohydrates. To the best of our knowledge, no reports are available for the carbohydrates conversion to 5-HMF over IL encapsulated zeolites. Therefore, we compared our results (conversions and 5-HMF yields) over [BMIM]Br/zeolite with those obtained with the physical mixture of IL + catalyst, by the previous research groups. Hu et al. (2014, 2013) in their various works, used the combination of HBeta and [BMIM]Cl (entry 1, Table 5.4); carbonaceous catalyst and [BMIM]Br (entry 2, Table 5.4) as catalyst system for the conversion of fructose and reported a yield of 5-HMF as 86.8 and 81.4% at slightly lower reaction conditions as compared to our system. Similarly, in the case of glucose and cellulose, the yield of 5-HMF are 50.3 and 46.4% (with HBeta + [BMIM]Cl catalyst system); 46.5 and 40.5% (with carbonaceous catalyst+[BMIM]Br catalyst system), respectively From this comparison, it could be noted that when IL is used as a co-catalyst/solvent, the operating conditions required to reach similar conversion and yield levels are milder as compared to those required for IL encapsulated zeolite catalysts, particularly when fructose is used as a substrate. However, with glucose and cellulose as substrates, the other studies showed lower yields. The higher

yields obtained with [BMIM]Br/NaY_5.1 could be attributed to the synergistic effect between the IL and the NaY_5.1 zeolite. Moreover, the major disadvantages associated with ionic liquid as a co-catalyst/solvent are higher cost and the difficulty in recovery and recyclability. The recovery of [BMIM]Br from the reaction mixture requires higher energy due to a higher boiling point of the [BMIM]Br.

Table 5.4: Comparison of the performance of [BMIM]Br encapsulated zeolites with literature data.

Sl. no.	Reactant	Catalyst	Reaction Temp. (°C) and time (h)	5-HMF Yield (%)	Reference
1	Fructose	HBETA + [BMIM]Cl	150, 0.84	86.8	(Hu et al., 2014)
2		Carbonaceous catalyst + [BMIM]Br	160, 0.25	81.4	(Hu et al., 2013)
3		$CrCl_3.6H_2O$ + TEAC	130, 0.16	73.8	(Hu et al., 2012)
4		[BMIM]Br/NaY_5.1	180, 1	80	PW
5	Glucose	HBETA + [BMIM]Cl	150, 0.84	50.3	(Hu et al., 2014)
6		[BMIM]Br/HMOR_20	170, 3	39	(Saxena et al., 2017)
7		Carbonaceous catalyst + [BMIM]Br	160, 0.25	46.4	(Hu et al., 2013)
8		Sn-Mont	160, 3	48.2	(Wang et al., 2012)
9		$CrCl_3.6H_2O$ + TEAC	130, 0.16	71.3	(Hu et al., 2012)
10		[BMIM]Br/NaY_5.1	180, 2	62	PW
11	Cellulose	HBETA + [BMIM]Cl	150, 0.84	46.5	(Hu et al., 2014)
12		$CuCl_2/CrCl_2$ + [EMIM]Cl	100, 8	57.5	(Su et al., 2009)
13		Carbonaceous catalyst+[BMIM]Br	160, 0.25	40.5	(Hu et al., 2013)
14		$CrCl_2/RuCl_3$ + [EMIM]Cl	120, 2	60	(Kim et al., 2011)
15		[BMIM]Br/NaY_5.1	180, 3	59	PW
16		[BMIM]Br/HY_80	180, 3	39	PW
17		[BMIM]Br/HMOR_20	180, 3	40	PW

5.2.2.4 Recycle test of used catalyst

Heterogeneous catalysis had an advantage of recyclability. Recycle study is performed for the catalyst, [BMIM]Br/NaY_5.1 at 180°C and 3 h (entries 02, 13 – 16, Table 5.3; Fig. 5.10). The yield of 5-HMF slightly decreased from 1st run (with fresh catalyst) to 3rd

run and then leveled-off after that up to 5th run. The yield of 5-HMF is 59% in 1st run, 47% in 2nd run and remained almost constant in 3rd, 4^{th,} and 5th runs. The slight decrease in the 5-HMF could be due to the blockage of pores by humins formed on the catalyst. The IL leaching from zeolites using ^{1}H-NMR analysis of the after experiment with D_2O as a solvent (Fig 5.11). The spectra did not show any peaks corresponding to IL. These results imply that [BMIM]Br encapsulated zeolites are stable and efficient catalysts for the conversion of carbohydrates to 5-HMF.

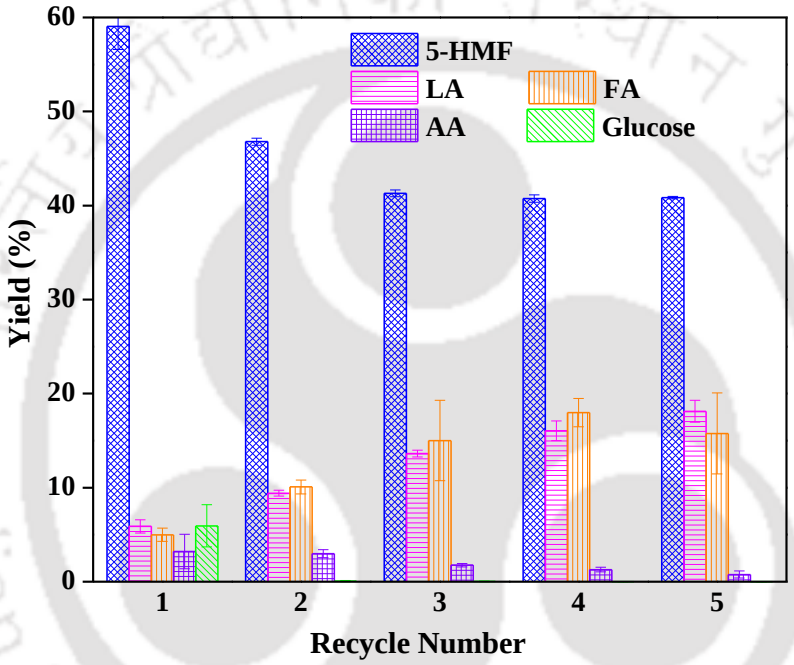

Figure 5.10: Recycle study of [BMIM]Br/NaY_5.1 catalyst with reactants: Cellulose (3 h) (other reaction conditions: 2 g DI water, 0.2 g substrate, substrate: catalyst = 3:1 w/w, 4 g MIBK, 0.6 g NaCl, and 180°C reaction temperature)

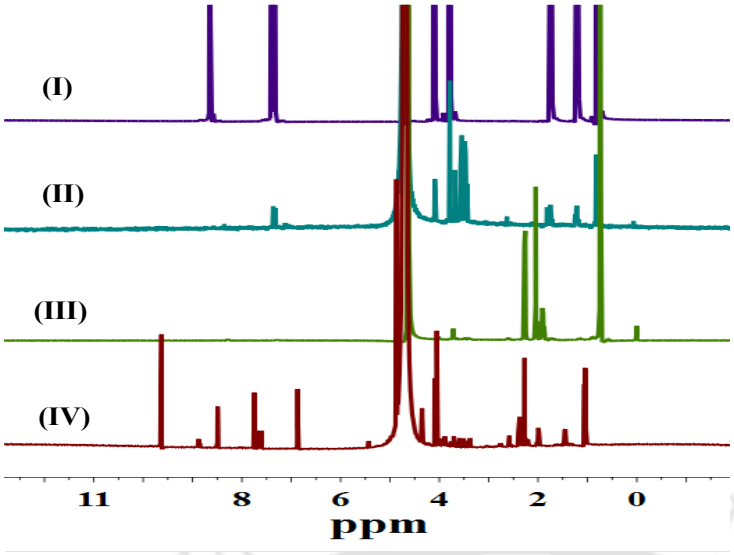

Figure 5.11 : ^{1}H NMR spectra for (I) pure [BMIM]Br, (II) [BMIM]Br /NaY_5.1 + D_2O suspension before exposing to reaction conditions (room temperature) and filtration (leaching test) (III) [BMIM]Br /NaY_5.1 + D_2O suspension after exposing to reaction conditions (180 °C and 3 h) and filtration (leaching test) and (IV) [BMIM]Br /NaY_5.1 + cellulose + Na Cl + D_2O suspension after exposing to reaction conditions (180 °C and 3 h) and filtration.

5.3 Conclusions

The [BMIM]Br ionic liquid is successfully encapsulated in the zeolites (NaY, HY, and HMOR) using a ship-in-a-bottle method and used for carbohydrates conversion to 5-HMF. The ionic liquid encapsulation is confirmed using various characterizations: XRD, TGA, CHN, N_2-sorption, Raman, EDX and ^{27}Al Solid-state (SS) NMR. The IL ionic interaction with H-form zeolite is stronger as compared to that of Na-form zeolite, as indicated by the TGA analysis. ^{27}Al SS NMR reveals that the HMOR loses its extra-framework Al upon the ionic liquid encapsulation. These catalysts showed significant improvements in the 5-HMF yield and carbohydrates conversions as compared to their bare zeolite counterparts. The 5-HMF yields obtained over [BMIM]Br/NaY with fructose, glucose, and cellulose are 80, 62, and 59% at 180^{o}C, respectively. The catalyst showed an excellent recycle stability with a moderate decrease in activity till the second cycle only.

References

Baerlocher, C., McCusker L.B., n.d. Database of Zeolite Structures [WWW Document].

Chen, S., Liu, Y., Fu, H., He, Y., Li, C., Huang, W., Jiang, Z., Wu, G., 2012. Unravelling the role of the compressed gas on melting point of liquid confined in nanospace. J. Phys. Chem. Lett. 3, 1052–1055. https://doi.org/10.1021/jz300225n

Choudhary, V., Mushrif, S.H., Ho, C., Anderko, A., Nikolakis, V., Marinkovic, N.S., Frenkel, A.I., Sandler, S.I., Vlachos, D.G., 2013. Insights into the interplay of lewis and Brønsted acid catalysts in glucose and fructose conversion to 5-(hydroxymethyl)furfural and levulinic acid in aqueous media. J. Am. Chem. Soc. 135, 3997–4006. https://doi.org/10.1021/ja3122763

Ennaert, T., Van Aelst, J., Dijkmans, J., De Clercq, R., Schutyser, W., Dusselier, M., Verboekend, D., Sels, B.F., 2016. Potential and challenges of zeolite chemistry in the catalytic conversion of biomass. Chem. Soc. Rev. 45, 584–611. https://doi.org/10.1039/c5cs00859j

Hsu, W.H., Lee, Y.Y., Peng, W.H., Wu, K.C.W., 2011. Cellulosic conversion in ionic liquids (ILs): Effects of H2O/cellulose molar ratios, temperatures, times, and different ILs on the production of monosaccharides and 5-hydroxymethylfurfural (HMF). Catal. Today 174, 65–69. https://doi.org/10.1016/j.cattod.2011.03.020

Hu, L., Sun, Y., Lin, L., 2012. Efficient conversion of glucose into 5-hydroxymethylfurfural by chromium(III) chloride in inexpensive ionic liquid. Ind. Eng. Chem. Res. 51, 1099–1104. https://doi.org/10.1021/ie202174f

Hu, L., Wu, Z., Xu, J., Sun, Y., Lin, L., Liu, S., 2014. Zeolite-promoted transformation of glucose into 5-hydroxymethylfurfural in ionic liquid. Chem. Eng. J. 244, 137–144. https://doi.org/10.1016/j.cej.2014.01.057

Hu, L., Zhao, G., Tang, X., Wu, Z., Xu, J., Lin, L., Liu, S., 2013. Catalytic conversion of carbohydrates into 5-hydroxymethylfurfural over cellulose-derived carbonaceous catalyst in ionic liquid. Bioresour. Technol. 148, 501–507. https://doi.org/10.1016/j.biortech.2013.09.016

Jiménez-Morales, I., Moreno-Recio, M., Santamaría-González, J., Maireles-Torres, P., Jiménez-López, A., 2015. Production of 5-hydroxymethylfurfural from glucose using aluminium doped MCM-41 silica as acid catalyst. Appl. Catal. B Environ. 164, 70–76. https://doi.org/10.1016/j.apcatb.2014.09.002

Kang, S., Fu, J., Zhang, G., 2018. From lignocellulosic biomass to levulinic acid: A review on acid-catalyzed hydrolysis. Renew. Sustain. Energy Rev. 94, 340–362. https://doi.org/10.1016/j.rser.2018.06.016

Kim, B., Jeong, J., Lee, D., Kim, S., Yoon, H.J., Lee, Y.S., Cho, J.K., 2011. Direct transformation of cellulose into 5-hydroxymethyl-2-furfural using a combination of metal chlorides in imidazolium ionic liquid. Green Chem. 13, 1503–1506. https://doi.org/10.1039/c1gc15152e

Kruger, J.S., Choudhary, V., Nikolakis, V., Vlachos, D.G., 2013. Elucidating the roles of zeolite H-BEA in aqueous-phase fructose dehydration and HMF rehydration. ACS Catal. 3, 1279–1291. https://doi.org/10.1021/cs4002157

Kuster, B.F.M., 1990. 5-Hydroxymethylfurfural (HMF). A Review Focussing on its Manufacture. Starch - Stärke 42, 314–321. https://doi.org/10.1002/star.19900420808

Li, H., Fang, Z., Smith, R.L., Yang, S., 2016. Efficient valorization of biomass to biofuels with bifunctional solid catalytic materials. Prog. Energy Combust. Sci. 55, 98–194. https://doi.org/10.1016/j.pecs.2016.04.004

Maton, C., Vos, N. De, Stevens, C. V, 2013. mechanisms and analysis tools the 5963–5977. https://doi.org/10.1039/c3cs60071h

Mohamedali, M., Ibrahim, H., Henni, A., 2018. Incorporation of acetate-based ionic liquids into a zeolitic imidazolate framework (ZIF-8) as efficient sorbents for carbon dioxide capture. Chem. Eng. J. 334, 817–828. https://doi.org/10.1016/j.cej.2017.10.104

Moliner, M., Rey, F., Corma, A., 2013. Towards the rational design of efficient organic structure-directing agents for zeolite synthesis. Angew. Chemie - Int. Ed. 52, 13880–13889. https://doi.org/10.1002/anie.201304713

Moumene, T., Belarbi, E.H., Haddad, B., Villemin, D., Abbas, O., Khelifa, B., Bresson, S., 2015. Study of imidazolium dicationic ionic liquids by Raman and FTIR spectroscopies: The effect of the nature of the anion. J. Mol. Struct. 1083, 179–186. https://doi.org/10.1016/j.molstruc.2014.11.061

Olivier-Bourbigou, H., Magna, L., Morvan, D., 2010. Ionic liquids and catalysis: Recent progress from knowledge to applications. Appl. Catal. A Gen. 373, 1–56. https://doi.org/10.1016/J.APCATA.2009.10.008

Peela, N.R., Yedla, S.K., Velaga, B., Kumar, A., Golder, A.K., 2019. Choline chloride functionalized zeolites for the conversion of biomass derivatives to 5-hydroxymethylfurfural. Appl. Catal. A Gen. 580, 59–70. https://doi.org/10.1016/j.apcata.2019.05.005

Saxena, P., Velaga, B., Peela, N.R., 2017. Ionic Liquid-Encapsulated Zeolite Catalysts for the Conversion of Glucose to 5-Hydroxymethylfurfural. ChemistrySelect 2, 10379–10386. https://doi.org/10.1002/slct.201701955

Su, Y., Brown, H.M., Huang, X., Zhou, X. dong, Amonette, J.E., Zhang, Z.C., 2009. Single-step conversion of cellulose to 5-hydroxymethylfurfural (HMF), a versatile platform chemical. Appl. Catal. A Gen. 361, 117–122. https://doi.org/10.1016/j.apcata.2009.04.002

Sudarsanam, P., Zhong, R., Van Den Bosch, S., Coman, S.M., Parvulescu, V.I., Sels, B.F., 2018. Functionalised heterogeneous catalysts for sustainable biomass valorisation. Chem. Soc. Rev. 47, 8349–8402. https://doi.org/10.1039/c8cs00410b

Tan, M.X., Zhao, L., Zhang, Y., 2011. Production of 5-hydroxymethyl furfural from cellulose in CrCl2/Zeolite/BMIMCl system. Biomass and Bioenergy 35, 1367–1370. https://doi.org/10.1016/j.biombioe.2010.12.006

Velaga, B., Peela, N.R., 2019. Seed-Assisted and OSDA-Free Synthesis of H-Mordenite Zeolites for Efficient Production of 5-Hydroxymethylfurfural from Glucose. Microporous Mesoporous Mater. 279, 211–219. https://doi.org/10.1016/J.MICROMESO.2018.12.028

Wang, J., Ren, J., Liu, X., Xi, J., Xia, Q., Zu, Y., Lu, G., Wang, Y., 2012. Direct conversion of carbohydrates to 5-hydroxymethylfurfural using Sn-Mont catalyst. Green Chem. 14, 2506–2512. https://doi.org/10.1039/c2gc35699f

Yang, J., De Vigier, K.O., Gu, Y., Jérôme, F., 2015. Catalytic dehydration of carbohydrates suspended in organic solvents promoted by ALCL3/SiO2coated with choline chloride. ChemSusChem 8, 269–274. https://doi.org/10.1002/cssc.201402761

Yu, Y., Mai, J., Huang, L., Wang, L., Li, X., 2014a. Ship in a bottle synthesis of ionic liquids in NaY supercages for CO 2 capture. RSC Adv. 4, 12756–12762. https://doi.org/10.1039/c3ra46971a

Yu, Y., Mai, J., Wang, L., Li, X., Jiang, Z., Wang, F., 2014b. Ship-in-a-bottle synthesis of amine-functionalized ionic liquids in NaY zeolite for CO2capture. Sci. Rep. 4, 1–8. https://doi.org/10.1038/srep05997

Yuan, D., He, D., Xu, Shutao, Song, Z., Zhang, M., Wei, Y., He, Y., Xu, Shuliang, Liu, Z., Xu, Y., 2015. Imidazolium-based ionic liquids as novel organic SDA to synthesize high-silica y zeolite. Microporous Mesoporous Mater. 204, 1–7. https://doi.org/10.1016/j.micromeso.2014.10.049

Yuan, Y.X., Niu, T.C., Xu, M.M., Yao, J.L., Gu, R.A., 2010. Probing the adsorption of methylimidazole at ionic liquids/Cu electrode interface by surface-enhanced Raman scattering spectroscopy. J. Raman Spectrosc. https://doi.org/10.1002/jrs.2480

Zhang, S., Zhang, J., Zhang, Y., Deng, Y., 2017. Nanoconfined Ionic Liquids. Chem. Rev. 117, 6755–6833. https://doi.org/10.1021/acs.chemrev.6b00509

Zhang, Z., Song, J., Han, B., 2017. Catalytic Transformation of Lignocellulose into Chemicals and Fuel Products in Ionic Liquids. Chem. Rev. 117, 6834–6880. https://doi.org/10.1021/acs.chemrev.6b00457

Zhu, L., Ren, L., Zeng, S., Yang, C., Zhang, H., Meng, X., Rigutto, M., Made, A. Van Der, Xiao, F.S., 2013. High temperature synthesis of high silica zeolite y with good crystallinity in the presence of N-methylpyridinium iodide. Chem. Commun. 49, 10495–10497. https://doi.org/10.1039/c3cc43974g

Chapter 6

Bio-inspired Ag-, Cu- and P-doped TiO_2 Catalysts for the Conversion of Glucose to 5-HMF

6.1 Specific overview

The synthesis of 5-HMF from fructose is extensively investigated and substantial progress has been achieved. However, in comparison to fructose, glucose is readily available and cheaper material (Torres et al., 2010). Therefore, effective productions of 5-HMF from direct conversion of glucose and its polymer (cellulose) still lack in the literature and desirable for industrial production.

The titanium dioxide (TiO_2) is a strong amphoteric metal oxide (Maleki et al., 2017) and is widely used as a photocatalyst (Peng et al., 2005), sensor (Teleki et al., 2006), and electrode materials (Kwak et al., 2009). The great chemical stability, acid-base property and rich surface chemistry of TiO_2 are the major advantages of this metal oxide (Kamat, 2007). A few researchers have tested the titania for the production of 5-HMF from carbohydrates. Watanabe et al. (2005) investigated the production of 5-HMF from glucose using anatase TiO_2 in a hot compressed water. The authors reported anatase TiO_2 dual functionality of basic and acidic sites is responsible for the higher activity of this catalyst. The basic sites facilitate the glucose isomerization to fructose, whereas, the acidic sites enable dehydration to 5-HMF. De et al. (2011) studied self-assembled mesoporous TiO_2 nanospheres for the catalytic dehydration of glucose to 5-HMF and reported that the mesoporous titania surface acidity mainly responsible for catalyzing the dehydration reaction. Similarly, sodium salicylate acted as a template over titania nanosphere was studied for the dehydration of several carbohydrate substrates (Dutta et al., 2011). The Lewis acidity and high surface area of nanoparticles played an important part in the conversion of the carbohydrates to 5-HMF by the microwave-assisted approach. Recently, Kuo et al. (2014) studied the acidic TiO_2 nanoparticle synthesis

and its application for the 5-HMF production from carbohydrates. They identified that TiO_2 is capable of conversation of carbohydrates to 5-HMF as well as to other value-added products such as LA and FA by the rehydration of 5-HMF.

The catalytic conversion of glucose to 5-HMF with significantly improves the 5-HMF yield with immobilized H_3PO_4 over TiO_2 (Nakajima et al., 2014). TiO_2 exhibits only Lewis acid sites which is a limitation reported so far. The bifunctional Lewis and Brønsted acidity catalytic systems show a better performance for the production of 5-HMF than monofunctional catalysts with only either Brønsted or Lewis acid (Fan et al., 2011; Nikolla et al., 2011). So, the optimum suitable catalyst design is an important factor in 5-HMF synthesis.

The conventional methods for the functionalization of TiO_2 using noble metals or transition metals are photo-deposition, wet impregnation, chemical reduction and sol-gel method (Ismail et al., 2013; Tayade et al., 2006). The present study reported a new bio-mediated method using several dopant metals, namely, Ag, Cu and nonmetal P on TiO_2 support at room temperature and pressure (Rao and Golder, 2016) using the *Sechium edule* fruit-extract based analytes such as ascorbic acid (Chelli and Golder, 2018; Ordonez et al., 2006). The analytes existing in *S. edule* fruit are collected in water as a green solvent and used as the electron donor compounds for the doping of optimally pre-immobilized metal ions on TiO_2 (Chakraborty et al., 2017). The doped bifunctional TiO_2 nanoparticles combining both Lewis and Brønsted acid functionalities are adequately characterized to study its structural and morphological properties. The catalytic activity of doped TiO_2 for glucose conversion to 5-HMF is tested in a biphasic system (water/MIBK). The effects of various dopant materials, reaction time, and temperature were also investigated to optimize the process of 5-HMF production.

6.2 Results and discussions

6.2.1 Catalyst characteristics

6.2.1.1 Determination of Ag-, Cu-, and P-loading on TiO_2

The amount of Ag-doped into the TiO_2 is determined from the difference between the initial concentration (1.5% equivalent) of Ag^+ and Cu^{2+} precursors taken for the adsorption/immobilization and the concentration of Ag^+ and Cu^{2+} in the solution after the adsorption (Rao and Golder, 2016). Nearly, 83 and 78% of initial concentrations of Ag and Cu, respectively, are doped. It implied that the actual loading of Ag or Cu on TiO_2 was about

1.25 and 1.17 wt % on TiO_2. The concentrations of Ag^+ or Cu^{2+} leached out into bio-extract during the reduction process with bio-extract is insignificant. The elemental EDX image mapping of P/TiO_2 (Fig. 6.1) confirmed the presence of Ti, O, and P elements. The weight percent of P-loaded on TiO_2 is 0.8 ± 0.1 and the Ti and O abundances are of 78.8 ± 0.6 and 20.5 ± 0.6, respectively (Fig. 6.1b). High dispersion of P in the TiO_2 support is evident (Figs. 6.1(c-e)).

Table 6.1: Crystallite size and phase contents of bare and doped TiO_2.

Catalyst type	Particle size from TEM, nm	Particle size from DLS, nm	Crystallite size, nm		Crystalline phase, %	
			Anatase, 25.3°	Rutile, 27.4°	Anatase, 25.3°	Rutile, 27.4°
TiO_2	29.15	48.61	16.26	17.32	79.78	20.22
Ag/TiO_2	39.06	72.02	31.05	37.88	72.39	27.61
Cu/TiO_2	40.31	75.32	32.31	51.36	73.45	26.55
P/TiO_2	46.73	82.02	38.01	32.24	70.55	29.41

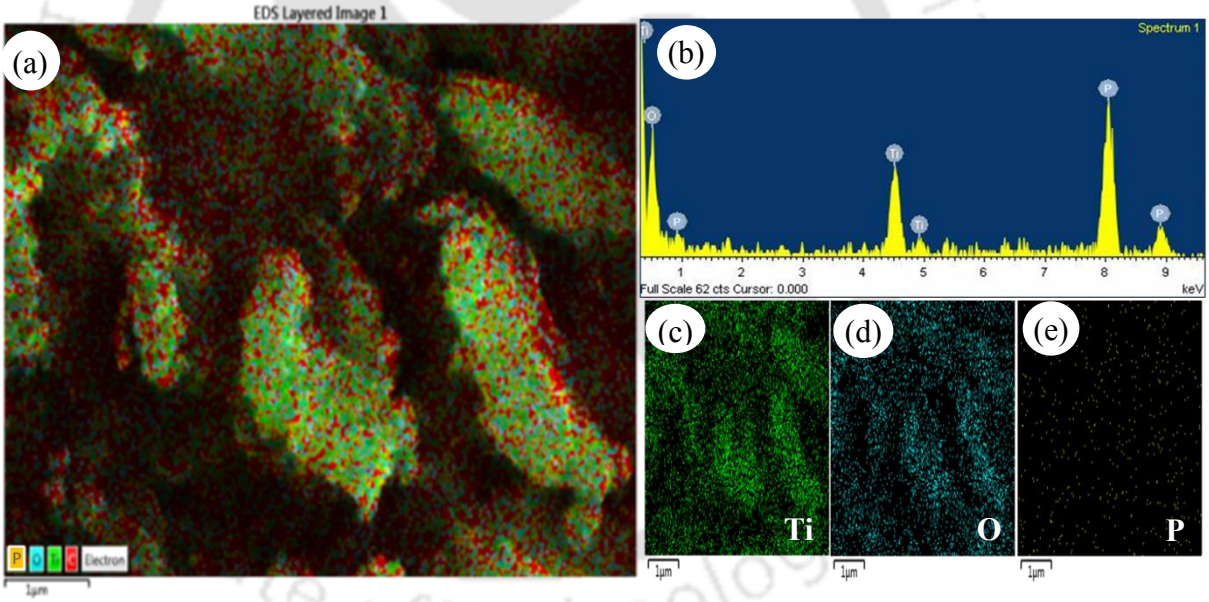

Figure 6.1: EDX image mapping of P/TiO_2 particles ((a): relative dispersity of C, O, Ti, and P elements, (b): Dispersity of individual element (c-e) Ti, O, and P dispersity).

6.2.1.2 Structural and morphological attributes

The intense diffraction peaks at 2θ values of 25.3, 37.8, 48.1, and 62.7° (Fig. 6.2) are due to the diffraction from the planes [1 0 1], [0 0 4], [0 2 0], and [0 2 4] of anatase phase (JCPDS file no. 21-1272), and the 2θ 27.4, 36.06, and 54.3° values for rutile, respectively (Rao and Golder, 2016). The XRD peaks corresponding to Ag, Cu, and P are not observed most

probably due to the presence of crystals with very small sizes, which are not detectable by XRD.

The rutile phase concentration is calculated using the following equation (Eq. 6.1):

$$\text{Rutile content (\%)} = \frac{A_R}{0.884(A_A + A_R)} \quad (6.1)$$

Where, A_R and A_A represent the integrated intensity from the planes [1 1 0] and [1 0 1] of the rutile and anatase phases, respectively. The lattice strains of bare TiO_2 and doped TiO_2 catalysts are determined from FWHM of the diffraction lines observed at different 2θ angles (20 to 80°) according to the Williamson-Hall's equation (Eq. 2) (Riazian et al., 2013).

$$\beta \cos\theta = \frac{k\lambda}{L} 4\varepsilon \sin\theta \quad (6.2)$$

where, β is the FWHM, ε is the lattice strain, and the shape factor k is assumed to be 0.9 similar to the Scherrer's equation, and λ is the wavelength of Kα(Cu) radiation.

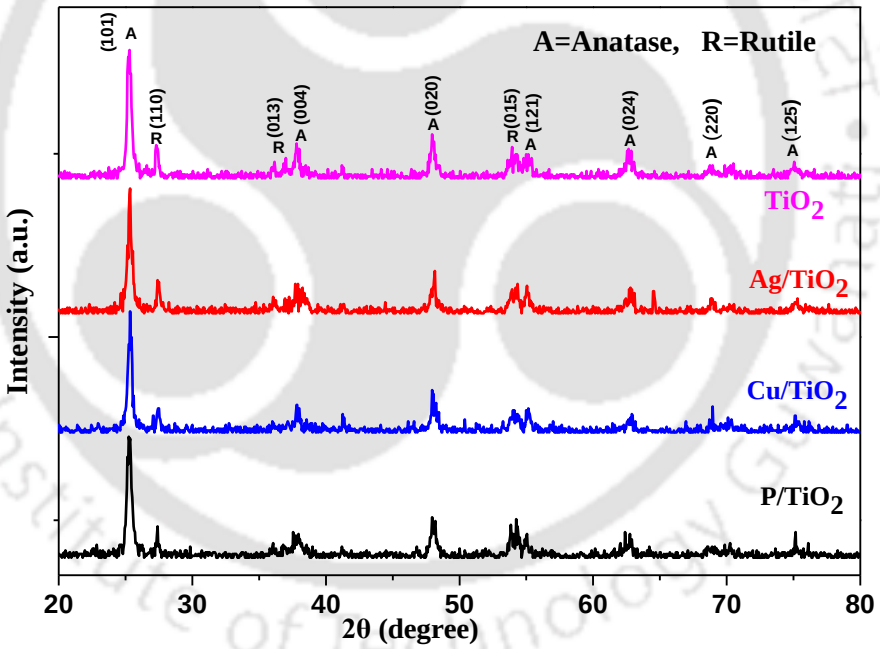

Figure 6.2: XRD patterns of bare, metal and phosphorous doped TiO_2.

The phase transformation from anatase to rutile (as determined using Eq. 6.1 and depicted in Table 6.1) is observed in all the catalysts via the surface reaction of metal with titanium sites (Ramakrishnan et al., 2012). This is also supported by the increment in the crystallite size for all the doped catalysts, which is determined by Scherrer's equation. For example, the average crystal size of TiO_2 increased by more than 2 folds from 16 to 38 nm for P-doped TiO_2, indicating significant crystal growth (Table 6.1). Moreover, from the XRD

lattice strain (as determined using Eq. 6.2) also it is decreased with doping from 0.0386 to 0.0365 (Ag/TiO_2), 0.0367 (Cu/TiO_2), and 0.0371 (P/TiO_2), respectively. The decrement in lattice strain corresponds to the phase transformation from anatase to rutile, which is consistent with the crystallite size increment. Hence, the decrement in lattice strain supports the incorporation of Ag, Cu, and P on TiO_2 due to ion-exchange or coordination reaction.

TEM micrographs (Fig. 6.3) indicate that the TiO_2 morphological features are influenced by the presence of other elements (in this case Ag, Cu, and P). The particle size of bare TiO_2 (Fig. 6.2a) is smaller than those of Ag-, Cu-, and P-doped TiO_2 (Figs. 6.3(b-d)), which partially explains the specific surface area reduction upon doping (Table 6.2). The silver, copper, and phosphate in TiO_2 are believed to stabilize the TiO_2 structure, increment of crystal size, which could have led to grain growth. The inter-planar spacing for TiO_2, Ag/TiO_2, Cu/TiO_2, and P/TiO_2 of fringes separation, as determined from HRTEM images, are 0.353, 0.353, 0.354, and 0.354 nm, respectively. These fringes correspond to the lattice plane (101) of the anatase phase (Fig. 6.2).

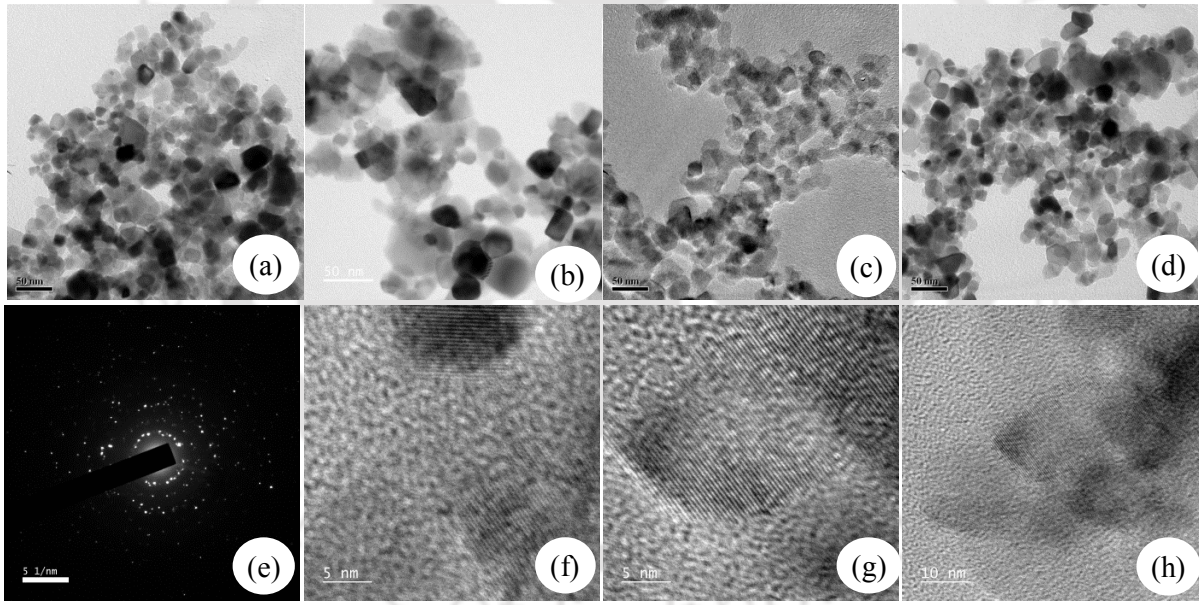

Figure 6.3: TEM micrographs of TiO_2 (a), Ag/TiO_2 (b), Cu/TiO_2 (c), P/TiO_2 (d), SAED patterns of P/TiO_2 (e), and high-resolution (HR) TEM images of Ag/TiO_2 (f), Cu/TiO_2 (g) and P/TiO_2 (h).

The TiO_2 crystal growth with Ag, Cu, and P doping, as observed from TEM and XRD analysis (Table 6.1), could be explained from the lattice strain relaxation phenomenon. The phenomenon involves the reduction of the induced strain arising from lattice distortion caused by the presence of Ag, Cu, and P. This behavior is facilitated by the induction of more oxygen species and thermal treatment which increases the mobility and allows transformation

of the TiO_2 to a thermodynamically more stable rutile phase (Atanda et al., 2015b). The increase of rutile phase percentage upon Ag-, Cu-, and P-doping onto TiO_2 is also observed from XRD data (Table 6.1).

The concentration of Lewis and Brønsted surface acid sites on bare and modified TiO_2 is determined by pyridine adsorption followed by FTIR (Fig. 6.4). Bare TiO_2 showed the intense absorption band at 1400 – 1450 cm^{-1}, which could be attributed to the coordinated Lewis acid sites, which indicates that the bare TiO_2 possesses more Lewis acid sites compared to Brønsted acid sites. The doped TiO_2 with Ag, Cu metals and oxides of phosphorus leads to significant modification of its nature of surface acid sites. The more intense absorption band observed at 1500 – 1560 cm^{-1}, after Ag-, Cu-, and P-doping on to TiO_2, corresponds to the existence of more Brønsted acid sites in these doped catalysts. The variation of the intensities of this band suggests a change in concentration of the available Brønsted acid sites. The concentration of Lewis (C_{LAS}) and Brønsted (C_{BAS}) acid sites are depicted in Table 6.2. The results indicate that Brønsted acidity decreases in the order: P/TiO_2 > Ag/TiO_2 > Cu/TiO_2. A strong interaction between the surface of TiO_2 and oxides of phosphorus is the possible reason for the increase of Brønsted acidity upon doping of TiO_2 with P. A similar trend of decreasing C_{LAS} and increase of C_{BAS} upon doping of P onto TiO_2 have been reported by Atanda et al. (2015a, 2015b).

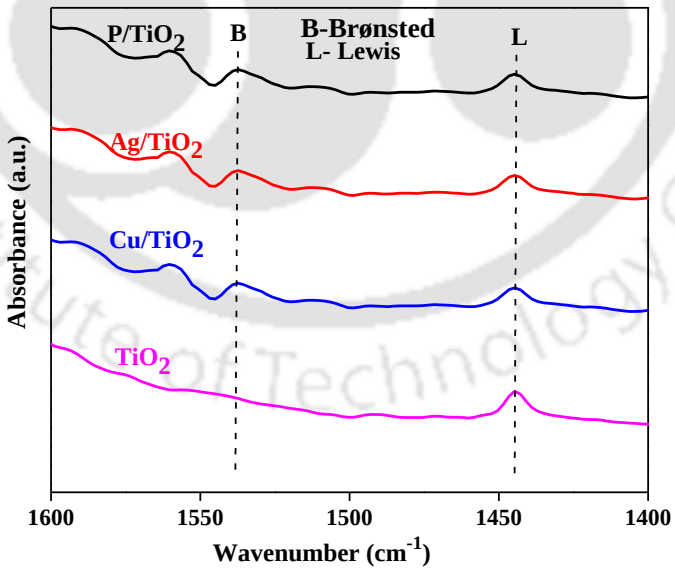

Figure 6.4: Py-FTIR of bare, metal and phosphorous doped TiO_2.

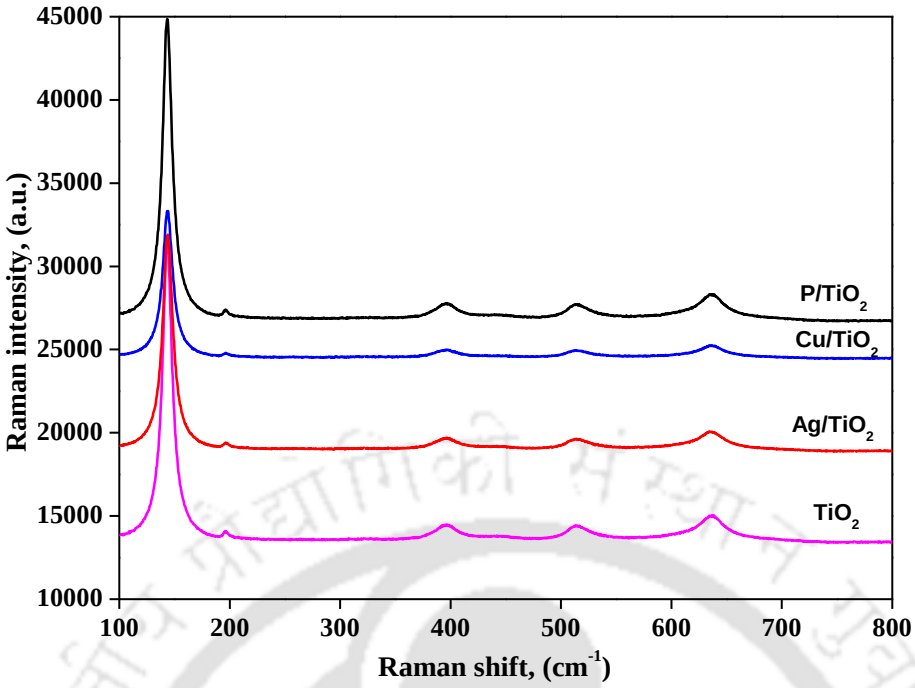

Figure 6.5: Raman spectra of bare, metal and phosphorous doped TiO_2.

The Raman spectra consisting of intense vibrational bands at 144, 400, 515, and 635 cm^{-1} (Fig. 6.5), corresponds to $v_1(E_g)$, $v_2(B_{1g})$, $v_3(A_{1g})$ or $v_3(B_{1g})$, and $v_4(E_g)$, respectively, of anatase phase of TiO_2 (Zhang et al., 2000). Bands of $v_1(E_g)$ and $v_2(B_{1g})$ represent the O–Ti–O bending vibrational mode, whereas v_3(A1g) or v_3(B1g), and *v4*(Eg) represent the Ti–O bond stretching vibrational mode (Ohsaka et al., 1978). The intensity of these bands from the Ag-, Cu-, and P-doped TiO_2 catalyst decreases as compared to that from bare TiO_2.

The BET surface area is decreased and the pore diameter and volume are increased with the Ag-, Cu- and P-doping on to TiO_2 (Table 6.2). The effect is maximum with P/TiO_2. The average pore diameter is 18 nm for the bare TiO_2 and is increased to 35, 37, and 38 nm, respectively, upon doping with Ag, Cu, and P. This could be attributed to the partial filling of TiO_2 pores by the doped elements (Ag, Cu, or P) leading to the blocking of small pore of TiO_2 support (Rao and Golder, 2016). The enhancement of average pore size with doping is due to the increase in crystallite size which gives the higher porosity of the nanoparticles. Also, Ag-, Cu-, and P-doping into TiO_2 crystal lattice may be the reason for the increase in the lattice tension. Therefore, the particle size became larger after doping, which is in agreement with the XRD results.

Table 6.2: Textural and acid properties of bare, metal and phosphorous doped TiO_2.

Catalyst	Surface area, $m^2.g^{-1}$	Pore diameter, nm	Pore volume, $cm^3.g^{-1}$	Bronsted Acid site conc. ($\mu mol.g^{-1}$)	Lewis Acid site conc. ($\mu mol.g^{-1}$)
TiO_2	66.5	17.68	0.29	55.3	166.9
Ag/TiO_2	64.8	19.90	0.31	176.8	182.0
Cu/TiO_2	59.3	26.26	0.41	175.4	163.2
P/TiO_2	57.0	32.40	0.47	184.6	191.0

6.2.1.3 Thermal and colloidal stabilities of doped catalysts

The thermal stability and the influence of temperature on the bare TiO_2 support and Ag-, Cu-, and P- doped TiO_2 are shown in Fig. 6.6a. The bare TiO_2 exhibited a steady weight loss of about 1.2% up to 950°C (Fig. 6.6a). The weight loss between 50 and 150°C due to the evaporation of water molecules for both Ag/TiO_2 and P/TiO_2. Another weight loss of around 1.1% within 200 - 540°C found due to the organic components degradation such as lignins, carbohydrates, ferulic acid, quercetins and ascorbic acid (Carballo et al., 2008; Rao and Golder, 2016) which play as stabilizing agents. The third weight loss of 0.35% was noticed at 540 – 950°C caused by the thermal decomposition of bioorganic salts such as resistive aromatic complexes and carbonates (Carballo et al., 2008).

The surface potential controls the adsorption of organic constituents on the surface of the catalyst. The zeta-potential (ζ) is related to the surface potential and, the difference of ζ with respect to the solution pH was shown in Fig. 6.6b.

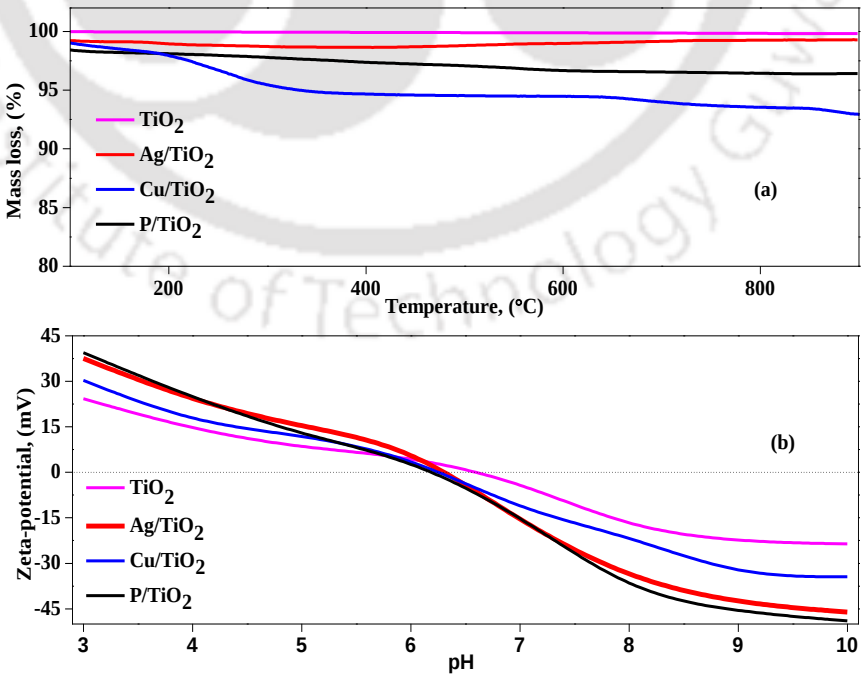

Figure 6.6: (a) TGA plots and (b) Zeta-potential studies of bare, metal and phosphorous doped TiO_2.

The point of zero-charge (pH_{zpc}) of bare TiO_2 is determined to be 6.63 ± 0.4 and, it decreased to 6.35 ± 0.4 and 6.23 for Ag/TiO_2 and P/TiO_2. In the case of TiO_2, ζ varied from 24 ± 0.5 to -23.8 ± 0.6 mV for pH between 3 and 10. Ag/TiO_2 exhibited ζ between -37.5 ± 0.3 and -46.14 ± 0.2 mV at pH 10. At a higher alkaline pH, the aggregates formation is minimized because of electrostatic repulsion (Behera et al., 2016; Rao and Golder, 2016). Consequently, the colloidal stability of particles was increased at a higher alkaline pH owing to a higher absolute ζ value (Popa et al., 2009). In the case of acidic pH range, the low absolute ζ directs to low surface charge could pose the lower particles stabilization. Therefore, ζ increased substantially in alkaline pH as compared to the acidic pH. The reaction formulation of the surface charge on TiO_2 surface was established both in acidic and alkaline pH is shown in Eqs. 6.3 and 6.4 (Behera et al., 2016).

$$Ti\text{-}OH + H^+ \leftrightarrow Ti\text{-}OH_2^+ \quad (6.3)$$

$$Ti\text{-}OH + OH^- \leftrightarrow Ti\text{-}O^- + H_2O \quad (6.4)$$

Furthermore, the higher valency of the Ti than the dopant (Ag, Cu, P) induces the oxygen vacancies in the heterostructures (Yang et al., 2015). This difference in valency, in-turn, results in higher colloidal stability of the particles by trapping more -OH groups or H_2O on Ag/TiO_2 or P/TiO_2 surface.

6.2.2 Catalyst performance for 5-HMF production

6.2.2.1 Production of 5-HMF from glucose: effect of catalyst and operating conditions

The glucose conversion along with the products yields over various catalysts (TiO_2, Ag/TiO_2, Cu/TiO_2, and P/TiO_2) is shown in Fig. 6.7. The bare TiO_2 showed the lowest yield of 5-HMF (35.4%) and the lowest glucose conversion (67.7%). All the doped catalysts (Ag-, Cu- and P-doped TiO_2) showed better catalytic activity as compared to bare TiO_2. The 5-HMF yields of 38.6, 39.5, and 46.4% are obtained over Ag-, Cu- and P-doped TiO_2 catalysts, respectively. P/TiO_2 showed the highest yield of 5-HMF which could be attributed to the higher Brønsted acid sites present in this catalyst (Table 6.2) as compared to those of other catalysts. The concentration of Brønsted and Lewis acid sites in this catalyst is nearly equal, which makes this catalyst the best among all the catalysts, tested in this study. The catalyst containing less number of Lewis acid sites resulted in the lower conversion of glucose. This may be due to the fact that the glucose to fructose isomerization reaction is catalyzed by Lewis acid sites. The side products (particularly, LA and FA) formation is also lowest with the P/TiO_2 catalyst. This indicates that P/TiO_2 suppresses the rehydration reaction of 5-HMF

to LA and FA. The other two side products (lactic acid and acetic acid) are forming in very low quantities (with yields less than 4%) overall the catalysts studied in this work. Atanda et al. (2015a) and (2015b) investigated the glucose to 5-HMF conversion over bare and P/TiO_2 catalysts in a biphasic system (water + n-butanol) and under various operating conditions. When the results of their work are compared with the present work, under similar operating conditions (175^{o}C, 3 h, 10 wt. % glucose), the yields of 5-HMF over P/TiO_2 catalysts are similar in both the works (46% in our work vs. 45% in their work). The glucose conversion (96%) is higher than that in our study (61%). Therefore, the selectivity to 5-HMF is much higher in our study (75% vs. 47%). Moreover, the amount of P doped onto TiO_2 is much smaller (0.8 wt.%) in our study as compared to that (15%) in their study. The better activity for the conversion of glucose to 5-HMF over P/TiO_2 could be attributed to better dispersion of the P over TiO_2 due to the bio-inspired method used in this study.

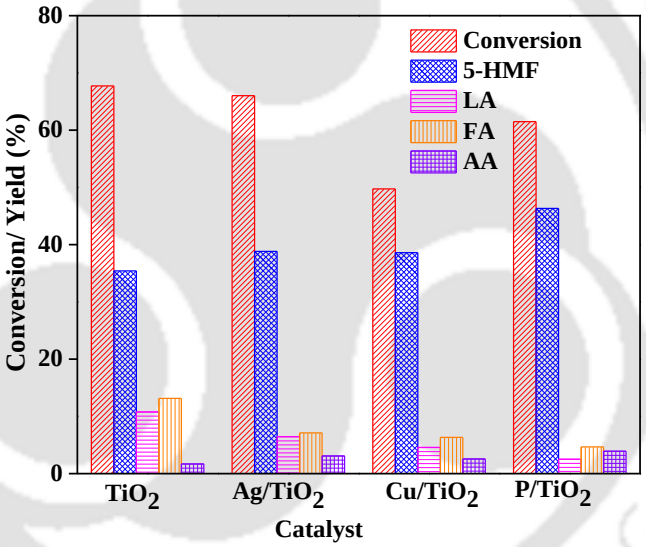

Figure 6.7: Conversion of glucose and yield of reaction products using bare, metal and phosphorous doped TiO_2. Reaction conditions: 2 g of DI water, 0.2 g of substrate, glucose: catalyst = 3:1 w/w, 4 g of MIBK, 0.6 g of NaCl, 3 h of reaction time, and 170°C of reaction temperature.

As the P/TiO_2 showed the best activity in this study, it is further tested at different temperatures and reaction times (Fig. 6.8). As can be noticed from the figure, the temperature shows a significant effect on glucose conversion as well as the 5-HMF yield. At all the temperatures, the glucose conversion increases linearly with reaction time at lower reaction times and levels-off at higher reaction times. The 5-HMF yield passed through maxima, at all the reaction temperatures. At 170^{o}C, the 5-HMF yield reached the maximum at the reaction time of 3 h. Whereas, at 180^{o}C as well as at 190^{o}C, it reached the maximum earlier, i.e., at 85

min. The maximum yield of 51% is obtained at 190°C and 85 min. A similar trend has been observed for glucose conversion as well as for 5-HMF yield by Atanda et al. (2015a). At all the reaction conditions used to test this catalyst, the yields of side products (LA, FA, lactic acid, and AA) are very less (< 5%). Which indicates that the catalyst P/TiO_2 suppresses the side reactions such as rehydration of 5-HMF to LA and FA, and decomposition of glucose to lactic acid, etc. This is the best property that we observed with this catalyst as compared to other catalysts studied in this thesis. For example, the ionic liquid encapsulated zeolites produce 5-HMF with higher yields but the yields of side products (particularly, LA and FA) are also higher.

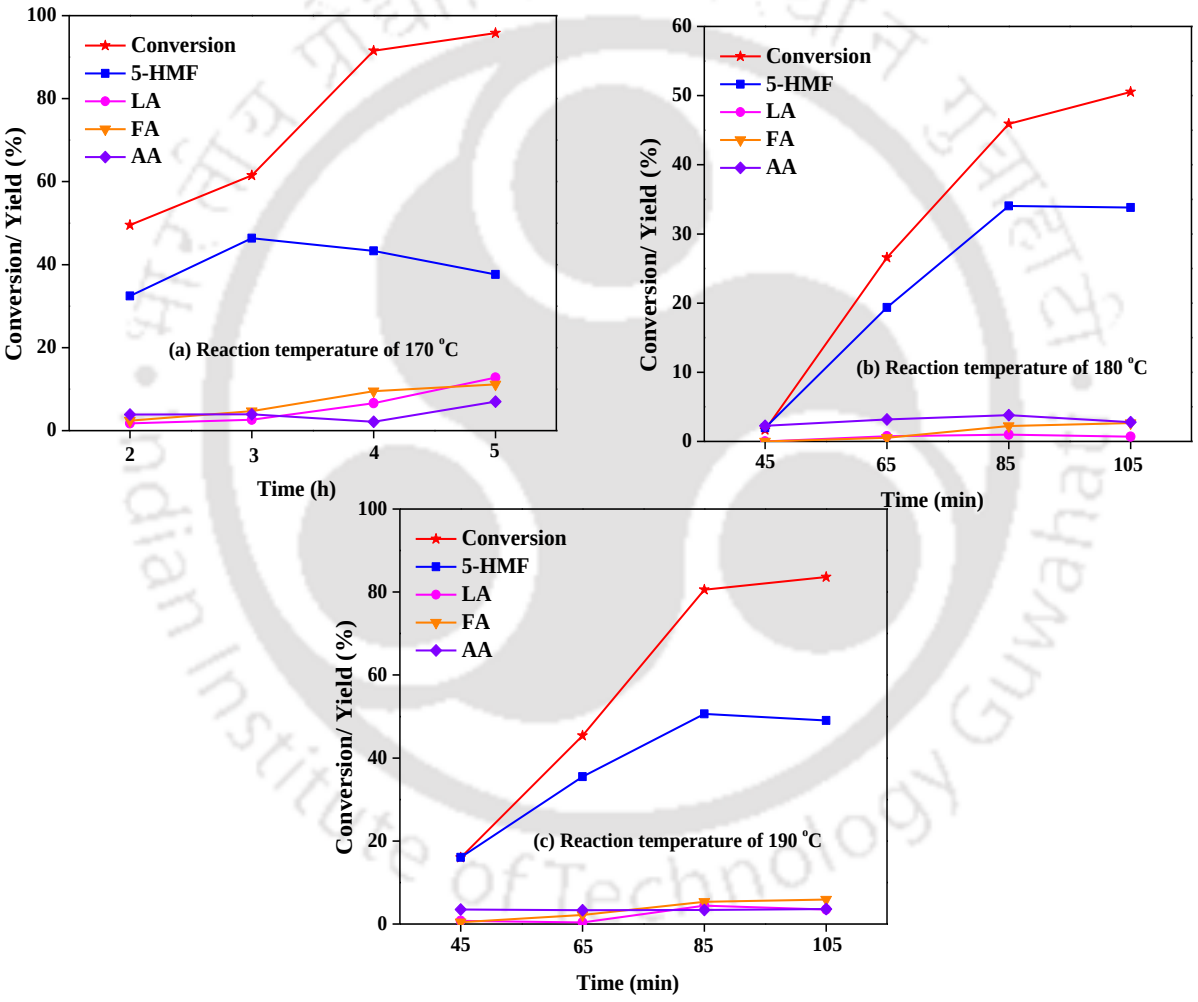

Figure 6.8: Variation of conversion of glucose and yield of reaction products as a function of reaction time using P/TiO_2 catalyst. Reaction conditions: 2 g DI water, 0.2 g glucose, substrate:catalyst ratio = 3:1 w/w, 4 g MIBK, 0.6 g NaCl, at reaction temperature of (a) 170°C, (b) 180°C, and (c) 190°C.

6.2.2.2 Recycle test for of used P/TiO_2 for glucose to 5-HMF conversion

The catalyst recycle test indicates that the P/TiO_2 catalyst is stable for at least four cycles (Fig. 6.9). In the four cycles, the glucose conversion is constant at 80% and the yield of 5-HMF is decreased marginally from 50 to 43% (14% decrease). After the first cycle, the yields of side products (LA and FA) increased marginally. The yield of AA remained constant in the four cycles. This data indicates that the catalyst can be reused for at least four cycles without significant loss of catalytic activity. A similar catalyst stability is reported by Atanda et al. (2015a) with a decrease of the 5-HMF yield by approximately 17% in three cycles.

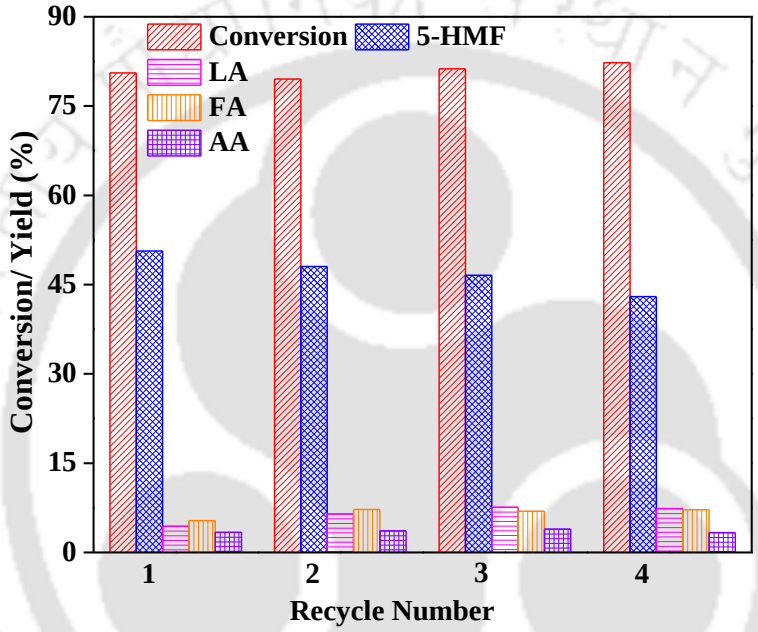

Figure 6.9: Conversion of glucose and yields of reaction products as a function of catalyst recycle number over P/TiO_2 catalyst.

6.3 Comparison of key results obtained in this doctoral studies

The comparison of the key results achieved in this thesis is summarized in Table 6.3. In this table we compared the best results obtained from various category of catalysts (bare zeolites vs. ChCl/zeolites vs. [BMIM]Br/zeolites vs. TiO_2 based catalysts) irrespective of reaction conditions. As can be seen from the table, the IL encapsulated zeolites showed a substantial increase in activity as compared to their bare zeolite counterparts. For example, the maximum 5-HMF yield obtained from glucose over bare zeolites is 46%. Whereas, it increased marginally to 48% with ChCl encapsulation and substantially to 62% with [BMIM]Br encapsulation. The 5-HMF yield over P/TiO_2 catalyst (51%) is lower as compared to that over [BMIM]Br encapsulated zeolites (62%). When the selectivities to 5-HMF are

compared, the selectivities to 5-HMF are similar over [BMIM]Br encapsulated zeolites (62%) and P/TiO_2 (63%). However, it is the highest over ChCl encapsulated zeolite (83%). A marginal increase of 5-HMF yield from 57 to 59% in the case of cellulose is also observed upon [BMIM]Br encapsulation. The ChCl/HMOR_20 showed the best 5-HMF yield of 98% from fructose, a moderate improvement as compared to the 5-HMF yield (92%) over bare zeolites. Therefore, from the overall comparison it can be concluded that the ionic liquid encapsulated zeolites (particularly, [BMIM]Br/NaY_5.1) perform better than the other catalysts used in this thesis.

Table 6.3: Key results of substrate conversion and 5-HMF yield over various catalysts used in this thesis.

Sl. no.	Catalyst	Substrate	Reaction conditions		Conversion (%)	Yield (%)[a]	Selectivity (%)[b]
			Temp. (°C)	Time (h)			
1	HBeta_360	Fructose	180	1	99.8	92.4	92.6
2	ChCl/HMOR_20	Fructose	180	1	99.1	97.9	98.8
3	[BMIM]Br/NaY_5.1	Fructose	180	1	99.9	80.9	81.0
4	HBeta_360	Glucose	180	2.83	72.9	51.5	70.5
5	ChCl/HMOR_20	Glucose	180	1	58.3	48.6	83.4
6	[BMIM]Br/NaY_5.1	Glucose	180	2	100	61.6	61.6
7	P/TiO_2	Glucose	190	1.25	80.5	50.7	63.0
8	HY_5.1	Cellulose	180	1	N/A	57.2	N/A
9	HBeta_360	Cellulose	180	3	N/A	40.0	N/A
10	ChCl/HY_5.1	Cellulose	180	1	N/A	55.3	N/A
11	[BMIM]Br/NaY_5.1	Cellulose	180	3	N/A	59.1	N/A

* Note: In all the above experiments, the amounts of DI water (2 g), substrate concentration (0.2 g), NaCl (0.6 g), and MIBK (4 g) are contant and the substrate:catalyst = 3:1 w/w. N/A: Not analyzed. [a]Yield of 5-HMF and [b]Selectivity to 5-HMF.

6.4 Conclusions

Ag, Cu, and P functionalized TiO_2 are successfully synthesized using a bio-inspired method and applied for the conversion of glucose to 5-HMF in a biphasic system (water/MIBK) and obtained high yields of 5-HMF. The incorporation of Ag, Cu, and P into the structural framework of TiO_2 is established using XRD and TEM analysis. Ag-, Cu-, and P-doping into TiO_2 enhanced the thermal and colloidal stability of TiO_2 and observed a moderate phase transformation from anatase to rutile phase. The crystallite size of doped-TiO_2 is increased due to Ag, Cu or P incorporation to the crystal structure of TiO_2 which is supported by the lattice strain of TiO_2. The adsorbed biomolecules, as well as the induced

oxygen vacancies, caused the reduction in the zeta-potential below and above pH_{zpc} giving doped-TiO_2 particles more stability in its aqueous colloid. N_2 sorption study revealed that the surface area decreased with doped-TiO_2 (14% reduction with P/TiO_2). Furthermore, Lewis and Bronsted acid sites are quantified by pyridine-FTIR. P/TiO_2 is the most effective catalyst for the conversion of glucose to 5-HMF due to its enhanced surface acidity. The highest 5-HMF yield of 50% at 81% glucose conversion is achieved at 190°C for 85 min reaction time. Lastly, the P/TiO_2 catalyst is stable for four cycles with only a marginal decrease in the 5-HMF yield.

References

Atanda, L., Mukundan, S., Shrotri, A., Ma, Q., Beltramini, J., 2015a. Catalytic conversion of glucose to 5-hydroxymethyl-furfural with a phosphated TiO2catalyst. ChemCatChem 7, 781–790. https://doi.org/10.1002/cctc.201402794

Atanda, L., Shrotri, A., Mukundan, S., Ma, Q., Konarova, M., Beltramini, J., 2015b. Direct Production of 5-Hydroxymethylfurfural via Catalytic Conversion of Simple and Complex Sugars over Phosphated TiO<inf>2</inf>. ChemSusChem 8, 2907–2916. https://doi.org/10.1002/cssc.201500395

Behera, A.K., Rao, C.V., Das, R.K., Giri, A.S., Golder, A.K., 2016. Fabrication and characterization of Ag-doped titania: impact of dye-sensitization, phenol decomposition kinetics and biodegradability index. Desalin. Water Treat. 57, 9488–9497. https://doi.org/10.1080/19443994.2015.1028457

Carballo, T., Gil, M.V., Gomez, X., Gonzalez-Andres, F., Moran, A., 2008. Characterization of different compost extracts using Fourier-transform infrared spectroscopy (FTIR) and thermal analysis. Biodegradation 19, 815–830.

Chakraborty, S., Rao, C.V., Das, R.K., Giri, A.S., Golder, A.K., 2017. Bio-mediated silver nanoparticle synthesis: Mechanism and microbial inactivation. Toxicol. Environ. Chem. 99, 434–447. https://doi.org/10.1080/02772248.2016.1214271

Chelli, V.R., Golder, A.K., 2018. Ag-doping on ZnO support mediated by bio-analytes rich in ascorbic acid for photocatalytic degradation of dipyrone drug. Chemosphere 208, 149–158. https://doi.org/10.1016/j.chemosphere.2018.05.158

De, S., Dutta, S., Patra, A.K., Bhaumik, A., Saha, B., 2011. Self-assembly of mesoporous TiO2nanospheres via aspartic acid templating pathway and its catalytic application for 5-hydroxymethyl-furfural synthesis. J. Mater. Chem. 21, 17505–17510.

https://doi.org/10.1039/c1jm13229f

Dutta, S., De, S., Patra, A.K., Sasidharan, M., Bhaumik, A., Saha, B., 2011. Microwave assisted rapid conversion of carbohydrates into 5-hydroxymethylfurfural catalyzed by mesoporous TiO2nanoparticles. Appl. Catal. A Gen. 409–410, 133–139. https://doi.org/10.1016/j.apcata.2011.09.037

Fan, C., Guan, H., Zhang, H., Wang, J., Wang, S., Wang, X., 2011. Conversion of fructose and glucose into 5-hydroxymethylfurfural catalyzed by a solid heteropolyacid salt. Biomass and Bioenergy 35, 2659–2665. https://doi.org/10.1016/j.biombioe.2011.03.004

Ismail, A.A., Al-Sayari, S.A., Bahnemann, D.W., 2013. Photodeposition of precious metals onto mesoporous TiO2 nanocrystals with enhanced their photocatalytic activity for methanol oxidation. Catal. Today 209, 2–7.

Kamat, P. V., 2007. Meeting the clean energy demand: Nanostructure architectures for solar energy conversion. J. Phys. Chem. C 111, 2834–2860. https://doi.org/10.1021/jp066952u

Kuo, C.-H., Poyraz, A.S., Jin, L., Meng, Y., Pahalagedara, L., Chen, S.-Y., Kriz, D.A., Guild, C., Gudz, A., Suib, S.L., 2014. Heterogeneous acidic TiO2 nanoparticles for efficient conversion of biomass derived carbohydrates. Green Chem. 16, 785. https://doi.org/10.1039/c3gc40909k

Kwak, E.S., Lee, W., Park, N.-G., Kim, J., Lee, H., 2009. Compact Inverse-Opal Electrode Using Non-Aggregated TiO2 Nanoparticles for Dye-Sensitized Solar Cells. Adv. Funct. Mater. 19, 1093–1099. https://doi.org/10.1002/adfm.200801540

Maleki, A., Kari, T., Aghaei, M., 2017. Fe3O4@SiO2@TiO2-OSO3H: an efficient hierarchical nanocatalyst for the organic quinazolines syntheses. J. Porous Mater. 24, 1481–1496. https://doi.org/10.1007/s10934-017-0388-z

Nakajima, K., Noma, R., Kitano, M., Hara, M., 2014. Selective glucose transformation by titania as a heterogeneous Lewis acid catalyst. J. Mol. Catal. A Chem. 388–389, 100–105. https://doi.org/10.1016/j.molcata.2013.09.012

Nikolla, E., Román-Leshkov, Y., Moliner, M., Davis, M.E., 2011. "One-pot" synthesis of 5-(hydroxymethyl)furfural from carbohydrates using tin-beta zeolite. ACS Catal. 1, 408–410. https://doi.org/10.1021/cs2000544

Ohsaka, T., Izumi, F., Fujiki, Y., 1978. Raman spectrum of anatase, TiO,. J. Raman Spectrosc. 7, 321–324.

Ordonez, A.A.L., Gomez, J.D., Vattuone, M.A., Isla, M.I., 2006. Antioxidant activities of Sechium edule (Jacq.) Swartz extracts. Food Chem. 97, 452–458.

https://doi.org/10.1016/j.foodchem.2005.05.024

Peng, T., Zhao, D., Dai, K., Shi, W., Hirao, K., 2005. Synthesis of titanium dioxide nanoparticles with mesoporous anatase wall and high photocatalytic activity. J. Phys. Chem. B 109, 4947–4952. https://doi.org/10.1021/jp044771r

Popa, I., Gillies, G., Papastavrou, G., Borkovec, M., 2009. Attractive electrostatic forces between identical colloidal particles induced by adsorbed polyelectrolytes. J. Phys. Chem. B Lett. 113, 8458–8461.

Ramakrishnan, R., Kalaivani, S., Amala Infant Joice, J., Sivakumar, T., 2012. Photocatalytic activity of multielement doped TiO2 in the degradation of congo red. Appl. Surf. Sci. 258, 2515–2521.

Rao, C.V., Golder, A.K., 2016. Development of a bio-mediated technique of silver-doping on titania. Colloids Surfaces A Physicochem. Eng. Asp. 506, 557–565. https://doi.org/10.1016/j.colsurfa.2016.07.031

Riazian, M., Rad, S.D., Azinabadi, R.R., 2013. Fabrication of pure and Ag-doped TiO2 nanorods and study of the lattice strain and the activation energy of the crystalline phases. J. Korean Phys. Soc. 62, 459–468. https://doi.org/10.3938/jkps.62.459

Tayade, R.J., Kulkarni, R.G., Jasra, R. V, 2006. Transition metal ion impregnated mesoporous TiO2 for photocatalytic degradation of organic contaminants in water. Ind. Eng. Chem. Res. 45, 5231–5238.

Teleki, A., Pratsinis, S.E., Kalyanasundaram, K., Gouma, P.I., 2006. Sensing of organic vapors by flame-made TiO2nanoparticles. Sensors Actuators, B Chem. 119, 683–690. https://doi.org/10.1016/j.snb.2006.01.027

Torres, A.I., Daoutidis, P., Tsapatsis, M., 2010. Continuous production of 5-hydroxymethylfurfural from fructose: A design case study. Energy Environ. Sci. 3, 1560–1572. https://doi.org/10.1039/c0ee00082e

Watanabe, M., Aizawa, Y., Iida, T., Aida, T.M., Levy, C., Sue, K., Inomata, H., 2005. Glucose reactions with acid and base catalysts in hot compressed water at 473 K. Carbohydr. Res. 340, 1925–1930. https://doi.org/10.1016/j.carres.2005.06.017

Yang, X., Wang, S., Sun, H., Wang, X., Lian, J., 2015. Preparation and photocatalytic performance of Cu-doped TiO2 nanoparticles. Trans. Nonferrous Met. Soc. China 25, 504–509.

Zhang, W.F., He, Y.L., Zhang, M.S., Yin, Z., Chen, Q., 2000. Raman scattering study on anatase TiO2 nanocrystals. J. Phys. D. Appl. Phys. 33, 912–916. https://doi.org/10.1088/0022-3727/33/8/305

Chapter 7

Major Findings and Future Directions

7.1 Major findings

Based on the investigations reported in Chapters 3, 4, 5, and 6, the following conclusions can be drawn:

i. Bare zeolites performance: Bare HBeta showed the highest 5-HMF yield of 94% with a fructose conversion of 98% at 180°C for 1 h. The highest yield to 5-HMF obtained with the glucose is 51.5% (at 72.9% conversion), respectively, at 180°C. The HBeta is highly selective to 5-HMF production with a negligible concentration of side products (< 3%).

ii. ChCl/zeolites performance: The choline chloride impregnated HMOR, HZSM5, HBeta, NaY, and HY zeolites are highly active for cellulose, glucose, and fructose conversion to 5-HMF. The crystal size is decreased for the zeolites with lower silica-to-alumina ratio upon impregnation with the ChCl. The 5-HMF yield from glucose and cellulose are the highest at 49 and 55% over ChCl/HMOR_20 and ChCl/HY_5.1, respectively.

iii. The activity of the zeolites with moderate silica-to-alumina ratios (SAR) is enhanced by the impregnation of ChCl on to these zeolites, particularly HZSM5. This is attributed to the better interaction of ChCl with HZSM5 through N-atoms of ChCl. However, the effect is negligible for the zeolites with either low or high SAR. The ChCl impregnated HZSM5 catalyst remained stable up to five consecutive cycles.

iv. [BMIM]Br/zeolites performance: The [BMIM]Br ionic liquid is successfully encapsulated in the zeolites (NaY, HY, and HMOR) using a ship-in-a-bottle method and used for carbohydrates conversion to 5-HMF. The [BMIM]Br encapsulation is confirmed using various characterizations: XRD, TGA, CHN, N_2-sorption, Raman, EDX and ^{27}Al SS NMR. The [BMIM]Br ionic interaction with H-form zeolite is stronger as compared to that of Na-form zeolite, as indicated by the TGA analysis. ^{27}Al SS NMR reveals that the HMOR loses its extra-framework Al upon the ionic liquid encapsulation.

v. The [BMIM]Br/zeolite catalysts showed significant improvements in the 5-HMF yield and carbohydrates conversions as compared to their bare zeolite counterparts. The 5-HMF yields obtained over [BMIM]Br/NaY with fructose, glucose, and cellulose are 80, 60, and 59%, at 180^{o}C, respectively. The catalyst showed excellent recycle stability with a moderate decrease in activity till the second cycle only.

vi. Ag-, Cu- and P-doped TiO_2 catalysts performance: Ag, Cu, and P functionalized TiO_2 are successfully synthesized using a bio-inspired method and applied for the conversion of glucose to 5-HMF in a biphasic system (water/MIBK) and obtained high yields of 5-HMF. The incorporation of Ag, Cu, and P into the structural framework of TiO_2 is established using XRD and TEM analysis. Ag-, Cu-, and P-doping into TiO_2 enhanced the thermal and colloidal stability of TiO_2 and observed a moderate phase transformation from anatase to rutile phase. The crystallite size of doped-TiO_2 is increased due to Ag, Cu or P incorporation to the crystal structure of TiO_2 which was supported by the lattice strain of TiO_2. The adsorbed biomolecules, as well as the induced oxygen vacancies, caused the reduction in the zeta-potential below and above pH_{zpc} giving doped-TiO_2 particles more stability in its aqueous colloid. N_2 sorption study revealed that the surface area decreased with doped-TiO_2 (14% reduction with P/TiO_2). Furthermore, the Lewis and Brønsted acid sites are quantified by pyridine-FTIR.

vii. P/TiO_2 is the effective catalyst for the conversion of glucose to 5-HMF due to its enhanced surface acidity. The highest 5-HMF yield of 50.4% at 80.6% glucose conversion is achieved at 190°C for 85 min reaction time. Lastly, the P/TiO_2 catalyst is stable for four cycles with only a marginal decrease in the 5-HMF yield.

vii. The best catalyst in the overall study is found to be [BMIM]Br/NaY with a 5-HMF yield of 59% from cellulose and of 60% from glucose. ChCl/HMOR showed the best 5-HMF yield of 98% from fructose. Moreover, the same catalyst (ChCl/HMOR) is highly selective to the formation of 5-HMF from glucose with a selectivity to 5-HMF of 83%.

viii. The ChCl/HZSM5 showed an enhancement in 5-HMF yield with an increase from 36 to 44%, whereas, the [BMIM]Br/NaY showed the best enhancement in 5-HMF yield with an increase from 41 to 59%, from cellulose, upon encapsulation with the respective IL.

The publications of the works reported in this doctoral thesis are already initiated, and it is very likely that these works will come up with a few quality publications soon.

7.2 Limitations of the thesis

i. The complete interactions of ionic liquid with the zeolite could not be identified: We carried out SS NMR, TGA, EDX, etc. to understand the interaction between the ionic liquid (ChCl or [BMIM]Br) and the zeolite. However, the complete understanding of interactions could not be established.

ii. The solid products (humins) are not characterized completely. Humins could be used in various potential applications. However, to do that a complete understanding of the structures of the humins formed is necessary.

iii. *In situ* techniques such as Operendo-FTIR are not used to fully understand the reaction mechanism. This understanding could be utilized to design even better catalysts for the conversion of carbohydrates to 5-HMF.

iv. The catalysts are not tested for actual lignocellulosic biomass: The understanding of the usefulness of the developed catalysts for actual lignocellulosic biomass could be highly beneficial.

7.3 Future work directions

i. A thorough investigation of ionic liquid encapsulated zeolites by using solid-state NMR, XPS, etc. to completely understand the ionic liquid interaction with the zeolite, so as to design these catalysts in a more efficient way.

ii. Zeolites could be synthesized ionothermally with tailor-made properties such as silica-to-alumina ratio, mesoporosity, etc. to obtain even better performances.

iii. Operendo-FTIR investigation for a complete understanding of the reaction mechanism.

iv. Systematic investigation of the effect of operating conditions (such as substrate dosage, catalyst dosage, etc.) and the catalyst composition in the case of P/TiO_2 catalyst functionalized by a bio-inspired approach.

v. Detailed characterizations of the solid products (such as humins) formed so as to identify their potential uses.

vi. The prepared catalysts could be tested for the direct actual lignocellulosic biomass conversion to 5-HMF.

vii. The prepared catalysts could be tested for the selective production of other value-added chemicals such as levulinic acid, lactic acid, 2,5-Diformylfuran, etc.

Research Output from the Thesis

Journal papers

1. N.R. Peela, **S.K. Yedla**, B. Velaga, A. Kumar, A.K. Golder; "Choline Chloride Functionalized Zeolites for the Conversion of Biomass Derivatives to 5-Hydroxymethylfurfural" Applied Catalysis A, General 580 (2019) 59 – 70 (DOI: 10.1016/j.apcata.2019.05.005)
2. **S.K. Yedla**, A.K. Golder, N.R. Peela, "Efficient Conversion of Carbohydrates to 5Hydroxymethylfurfural over Mesoporous Zeolites" Journal of Emerging Technologies and Innovative Research, May 2019,Volume 6, Issue 5,239-250, ISSN-2349-5162
3. **S.K. Yedla,** B.Velaga, S.Chowdary, A. Namdeo, A.K. Golder, N.R.Peela. "1-Butyl-3-Methylimidazolium Bromide Functionalized Zeolites: Nature of Interactions and Catalytic Activity for Carbohydrates Conversion to Value-added Chemicals" (Under Review)

National and international conferences

1. **S.K Yedla,** A. K. Golder, N. R. Peela, "Studies on the Production of 5-hydroxymethylfurfural (5-HMF) from Cellulose- A Mini Review" presented (poster) at CHEMCON 2015, December 27-30th 2015, Indian Institute of Technology Guwahati, India.
2. **S.K Yedla**, A. K. Golder, N. R. Peela, "One-Pot Production of 5-Hydroxymethylfurfural (5-HMF) from Carbohydrates by using different Solid Acid Catalysts", presented (oral) at REFLUX 2017, March 24-26th 2017, Indian Institute of Technology Guwahati, India
3. **S.K Yedla**, A. K. Golder, N. R. Peela"Production of 5-Hydroxymethylufurfural (5-HMF) from Fructose over H-MOR Zeolite Catalyst" presented (poster) at REFLUX 2017, March 24-26th 2017, Indian Institute of Technology Guwahati, India
4. **S.K Yedla,** A. K. Golder, N. R. Peela, "Glucose Dehydration to 5-Hydroxymethylfurfural over H-Type Zeolites in a Water/MIBK Biphasic System", presented (oral) at ICPOLC-19, January, 27th 2019, Hyderabad, India.
5. **S.K Yedla,** A. K. Golder, N. R. Peela"Efficient Conversion of Carbohydrates to 5-Hydroxymethylfurfural over Mesoporous Zeolites" presented (oral) at ICET-19, March, 2nd 2019, Hyderabad, India.

6. **S.K Yedla,** A. K. Golder, N. R. Peela, "Choline Chloride Grafted Zeolites for the production of 5-Hydroxymethylfurfural from Carbohydrates Conversion" presented (poster) at RESEARCH CONCLAVE 2019, March 14-17th 2019, Indian Institute of Technology Guwahati, India.

Awards

1. Best presentation award for the paper entitled "One-Pot Production of 5-Hydroxymethylfurfural (5-HMF) from Carbohydrates by using different Solid Acid Catalysts." in Reflux-2017-Annual Chemical Engineering Symposium, Department of Chemical Engineering, 24-26 March, IIT Guwahati, Assam, India
2. Best presentation award for the paper entitled, "Choline Chloride Grafted Zeolites for the production of 5-Hydroxymethylfurfural from Carbohydrates Conversion" presented (poster) at RESEARCH CONCLAVE 2019, March 14-17th 2019, Indian Institute of Technology Guwahati, India

Other publications/book chapters

1. M. Alam, **S. K. Yedla,** S. T. Bhutia, V. V. Goud, N. R. Peela, Advancement in Development of Biodiesel Production in the Last Two Decades: An Indian Overview on Raw Materials, Synthesis, By-products, and Application. A.K. Chandel, R.K. Sukumaran (eds.), Springer, (2017), Pages (167-188)